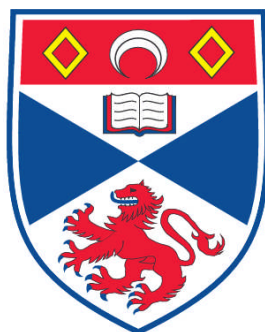


**STUDIES AND APPLICATION OF THE ENZYMES OF
FLUOROMETABOLITE BIOSYNTHESIS IN STREPTOMYCES
CATTLEYA**

Mayca Onega

**A Thesis Submitted for the Degree of PhD
at the
University of St Andrews**



2009

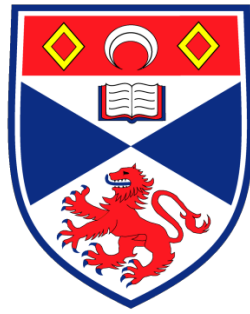
**Full metadata for this item is available in
Research@StAndrews:FullText
at:**

<http://research-repository.st-andrews.ac.uk/>

Please use this identifier to cite or link to this item:

<http://hdl.handle.net/10023/991>

This item is protected by original copyright



University
of
St Andrews

Studies and application of the enzymes
of fluorometabolite biosynthesis
in *Streptomyces cattleya*

by

Mayca Onega

*Thesis submitted to the University of St Andrews
in application for the degree of
Doctor of Philosophy*

March 2009

I, Mayca Omega, hereby certify that this thesis, which is approximately 40,000 words in length, has been written by me, that it is the record of work carried out by me and that it has not been submitted in any previous application for a higher degree.

I was admitted as a research student in October 2004 and as a candidate for the degree of Doctor of Philosophy in October 2005; the higher study for which this is a record was carried out in the University of St Andrews between 2004 and 2009.

Date Signature of candidate

I hereby certify that the candidate has fulfilled the conditions of the Resolution and Regulations appropriate for the degree of Doctor of Philosophy in the University of St Andrews and that the candidate is qualified to submit this thesis in application for that degree.

Date Signature of supervisor

In submitting this thesis to the University of St Andrews we understand that we are giving permission for it to be made available for use in accordance with the regulations of the University Library for the time being in force, subject to any copyright vested in the work not being affected thereby. We also understand that the title and the abstract will be published, and that a copy of the work may be made and supplied to any bona fide library or research worker, that my thesis will be electronically accessible for personal or research use unless exempt by award of an embargo as requested below, and that the library has the right to migrate my thesis into new electronic forms as required to ensure continued access to the thesis. We have obtained any third-party copyright permissions that may be required in order to allow such access and migration, or have requested the appropriate embargo below.

The following is an agreed request by candidate and supervisor regarding the electronic publication of this thesis:

Embargo on both all or part of printed copy and electronic copy for the same fixed period of 1 year on the following ground: publication would be commercially damaging to the researcher, or to the supervisor, or the University and would preclude future publication.

Date Signature of candidate

Date Signature of supervisor

To my grandfather, Luxís.

A mi abuelo, Luxís.

*Porque no recuerdo la última vez que te vi
pero sí lo mucho que me quisiste.
Y lo que yo te quiero a ti.*

Acknowledgements

First and foremost, I would like to thank and express my appreciation to my supervisor Professor David O'Hagan for giving me the invaluable opportunity to work in his group on such exhilarating and inspiring project. I appreciate very much his encouragement, patience and support during my PhD. I am also thankful to EPSRC for financial support.

Special thanks must go to the technical staff at the University of St Andrews for support and advice: Mrs Melanja Smith and Dr Tomas Lebl for the NMR service and Caroline Horsburgh for MS analysis. Thanks also go to Dr J. Hamilton (University of Belfast) for GC-MS analysis. I am very grateful to Mrs Jean Johnston and Mrs Margaret Wilson in the BMS office for their continuous friendly help.

I appreciate very much the support and help of Dr Christophe Plisson at GlaxoSmithKline, and Dr Lutz Schweiger, Dr Juozas Domarkas and Dr Timothy Smith at the University of Aberdeen. Without their collaboration, most of the PET work could not have been possible.

I would like to thank everybody in the DOH group. It has been a great pleasure to work with all of you! A very special thanks goes to Dr Hai Deng for teaching me and helping me so much in the lab. Thanks must also go to Stuart and Ryan for helpful discussions. I truly appreciate all the help and support from my 'academic father' Cosimo (*papá*) and from my 'chemical brother' Matthieu. My heartfelt thanks also go to Natalie for being more than a labmate: a great friend always willing to help. Thanks to Vincent, 'partner in crime' during writing up, submission, viva and celebration.

I want to express my gratitude to the person who encouraged me most to start this work. Thank you Tomás for your endless support and for a marvellous friendship!

Special thanks go to Fernando, who has been like an older brother for me. Karen 'Karenina', FFS I just cannot thank you enough! Vita, for all the chats and hot chocolates together and the best tiramisù ever! I am very lucky to have been surrounded by such remarkable group of people who provided me a lot of support and good times in St Andrews. Thanks also go to: Aga, Annick, Diego, Federica, Helena, María, Marzia, Nikos, Raquel, Ricardo and Sidhes.

Many thanks must also go to the ones who came to visit me and shared part of their lives with me in St Andrews. In order of visit thanks go to: my cousin Nani, my friend Ale and my cousin Sonia 'a miña prima do coiro' for the unforgettable days we spent together.

A very special thanks to M.K. for composing the soundtrack of this thesis and my life.

ACKNOWLEDGEMENTS

I will always be indebted to my friends in Lugo. Because they have been walking beside me and helping me when I most needed it, a huge 'thank you' goes to: Abel and David, Fátima, Sandra Allo and Sandra Rivas. Special thanks go also to Ángel for being simply a great person. I feel truly fortunate to have met you and to have you as friends. You all have a very especial place in my heart.

And finally, and most importantly, I want to thank everybody in my family. A warm 'thank you' to my grandmothers, Tata and María, for always having a smile for me and being so concerned about my happiness. To my parents for their constant support (daily!) and for showing me what is really important in life and for everything they have given to me. To the best gift they ever gave to me: Her, my sister (Eva). Her, to the infinity and beyond! Thank you for the chats, the laughs, the endless nights on the phone, for calming me down and keeping me sane. Because without you, I would have never reached this far. Thank you always.

Porque sin vosotros, nunca habría llegado tan lejos. Siempre gracias.

Contents

| | |
|--|------------|
| Declaration | i |
| Acknowledgements | ii |
| Contents | iv |
| Abbreviations | x |
| Abstract | xiv |
| | |
| 1 Introduction | 2 |
| | |
| 1.1 Halogens in natural products | 6 |
| | |
| 1.2 Fluorinated natural products | 9 |
| 1.2.1 The element fluorine in nature | 10 |
| 1.2.2 Fluorinated natural products from plants | 11 |
| 1.2.2.1 Fluoroacetate | 11 |
| 1.2.2.2 Fluorocitrate | 12 |
| 1.2.2.3 Fluoroacetone | 13 |
| 1.2.2.4 Fluorinated fatty acids | 14 |
| 1.2.3 Fluorinated natural products from marine sources | 16 |
| 1.2.4 Fluorinated natural products from bacteria | 17 |
| 1.2.4.1 Nucleocidin from <i>Streptomyces calvus</i> | 17 |
| 1.2.4.2 Fluoroacetate and 4-fluothreonine from <i>Streptomyces cattleya</i> | 18 |
| | |
| 1.3 Techniques used for studying the biosynthesis of natural products | 19 |
| 1.3.1 Isotopic labelling | 19 |
| 1.3.2 Enzyme experiments | 20 |
| 1.3.3 ¹⁹ F NMR spectroscopy | 21 |

| | | |
|------------|---|------------|
| 1.4 | Biosynthesis of fluorinated secondary metabolites by <i>Streptomyces cattleya</i> | 24 |
| 1.4.1 | Fluoroacetaldehyde as a biosynthetic intermediate | 24 |
| 1.4.2 | Identification of fluoacetaldehyde dehydrogenase from <i>S. cattleya</i> | 25 |
| 1.4.3 | Identification of PLP-dependent threonine transaldolase from <i>S. cattleya</i> | 25 |
| 1.4.4 | Identification of a fluorination enzyme from <i>Streptomyces cattleya</i> | 28 |
| 1.4.4.1 | Purification, crystal structure and properties | 35 |
| 1.4.4.2 | Mechanism of the fluorinase | 42 |
| 1.4.5 | Identification of 5-deoxy-5-fluoro- α ,D-ribose-1-phosphate as an intermediate | 46 |
| 1.4.6 | Fluorometabolite gene cluster in <i>S. cattleya</i> | 48 |
| 1.4.7 | Overview of fluorometabolite biosynthesis in <i>Streptomyces cattleya</i> | 49 |
| 1.5 | References | 51 |
| 2 | Identification of 5-FDRulP as an intermediate in fluorometabolite biosynthesis in <i>Streptomyces cattleya</i> | 62 |
| 2.1 | L-Methionine salvage pathway | 63 |
| 2.1.1 | 5-Deoxy-5-methylthio- α ,D-ribose-1-phosphate isomerases | 65 |
| 2.2 | The metabolism of 5'-FDA in <i>S. cattleya</i> | 67 |
| 2.3 | The metabolism of 5-FDRP in <i>S. cattleya</i> | 70 |
| 2.3.2 | Preparation of 5-FDRP | 61 |
| 2.3.3 | The effect of EDTA on fluorometabolite production | 72 |
| 2.3.4 | Isomerisation of 5-FDRP to 5-FDRulP | 74 |
| 2.3.4.1 | 5-FDRulP as a biosynthetic intermediate | 75 |
| 2.3.4.2 | Purification of the isomerase | 85 |
| 2.3.4.3 | Identification of the isomerase gene in <i>S. cattleya</i> | 92 |
| 2.3.4.4 | Mechanism of the isomerase enzyme | 94 |
| 2.4 | The metabolism of 5-FDRulP in <i>S. cattleya</i> | 97 |
| 2.4.1 | Aldolases in <i>S. cattleya</i> | 97 |
| 2.5 | Conclusions | 102 |
| 2.6 | References | 103 |

| | |
|---|------------|
| 3 Synthesis of key molecules | 108 |
| 3.1 Synthesis of 5'-deoxy-5'-fluoroadenosine | 47 108 |
| 3.2 Synthesis of 5-deoxy-5-fluoro-D-ribose | 71 117 |
| 3.3 Synthesis of 5-deoxy-5-fluoro-D-xylose | 74 121 |
| 3.4 Synthesis of fluoroacetaldehyde | 26 123 |
| 3.5 References | 124 |
| 4 The fluorinase as a tool for the synthesis of new fluorine-18 labelled sugars for positron emission tomography | 127 |
| 4.1 Introduction to positron emission tomography | 128 |
| 4.2 Application of the fluorinase enzyme in PET | 135 |
| 4.2.1 New enzymatic method for the synthesis of [¹⁸ F]FDR | 138 |
| 4.2.1.1 Development of the “cold” experiment | 139 |
| 4.2.1.2 Development of the “hot” experiment | 153 |
| 4.2.2 Enzymatic synthesis of [¹⁸ F]FDA | 162 |
| 4.2.3 Enzymatic synthesis of [¹⁸ F]FDI | 163 |
| 4.3 Adenosine analogues as potential radiotracers for investigating adenosine receptors by PET | 164 |
| 4.3.1 PET imaging studies <i>in vitro</i> | 166 |
| 4.3.1.1 5'-Deoxy-5'-[¹⁸ F]fluoroadenosine | 166 |
| 4.3.1.2 5'-Deoxy-5'-[¹⁸ F]fluorinosine | 169 |
| 4.3.2 PET imaging studies <i>in vivo</i> : a small animal study with [¹⁸ F]FDA | 170 |
| 4.4 Preliminary results of [¹⁸ F]FDR as a radiotracer of potential diagnostic interest | 173 |
| 4.5 Conclusions | 174 |
| 4.6 References | 175 |

| | | |
|------------|--|------------|
| 5 | Chemical and biochemical experimental | 184 |
| 5.1 | Chemical syntheses | 184 |
| 5.1.1 | General experimental procedures | 184 |
| 5.1.1.1 | Reagents and solvents | 184 |
| 5.1.1.2 | Reaction conditions | 185 |
| 5.1.1.3 | Chromatography | 185 |
| 5.1.1.4 | Nuclear Magnetic Resonance Spectroscopy (NMR) | 186 |
| 5.1.1.5 | Mass Spectroscopy | 186 |
| 5.1.1.6 | Melting point analyses | 187 |
| 5.1.1.7 | GC-MS | 187 |
| 5.1.2 | Synthesis of 5'-deoxy-5'-fluoroadenosine 47 | 188 |
| 5.1.2.1 | 2',3'- <i>O</i> -Isopropylidene-5'- <i>O</i> -mesyladenosine 95 | 188 |
| 5.1.2.2 | 2',3'- <i>O</i> -Isopropylidene-5'-deoxy-5'-fluoroadenosine 96 | 189 |
| 5.1.2.3 | Chloro-9-(2',3'- <i>O</i> -isopropylidene-β-D-ribofuranosyl)-purine 99 | 191 |
| 5.1.2.4 | 2',3'- <i>O</i> -Isopropylidene-5'-deoxy-5'-fluoro-6-chloropurine riboside 100^a 2',3'- <i>O</i> -Isopropylidene-5'-deoxy-5',6-difluoropurine riboside 100b | 192 |
| 5.1.2.5 | 5'-Deoxy-5'-fluoroadenosine 47 | 193 |
| 5.1.3 | Synthesis of 5-deoxy-5-fluoro-D-ribose 71 | 194 |
| 5.1.3.1 | Methyl-2,3- <i>O</i> -isopropylidene-β-D-ribofuranoside 82 | 194 |
| 5.1.3.2 | Methyl-2,3- <i>O</i> -isopropylidene-5- <i>O</i> -tosyl-β-D-ribofuranoside 102 | 195 |
| 5.1.3.3 | Methyl-2,3- <i>O</i> -isopropylidene-5-deoxy-5-fluoro-β-D-ribofuranoside 84 | 196 |
| 5.1.3.4 | 5-Deoxy-5-fluoro-D-ribose 71 | 197 |
| 5.1.4 | Synthesis of 5-deoxy-5-fluoro-D-xylose 74 | 198 |
| 5.1.4.1 | 1,2-Di- <i>O</i> -isopropylidene-5- <i>O</i> -tosyl-D-xylofuranose 105 | 198 |
| 5.1.4.2 | 1,2- <i>O</i> -Isopropylidene-5-deoxy-5-fluoro-α-D-xylofuranose 106 | 199 |
| 5.1.4.3 | 5-Deoxy-5-fluoro-D-xylofuranose 74 | 200 |
| 5.1.5 | Fluoroacetaldehyde 26 | 201 |
| 5.2 | Biochemical protocols | 202 |
| 5.2.1 | General experimental procedures | 202 |
| 5.2.1.1 | Reagents and enzymes | 202 |
| 5.2.1.2 | Cell culture and microbiological work | 202 |
| 5.2.1.3 | Nuclear Magnetic Resonance Spectroscopy (NMR) | 203 |

| | | |
|----------|--|-----|
| 5.2.1.4 | Gas Chromatography Mass Spectrometry (GC-MS) | 204 |
| 5.2.1.5 | High Performance Liquid Chromatography (HPLC) | 204 |
| 5.2.1.6 | Fast Performance Liquid Chromatography (FPLC) | 205 |
| 5.2.1.7 | SDS-Polyacrylamide gel electrophoresis (SDS-PAGE) | 206 |
| 5.2.2 | Culturing conditions of <i>S. cattleya</i> | 207 |
| 5.2.2.1 | Growth and maintenance of <i>S. cattleya</i> on agar | 207 |
| 5.2.2.2 | Culture medium and growth conditions of <i>S. cattleya</i> | 207 |
| 5.2.2.3 | Media procedure for growing <i>S. cattleya</i> | 208 |
| 5.2.3 | Preparation of resting cell cultures of <i>S. cattleya</i> | 209 |
| 5.2.4 | Preparation of cell-extract (CFE) of <i>S. cattleya</i> | 209 |
| 5.2.5 | Assay to determine biosynthetic activity in a CFE of <i>S. cattleya</i> | 209 |
| 5.2.6 | Protein purification by ammonium sulfate precipitation | 210 |
| 5.2.7 | Partial purification of an isomerase from <i>S. cattleya</i> | 211 |
| 5.2.7.1 | Hydrophobic interaction chromatography (HIC) | 212 |
| 5.2.7.2 | Size exclusion chromatography | 212 |
| 5.2.7.3 | Ion exchange chromatography (IEC) | 212 |
| 5.2.8 | Chemo-enzymatic preparation of 5'-FDI 50 | 213 |
| 5.2.9 | Chemo-enzymatic preparation of 5-FDRP 61 | 213 |
| 5.2.10 | Chemo-enzymatic preparation of 5-FDRul 73 | 214 |
| 5.2.11 | Chemo-enzymatic preparation of 5-FDXul 75 | 214 |
| 5.2.12 | Incubations in CFEs of <i>S. cattleya</i> | 215 |
| 5.2.12.1 | Preparation of 5-FDRulP 69 | 215 |
| 5.2.12.2 | Preparation of 5-FDRul 73 | 215 |
| 5.2.12.3 | Incubation 5-FDRul 73 in a CFE of <i>S. cattleya</i> | 215 |
| 5.2.13 | GC-MS Determination of the persilylated derivative of 5-FDRulP 69 | 216 |
| 5.2.14 | Expression of recombinant flA and purification | 217 |
| 5.2.14.1 | Assay for the over-expressed flA | 218 |
| 5.2.15 | <i>T. vivax</i> IAG-NH over-expression and purification | 219 |
| 5.2.15.1 | Expression vector | 219 |
| 5.2.15.2 | Transformation of competent cells with the <i>iagnh</i> ORF in pQE-30 | 219 |
| 5.2.15.3 | Expression of <i>iagnh</i> and purification of IAG-NH | 220 |
| 5.2.15.4 | Assay for the over-expressed <i>iagnh</i> | 223 |
| 5.2.16 | 5'-FDA as a substrate for the <i>T. vivax</i> IAG-NH | 223 |
| 5.2.16.1 | Incubation of 5'-FDA 47 in a CFE of <i>T. vivax</i> IAG-NH | 223 |

| | | |
|------------|--|------------|
| 5.2.17 | Enzymatic preparation of 5'-FDA 47 | 224 |
| 5.2.18 | Enzymatic preparation of 5-FDR 71 from SAM 49 | 225 |
| 5.2.18.1 | Sequential one-pot synthesis | 225 |
| 5.2.18.2 | One-pot synthesis | 225 |
| 5.2.18.3 | Enzymatic preparation of [¹⁸ F]FDR [¹⁸ F] 71 from SAM 49 | 226 |
| 5.3 | References | 228 |
| | Appendix | 231 |

Abbreviations

| | |
|----------|--|
| ~ | Approximately |
| μg | Microgram |
| μl | Microlitre |
| μM | Micromolar |
| 5'-BrDA | 5'-Bromo-5'-deoxyadenosine |
| 5'-CIDA | 5'-Chloro-5'-deoxyadenosine |
| 5'-CIDI | 5'-Chloro-5'-deoxyinosine |
| 5'-FDA | 5'-Deoxy-5'-fluoroadenosine |
| 5'-FDI | 5'-Deoxy-5'-fluoroinosine |
| 5-FDR | 5-Deoxy-5-fluoro-D-ribose |
| 5-FDRP | 5- Deoxy-5-fluoro-D-ribose-1-phosphate |
| 5-FDRul | 5- Deoxy-5-fluoro-D-ribulose |
| 5-FDRulP | 5-Deoxy-5-fluoro-D-ribulose-1-phosphate |
| 5-FDX | 5-Deoxy-5-fluoro-D-xylose |
| 5-FDXul | 5- Deoxy-5-fluoro-D-xylulose |
| 5-FDXulP | 5- Deoxy-5-fluoro-D-xylulose-1-phosphate |
| Å | Ångstrom |
| amu | Atomic mass unit |
| ADP | Adenosine diphosphate |
| AMP | Adenosine monophosphate |
| ATP | Adenosine triphosphate |
| CFE | Cell-free extract |
| CI | Chemical ionisation |

ABBREVIATIONS

| | |
|-----------------------|--|
| CoA | Coenzyme A |
| conc. | Concentration |
| d | Doublet |
| DCM | Dichloromethane |
| ddd | Doublet of doublet of doublets |
| dec. | Decompose |
| DHAP | Dihydroxyacetone phosphate |
| EDTA | Ethylenediaminetetraacetic acid |
| ES-MS | Electrospray mass spectrometry |
| FAD | Flavin adenine dinucleotide (oxidised form) |
| FADH ₂ | Flavin adenine dinucleotide (reduced form) |
| FPLC | Fast protein liquid chromatography |
| Fr-1,6-P ₂ | Fructose-1,6-bisphosphate |
| g | Gram |
| GC-MS | Gas chromatography mass spectrometry |
| GDP | Guanosine diphosphate |
| GTP | Guanosine triphosphate |
| h | Hour |
| HEPES | 4-(2-Hydroxyethyl)piperazine-1-ethanesulfonic acid |
| HIC | Hydrophobic interaction chromatography |
| HP | High performance |
| HPLC | High pressure liquid chromatography |
| Hz | Hertz |
| IPTG | Isopropyl β -D-1-thiogalactopyranoside |
| <i>J</i> | Coupling constant |

ABBREVIATIONS

| | |
|------------------|---|
| kDa | Kilodalton |
| L | Litre |
| LB | Luria-Bertani |
| L-FruA | L-Fructose-1,6-bisphosphate aldolase |
| L-FucA | L-Fuculose-1-phosphate aldolase |
| M | Molar |
| <i>m/z</i> | Mass over charge ratio |
| mA | Milliamp |
| MeCN | Acetonitrile |
| MES | 2-Morpholinoethanesulfonic acid |
| mg | Milligram |
| min | Minutes |
| ml | Millilitre |
| mM | Millimolar |
| MSTFA | <i>N</i> -Methyl- <i>N</i> -(trimethylsilyl)-trifluoroacetamide |
| MTA | 5'-Methylthio-5'-deoxyadenosine |
| MTAP | Methylthioadenosine phosphorylase |
| MTR | 5-Methylthio-5-deoxy-D-ribose |
| MTRP | 5-Methylthio-5-deoxy-D-ribose-1-phosphate |
| MTRuIP | 5-Methylthio-5-deoxy-D-ribulose-1-phosphate |
| MW | Molecular weight |
| NAD ⁺ | Nicotinamide adenine dinucleotide (oxidised form) |
| NADH | Nicotinamide adenine dinucleotide (reduced form) |
| NADPH | Nicotinamide adenine dinucleotide phosphate (reduced form) |
| NMR | Nuclear magnetic resonance |

ABBREVIATIONS

| | |
|----------------|---|
| OD | Optical density |
| PBS | Phosphate buffered saline |
| PET | Positron emission tomography |
| PLP | Pyridoxal 5'-phosphate |
| PNPase | Purine nucleoside phosphorylase |
| ppm | Parts per million |
| RCY | Radiochemical yield |
| rpm | Revolutions per minute |
| s | Singlet |
| SAH | <i>S</i> -Adenosyl-L-homocysteine |
| SAM | <i>S</i> -Adenosyl-L-methionine |
| SDS-PAGE | Sodium dodecyl sulfate-polyacrylamide gel electrophoresis |
| sp. | Species |
| t | triplet |
| TB | Terrific broth |
| TBAF | Tetrabutyl ammonium fluoride |
| <i>t</i> -BuOH | <i>tert</i> -butanol |
| td | triplet of doublets |
| TFA | Trifluoroacetic acid |
| THF | Tetrahydrofuran |
| TMS | Trimethylsilyl |
| Tris | Tris(hydroxymethyl)aminoethane |
| TsCl | <i>p</i> -tosylchloride |
| UV | Ultra-violet |
| V | Volt |

Abstract

This thesis focuses on studies investigating the structure of intermediates involved in fluorometabolite biosynthesis, and the potential applications of the fluorinase enzyme in positron emission tomography (PET).

Chapter 1 introduces the rare natural occurrence of fluorinated compounds. The bacterium *Streptomyces cattleya* is known to biosynthesise two fluorinated secondary metabolites: the toxin fluoroacetate (FAc) and the antibiotic 4-fluorothreonine (4-FT). The enzymes and intermediates identified on this fluorometabolite biosynthetic pathway in *S. cattleya*, prior to this research, are discussed in detail.

Chapter 2 presents studies towards the unambiguous structural identification of (3*R*,4*S*)-5-deoxy-5-fluoro-D-ribulose-1-phosphate (5-FRulP) as the third fluorinated intermediate on the biosynthetic pathway to fluoroacetate and 4-fluorothreonine in *S. cattleya*.

Chapter 3 describes the synthetic routes to key molecules, necessary as reference compounds and substrates, to underpin the subsequent studies in this thesis. In particular, synthetic routes to 5'-deoxy-5'-fluoroadenosine (5'-FDA), 5'-deoxy-5'-fluorinosine (5'-FDI), 5-deoxy-5-fluoro-D-ribose (5-FDR) and 5-deoxy-5-fluoro-D-xylose (5-FDX) are described.

Chapter 4 describes the use of the fluorinase enzyme from *S. cattleya* as a tool for the synthesis of new [¹⁸F]-labelled sugars with potential application in positron emission tomography (PET). A new route to 5-deoxy-5-[¹⁸F]fluoro-D-ribose ([¹⁸F]FDR) is developed in a two-step enzymatic synthesis. A total of three potential radiotracers ([¹⁸F]FDA, [¹⁸F]FDR and [¹⁸F]FDI) are synthesised using fluorinase-coupled enzyme reactions. In addition, *in vitro* studies are reported with these [¹⁸F]-labelled sugars to investigate their uptake and potential as PET radiotracers in cancer cells. A preliminary rat imaging study with [¹⁸F]FDA is reported.

Chapter 5 details the experimental procedures for the compounds synthesised in this research and the biological procedures for chemo-enzymatic syntheses and protein purification.

CHAPTER 1

Introduction

Introduction

Throughout history human cultures have always been searching for substances for the treatment of pain and suffering, for life-enhancement, for rituals to get closer to God and also, if necessary, for a quick and easy death. Thus, there are ancient records describing the use of natural extracts, for a wide variety of purposes, long before they were isolated and named.^{1,2} This is the case of opium, which use and cultivation was documented by Homer in *The Odyssey* (ca. ninth century B.C.): “Presently she cast a drug into the wine whereof they drank, a drug to lull all pain and anger, and bring forgetfulness of every sorrow [...] Where earth the grain-giver yields herbs in greatest plenty, many that are healing in the cup, and many baneful.”³

Likewise, native people in South America were well aware of natural toxins and learned to extract potent and deadly poisons, as reported by the Spaniard Gaspar de Carvajal, chronicler of the discovery of the Amazon⁴: “In this village the Indians were familiar with some kind of poisonous plant, for this became evident from the wound of the aforesaid man, because at the end of twenty-four hours he surrendered [...] The centre must have been Curaray, name from which ‘curare’ is perhaps derived, as the poison with which these Indians poisoned their arrows was called.” About 400 years later, curare became part of the practice of anaesthesia.⁵

Nature has provided the active ingredients for the traditional medicine and the unsurpassable biological activity of these substances has given leads for the design of valuable and important medicines in today’s health care. However, the idea of ‘pure’ compounds as drugs evolved from the isolation of the active principles of commonly used plants and herbs, such as morphine **1** and caffeine **2** in the early 1800s (see Figure 1.1). These isolations were then

followed by what can be considered the first commercial pure natural product, morphine **1**, by E. Merck in 1826 and the first semi-synthetic pure drug, aspirin, based on a natural product (salicin **3**) by Bayer in 1899.⁶ These bioactive molecules, extracted not only from plants and trees but also from microorganisms (*e.g.*, **5** and **8**, Figure 1.1), have been used as medicines, narcotics and hallucinogens, stimulants and poisons. Some common selected natural products are shown below in Figure 1.1.

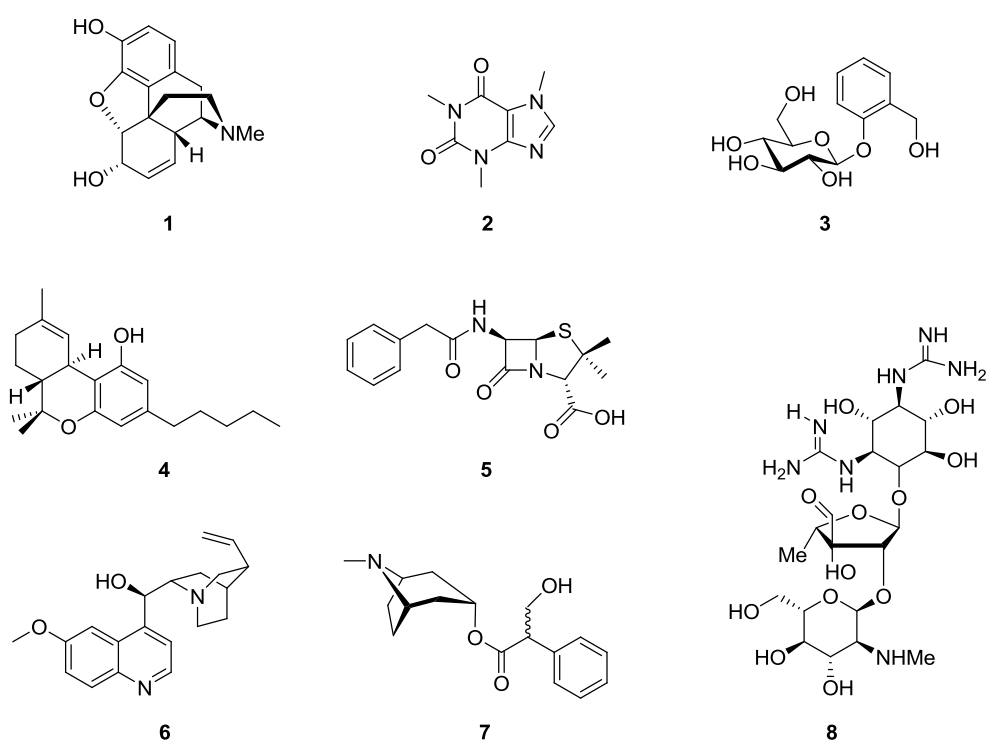


Figure 1.1 Morphine **1**, caffeine **2**, salicin **3**, tetrahydrocannabinol **4**, penicillin G **5**, quinine **6**, atropine **7**, streptomycin **8**.

On the other hand, it is of note the significant role that natural products have played in the development of organic chemistry. The study of these bioactive compounds resulted in the advancement of the major chemical and physical methods for structure elucidation, as well as the discovery of many reactions of great synthetic importance.⁷

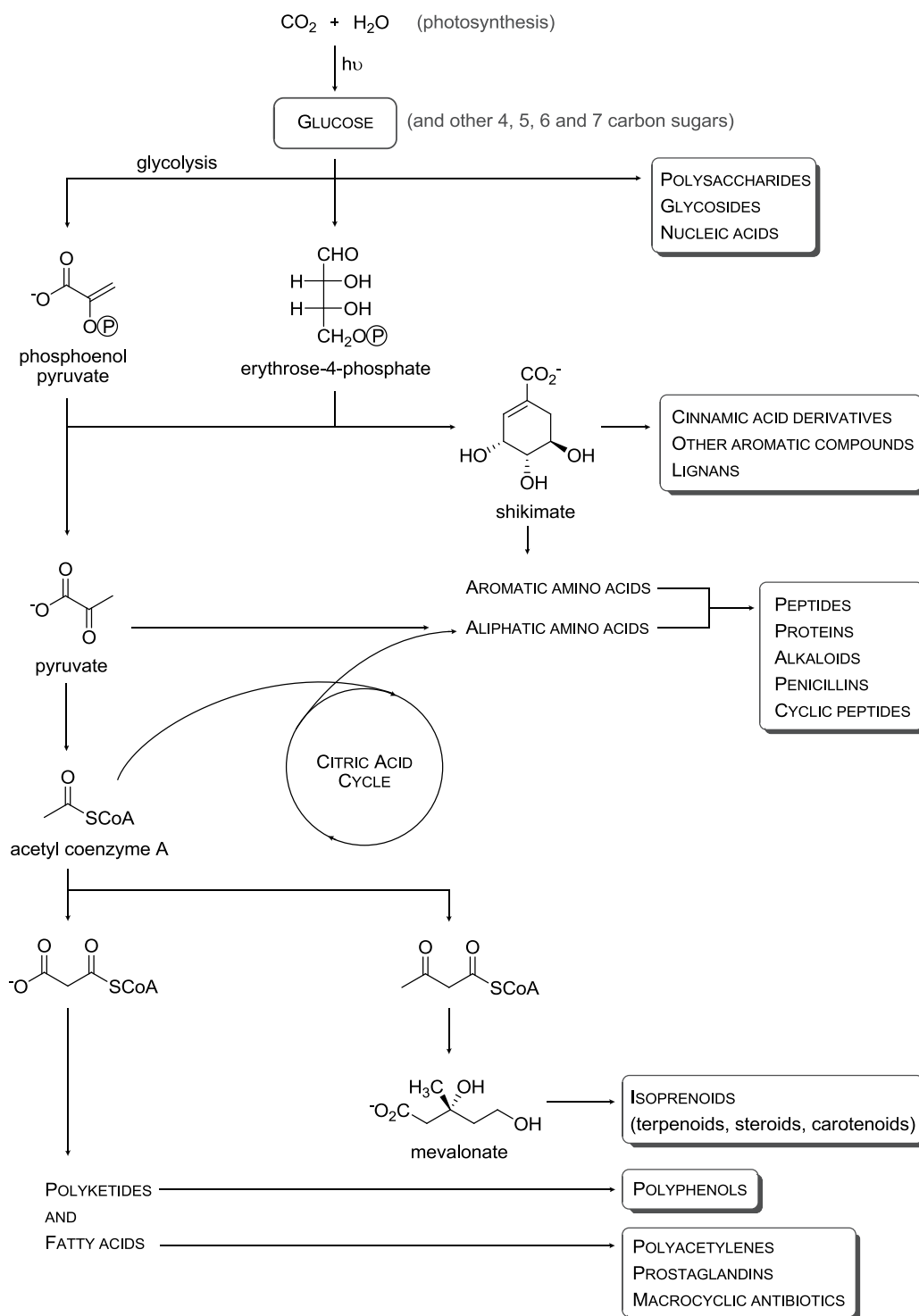
CHAPTER 1

Natural products may be divided in two main categories:

- *Primary metabolites*, which are the common compounds to all cells that play a central role in the metabolism and reproduction of those cells (*e.g.*, nucleic acids, the common amino acids and sugars)
- *Secondary metabolites*, the characteristic compounds of a limited range of species that have a biological effect on other organisms. They are subdivided into: polyketides and fatty acids; terpenoids and steroids; phenylpropanoids; alkaloids; specialised amino acids and peptides; and specialised sugars.

The principal building blocks for the biosynthesis of secondary metabolites are acetate, shikimate and the amino acids.⁷ The relationship between the primary and secondary pathways of metabolism is illustrated in Scheme 1.1.

CHAPTER 1



Scheme 1.1 Primary and secondary metabolism pathways.

1.1 Halogens in natural products

Some organisms are capable of incorporating halogens into their biosynthetic metabolic pathways. Thus, nature has synthesised an impressive collection of halogenated natural products, referred to as halometabolites, showing very different chemical structures and properties. Chloro-metabolites and bromo-metabolites predominate; iodinated and fluorinated natural products are much less common. The great diversity of these organohalogens, both in their chemistry and their origin, suggests considerable biochemical importance to living organisms. Thus, the functions of these halometabolites are varied and they can have distinct physiological or biochemical roles. For example, the ‘lone star tick’ uses 2,6-dichlorophenol **9** (*vide infra*, Figure 1.2) as a sex pheromone,^{8,9} while 4-chloroindolyl-3-acetic acid **10** (Figure 1.2) is a universal growth hormone biosynthesised by numerous *Leguminosae* plants,^{10,11} and the Ecuadorian poison tree frog *Epipedobates tricolor* secretes epibatidine **11** (Figure 1.2), a unique chlorinated compound with a novel 7-azanorbornane structure, that is 500 times more potent than morphine as an analgesic.¹²

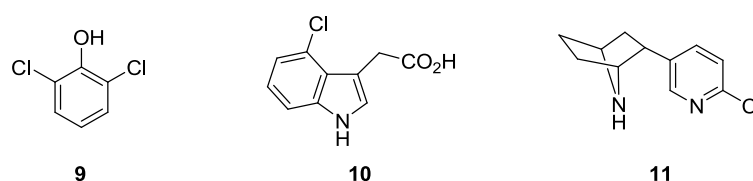


Figure 1.2 2,6-Dichlorophenol **9**; 4-chloroindolyl-3-acetic acid **10**; (+)-epibatidine **11**.

The first reported naturally-occurring halogenated organic compound was an iodinated amino acid isolated from the coral *Gorgonia cavolinii* in 1896, and subsequently identified as 3,5-diiodotyrosine.¹³ Later, in the 1960s, the few known natural organohalogens (*e.g.*, griseofulvin, chloramphenicol, aureomycin, vancomycin) were considered bizarre compounds of nature or even artefacts of the isolation process, and were not recognised as the

CHAPTER 1

unique organic compounds with great biological activity part of an enormous class of natural products yet to be discovered. For example: “Present information suggests that organic compounds containing covalently bound halogen are found only infrequently in living organisms.”¹⁴ As of February 2005, the number of known natural organohalogens was over 4100.¹⁵ This is a consequence of the general interest in natural products as a potential source of new medicinal drugs. The breakdown of these naturally occurring organohalogens was approximately: 2300 organochlorines, 2100 organobromines, 110 organoiodines and 30 organofluorines. A few of these compounds contain both chlorine and bromine. Although most of the organohalogens discovered in the past thirty-five years are marine-derived, many other halogenated compounds are produced by bacteria, fungi, lichen, terrestrial plants, insects, some higher animals (including humans) and geothermal processes, making natural organohalogens ubiquitous in both marine and terrestrial environments. A selection of examples from the wide spectrum of halogenated compounds from many natural sources is shown in Figure 1.3 (*vide infra*).

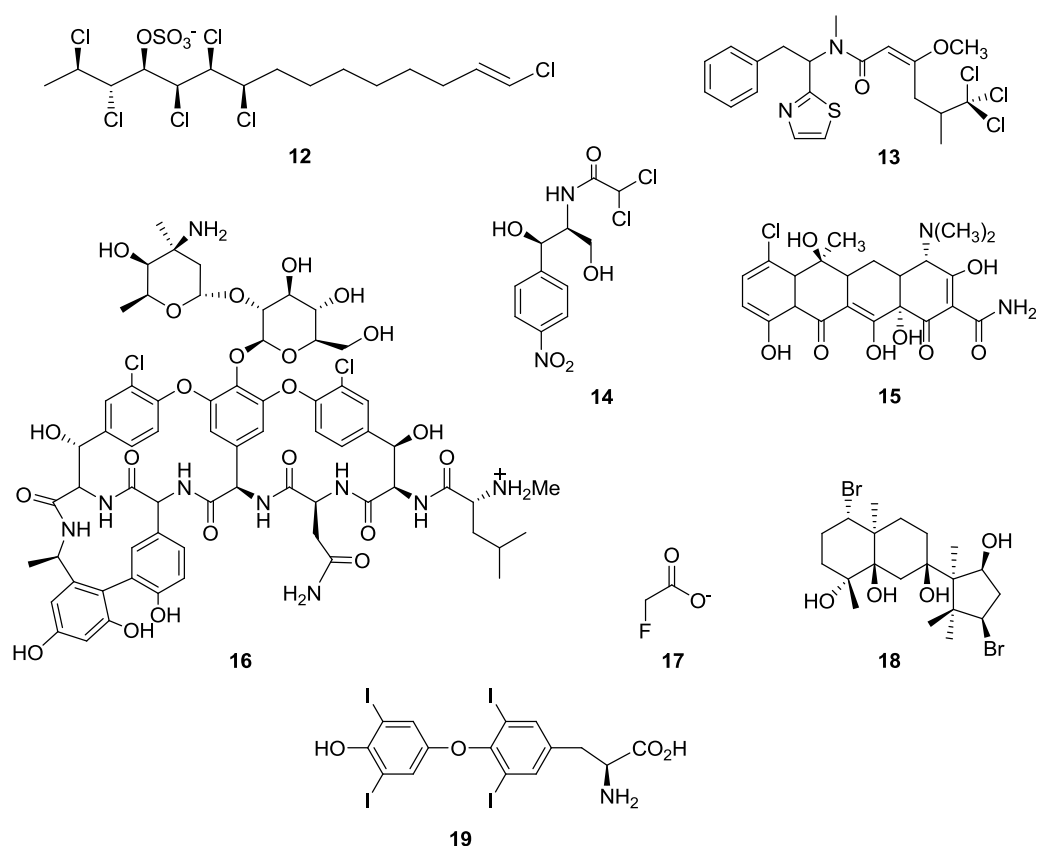


Figure 1.3 Selection of halogenated natural products: biotoxin **12** (*Mytilus galloprovincialis*), barbamide **13** (*Lyngbya majuscula*), chloramphenicol **14** (*Streptomyces venezuelae*), 7-chlorotetracycline **15** (*Streptomyces aureofaciens*), vancomycin **16** (*Amycolatopsis orientalis*), fluoroacetate **17** (*Streptomyces cattleya*), 5-neoirietetraol **18** (*Laurencia* species), and thyroxine **19** (human thyroid gland).

The marine environment is the richest source of halometabolites and halogenating enzymes, thus generating most of the halogenated secondary metabolites known to date. The majority of these marine organohalogenes contain bromine, whereas chlorine-containing compounds are usually synthesised by terrestrial organisms. Bacteria are amazing chemical factories and they produce some of the most commercially important chlorinated antibiotics, such as the antibiotics chloramphenicol **14**^{16,17,18} and the polyketide-derived chlorotetracycline **15**^{19,20} (Figure 1.3). More than 50 *Streptomyces* bacteria have yielded biologically active

organochlorine compounds, many of which possess complex structures and show unique and powerful biological activity. Among them, there is the life-saving antibiotic vancomycin **16** (Figure 1.3, *vide supra*), produced by *Amycolatopsis orientalis*.²¹ It has been used for nearly 50 years to treat penicillin-resistant life-threatening infections, and the two chlorine atoms in this glycopeptide are essential for optimal biological activity.^{22,23}

Barbamide **13** (Figure 1.3), produced by the biosynthetically prolific cyanobacterium *Lyngbya majuscula*,²⁴ is an example of marine organohalogen. It contains an unusual trichloromethyl group, the metabolic origin of which has been investigated in order to elucidate the chlorination mechanism.^{25,26,27} Also from the marine environment a large number of halogenated terpenes are produced by the red alga genus *Laurencia*, as for example neoirietetraol **18**^{28,29} (Figure 1.3). One of the most toxic organohalogens is fluoroacetate **17** (Figure 1.3). It is synthesised, along with the similarly toxic long chain ω -fluorocarboxylic acids, by several plants indigenous to West Africa, Australia and other countries.^{30,31,32} Examples of organohalogen natural products from animals are compounds **12** and **19**, illustrated in Figure 1.3. The novel cytotoxic polychlorinated sulfolipid **12** has been isolated from toxic mussels (*Mytilus galloprovincialis*) located along the Emilia Romagna coasts of Italy.³³ Thyroxine **19** is another example of halometabolite with animal origin; isolated from the human thyroid gland, where it plays an important role in its control.^{34,35}

1.2 Fluorinated natural products

Only a few fluorinated metabolites have been identified in nature. So far, there are no examples of organofluorine natural products from higher animals or insect sources. However, some reported findings suggest that the occurrence of organofluorine compounds in nature may not be only restricted to plants and microorganisms.³⁶

1.2.1 The element fluorine in nature

Fluorine, in the form of fluoride ion, is the most abundant halogen in the earth's crust (Table 1.1) with concentrations in the range of 270–740 ppm.^{32,37}

Table 1.1 Halides and abundance.³⁸

| Halide | Abundance (ppm) | | Order of abundance |
|-----------------|-----------------|-------------|--------------------|
| | Crustal rocks | Ocean water | |
| F ⁻ | 544 | 1.3 | 13 |
| Cl ⁻ | 126 | 19,000 | 20 |
| Br ⁻ | 2.5 | 65 | 46 |
| I ⁻ | 0.46 | 0.05 | 60 |

This low frequency of organofluorine compounds lies to a great extent in the chemical properties of fluoride ion. Only 13 fluorinated natural products have been characterised.³² One of the principle reasons for this is the low solubility of fluoride-containing minerals (*e.g.*, fluorospar: CaF₂), which reduces the bioavailability of fluoride to living organisms. This is highlighted by the fact that sea water contains only 1.3 ppm of fluoride³⁹ in comparison to 19,000 ppm of chloride (Table 1.1).

Another factor that limits the participation of fluoride in biochemical processes is the high heat of hydration of fluoride ion.^{40,41} Thus, in aqueous solution fluoride ion is heavily hydrated making it a substantially weaker nucleophile in water than all of the other halogen ions, as shown in Table 1.2 (*vide infra*). This reduces its ability to act as a nucleophile in displacement reactions.

Table 1.2 Heat of hydration and standard redox potential for the halogen group.^{40,41}

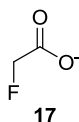
| Halogen X ⁻ | Heat of hydration KJ mol ⁻¹ | Standard redox potential E ⁰ |
|---------------------------|---|--|
| F ⁻ | 490 | -3.06 |
| Cl ⁻ | 351 | -1.36 |
| Br ⁻ | 326 | -1.07 |
| I ⁻ | 285 | -0.54 |

Furthermore, the haloperoxidase reaction,⁴² which plays a significant role in the formation of natural organohalogen compounds by generating X⁺ at the expense of hydrogen peroxide reduction, does not extend to fluorination³⁷ due to the high redox potential necessary to generate F⁺ from F⁻ (Table 1.2).

1.2.2 Fluorinated natural products from plants

1.2.2.1 Fluoroacetate

Fluoroacetate **17** was the first organofluorine natural product to be reported and is by far the most widespread of this class. It was initially identified and isolated by Marais in 1943 from the South African shrub *Dichapetalum cymosum*.^{43,44} The plant was known to be extremely toxic and had long been recognised as a hazard to livestock.



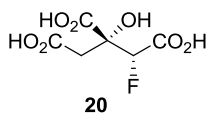
Fluoroacetate **17** has subsequently been found in a variety of plants throughout the world.^{45,46} Many other species of the genus *Dichapetalum*, such as *D. heudelotti*,⁴⁷ *D. stuhlmannii*,^{45,46}

and *D. toxicarium*^{47,48} are known to produce fluoroacetate. The highest concentrations reported to date are those found in *D. braunii*, with 8 mg/g dry weight in young leaves and seeds.⁴⁹

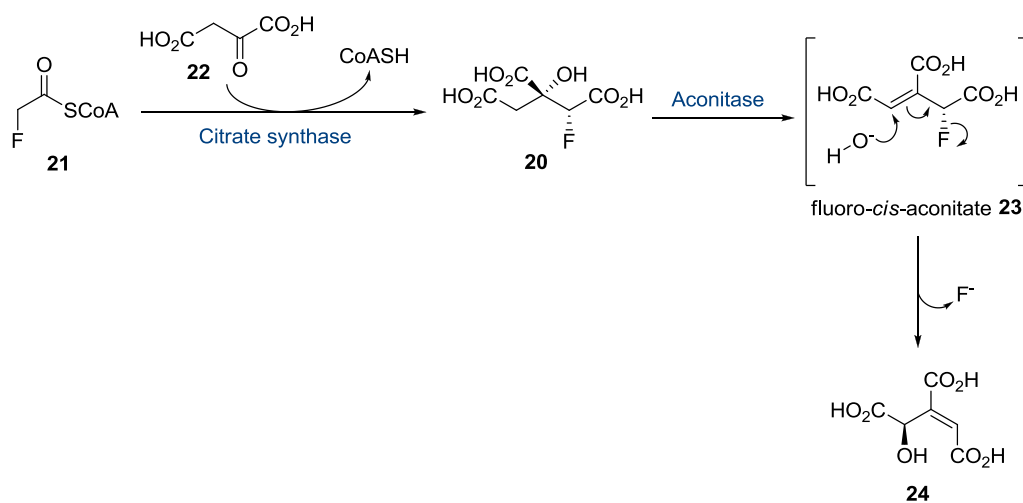
A great number of the species that produce fluoroacetate **17** can be found in Australia,⁵⁰ where over 40 plant species have been identified, most of them belonging to the genus *Gastrolobium* and *Oxylobium*.^{51,52} Although fluoroacetate-producing plants are in general confined to Africa and Australia, fluoroacetate **17** has also been reported in Brazilian and Indian species.^{53,54} In addition, it has been detected in very low concentrations in other plant materials which are not normally regarded as toxic.^{55,56 57,58,59,60}

1.2.2.2 Fluorocitrate

The toxicity of fluoroacetate **17** was investigated by Sir Rudolph Peters in the early 1950s. He proposed that the high toxicity of this fluorometabolite arises from its *in vivo* conversion to (2*R*, 3*R*)-fluorocitrate **20** by the action of citrate synthase, the enzyme that normally feeds acetyl-CoA into the citric acid cycle.^{61,62} This is consistent with trace amounts of fluorocitrate **20** which are found in many plants that accumulate fluoroacetate **17**.^{55,58,60,63}



The stereospecific condensation of fluoroacetyl-CoA with oxaloacetate to form fluorocitrate **20** gives the only toxic stereoisomer of fluorocitrate⁶⁴ as shown in Scheme 1.2 (*vide infra*). This metabolic conversion of fluoroacetate **17** to (2*R*, 3*R*)-fluorocitrate **20** has been termed the ‘lethal synthesis’.^{65,66}

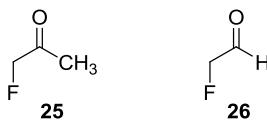


Scheme 1.2 Stereospecific condensation of fluoroacetyl-CoA **21** with oxaloacetate **22** to form fluorocitrate **20** and its subsequent conversion to 4-hydroxy-*trans*-aconitate **24**.

Fluorocitrate **20** is a potent inhibitor of aconitase,⁶⁷ the enzyme responsible for the conversion of citrate to isocitrate. It has been revealed that (2*R*, 3*R*)-fluorocitrate **20** acts as a mechanism based inhibitor of aconitase by first being converted to fluoro-*cis*-aconitate **23**, followed by addition of hydroxide and loss of fluoride to form 4-hydroxy-*trans*-aconitate **24** as illustrated in Scheme 1.2. This product has a high binding affinity for aconitase and is a potent competitive inhibitor.⁶⁸ Additionally, it has been proposed that (2*R*, 3*R*)-fluorocitrate **20** interferes with membrane transport processes by covalently binding to proteins.⁶⁹

1.2.2.3 Fluoroacetone

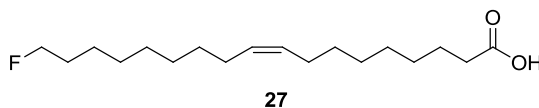
Fluoride metabolism in some fluoroacetate-producing plants was explored by Peters and Shorthouse in the late 1960s. They reported some evidence for the presence of fluoroacetone **25** as a metabolite of the Australian plant *Acacia georginae*.^{70,71}



Nonetheless, the method used for detecting fluoroacetone **25**, which involved derivatisation of the fluorinated molecules with a 2,4-dinitrophenylhydrazine solution, could not distinguish between fluoroacetone **25** and fluoroacetaldehyde **26**. As a result, the authors admit some uncertainty over the existence of this fluorometabolite. Considering the identification of fluoroacetaldehyde **26** as an intermediate in fluorometabolite biosynthesis in *Streptomyces cattleya*,⁷² it is possible that the fluorinated hydrazone derivative isolated in those experiments was actually that of fluoroacetaldehyde **26**. Hence, the identification of fluoroacetone **25** as a natural product is still unclear.

1.2.2.4 Fluorinated fatty acids

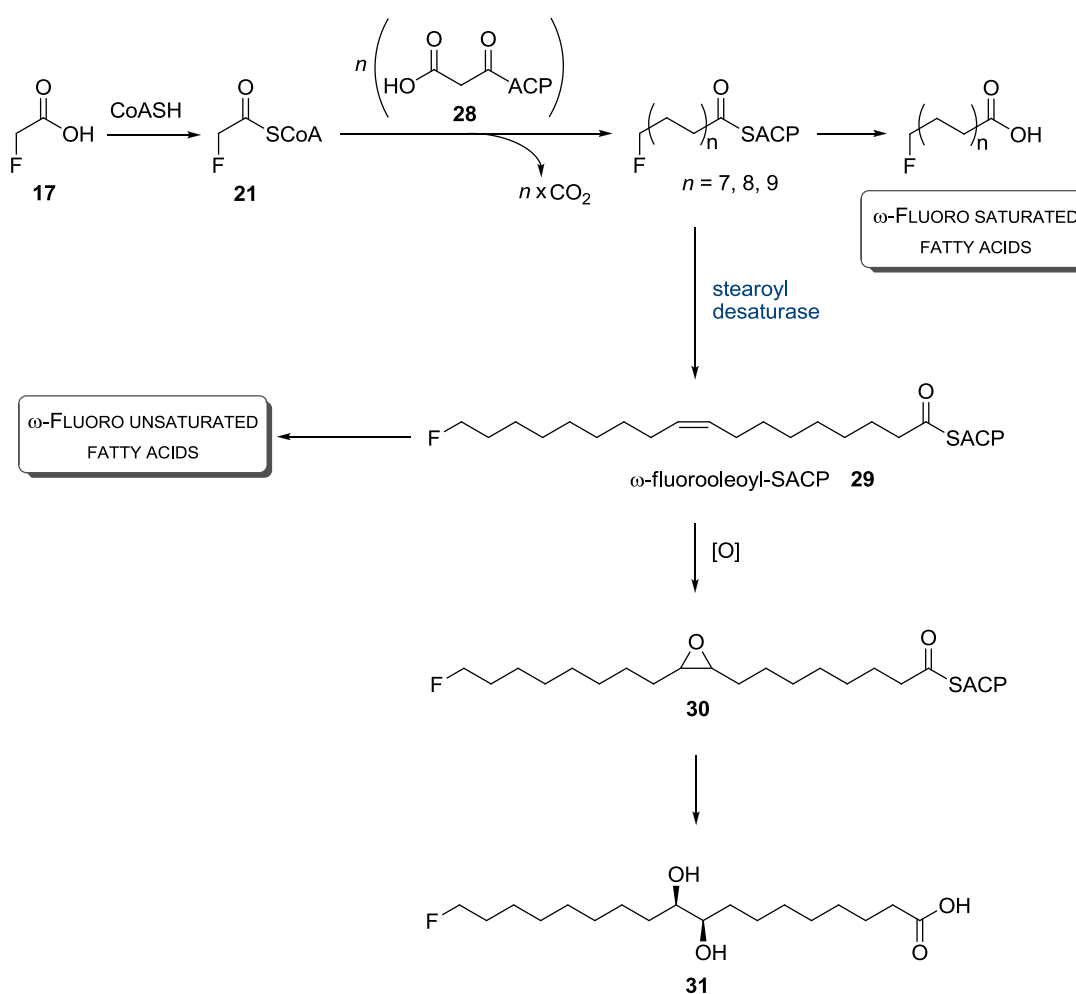
In 1959, Peters and co-workers succeeded in isolating the principal fluorinated compound in the seed oil of the shrub *Dichapetalum toxicarium*.^{73,74} This fluorinated natural product was identified conclusively as ω -fluorooleic acid (C_{18:1F}) **27** by synthesis, and accounted for around 80% of the organic fluorine present in the seeds.⁷⁵ Small amounts of ω -fluoropalmitic acid (C_{16:0F}) were also purified from the oil.⁷⁶



Further analysis of the seeds resulted in the identification of an additional five ω -substituted fluorinated acids.^{77,78,79} All of these metabolites clearly derive from ω -fluorooleic acid **27**. These are ω -fluoropalmitoleic acid (C_{16:1F}), ω -fluorostearic acid (C_{18:0F}), ω -fluorolinoleic acid

(C_{18:2F}), ω-fluoroarachidic acid (C_{20:0F}), and ω-fluoroeicosenoic acid (C_{20:1F}). The position of the double bonds was located after GC-MS analysis.⁷⁸

The chain lengths and degree of unsaturation of these ω-fluorofatty acids seems to accompany those of their non-fluorinated analogues, but the former are 5–10-fold less abundant.^{77,79} The postulated biosynthetic route for the formation of ω-fluorofatty acids from fluoroacetate in *D. toxicarium*⁸⁰ is illustrated below in Scheme 1.3.



Scheme 1.3 Putative biosynthetic pathway to ω-fluorofatty acids in *D. toxicarium* showing fluoroacetate **17** as a starter unit.

Fluorine is always confined to the terminal position in these fluorofatty acids. This suggests some kind of enzymatic restriction on the use of fluorinated analogues at later stages of the biosynthetic process. Thus, it is plausible that either acetyl-CoA carboxylase cannot synthesise fluoromalonyl-CoA or chain elongation involving the incorporation of fluoromalonyl-ACP instead of malonyl-ACP does not occur.^{14,81}

1.2.3 Fluorinated natural products from marine sources

The first fluorinated natural products **32–36** from a marine source were isolated recently from the sponge *Phakellia fusca* collected in the South China Sea.⁸² Sponges of the genus *Phakellia* are well known to yield alkaloids, sterols, peptides and polyether acids.

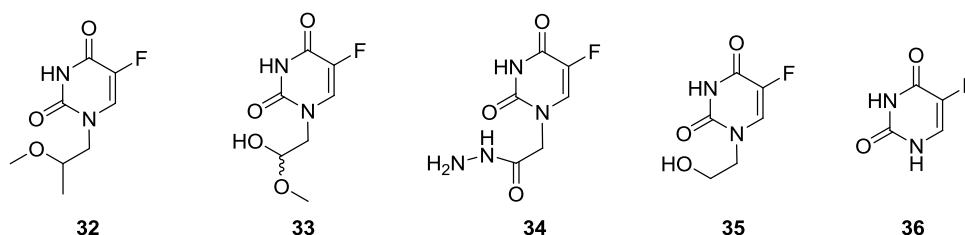


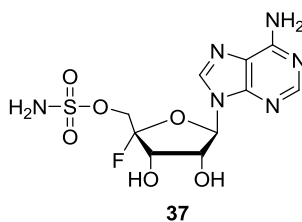
Figure 1.4 Fluorouracil alkaloids **32–36** isolated from *Phakellia fusca*.

Two of these 5-fluorouracil derivatives, metabolites **35**⁸³ and **36**⁸⁴ were previously known as synthetic anti-tumour agents,⁸⁵ and metabolites **32**, **33** and **34** were reported as novel fluorinated natural products.⁸² However, there is no evidence of how these compounds are accumulated in the sponge, and the possibility that they are products of industrial contamination cannot be discarded, particularly because 5-fluorouracil **36** is a major pharmaceutical product.⁸⁶

1.2.4 Fluorinated natural products from bacteria

1.2.4.1 Nucleocidin from *Streptomyces calvus*

The bacterium *Streptomyces calvus*, isolated from an Indian soil sample, was shown in 1957 to produce the antibiotic nucleocidin **37**.^{87,88}



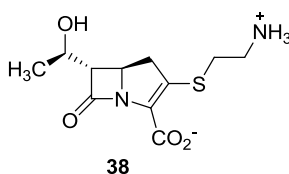
This adenosine derivative⁸⁹ proved to exhibit a rather broad antibacterial spectrum, being particularly active against trypanosomes.^{88,90} However, it was not until 1969 that it was realised that nucleocidin **37** actually contained fluorine,⁹¹ and subsequent synthetic work by Shuman *et al.*⁹² suggested the β -D-configuration for the pentose moiety. The assignment of the D-ribose configuration and the proposed structure of nucleocidin **37** were confirmed by total synthesis in 1976.⁹³

This fluorometabolite is significantly different from the other known fluorinated metabolites in that the position of the fluorine atom on the ribose ring shows no obvious biosynthetic origin from fluoroacetate **17** and suggests the presence of a novel enzymatic fluorination step. So far there are no experimental data on the biosynthesis of this unique fluorocarbohydrate. Even the source of fluoride for the synthesis of nucleocidin **37** is not clear, since the fermentation medium was not specifically supplemented with fluoride.⁸⁸ Therefore, trace contamination of fluoride ion in the medium salts of the water appears to be its source.

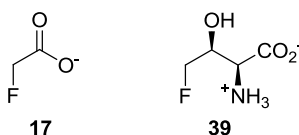
Several attempts to re-isolate nucleocidin **37** from cultures of *S. calvus* have been unsuccessful and biosynthetic studies have therefore been frustrated.^{94,95}

1.2.4.2 Fluoroacetate and 4-fluorothreonine from *Streptomyces cattleya*

The actinomycete *Streptomyces cattleya* was known to produce, along with *Streptomyces penemifaciens*, the antibiotic thienamycin **38**.^{96,97,98} This naturally occurring β -lactam antibiotic was the first to be isolated that contained the carbapenem ring system.^{99,100}



In 1986, experiments carried out by Merck to optimise thienamycin **38** production led to the observation of a novel antibiotic activity in *S. cattleya*, generated when a particular soya protein was used in the culture medium.¹⁰¹ This soya protein contained significant levels of fluoride ion, which explained the accumulation of fluorometabolites. These secondary fluorometabolites were identified as the well-known toxic natural product fluoroacetate **17** and the amino acid 4-fluorothreonine **39**, responsible for the novel antibiotic activity.



Streptomyces cattleya and *Streptomyces calvus* are the only identified microorganisms capable of biosynthesising fluorometabolites. Since all attempts to re-isolate nucleocidin **37** from *S. calvus* have been unsuccessful, work carried out to investigate the enzymology of fluorometabolite production has been focused on *S. cattleya*.^{95,102}

1.3 Techniques used for studying the biosynthesis of natural products

Once the structure of a secondary metabolite is elucidated, it is usually possible to propose a biosynthetic hypothesis for its formation from one of the basic building blocks: acetate, mevalonate, shikimate, or the amino acids. A biosynthetic pathway can only be considered delineated once each individual intermediate and enzyme has been identified.

A biosynthetic pathway involves the enzyme-catalysed conversion of a series of intermediates ($A \rightarrow B \rightarrow C \rightarrow D$) to a natural product. Biosynthetic investigations involve both labelling and enzymatic experiments. The complementary role of these approaches provides information on building blocks and the structures of the intermediates, together with the order, stereochemistry, and mechanisms of biosynthetic events.^{7,103}

1.3.1 Isotopic labelling

In order to investigate biosynthetic pathways, the fate of a labelled precursor can be determined after incubation with the living system. In early studies, isotopic labelling studies for the elucidation of biosynthetic pathways commenced with the availability of the radioisotopes carbon-14 (^{14}C) and tritium (^3H). The disadvantages associated with the handling and storage of radioactive isotopes have subsequently been overcome with the deployment of stable isotopes. The use of the non-radioactive isotopes carbon-13 (^{13}C) and deuterium (^2H), and to a lesser extent the isotopes ^{15}N and ^{18}O , have revolutionised the study of biosynthetic pathways, since these isotopes have non-zero nuclear spin and are thus detectable using nuclear magnetic resonance (NMR) techniques. Carbon-13 and deuterium are widely used to probe pathways, and can be assayed by mass spectrometry or NMR spectroscopy, either directly using ^2H NMR spectroscopy or indirectly *via* ^{13}C NMR

spectroscopy. Moreover, the extent of incorporation of label and the distribution can be determined by mass spectrometry and GC-MS analysis.^{7,103}

The incorporation of stable isotopes into natural products represents an effective and attractive method for studying biochemical pathways and has proven to be a very powerful technique for exploring such pathways. In the mid 1930s, Schoenheimer and co-workers proposed the use of deuterium for the study of intermediary metabolic processes, such as fatty acid biosynthesis.¹⁰⁴

The biosynthetic origin of the secondary metabolites fluoroacetate (FAc) **17** and 4-fluorothreonine (4-FT) **39** was investigated in cell suspensions of *S. cattleya* using labelled precursors,^{102,105} and this will be discussed later in the chapter.

1.3.2 Enzyme experiments

Questioning of the enzymes that mediate biosynthetic events provides further information on particular steps. If an enzyme that catalyses a specific step is absent, either in a genetically deficient mutant or because the enzyme system has been inhibited or poisoned, the biosynthetic substrate which is normally transformed may accumulate. Biosynthesis takes place in highly structured living cells. If the cell membrane is disrupted, it is often possible to develop cell-free enzyme preparations which catalyse individual steps. It can then be possible to purify the enzyme itself for assay and even to obtain it in a crystalline form. The enzyme may then be examined by X-ray crystallography, with or without a bound substrate.

Now that it is possible to identify the genetic sequences that code for specific enzymes and to clone these systems, this has become a very powerful tool in biosynthesis. The transfer and over-expression of genetic information into an easily grown bacterium permits the preparation of quantities of the relevant enzyme systems, and enables individual steps in a biosynthesis to be studied in detail.^{7,103}

1.3.3 ^{19}F NMR spectroscopy

Nuclear magnetic resonance (NMR) spectroscopy has significantly advanced the investigation of ^{13}C and ^2H incorporation of metabolic precursors into natural products after isotopic labelling studies.¹⁰⁶ However, the 12-year gap between the discovery of nucleocidin and the detection of fluorine in the molecule^{90,91} illustrates the complexity in identifying organofluorine compounds in the past. Without the present-day tools of analytical chemistry (*e.g.*, ^{19}F NMR, mass spectrometry, ion chromatography, F^- -selective electrodes), it would be difficult to distinguish between a C-H bond and a C-F bond. Therefore, an extension to ^{19}F NMR spectroscopy offers an extremely powerful method by which fluorometabolite biosynthetic pathways can be monitored in real time and in a non-invasive manner. Fluorine-19 has a natural abundance of 100% and has a sensitivity to NMR detection that is approximately 83% that of the sensitivity of ^1H , as shown below in Table 1.3.¹⁰⁷

Table 1.3 Nuclear properties of ^1H , ^{13}C and ^{19}F .

| Nuclide | Nuclear spin | Relative sensitivity | Natural abundance |
|-----------------|--------------|----------------------|-------------------|
| | I | % | % |
| ^1H | 1/2 | 100 | 99.98 |
| ^{13}C | 1/2 | 1.59 | 1.11 |
| ^{19}F | 1/2 | 83.3 | 100.00 |

Whilst the definitive identification of natural fluorine-containing products requires purification and full structural elucidation, ^{19}F NMR spectroscopy can provide rapid insights into the biosynthesis and biodegradation of such compounds and their regulation *in vivo*, without purification or derivatisation. In addition, once the products have been identified, NMR experiments allow assessment of the changes related to genetic and physiological

manipulation.^{108,109} This originates from the favorable features of the fluorine isotope,^{107,110} such as:

- Fluorine-19 is a spin $I = \frac{1}{2}$ nuclide, and is present in 100% abundance. It has receptivity to NMR detection almost comparable to ^1H .
- The sensitivity is further increased because of the absence of naturally occurring background signals, since biological systems do not contain endogenous NMR-visible fluorinated compounds. This implies that all resonances observed can be assigned to the metabolite or compound under study.
- The fluorine nucleus in a molecule is on average surrounded by 9 electrons rather than a single electron (as is the case with hydrogen). Thus, it is highly sensitive to its molecular surroundings and to changes in the local environment. The ^{19}F nucleus is characterised by a broad chemical shift range of about 500 ppm (this is large compared to the chemical shift range of, for example, ^1H and ^{13}C NMR spectra; 15 ppm and 250 ppm, respectively), which results in virtually no resonance overlap.

As a result, ^{19}F NMR spectroscopy has emerged as an efficient tool for elucidating pathways for the conversion of fluorine-containing molecules by microorganisms, with a special emphasis on possibilities for investigating biohalogenation and the type of fluorometabolites involved.

The utility of ^{19}F NMR spectroscopy for studying the fate of organofluorine compounds in biological systems has been recognised for more than 40 years.¹¹¹ In the late 1980s, Baron *et al.* used ^{19}F NMR spectroscopy for the detection and measurement of fluoroacetate **17** in plant extracts,¹¹² while Cass and co-workers studied the fate of fluoro-aromatic compounds in a mutated strain of *Pseudomonas putida* using the same technique.¹¹³ From the recent literature, many examples demonstrate the ability of ^{19}F NMR experiments to provide data about ligand binding, unfolding, mobility, and other aspects

related with the study of biological systems, such as quantification of fluorinated contaminants and pharmacokinetics of fluorinated drugs.^{114,115,116}

Since ^{19}F NMR spectroscopy has proved to be an effective and sensitive method for investigating fluorine-containing metabolic pathways, this has been the main technique, before protein isolation, for the study of fluorometabolite biosynthesis in *S. cattleya*. The chemical environment in which the fluorine is located can be established with some degree of accuracy by ^{19}F - ^1H coupling constants. This is exemplified in the ^{19}F NMR spectra for the known fluorinated secondary metabolites fluoroacetate (FAc) **17** and 4-fluorothreonine (4-FT) **39**, as illustrated below in Figure 1.5.

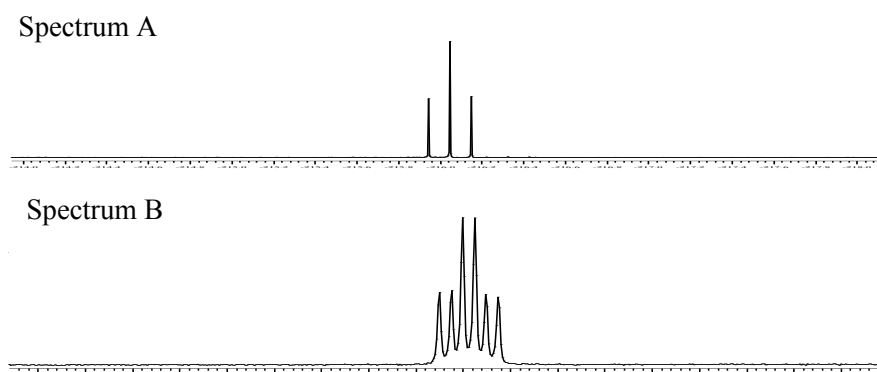


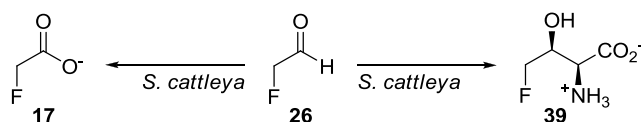
Figure 1.5 ^{19}F NMR spectra (in D_2O at 25 $^\circ\text{C}$) showing the fluorine signals of FAc **17** (Spectrum A) and 4-FT **39** (Spectrum B).

For fluoroacetate **17** (Figure 1.5, spectrum A) the ^{19}F NMR signal is a triplet (t) (^{19}F NMR, t, -216.9 ppm, 2J 48.3 Hz). For 4-fluorothreonine **39** (Figure 1.5, spectrum B) the signal is a doublet of triplets (dt) (^{19}F NMR, dt, -231.6 ppm, 2J 46.9 Hz and 3J 25.0 Hz) due to the additional vicinal coupling with the vicinal hydrogen.¹⁰¹

1.4 Biosynthesis of fluorinated secondary metabolites by *Streptomyces cattleya*

1.4.1 Fluoroacetaldehyde as a biosynthetic intermediate

Fluoroacetate **17** and 4-fluorothreonine **39** are the end products of the fluorometabolite pathway in *S. cattleya*. Initial investigations to determine the metabolic relationship between FAc **17** and 4-FT **39**, and to identify the carbon substrate for the fluorinating enzyme, consisted of the use of isotope labelled precursors in resting cells of *S. cattleya* and subsequent analysis by ^{19}F NMR spectroscopy and GC-MS analysis.^{102,105,117} From these studies it was concluded that fluoroacetate **17** was not a precursor of 4-fluorothreonine **39** and *vice versa*, suggesting that each metabolite must therefore arise by further metabolism of a common fluorinated intermediate. Further investigations into the origin of these fluorometabolites indicated that their metabolic precursor was fluoroacetaldehyde (FAd) **26**.⁷²

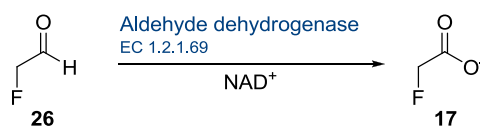


Scheme 1.4 Fluoroacetaldehyde **26** is a common intermediate in the biosynthesis of FAc **17** and 4-FT **39**.

This was confirmed by incubating a synthetically-prepared sample of FAd **26** in resting cell suspensions of *S. cattleya*, which resulted in the efficient conversion of **26** to fluoroacetate **17**.⁷²

1.4.2 Identification of fluoroacetaldehyde dehydrogenase from *S. cattleya*

The identification of fluoroacetaldehyde **26** as a precursor of fluoroacetate **17** and 4-fluorothreonine **39** opened up prospects for the identification and isolation of the last enzyme on the pathway. Cell-free extracts of *S. cattleya* were analysed for their capacity to oxidise FAd **26** to FAc **17** in the presence of NAD^+ . Hence, the enzyme responsible for the oxidation of **26** (Scheme 1.5) was isolated and characterised.¹¹⁸



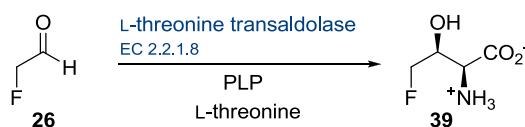
Scheme 1.5 Biotransformation of fluoroacetaldehyde **26** to fluoroacetate **17** catalysed by fluoroacetaldehyde dehydrogenase in *S. cattleya*.

The native NAD^+ -dependent aldehyde dehydrogenase showed a molecular weight of 200 kDa, suggesting a tetramer. The optimum pH was found to be pH 9. The activity of the enzyme was significantly reduced in the presence of iodoacetamide, indicating an important thiol residue. In terms of substrate specificity, the enzyme showed high affinity for fluoroacetaldehyde **26** ($K_m = 0.08$ mM) and, surprisingly, acetaldehyde is a poor substrate.¹¹⁸

1.4.3 Identification of PLP-dependent threonine transaldolase from *S. cattleya*

Labelling studies and feeding experiments revealed $[1\text{-}^2\text{H}_1]$ fluoroacetaldehyde **26** as the metabolic precursor of 4-fluorothreonine **39**.⁷² In order to explore the production of this secondary metabolite in *S. cattleya*, cell-free extracts of the bacterium were then incubated

with FAd **26** and various amino acids and co-factors. The co-factor pyridoxal 5'-phosphate (PLP) is well known to be utilised by bacterial threonine aldolases in condensations of acetaldehyde with glycine to generate L-threonine.¹¹⁹ With this in mind, PLP was explored as a possible co-factor for the analogous transformation in *S. cattleya* (Scheme 1.6). Thus, incubation of L-threonine, fluoroacetaldehyde **26** and PLP in a cell-free extract of the bacterium¹²⁰ led to the formation of 4-fluorothreonine **39**, detected by ¹⁹F NMR spectroscopy, as illustrated below in Figure 1.6.¹²¹



Scheme 1.6 Biotransformation of fluoroacetaldehyde **26** to fluoroacetate **17** catalysed by fluoroacetaldehyde dehydrogenase in *S. cattleya*.

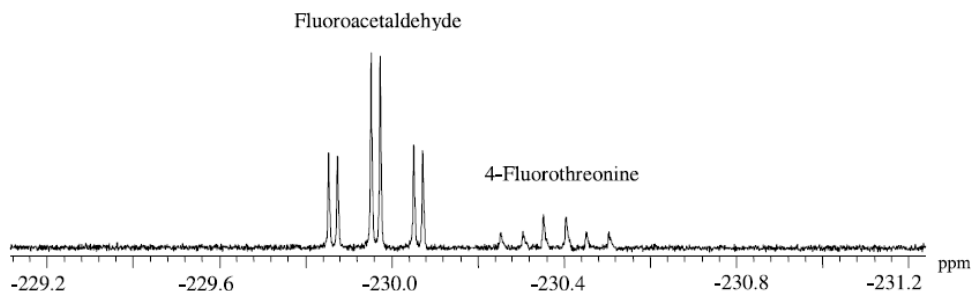
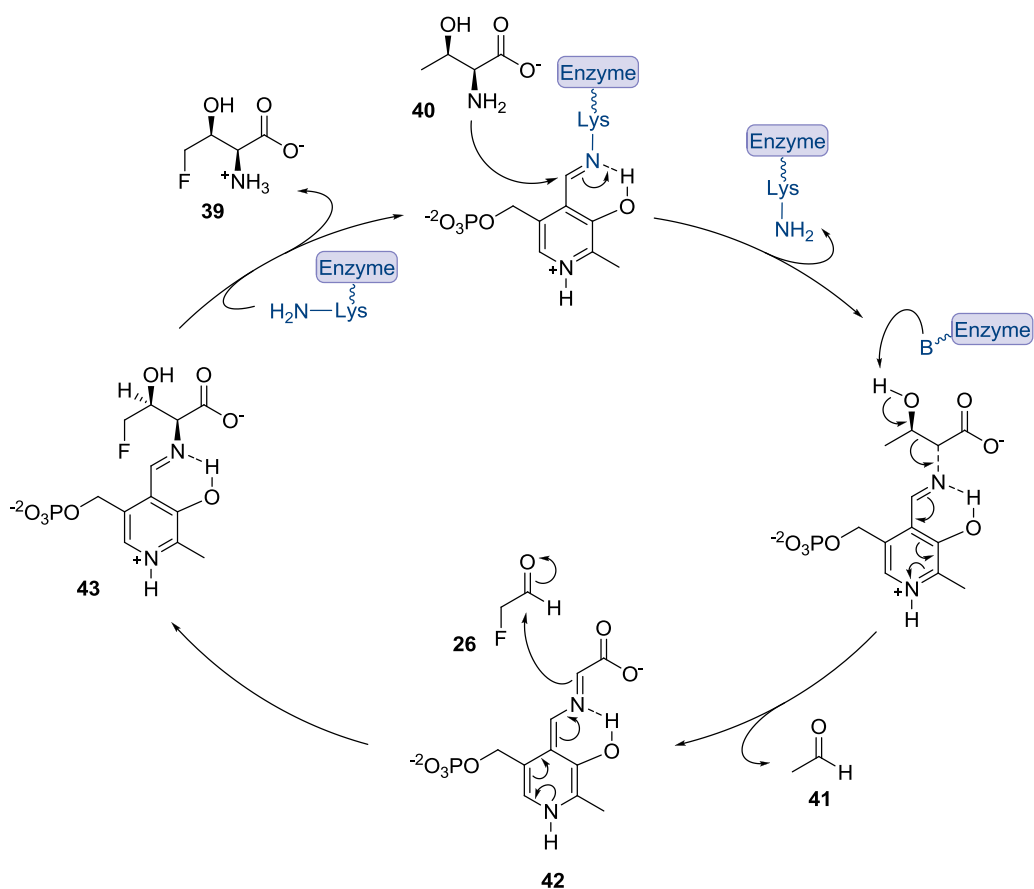


Figure 1.6 ¹⁹F NMR spectrum showing production of 4-fluorothreonine **39** in a CFE of *S. cattleya* incubated with PLP, fluoroacetaldehyde **26** and L-threonine.¹²¹

Assays with partially purified enzyme and a range of amino acids (glycine, L-serine, L-cysteine, L-aspartate, L-alanine, and L-*allo*-threonine) revealed the requirement for PLP and the amino acid L-threonine **40** for the production of 4-fluorothreonine **39** in the bacterium.¹²⁰ These results indicated the presence of a novel threonine transaldolase enzyme. The proposed mechanism is shown in Scheme 1.7 (*vide infra*).



Scheme 1.7 Proposed mechanism for the enzymatic production of 4-FT **39** catalysed by the PLP-dependent threonine transaldolase (EC 2.2.1.8) from *S. cattleya*.

The PLP-dependent threonine transaldolase was purified to homogeneity, showing a native molecular weight of 120 kDa and a monomer of approximately 60 kDa. This threonine transaldolase from *S. cattleya* does not use glycine as a substrate, which makes it distinct from more classical threonine aldolases.¹²⁰

1.4.4 Identification of a fluorination enzyme from *Streptomyces cattleya*

The enzymatic synthesis of fluorophosphates in mammalian cells was first described by Ochoa,¹²² when pyruvate kinase was incubated with adenosine-triphosphate (ATP) and fluoride ion in the presence of magnesium ions.

Experiments exploring fluorophosphate production in resting cell cultures of *S. cattleya* led to the detection of the cell-free production of an organofluorine compound.¹²³ Small amounts of fluorophosphates were detected by ¹⁹F NMR spectroscopy (Figure 1.7, *vide infra*) in whole cell incubations supplemented with glycerol and KF, after 5 days at 28 °C.

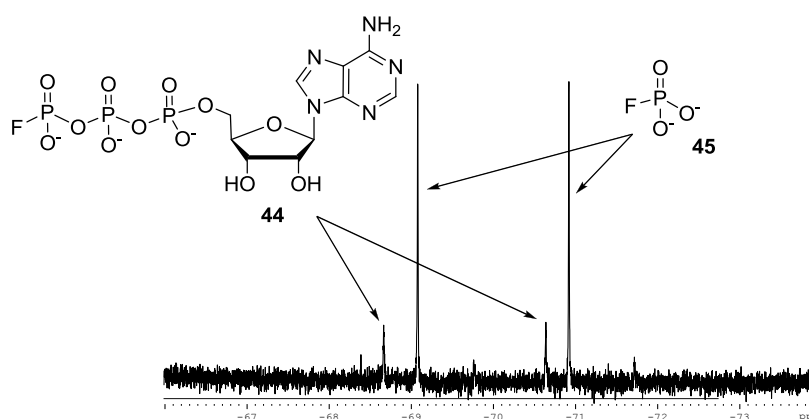


Figure 1.7 ¹⁹F NMR spectrum of supernatant of resting cells of *S. cattleya* after incubation with glycerol (5 mM) and KF (2 mM) for 5 days at 28 °C. The major signal (d, -70 ppm, J_{FP} 865.3 Hz) corresponds to monofluorophosphate **45** whereas the smaller one (d, -69.7 ppm, J_{FP} 929.2 Hz) is assigned to β -fluoroadenosine diphosphate (β -FADP) **44**.¹²³

Initially it was considered that activated fluoride in the form of fluorophosphates may play a role in the fluorination process in *S. cattleya* towards the secondary metabolites fluoroacetate **17** and 4-fluorothreonine **39**, since the production of fluorophosphates could

overcome some of the problems associated with water solvation of fluoride and provide an activated form of fluoride ion for further metabolism.¹²⁴

To investigate this hypothesis, cell-free extract experiments were carried out in which adenosine triphosphate (ATP) and several other phosphate sources such as uridine triphosphate (UTP), guanosine triphosphate (GTP) and cytidine triphosphate (CTP) were added with fluoride ion to a CFE of *S. cattleya*. From the analysis by ¹⁹F NMR spectroscopy no signal for fluorophosphate could be detected. However, the CFE incubation with ATP gave rise to the production of three organofluorine products, as shown by ¹⁹F NMR analysis (Figure 1.8).¹²³

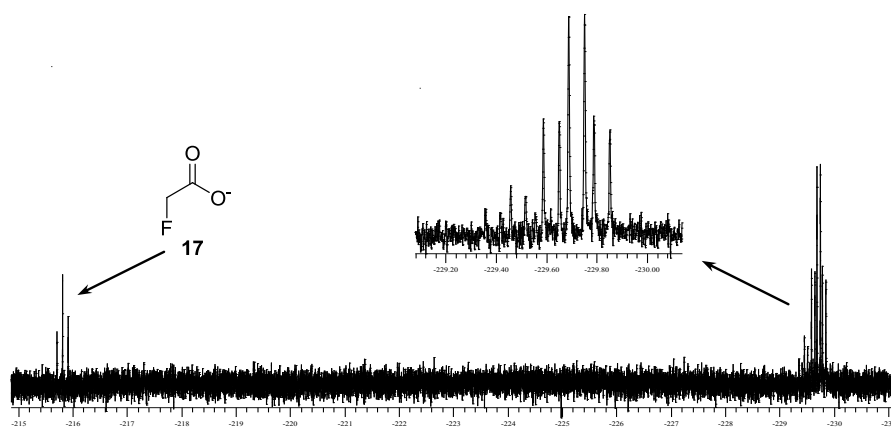


Figure 1.8 ¹⁹F NMR spectrum of CFE incubation with ATP and fluoride ion at 37 °C for 18 h.

The ¹⁹F NMR spectrum showed three signals,¹²³ one of which was assigned to FAc **17** (t, -215.8 ppm, ²J_{HF} 48.3 Hz) and two were unknown (-229.5 ppm and -229.7 ppm).

The production of fluoroacetate **17** in the CFE of *S. cattleya* can only be explained by the enzymatic fluorination of an organic molecule which then proceeds through further enzymatic steps to **17**. The presence of two additional signals raised the possibility of the identification of intermediates on the biosynthetic pathway. Both signals are doublets of triplets (dt) with identical *J*_{HF} coupling constants (²*J*_{HF} 47 Hz, ³*J*_{HF} 29 Hz), indicating closely related structures.

Previously, labelling experiments with $[2\text{-}^2\text{H}_1, 2\text{-}^{18}\text{O}]$ glycerol had shown that the C-O bond is retained during the biosynthesis, as the isotope was found in both FAc **17** and 4-FT **39**.¹²⁵ With this information, a minimal structure for the two potential intermediates was devised (Figure 1.9).

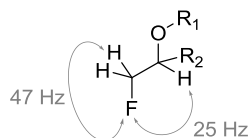
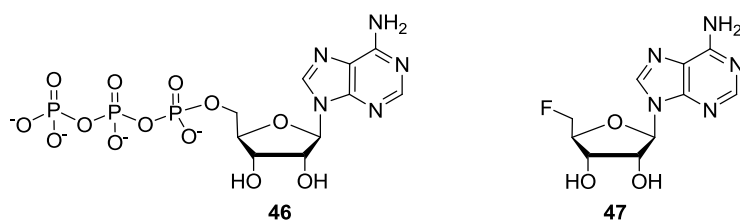
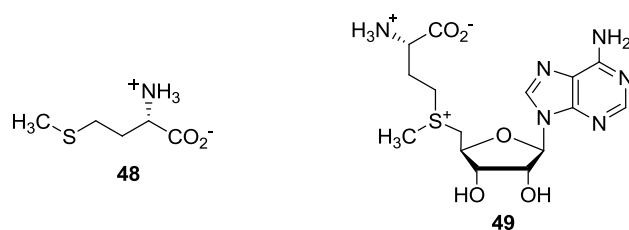


Figure 1.9 Minimal structure devised from the signals of the unknown fluorometabolites.

These experiments showed that ATP **46** supported fluorometabolite biosynthesis in *S. cattleya*. Thus, at this stage, it appeared reasonable that adenosine triphosphate **46** was involved in the fluorination reaction, being acted upon by a fluorinase enzyme that would displace the triphosphate group. The product of such enzymatic fluorination would clearly be 5'-deoxy-5'-fluoroadenosine (5'-FDA) **47**, which is consistent with the minimal structure previously shown in Figure 1.9 (*vide supra*).



However, further investigations into the enzymatic C-F bond formation using ATP **46** revealed that the amino acid L-methionine **48** enhanced the production of fluoroacetate **17** and both the other two fluorinated compounds. These results suggested that *S*-adenosyl-L-methionine (SAM) **49**, and not ATP **46**, was involved in the biosynthesis of fluorometabolites in *S. cattleya*.



The formation of *S*-adenosyl-L-methionine **49** could be rationalised by the presence of SAM synthase in CFE of the bacterium, which mediates a reaction between ATP **46** and L-methionine **48**.¹²⁶

When cell-free extracts of *S. cattleya* were incubated with ATP **46** and KF, the *in situ* production of SAM **49** by SAM synthase, proved *in vitro* fluorometabolite production to render 5'-FDA **47**.

The fluorination process was studied in real time by incubating SAM **49** and KF in a CFE of *S. cattleya*. The progress of the biosynthesis was monitored by ¹⁹F NMR analysis. This experiment showed the production of FAc **17** and confirmed SAM **49** as the substrate of the fluorination enzyme, capable of supporting fluorometabolite biosynthesis.¹²⁷ The resulting ¹⁹F NMR spectra are shown in Figure 1.10 (*vide infra*).

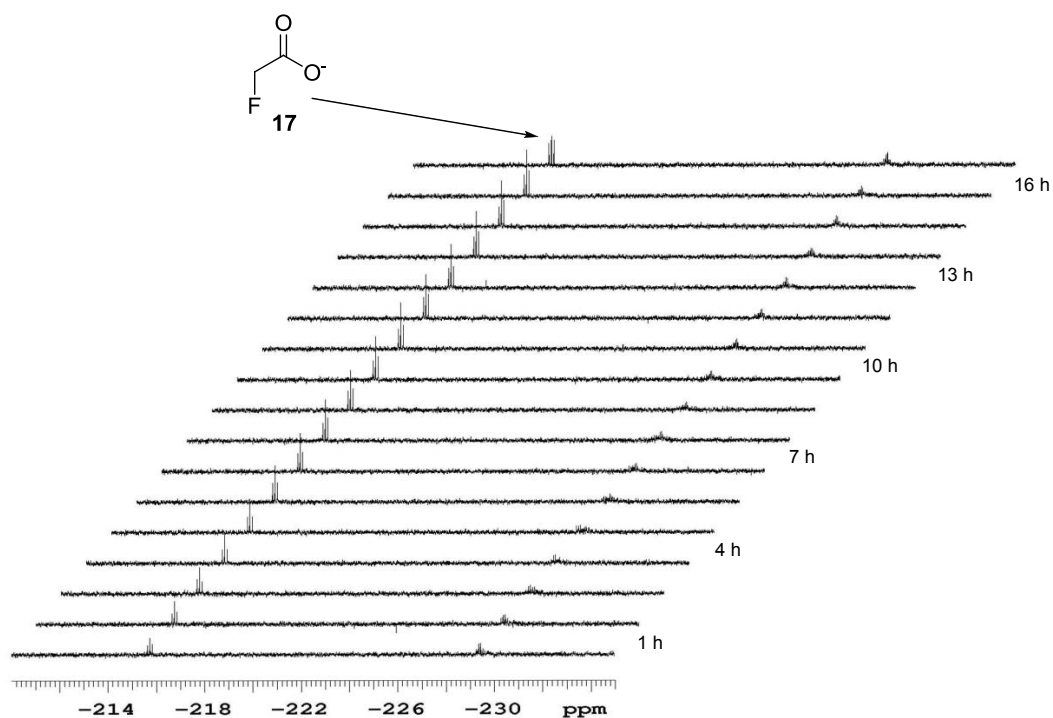


Figure 1.10 ^{19}F NMR time course of CFE incubations with SAM **49** and fluoride ion showing production of FAc **17** and two fluorometabolites at -229.4 ppm (5'-FDA **47**) and -229.7 ppm (unknown).

The preparation of a synthetic sample of 5'-FDA **47** and subsequent CFE experiments, confirmed the role of **47** as an intermediate in the biosynthetic pathway to fluoroacetate **17**. The ^{19}F NMR time course clearly showed formation of 5'-FDA **47** (-229.4 ppm) followed by another metabolite with a ^{19}F NMR signal at -229.7 ppm.

The identity of this unknown fluorometabolite was determined by further incubations of CFE with SAM **49** and KF in the presence of iodoacetamide (Figure 1.11, *vide infra*). Iodoacetamide arrests fluoroacetate **17** biosynthesis by inhibiting one or more of the enzymes on the pathway.¹¹⁸

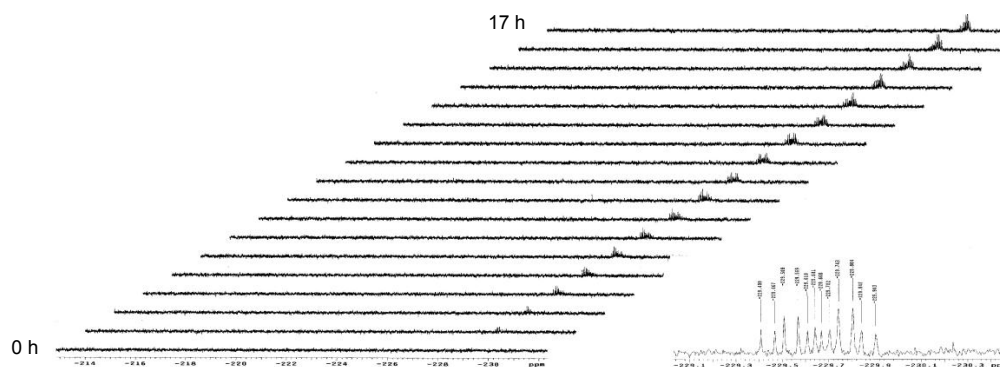


Figure 1.11 ^{19}F NMR time course of CFE incubations with SAM **49** and fluoride ion in the presence of iodoacetamide. Inset shows the ^{19}F NMR signals for the two fluorometabolites formed.

The spectra in Figure 1.11 show accumulation of two fluorometabolites without formation of FAc **17**. Of the two fluorometabolites generated, one was identified as the product of the fluorination reaction, 5'-FDA **47**. The other (^{19}F NMR, δ_{F} -229.7 ppm), had an identical coupling pattern (dt, $^2J_{\text{HF}}$ 47 Hz, $^3J_{\text{HF}}$ 29 Hz) to 5'-FDA **47**. Further analysis by ^1H NMR and ^{19}F NMR spectroscopy on a purified sample of this unknown fluorometabolite indicated that it was a 5'-deoxy-5'-fluororibose nucleoside. ES-MS analysis gave a mass ion which was one atomic mass unit higher than 5'-FDA **47** ($\text{MH}^+ = 269$ amu *versus* $\text{MH}^+ = 268$ amu). The presence of a deaminase activity¹²⁸ in *S. cattleya*, converting the NH_2 group of adenine to an OH of inosine, would account for this mass difference. To explore the possibility that 5'-FDA **47** was converted to 5'-deoxy-5'-fluorinosine (5'-FDI) **50**, isotopic labelling experiments were carried out with [^{18}O]-labelled water. ES-MS analysis showed a product which was now three atomic mass units higher than 5'-FDA **47**, indicating the incorporation of 18-oxygen during the biotransformation of 5'-FDA **47** to 5'-FDI **50** mediated by a deaminase. This result was confirmed by GC-MS analysis of the derivatised fluorometabolites with MSTFA,^{127,129} as shown in Figure 1.12 (*vide infra*).

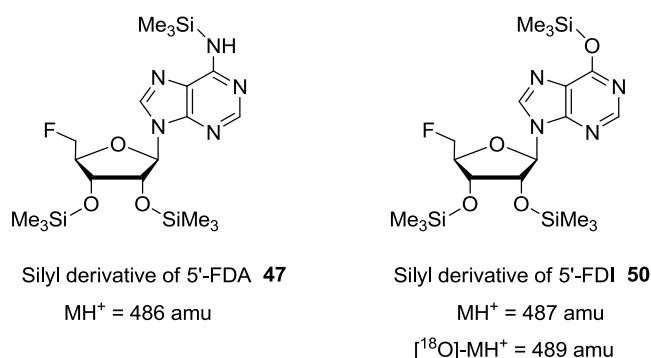
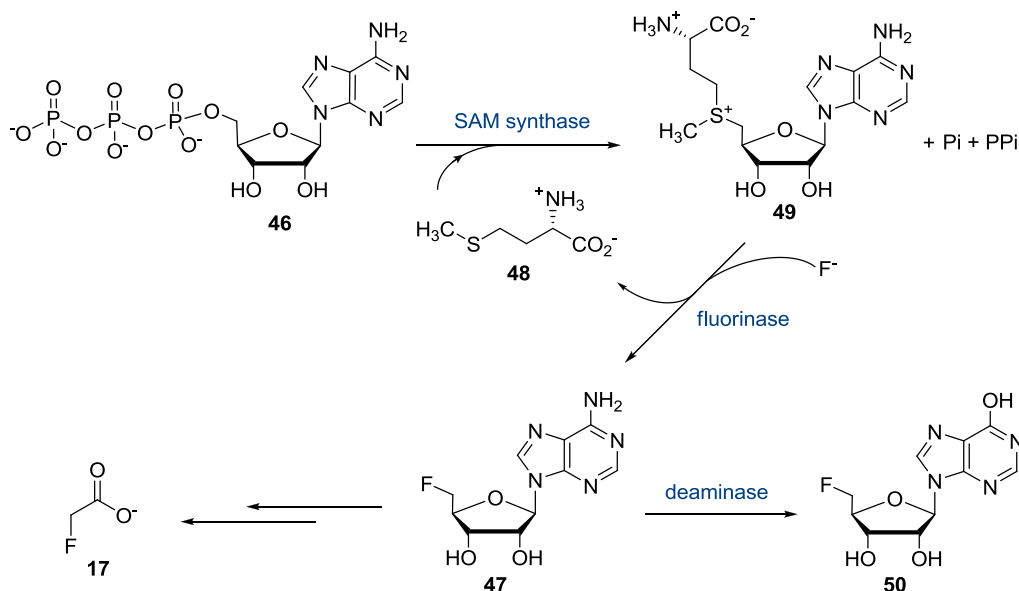


Figure 1.12 Persilylated derivatives of 5'-FDA **47** and 5'-FDI **50** analysed by GC-MS (CI) after treatment with MSTFA.

Incubations of cell-free extracts of *S. cattleya* with a purified sample of 5'-FDI **50** showed no production of FAc **17** or 4-FT **39**. Thus, the conversion of 5'-FDA **47** to 5'-FDI **50** is irreversible, and 5'-FDI **50** does not support fluorometabolite biosynthesis,¹²⁹ therefore it remains as a stable shunt product in the biotransformation of fluoride to fluoroacetate **17** (Scheme 1.8, *vide infra*).



Scheme 1.8 Enzymatic formation of 5'-FDA **47** from SAM **49** generated *in situ*, leading to the production of the secondary metabolite FAc **17** and the shunt product 5'-FDI **50**.

1.4.4.1 Purification, crystal structure and properties

With 5'-deoxy-5'-fluoroadenosine (5'-FDA) **47** identified as the product of the fluorination enzyme and SAM **49** as the substrate,¹³⁰ an HPLC assay was established to pursue purification of the fluorinating enzyme in *Streptomyces cattleya*. Purification of 5'-fluoro-5'-deoxyadenosine synthase (5'-FDAS, 'fluorinase'; EC 2.5.1.63) from *S. cattleya* was carried out by C. Schaffrath at the University of St Andrews and full details have been published.¹³¹ The molecular weight of the monomeric protein (M_r) was estimated to be around 32 kDa by SDS-PAGE electrophoresis. The purified enzyme showed a native mass of approximately 180 kDa after gel filtration chromatography, indicating that it is a hexamer.

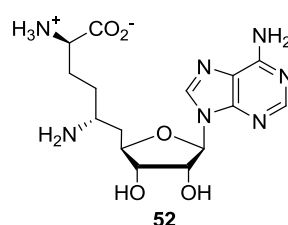
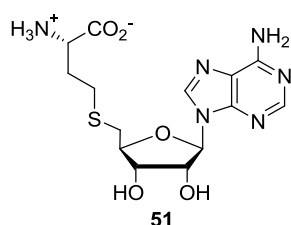
The partial amino acid sequence of the wild-type enzyme was used to design polymerase chain reaction (PCR) primers. The gene of the fluorinase (*flA*) was then cloned by degenerate PCR using genomic DNA from *S. cattleya* as a template. The complete gene and the amino acid sequence for the fluorinase (*flA*) was obtained after sequencing the amplified DNA. The *flA* gene is 897 base pairs (bp) in size and encodes a protein containing 299 amino acids. The *flA* gene amplified by PCR was inserted into the pET28a(+) plasmid and expressed in *Escherichia coli* BL21(DE3) cells. The over-expressed and purified recombinant FIA protein showed a molecular weight in agreement with ESI-MS data for the wild-type enzyme.¹³²

Access to recombinant fluorinase allowed a fuller characterisation of its activity.¹³² The catalytic rate constant (k_{cat}) of the fluorinase is 0.07 min^{-1} and the Michaelis constant (K_m) for F^- is 2 mM, and the K_m for SAM **49** is 74 μM .

The effect of temperature on the enzyme was investigated by conducting an assay over a range of temperatures from 25 °C to 70 °C. The optimum temperature was determined to be 55 °C. Addition of EDTA (1 mM) showed an increase activity by 25%, suggesting that the enzyme may be sensitive to trace amounts of metal ions. However, the presence of Mg^{2+} ion (1 mM) did not affect the activity.

CHAPTER 1

Inhibitory studies were carried out with *S*-adenosyl-L-homocysteine (SAH) **51** and the antibiotic sinefungin **52**, both previously reported to inhibit reactions of SAM-dependent enzymes.^{133,134}



SAH **51** was a competitive inhibitor of the fluorinase with a K_i value of 29 μM , whereas the presence of sinefungin **52** caused only 15% loss of enzyme activity, indicating much weaker inhibition.

Crystallisation of the fluorinase was initiated with the wild type enzyme. However, the successful solution of the structure was completed with the cloning and over-expression of the fluorinase (EC 2.5.1.63), by Dr J. Spencer at Cambridge University, that allowed crystallisation trials to be carried out to obtain protein X-ray diffraction data.^{132,135} The fluorinase structure revealed a hexamer constructed as a dimer of trimers (Figure 1.13, *vide infra*). The fold of the monomeric unit was novel and had no obvious relationship to any other protein superfamily known at that time.

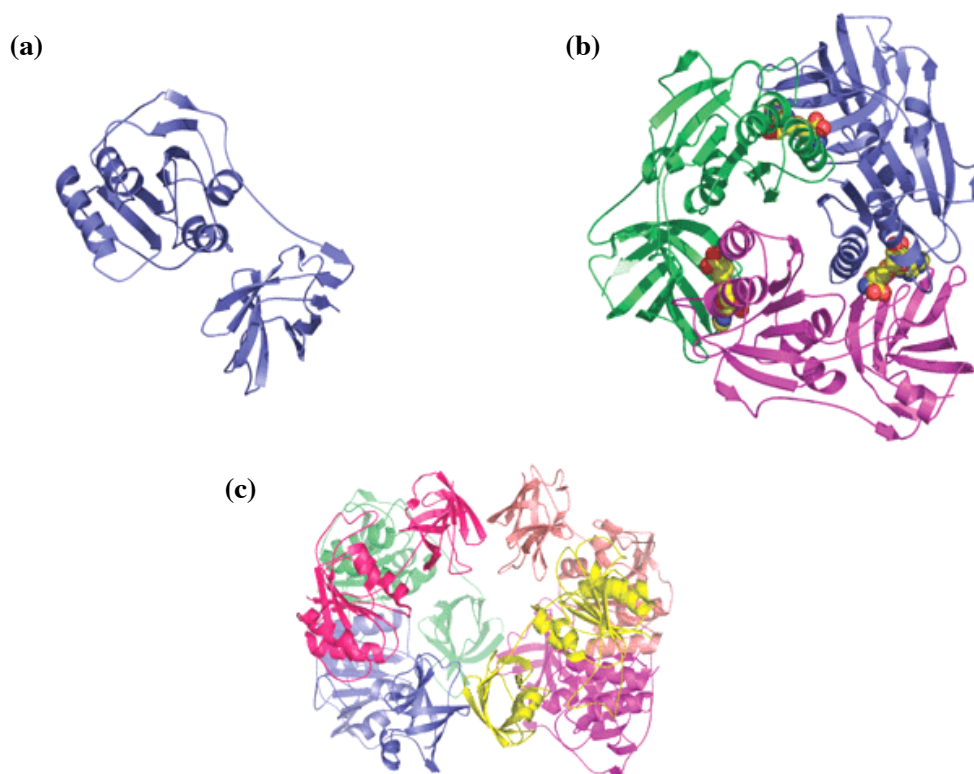


Figure 1.13 The structure of the fluorinase (EC 2.5.1.63). **(a)** Monomer **(b)** Trimer with SAM **49** bound at the subunit interfaces **(c)** The overall hexamer structure showing a dimer of trimers.

The crystal structure revealed that the trimer has three active sites where SAM **49** binds at the subunit interfaces. The substrate **49** binds tightly to the fluorinase, consistent with its co-purification with the protein. The three components of SAM **49**: the adenine ring, the ribose ring and L-methionine are recognised by a combination of hydrogen bonds and van der Waals contacts. Of particular note is the ribose ring of **49**, which is held in an unusually planar conformation by hydrogen bonding contacts between the 2'- and 3'-hydroxyl groups and the carboxylate group of Asp 16, as shown in Figure 1.14 (*vide infra*).

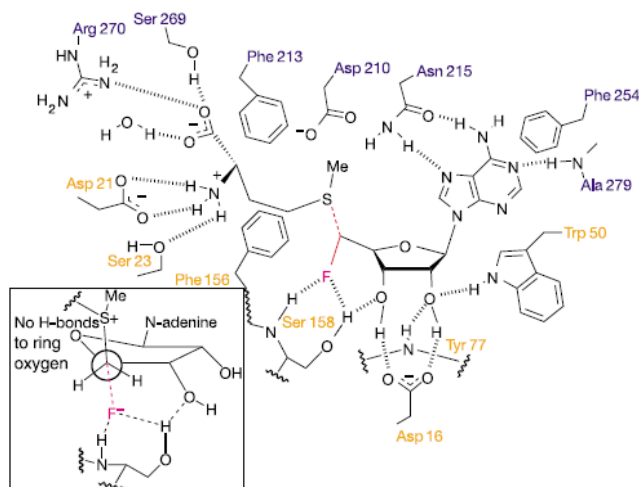
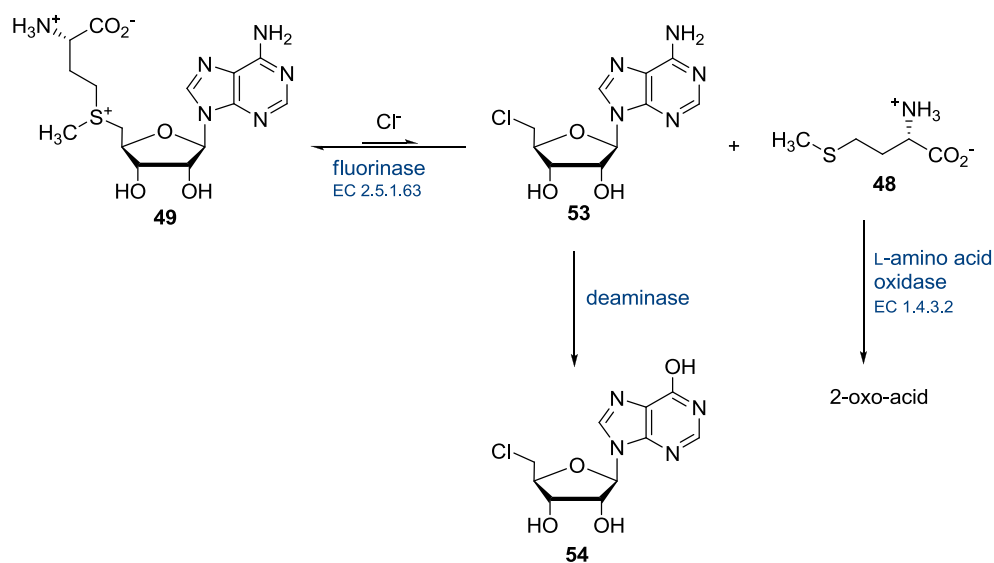


Figure 1.14 Schematic representation of hydrogen bonding contacts of 5'-FDA **47** and L-methionine **48** on the surface of the fluorinase as deduced from X-ray crystallography data.¹³²

The crystal structure revealed that most of the heteroatoms of the adenine ring are involved in hydrogen bonding, and the amino acid residues of the methionyl moiety are compensated by interactions to the surface of the protein. It is also noteworthy that the ribosyl ether oxygen is the only heteroatom of SAM **49** which is not involved as a hydrogen bond acceptor.

Co-crystallisation of the fluorinase with SAM **49** in the presence of fluoride ion resulted in a bound product complex with 5'-FDA **47** and L-methionine **48** at the active site. A comparison of this product structure with the wild-type (SAM-bound) protein was particularly informative in suggesting a mechanism for the reaction. Very small structural changes were observed between the two crystal structures, except in the bond forming/breaking region. The orientation of the new C-F bond (Figure 1.14, *vide supra*), approximately antiperiplanar to the old C-S bond, is indicative of a substitution reaction (S_N2) occurring with an inversion of configuration.¹³⁶ This conclusion is reinforced by the stereochemical studies described in Section 1.4.4.2.

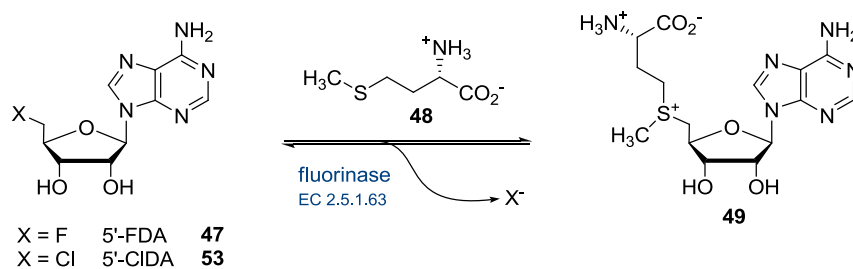
Despite the high bond-dissociation energy of the C-F bond, assays with the FDAS, both in the forward and reverse directions, have suggested that the fluorinase enzyme is reversible and therefore, it also catalyses the conversion of 5'-FDA **47** to SAM **49**.¹³⁷ This was proved by incubation of 5'-FDA **47** with L-(¹³C-methyl)methionine, which resulted in the formation of ¹³C-methyl-SAM, identified by HPLC-ES-MS analysis. Further experiments replacing fluoride ion with a chloride ion in the presence of SAM **49**, showed the production of 5'-chloro-5'-deoxyadenosine (5'-CIDA) **53**. Nevertheless, this was only possible when the reaction equilibrium was moved in favour of the organochlorine product by coupling the fluorinase to an L-amino acid oxidase that acts upon L-methionine **48**, as shown in Scheme 1.9.



Scheme 1.9 Coupled enzymatic strategy towards C-Cl bond formation catalysed by the fluorinase.

The incorporation of bromine and iodine was explored using a similar coupled-enzyme system. However, no organohalogen products were detected.¹³⁷

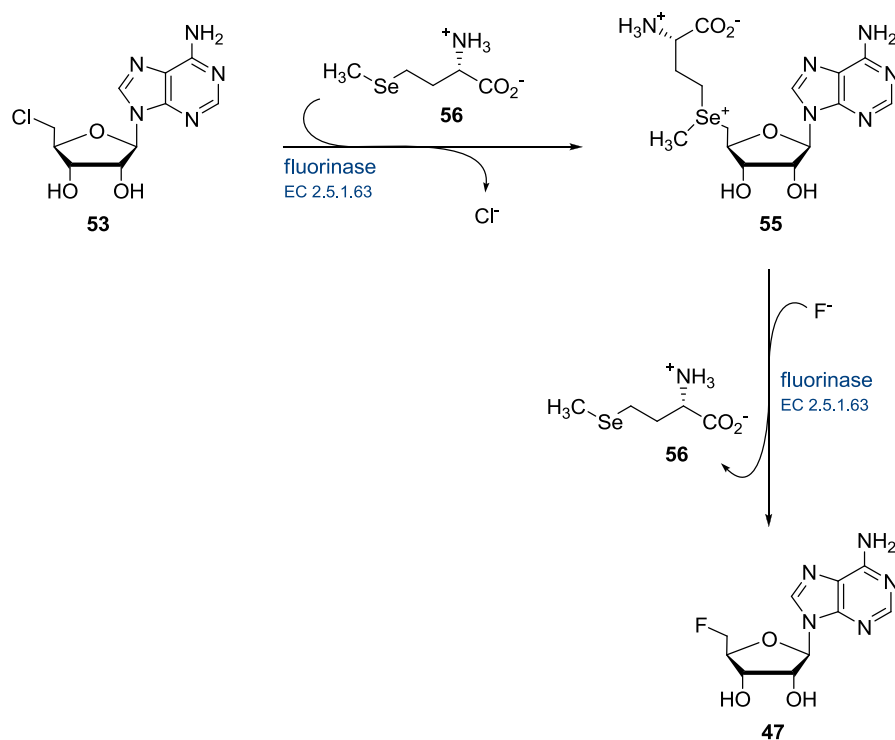
As a result, the fluorinase can catalyse the conversion of L-methionine **48** and either 5'-FDA **47** or the chlorinated analogue, 5'-CIDA **53**, to SAM **49**, with the concomitant release of the corresponding halide ion, as illustrated in Scheme 1.10.



Scheme 1.10 The fluorinase operates in reverse with both 5'-FDA **47** and 5'-CIDA **53**.

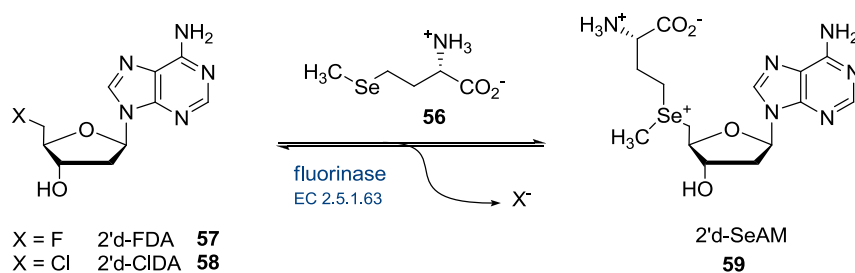
Experiments to explore the reaction catalysed by the fluorinase in the reverse direction showed that 5'-CIDA **53** is the more efficient substrate, since chloride is a better leaving group. Also the selenomethionine analogue of **49**, SeAM **55**, is the more efficient substrate in the reverse direction, because Se is the better nucleophile.

However, the fluorinase shows a preference for F⁻ over Cl⁻ by a factor of 120. This was demonstrated in a fluorinase-mediated trans-halogenation reaction as illustrated in Scheme 1.11 (*vide infra*).



Scheme 1.11 Trans-halogenation reaction of 5'-CIDA **53** to 5'-FDA **47** catalysed by the fluorinase.

Interestingly, when a 2'-deoxy-ribonucleoside (*e.g.*, 2'-deoxy-5'-FDA) is presented to the enzyme, it is also turned over, although less efficiently than the natural substrate, 5'-FDA **47** (Scheme 1.12).¹³⁸

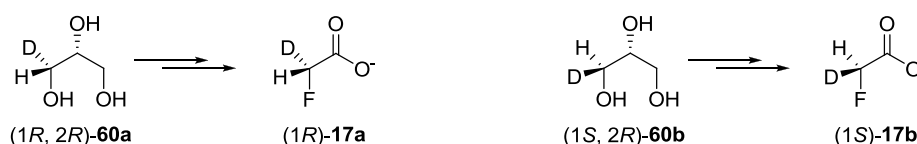


Scheme 1.12 The fluorinase can catalyse the conversion of 2'-d-FDA **57** and 2'-d-CIDA **58** substrates with L-SeMet **56** to generate 2'-d-SeAM **59**.

It is clear from these studies that, although the 2'-hydroxyl group of the ribose ring has been removed, the fluorinase accepts the 2'-deoxy analogues, 2'-d-FDA **57** and 2'-d-CIDA **58**, as substrates to generate 2'-d-SeAM **59**. A crystal structure of the 2'-d-FDA-fluorinase co-complex confirmed that the 2-deoxy substrates bind at the active site, therefore retaining some level of activity.¹³⁸

1.4.4.2 Mechanism of the fluorinase

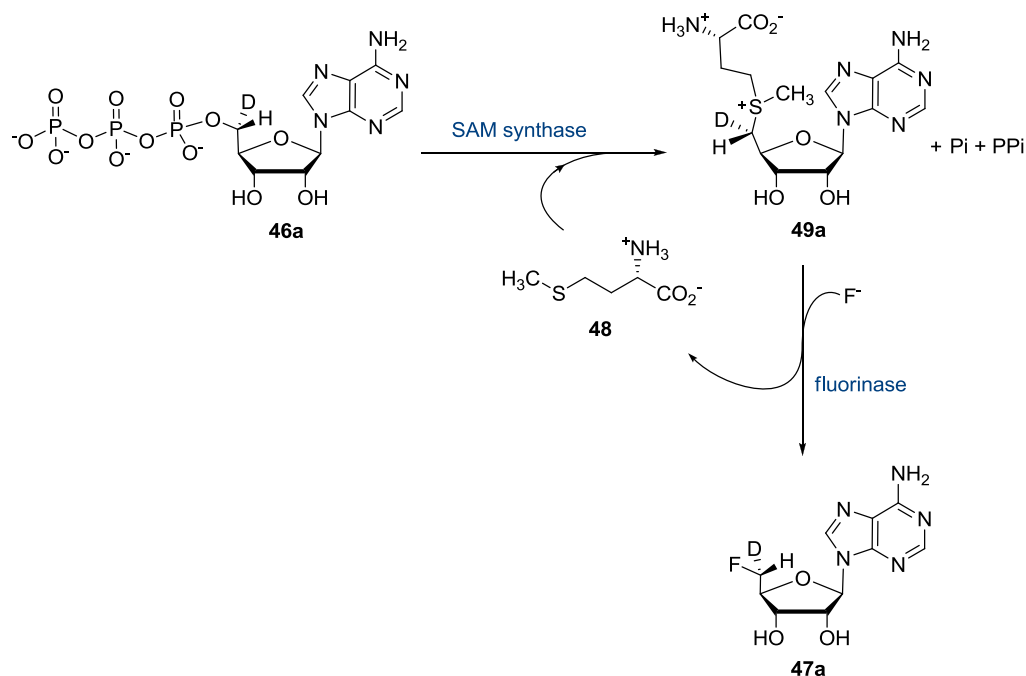
The stereochemical course of biological fluorination was explored using deuterium isotope labelling, firstly in whole-cell incubations¹³⁶ of *S. cattleya* and subsequently with the purified enzyme.¹³⁹ This consisted of a set of feeding experiments with isotopically labelled glycerols in *S. cattleya*. In particular, (1*R*, 2*R*)- and (1*S*, 2*R*)-[1-²H₁]glycerol, **60a** and **60b** (Scheme 1.13, *vide infra*), were incubated with washed cells of the bacterium. These glycerols were labelled with a single deuterium atom only on the pro-*R* hydroxymethyl group of glycerol, the pro-chiral arm which was already established to undergo fluorination.¹¹⁷ The OH group is formally replaced by fluorine during fluorometabolite biosynthesis in *S. cattleya*. The incorporation of these chiral glycerols, **60a** and **60b**, resulted in the production of chiral fluoromethyl groups on the resultant fluoroacetates, **17a** and **17b**, generated *in vivo* during incubations with washed resting cells of the bacterium, as illustrated below in Scheme 1.13.



Scheme 1.13 Incorporation of chiral deuterium labelled glycerols in whole-cell incubations of *S. cattleya*.¹³⁶

This set of feeding experiments demonstrated that the biosynthetic process is stereospecific. The fact that the *in vivo*-generated fluoroacetates **17a** and **17b** showed the same stereochemistry as their respective incubated labelled glycerols, suggested that the enzymatic C-F bond formation occurs with an inversion of configuration between SAM **49** and fluoroacetate **17**.

With the purified and over-expressed fluorinase available, a study was carried out to examine the stereochemical course of the fluorination event on the enzyme directly.¹³⁹ With this as an objective, synthetically prepared (5'*R*)-[5'-²H₁]ATP **46a** was incubated with purified SAM synthase to generate a sample of (5'*S*)-[5'-²H₁]SAM **49a** (*vide infra* Scheme 1.14). Treatment of this isotopically labelled SAM with fluoride ion in the presence of the fluorinase provided a sample of [5'-²H₁]-5'-FDA **47a**, stereospecifically labelled at the C5' position. The entire strategy is illustrated in Scheme 1.14.



Scheme 1.14 Coupled-enzyme assay involving SAM synthase and the fluorinase, indicating that there are two sequential inversions of configuration resulting in an overall retention of configuration.

Since SAM synthase operates *via* a S_N2 mechanism,¹⁴⁰ the resultant configuration at C5' of [5'-²H₁]-5'-FDA **47a** indicated that the fluorination reaction also occurs with an inversion of the configuration. Thus, the stereochemical study suggests that the enzyme catalyses the S_N2 displacement of L-methionine **48** by nucleophilic attack at C5' of SAM **49**, a process which requires at least partial desolvation of fluoride ion.¹³⁹ However, computational studies showed that stripping the fluoride ion of its last two remaining water molecules requires significantly more than half of the overall desolvation energy,¹⁴¹ suggesting a mechanism that leaves at least two hydrogen bonds to F⁻ to be favoured. Two recent theoretical studies shed light on possible mechanisms.^{141,142} Quantum mechanical/molecular mechanical (QM/MM) calculations¹⁴² indicated that the fluorinase accelerates the reaction by between 10⁶ to 10⁸ in comparison with the uncatalysed process, activation energy of which is approximately 100 kJmol⁻¹. On the other hand, a theoretical study in the gas phase indicated that only partial desolvation of the fluoride ion was required to make F⁻ a potent nucleophile.¹⁴¹ This latter study also highlighted a role of the charge on the organic moiety in stabilising the fluoride ion as it becomes partially desolvated, and in giving a reactant conformation appropriate for nucleophilic attack at the substitution centre.

Although the structure of the fluorinase bound to both SAM **49** and the products were solved, and the theoretical studies revealed possible mechanisms, it was only very recently that the molecular mechanism of enzymatic fluorination was elucidated. Site-directed mutagenesis studies, structural analyses and isothermal calorimetry (ITC) experiments provided the necessary data to establish the key residues required for catalysis and the order of substrate binding.¹⁴³ As fluoride ion is not easily distinguished from water by protein X-ray crystallography, chloride ion was used in combination with a mutant of low activity. Thus, it was possible to locate the halide ion in non-productive co-complexes with SAM **49** and SAH **51**. The kinetic data revealed that the positively charged sulfur atom of SAM **49** plays a

key role in stabilising the transition state. These experiments also allowed the order of binding of the reactants to be determined and thus, a detailed molecular mechanism for the fluorinase was proposed as illustrated in Figure 1.15.

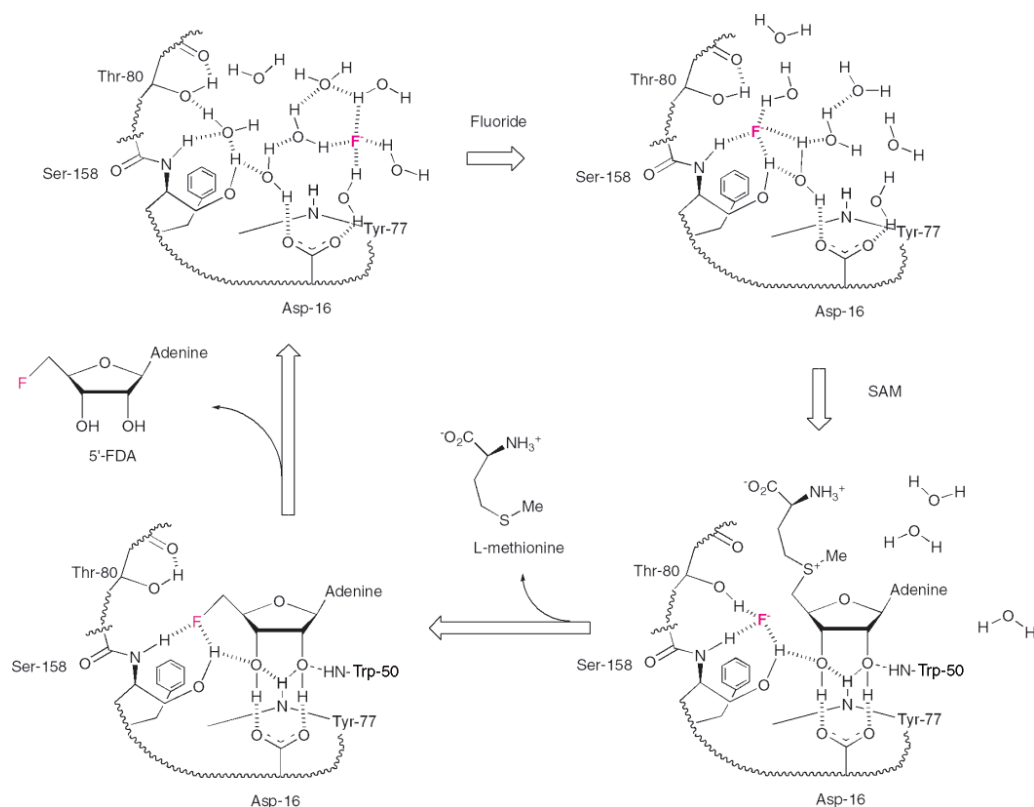
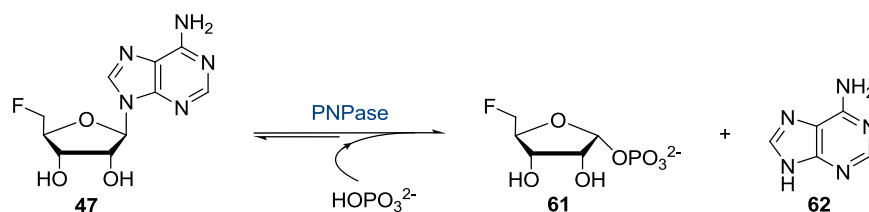


Figure 1.15 Schematic illustration of the sequential mechanism of the fluorinase.¹⁴³

The molecular mechanism for FDAS is explained in the following manner. The solvated fluoride ion binds to an unoccupied binding site of the fluorinase. The affinity of binding is increased by exchanging two water molecules for hydrogen bonds to polar residues of the protein (a process that is entropically favoured). Then a molecule of SAM **49** binds tightly and specifically to the enzyme forcing the release of water and trapping the fluoride ion in a reactive position, stabilised by the positive charge on SAM **49**. The partially desolvated fluoride ion acts now as a nucleophile attacking at the C5' of SAM **49** via a $\text{S}_{\text{N}}2$ mechanism. After that, L-methionine **48** is then released by the enzyme followed by 5'-FDA **47**.

1.4.5 Identification of 5-deoxy-5-fluoro- α ,D-ribose-1-phosphate as an intermediate

In order to decipher the next step in the fluorometabolite pathway in *S. cattleya*, the role of a putative purine-nucleoside phosphorylase (PNPase)^{144,145} was investigated using a CFE of the bacterium.¹⁴⁶ The action of such enzyme would then generate 5-deoxy-5-fluoro- α ,D-ribose-1-phosphate (5-FDRP) **61** and adenine **62**, as a result of a specific reaction for β -nucleosides to give only the α -anomer of the phosphorylated sugar, as shown below in Scheme 1.15.



Scheme 1.15 A putative purine-nucleoside phosphorylase in *S. cattleya* catalyses the cleavage of the C-N glycosidic bond of 5'-FDA **47** by a phosphorolysis reaction to render 5-FDRP **61** and adenine **62**.

To this end, a sample of 5-FDRP **61** was prepared to explore its role as an intermediate during fluorometabolite biosynthesis in *S. cattleya*. This was achieved using a chemo-enzymatic approach with two commercially available enzymes: a 5'-adenylic acid deaminase (EC 3.5.4.6; *Aspergillus species*) and a bacterial PNPase (EC 2.4.2.1; unknown source). Incubation of this sample of 5-FDRP **61** in a cell free extract of *S. cattleya* resulted in the accumulation of the secondary metabolite FAc **17**, as determined by ¹⁹F NMR spectroscopy. Thus, it was shown that 5-deoxy-5-fluoro- α ,D-ribose-1-phosphate (5-FDRP) **61** supported the biosynthesis of fluorometabolites in *S. cattleya*, being the next formed intermediate after 5'-FDA **47** on the biosynthetic pathway to FAc **17** and 4-FT **39**.¹⁴⁷

The identification of 5-FDRP **61** and the phosphorylase activity responsible for its formation, led to a partially purified PNPase from *S. cattleya*.¹⁴⁸ Feeding experiments with 5'-FDA **47** were carried out with a partially purified protein fraction after ammonium sulfate precipitation, hydrophobic interaction chromatography and ion exchange chromatography. The bioconversion of 5'-FDA **47** to 5-FDRP **61** was then monitored by ¹⁹F NMR spectroscopy (Figure 1.16, *vide infra*), and the formation of **61** demonstrated the ability of this partially purified PNPase from *S. cattleya* to catalyse the phosphorolysis reaction on the fluorinase product.¹⁴⁷

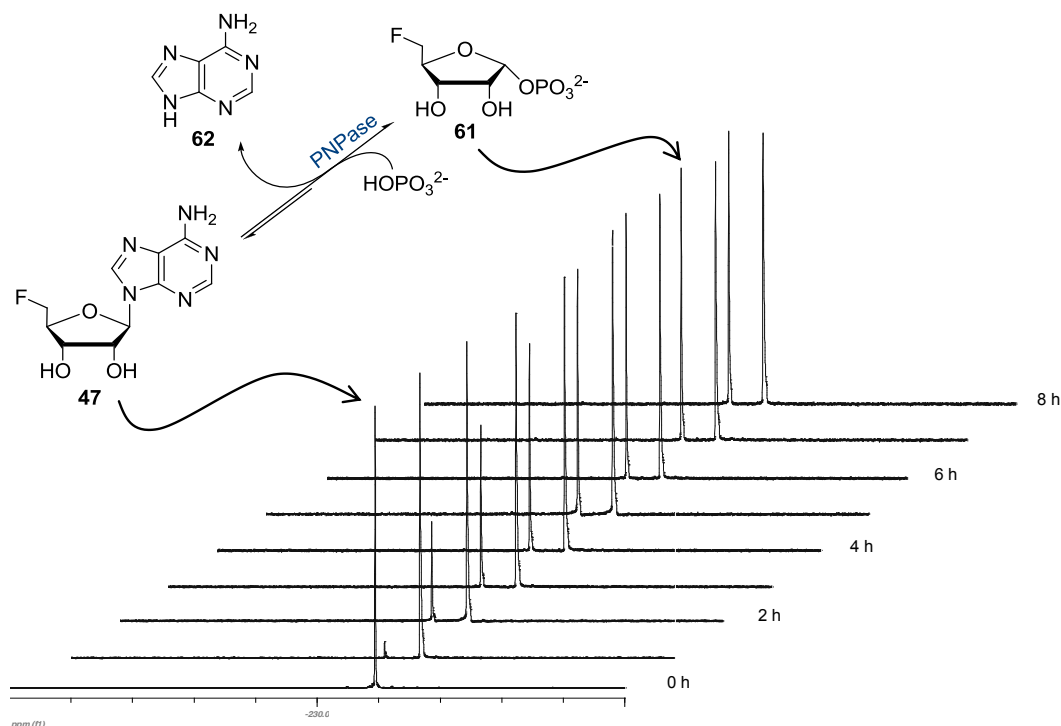


Figure 1.16 ¹⁹F {¹H} NMR time course, recorded every hour for 8 h, showing the production of 5-FDRP **61** from 5'-FDA **47**, catalysed by a purine nucleotide phosphorylase contained in a partially purified extract from *S. cattleya*.

This set of experiments confirmed 5-deoxy-5-fluoro- α ,D-ribose-1-phosphate (5-FDRP) **61** as the second intermediate in fluorometabolite biosynthesis in *S. cattleya*, and also the presence

of a purine-nucleoside phosphorylase (PNPase), which is responsible for the reversible phosphorolysis of the glycosidic bond of 5'-FDA **47** to 5-FDRP **61** (Scheme 1.15, *vide supra*). The partially purified PNPase has revealed narrow substrate specificity and similarities to bacterial 5'-methylthioadenosine phosphorylases (MTAPs).¹⁴⁸

With the identification of the *flB* gene encoding a putative purine nucleoside phosphorylase,¹⁴⁹ over-expression and purification of the PNPase from *S. cattleya* was possible, with subsequent work on crystallisation trials. The purified over-expressed PNPase from *S. cattleya* showed an estimated mass of 33 kDa by SDS-PAGE electrophoresis.¹⁴⁸

1.4.6 Fluorometabolite gene cluster in *S. cattleya*

Recently, in the search of the genes encoding the enzymes involved in fluorometabolite biosynthesis in *S. cattleya*, a 10 kb gene cluster has been identified in Cambridge from a genomic DNA cosmid library of the bacterium.¹⁴⁹ In total, a further eleven open reading frames (ORF) have been located around the previously characterised fluorinase gene (*flA*) of *S. cattleya*. Contiguous to *flA* was found a putative ORF (*flB*) which encodes for the purine nucleoside phosphorylase (PNPase) enzyme responsible for the transformation of 5'-FDA **47** to 5-FDRP **61** (as previously described in Section 1.4.5, *vide supra*). The functions of these genes contained in the *fl* locus (Figure 1.17, *vide infra*) have been tentatively assigned based on other known protein sequences, and most of them are likely to play a role in regulation. Interestingly, the gene *flK* has been shown to encode a thioesterase responsible for the breakdown of fluoroacetyl-CoA **21** but not acetyl-CoA. The presence of such selective thioesterase activity suggests a resistance mechanism to fluoroacetate **17** in the organism. In this way, any fluoroacetyl-CoA **21** formed is hydrolysed, avoiding its entry into the tricarboxylic acid cycle.

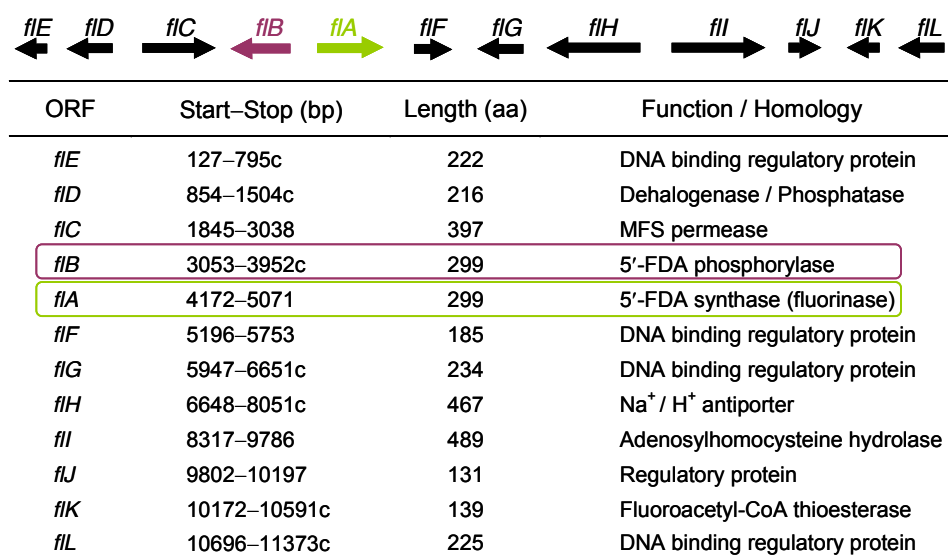


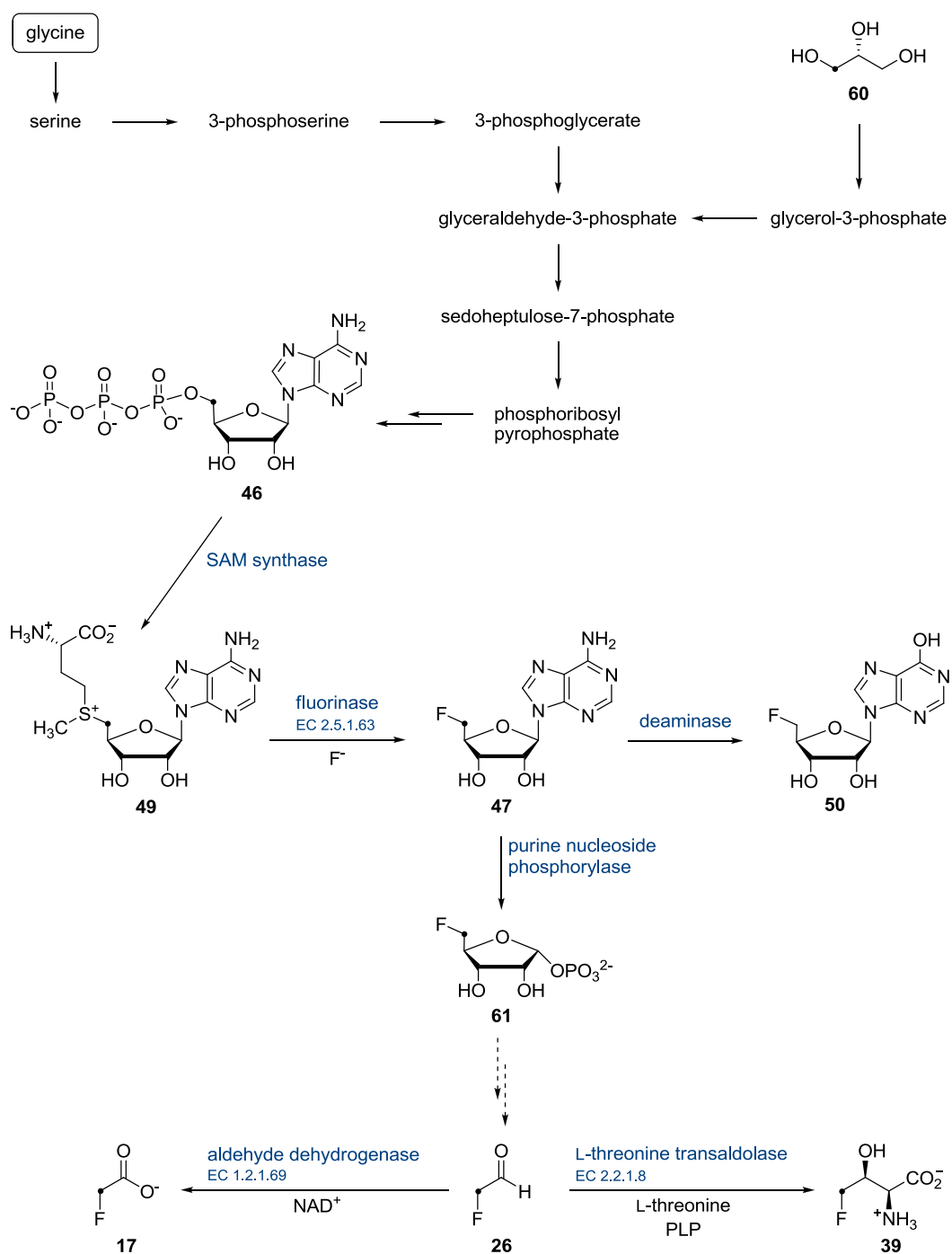
Figure 1.17 The Spencer cluster: map of the *fl* gene locus and possible functions for the proteins encoded by the open reading frames.¹⁴⁹

However, the genes encoding for the previously characterised enzymes, responsible of the later steps in fluorometabolite biosynthesis in *S. cattleya*, were not located in the Spencer cluster. Thus, it is unclear whether there is a second locus containing these missing genes or whether the enzymes catalysing similar reactions in primary metabolism may also accept the fluorinated substrates.¹⁴⁹

1.4.7 Overview of fluorometabolite biosynthesis in *Streptomyces cattleya*

As discussed so far, isotope labelling experiments and biochemical studies led to the rationalisation of the biosynthetic pathway in the fluorometabolite-producer *S. cattleya*.^{32,95}

An illustration of the metabolites and enzymes involved in the biosynthesis of fluoroacetate **17** and 4-fluorothreonine **39**, prior to the work carried out in this thesis, is illustrated in Scheme 1.16 (*vide infra*).



Scheme 1.16 Overview of the biosynthetic pathway in *S. cattleya* showing the relationships between primary metabolites and fluorinated secondary metabolites and the enzymes involved in such transformations. The dot traces the fate of the pro-*R* hydroxymethyl group of glycerol through to FAc **17** and 4-FT **39**.

1.5 References

1. J. Pérez-Cajaraville, D. Abejón, J. R. Ortiz and J. R. Pérez, *Rev. Soc. Esp. Dolor*, 2005, **12**, 373-384.
2. C. González Wagner, *Gerión*, 1984, **2**, 31-59.
3. Homer, in *The Odyssey*, The Harvard Classics, Book IV, 1909, pp. 34.
4. Gaspar de Carvajal, in *The discovery of the Amazon according to the account of Friar Gaspar de Carvajal and other documents*, 1934, p.224.
5. M. R. Lee, *J. R. Coll. Physicians Edinb.*, 2005, **35**, 83-92.
6. D. J. Newman, G. M. Cragg and K. M. Snader, *Nat. Prod. Rep.*, 2000, **17**, 215-234.
7. J. R. Hanson, in *Natural Products: The Secondary Metabolites*, The Royal Society of Chemistry, Cambridge, **2003**, pp. 1-2.
8. R. S. Berger, J. C. Dukes and Y. C. Chow, *J. Med. Entomol.*, 1971, **8**, 84-86.
9. R. S. Berger, *J. Med. Entomol.*, 1983, **20**, 103.
10. S. Marumo, H. Hattori, H. Abe and K. Munakata, *Nature*, 1968, **219**, 959-960.
11. M. Katayama, S. V. Thiruvikraman and S. Marumo, *Plant Cell Physiol.*, 1987, **28**, 383-386.
12. T. F. Spande, H. M. Garraffo, M. W. Edwards, H. J. C. Yeh, L. Pannell and J. W. Daly, *J. Am. Chem. Soc.*, 1992, **114**, 3475-3478.
13. E. Drechsel, *Z. Biol.*, 1896, **33**, 85-107.
14. L. Fowden, *Proc. Roy. Soc. B*, 1968, **171**, 5-18.
15. G. W. Gribble, *The Nucleus*, 2005, **2**, 8-12.
16. D. Gottlieb, P. K. Bhattacharyya, H. W. Anderson and H. E. Carter, *J. Bact.*, 1948, **55**, 409-417.

CHAPTER 1

17. J. Ehrlich, D. Gottlieb, P. R. Burkholder, L. E. Anderson and T. G. Pridham, *J. Bact.*, 1948, **56**, 467-477.
18. J. Ehrlich, Q. R. Bartz, R. M. Smith, D. A. Joslyn and P. R. Burkholder, *Science*, 1947, **106**, 417.
19. B. M. Duggar, *Ann. NY Acad. Sci.*, 1948, **51**, 177-181.
20. *US Pat.*, 2482055, 1949.
21. M. H. McCormick, W. M. Stark, G. E. Pittenger, R. C. Pittenger and J. M. McGuire, *Antibiotics Ann.*, 1955-1956, 606-611.
22. D. H. Williams, *Nat. Prod. Rep.*, 1996, **13**, 469-477.
23. D. H. Williams and B. Bardsley, *Angew. Chem., Int. Ed.*, 1999, **38**, 1173-1193.
24. J. Orjala and W. H. Gerwick, *Nat. Prod. Rep.*, 1996, **59**, 427-430.
25. J. Hartung, *Angew. Chem., Int. Ed.*, 1999, **38**, 1209-1211.
26. N. Sitachitta, B. L. Márquez, R. T. Williamson, J. Rossi, M. A. Roberts, W. H. Gerwick, V.-A. Nguyen and C. L. Willis, *Tetrahedron*, 2000, **56**, 9103-9113.
27. N. Sitachitta, J. Rossi, M. A. Roberts, W. H. Gerwick, M. D. Fletcher and C. L. Willis, *J. Am. Chem. Soc.*, 1998, **120**, 7131-7132.
28. Y. Takahashi, M. Daitoh, M. Suzuki, T. Abe and M. Masuda, *J. Nat. Prod.*, 2002, **65**, 395-398.
29. H. Takahashi, Y. Takahashi, M. Suzuki, T. Abe and M. Masuda, *Anal. Sci.*, 2007, **23**, x103-x104.
30. G. W. Gribble, *Naturally Occurring Organofluorines*. In *Handbook of Environmental Chemistry*, Vol. 3, Part N: Organofluorines (ed. by A. H. Neilson), Springer-Verlag, Berlin Heidelberg, 2002, pp. 121-136.
31. G. W. Gribble, *J. Chem. Edu.*, 1973, **50**, 460-462.

CHAPTER 1

32. D. O'Hagan and D. B. Harper, *J. Fluorine Chem.*, 1999, **100**, 127-133.
33. P. Ciminiello, E. Fattorusso, M. Forino, M. Di Rosa, A. Ianaro and R. Poletti, *J. Org. Chem.*, 2001, **66**, 578-582.
34. C. R. Harington, *Biochem. J.*, 1926, **20**, 293-299.
35. C. R. Harington and G. Barger, *Biochem. J.*, 1926, **21**, 169-183.
36. D. B. Harper and D. O'Hagan, *Nat. Prod. Rep.*, 1994, **11**, 123-133.
37. S. L. Neidleman and J. Geigert, in *Biohalogenation: Principles, Basic Roles and Applications*, Ellis Horwood Limited, Chichester, 1986.
38. N. N. Greenwood and A. Earnshaw, in *Chemistry of the Elements*, Pergamon Press, Oxford, 1989.
39. F. A. Cotton and G. Wilkinson, in *Advanced Inorganic Chemistry*, 5th Edition, John Wiley and Sons, New York, 1988.
40. B. E. Smart, *Fluorinated organic molecules*. In *Molecular structure and energetics*, Vol.3, VCH Publishers, Weinheim, Germany, 1986, p. 141.
41. C. Walsh, *Adv. in Enzymology*, 1982, **55**, 197-289.
42. K.-H. van Pée, and S. Unversucht, *Chemosphere*, 2003, **52**, 299-312.
43. J. S. C. Marias, *Onderstepoort J. Vet. Res.*, 1943, **18**, 203-206.
44. J. S. C. Marias, *Onderstepoort J. Vet. Res.*, 1944, **20**, 67-73.
45. R. J. Hall R. B. Cain, *New Phytol.*, 1972, **71**, 839-853.
46. R. J. Hall, *New Phytol.*, 1972, **71**, 855-871.
47. B. Vickery, M. L. Vickery and J. T. Ashu, *Phytochemistry*, 1973, **12**, 145-147.
48. B. Vickery and M. L. Vickery, *Phytochemistry*, 1972, **11**, 1905-1909.
49. D. O'Hagan, R. Perry, J. M. Lock, J. J. M. Meyer, L. Dasaradhi, J. T. G. Hamilton and D. Harper, *Phytochemistry*, 1993, **33**, 1043-1045.

CHAPTER 1

50. L. E. Twigg and D. R. King, *Oikos*, 1991, **61**, 412-430.
51. L. E. Twigg, D. R. King, L. H. Bowen, G. R. Wright and C. T. Eason, *Aus. J. Bot.*, 1996, **44**, 411-412.
52. L. E. Twigg, D. R. King, and M. D. Potts, *Aus. J. Bot.*, 1999, **47**, 877-880.
53. M. M. De Oliveira, *Cell. Mol. Life Sci.*, 1963, **19**, 586-587.
54. T. Vartiainen and J. Gynther, *Food Chem. Toxicol.*, 1984, **22**, 307-308.
55. J. Lovelace, G. W. Miller and G. W. Welkie, *Atmos. Environ.*, 1968, **2**, 187-190.
56. J. Y.-O. Cheng, M.-H. Yu, G. W. Miller and G. W. Welkie, *Environ. Sci. Technol.*, 1968, **2**, 367-370.
57. P. F. V. Ward and N. S. Huskisson, *Biochem. J.*, 1969, **113**, 9P.
58. M.-H. Yu and G. W. Welkie, *Environ. Sci. Technol.*, 1970, **4**, 492-495.
59. R. A. Peters and M. Shorthouse, *Phytochemistry*, 1972, **11**, 1337-1338.
60. R. A. Peters, *Phytochemistry*, 1972, **11**, 1339.
61. R. A. Peters, R. W. Wakelin and P. Buffa, *Proc. Roy. Soc. B*, 1953, **140**, 497-506.
62. J. F. Morrison and R. A. Peters, *Biochem. J.*, 1954, **58**, 473-479.
63. L. E. Twigg and R. J. Mead, *Aust. J. Zool.*, 1990, **37**, 617-626.
64. R. J. Dummel and E. Kun, *J. Biol. Chem.*, 1969, **11**, 2966-2969.
65. R. A. Peters, *Adv. Enzymol.*, 1957, **18**, 113-159.
66. R. Keck, H. Haas and J. Rétey, *FEBS Lett.*, 1980, **114**, 287-290.
67. H. L. Carrell, J. P. Glusker, J. J. Villafranca, A. S. Mildvan, R. J. Dummel and E. Kun, *Science*, 1970, **170**, 1412-1414.
68. H. Lauble, M. C. Kennedy, M. H. Emptage, H. Beinert and C. D. Stout, *Proc. Natl. Acad. Sci. USA*, 1996, **93**, 13699-13703.

CHAPTER 1

69. E. Kun, E. Kirsten and M. L. Sharma, *Proc. Natl. Acad. Sci. USA*, 1977, **74**, 4942-4946.
70. R. A. Peters and M. Shorthouse, *Nature*, 1967, **216**, 80-81.
71. R. A. Peters and M. Shorthouse, *Nature*, 1971, **231**, 123-124.
72. S. J. Moss, C. D. Murphy, J. T. G. Hamilton, W. C. McRoberts, D. O'Hagan, C. Schaffrath and D. B. Harper, *Chem. Commun.*, 2000, 2281-2282.
73. R. A. Peters and P. J. Hall, *Biochem. Pharmacol.*, 1959, **2**, 25-36.
74. R. A. Peters, P. J. Hall, P. F. V. Ward and N. Sheppard, *Biochem. J.*, 1960, **77**, 17-22.
75. R. E. A. Dear and F. L. M. Pattison, *J. Am. Chem. Soc.*, 1963, **85**, 622-626.
76. P. F. V. Ward, P. J. Hall and R. A. Peters, *Nature*, 1964, **201**, 611-612.
77. J. T. G. Hamilton and D. B. Harper, *Phytochemistry*, 1997, **44**, 1129-1132.
78. W. W. Christie, J. T. G. Hamilton and D. B. Harper, *Chem. Phys. Lipids*, 1998, **97**, 41-47.
79. D. B. Harper, J. T. G. Hamilton and D. O'Hagan, *Tetrahedron Lett.*, 1990, **31**, 7661-7662.
80. D. B. Harper, D. O'Hagan and C. D. Murphy, *Fluorinated natural products: occurrence and biosynthesis*. In *The Handbook of Environmental Chemistry*, Vol. 3, Part P, ed. G. W. Gribble, Springer-Verlag, Berlin Heidelberg, 2003, p. 148.
81. J. N. Eloff and B. von Sydow, *Phytochemistry*, 1971, **10**, 1409-1415.
82. X.-H. Xu, G.-M. Yao, Y.-M. Li, J.-H. Lu, C.-J. Lin, X. Wang and C.-H. Kong, *J. Nat. Prod.*, 2003, **66**, 285-288.
83. S. Ozaki, Y. Watanabe, T. Hoshiko, H. Mitzuno, K. Ishirawa and H. Mori, *Chem. Pharm. Bull.*, 1984, **32**, 733-738.
84. J. A. Montgomery and K. Hewson, *J. Am. Chem. Soc.*, 1957, **79**, 4559.

CHAPTER 1

85. S. Spiegelman, R. Sawyer, R. Nayak, E. Ritzi, R. Stolfi and D. Martin, *Proc. Natl. Acad. Sci. USA*, 1980, **77**, 4966-4970.
86. S. Ozaki, *Med. Res. Rev.*, 1996, **16**, 51-86.
87. S. O. Thomas, V. L. Singleton, J. A. Lowery, R. W. Sharpe, L. M. Pruess, J. N. Porter, J. H. Mowat and N. Bohonos, *Antibiotics Ann.*, 1957, 716-721.
88. *US Pat.*, 2914525, 1959.
89. C. W. Waller, J. B. Patrick, W. Fulmor and W. E. Meyer, *J. Am. Chem. Soc.*, 1957, **79**, 1011-1012.
90. R. I. Hewit, A. R. Gumble, L. H. Taylor and W. S. Wallace, *Antibiotics Ann.*, 1957, 722-729.
91. G. O. Morton, J. E. Lancaster, G. E. Van Lear, W. Fulmor and W. E. Meyer, *J. Am. Chem. Soc.*, 1969, **91**, 1535-1537.
92. D. A. Shuman, R. K. Robins and M. J. Robins, *J. Am. Chem. Soc.*, 1969, **91**, 3391-3392.
93. I. D. Jenkins, J. P. H. Verheyden and J. G. Moffatt, *J. Am. Chem. Soc.*, 1976, **98**, 3346-3357.
94. A. R. Maguire, W.-D. Meng, S. M. Roberts and A. J. Willetts, *J. Chem. Soc., Perkin Trans. 1*, 1993, 1795-1808.
95. H. Deng, D. O'Hagan and C. Schaffrath, *Nat. Prod. Rep.*, 2004, **21**, 773-784.
96. J. M. Williamson, E. Inamine, K. E. Wilson, A. W. Douglas, J. M. Liesch and G. Albers-Schönberg, *J. Biol. Chem.*, 1985, **260**, 4637-4647.
97. *US Pat.*, 4304867, 1981.
98. *US Pat.*, 4371617, 1983.
99. *US Pat.*, 3950357, 1976.

CHAPTER 1

100. J. S. Kahan, F. M. Kahan, R. Goegelman, S. A. Currie, M. Jackson, E. O. Stapley, T. W. Miller, A. K. Miller, D. Hendlin, S. Mochales, S. Hernandez, H. B. Woodruff and J. Birnbaum, *J. Antibiot.*, 1979, **32**, 1-12.
101. M. Sanada, T. Miyano, S. Iwadare, J. M. Williamson, B. H. Arison, J. L. Smith, A. W. Douglas, J. M. Liesch and E. Inamine, *J. Antibiot.*, 1986, **39**, 259-265.
102. K. A. Reid, J. T. G. Hamilton, R. D. Bowden, D. O'Hagan, L. Dasaradhi, M. R. Amin and D. B. Harper, *Microbiology*, 1995, **141**, 1385-1393.
103. J. Mann in *Chemical Aspects of Biosynthesis*, 1st Edition, Oxford University Press, 1994.
104. R. Schoenheimer and D. Rittenberg, *J. Biol. Chem.*, 1935, **111**, 163-168.
105. J. T. G. Hamilton, C. D. Murphy, M. R. Amin, D. O'Hagan and D. Harper, *J. Chem. Soc., Perkin Trans. I*, 1998, 759-767.
106. T.W.-M. Fan and A. N. Lane, *Prog. Nucl. Mag. Res. Sp.*, 2008, **52**, 69-117.
107. P. D. Stanley, in *The Handbook of Environmental Chemistry*, Vol. 3, Part N Organofluorines, Springer-Verlag, Berlin Heidelberg, 2002, pp. 4-5.
108. Y. G. Gakh, A. A. Gakh and A. M. Gronenborn, *Magn. Reson. Chem.*, 2000, **38**, 551-558.
109. C. D. Murphy, *OMICS*, 2007, **11**, 314-324.
110. M. G. Boersma, T.Y. Dinarieva, W. J. Middelhoven, W. J. H. Van Berkel, J. Doran, J. Vervoort and I. M. C. M. Rietjens, *Appl. Environ. Microbiol.*, 1998, **64**, 1256-1263.
111. P. Bachert, *Prog. Nucl. Mag. Res. Sp.*, 1997, **33**, 1-56.
112. M. L. Baron, C. M. Bothroyd, G. I. Rogers, A. Staffa and I. D. Rae, *Phytochemistry*, 1987, **26**, 2293-2295.

CHAPTER 1

113. A. E. G. Cass, D. W. Ribbons, J. T. Rossiter and S. R. Williams, *FEBS Lett.*, 1987, **220**, 353-357.
114. B. J. Stockman, *J. Am. Chem. Soc.*, 2008, **130**, 5870-5871.
115. J. M. Tront and F. M. Saunders, *Environ. Pollut.*, 2007, **145**, 708-714.
116. W. Wolf, C. A. Presant and V. Waluch, *Adv. Drug Delivery Rev.*, 2000, **41**, 55-74.
117. J. Nieschalk, J. T. G. Hamilton, C. D. Murphy, D. B. Harper and D. O'Hagan, *Chem. Commun.*, 1997, 799-780.
118. C. D. Murphy, S. J. Moss and D. O'Hagan, *Appl. Environ. Microbiol.*, 2001, **67**, 4919-4921.
119. J. A. Robinson and D. Gani, *Nat. Prod. Rep.*, 1985, **2**, 293-319.
120. C. D. Murphy, D. O'Hagan and C. Schaffrath, *Angew. Chem., Int. Ed.*, 2001, **40**, 4479-4481.
121. C. D. Murphy, C. Schaffrath and D. O'Hagan, *Chemosphere*, 2003, **52**, 455-461.
122. A. Tietz and S. Ochoa, *Arch. Biochem. Biophys.*, 1958, **78**, 477-493.
123. C. Schaffrath, Ph.D. Thesis, *Biosynthesis and Enzymology of Fluorometabolite Production in Streptomyces cattleya*, University of St Andrews, 2002.
124. R. E. London and S. A. Gabel, *Arch. Biochem. Biophys.*, 1996, **334**, 332-340.
125. C. Schaffrath, C. D. Murphy, J. T. G. Hamilton and D. O'Hagan, *J. Chem. Soc., Perkin Trans. I*, 2001, 3100-3105.
126. T.-C. Chou, and P. Talalay, *Biochemistry*, 1972, **11**, 1065-1073.
127. C. Schaffrath, S. L. Cobb and D. O'Hagan, *Angew. Chem., Int. Ed.*, 2002, **41**, 3913-3915.
128. W. Jones, L. C. Kurz and R. Wolfenden, *Biochemistry*, 1989, **28**, 1242-1247.

CHAPTER 1

129. S. L. Cobb, H. Deng, J. T. G. Hamilton, R. P. McGlinchey, D. O'Hagan and C. Schaffrath, *Bioorg. Chem.*, 2005, **33**, 393-401.
130. D. O'Hagan, C. Schaffrath, S. L. Cobb, J. T. G. Hamilton and C. D. Murphy, *Nature*, 2002, **416**, 279.
131. C. Schaffrath, H. Deng and D. O'Hagan, *FEBS Lett.*, 2003, **547**, 111-114.
132. C. Dong, F. Huang, H. Deng, C. Schaffrath, J. B. Spencer, D. O'Hagan and J. H. Naismith, *Nature*, 2004, **427**, 561-465.
133. A. M. Reeve, S. D. Breazeale and C. A. Townsend, *J. Biol. Chem.*, 1998, **273**, 30695-30703.
134. A. K. Ghosh and Y. Wang, *J. Chem. Soc., Perkin Trans. 1*, 1999, 3597-3601.
135. C. Dong, H. Deng, M. Dorward, C. Schaffrath, D. O'Hagan and J. H. Naismith, *Acta Crystallogr. D*, 2003, **59**, 2292-2293.
136. D. O'Hagan, R. J. M. Goss, A. Meddour and J. Courtieu, *J. Am. Chem. Soc.*, 2003, **125**, 379-387.
137. H. Deng, S. L. Cobb, A. R. McEwan, R. P. McGlinchey, J. H. Naismith, D. O'Hagan, D. A. Robinson and J. B. Spencer, *Angew. Chem., Int. Ed.*, 2006, **45**, 759-762.
138. S. L. Cobb, H. Deng, A. R. McEwan, J. H. Naismith, D. O'Hagan and D. A. Robinson, *Org. Biomol. Chem.*, 2006, **4**, 1458-1460.
139. C. D. Cadicamo, J. Courtieu, H. Deng, A. Meddour and D. O'Hagan, *ChemBioChem*, 2004, **5**, 685-690.
140. R. J. Parry and A. Minta, *J. Am. Chem. Soc.*, 1982, **104**, 871-872.
141. M. A. Vincent and I. H. Hillier, *Chem. Commun.*, 2005, 5902-5903.
142. H. M. Senn, D. O'Hagan and W. Thiel, *J. Am. Chem. Soc.*, 2005, **127**, 13643-13655.

CHAPTER 1

143. X. Zhu, D. A. Robinson, A. R. McEwan, D. O'Hagan and J. H. Naismith, *J. Am. Chem. Soc.*, 2007, **129**, 14597-14604.
144. M. J. Pugmire and S. E. Ealick, *Biochem. J.*, 2002, **361**, 1-25.
145. M. D. Erion, K. Takabayashi, H. B. Smith, J. Kessi, S. Wagner, S. Honger, S. L. Shames and S. E. Ealick, *Biochemistry*, 1997, **36**, 11725-11734.
146. S. L. Cobb, Ph.D. Thesis, *The origin and metabolism of 5'-FDA in Streptomyces cattleya*, University of St Andrews, 2005.
147. S. L. Cobb, H. Deng, J. T. G. Hamilton, R. McGlinchey and D. O'Hagan, *Chem. Commun.*, 2004, 592-593.
148. R. P. McGlinchley, Ph.D. Thesis, *Intermediates and enzymes involved in fluorometabolite biosynthesis in Streptomyces cattleya*, University of St Andrews, 2006.
149. F. Huang, S. F. Haydock, D. Spiteller, T. Mironenko, T.-L. Li, D. O'Hagan, P. F. Leadlay and J. B. Spencer, *Chem. Biol.*, 2006, **13**, 475-484.

CHAPTER 2

**Identification of 5-FDRuIP
as an intermediate in
fluorometabolite biosynthesis
in *Streptomyces cattleya***

Identification of 5-FDRulP as an intermediate in fluorometabolite biosynthesis in *Streptomyces cattleya*

5-Deoxy-5-fluoro- α ,D-ribose-1-phosphate (5-FDRP) **61** has been identified as the second intermediate on the fluorometabolite biosynthetic pathway in *S. cattleya*.¹ It arises by the action of a purine-nucleoside phosphorylase (PNPase) on 5'-deoxy-5'-fluoroadenosine (5'-FDA) **47**. Fluoroacetaldehyde **26** was already known to be the last common intermediate to both fluoroacetate **17** and 4-fluorothreonine **39**.² However, metabolic intermediates that exist between 5-FDRP **61** and fluoroacetaldehyde **26** remained to be characterised. It was the focus of this work to identify these intermediates.

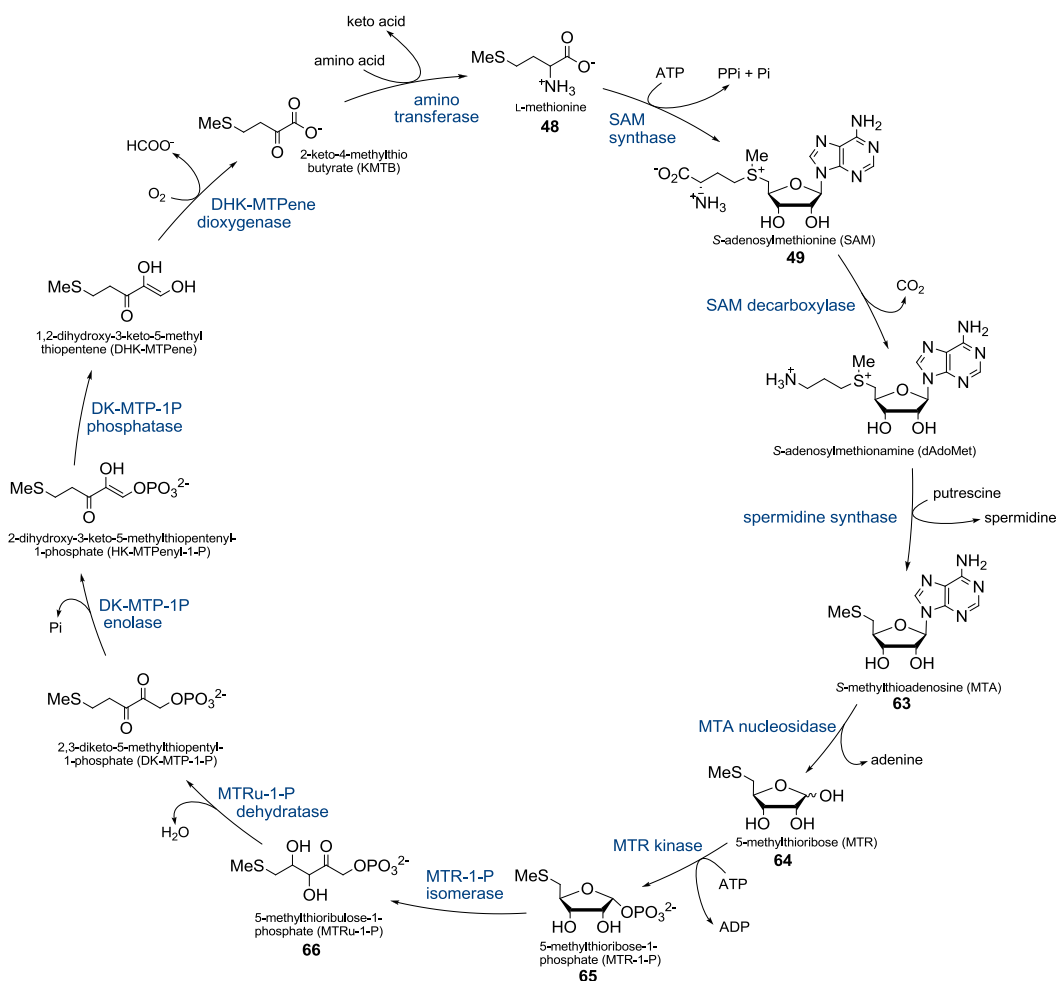
The results described in this chapter indicate that 5-deoxy-5-fluoro-D-ribulose-1-phosphate (5-FDRulP) **69** is the next formed fluorometabolite after 5-FDRP **61**.³ The enzyme responsible for the conversion of 5-FDRP **61** to 5-FDRulP **69** has been identified as an isomerase. In order to understand the metabolic fate of 5'-FDA **47** and the next fluorinated intermediates on the pathway, a short overview of biochemical processes involving the metabolism of structurally similar nucleosides is given below.

2.1 L-Methionine salvage pathway

The methionine salvage pathway is universally used to regenerate the amino acid L-methionine **48**, crucial in many cellular functions, and to maintain its levels *in vivo*. Most organisms, from bacteria through plants to mammals, have evolved this route to surmount the energy consuming assimilation of sulfur.⁴ In this way, organic sulfur is recovered from 5-methylthioribose (MTR) **64**, which is derived from the *S*-methylthioadenosine (MTA) **63** that is a by-product of other reactions involving SAM **49** (Scheme 2.1, *vide infra*). This metabolic pathway has been the subject of study due to its role in a variety of human tumour tissues.^{5,6,7} Also some analogs of MTR **64** have been shown to be growth inhibitors of the malarial protozoan, *Plasmodium falciparum*.^{8,9,10}

This metabolic route has been extensively studied in the gram-negative bacterium *Klebsiella pneumoniae*, where all of the genes and reactions have been revealed.^{11,12,13,14,15,16}

Very recently, the genes encoding the enzymes of all steps in this cycle have been also identified in the commonly used eukaryotic model system, the yeast *Saccharomyces cerevisiae*,¹⁷ as well as in the non-photosynthetic bacterium *Bacillus subtilis*.¹⁸ Scheme 2.1 illustrates the methionine salvage pathway, as revealed in *Bacillus subtilis*.¹⁹



Scheme 2.1 Methionine salvage pathway in *Bacillus subtilis*.¹⁹

The beginning of the pathway is variable, even in phylogenetically related organisms. Briefly, MTA **63**, a product of spermidine metabolism, is converted into MTR **64** by the action of a MTA nucleosidase. Then, a MTR kinase acts upon MTR **64** to yield 5-methylthio- α ,D-ribose-1-phosphate (MTR-1-P) **65**, a compound that is isomerised to 5-methylthio-ribulose-1-phosphate (MTRu-1-P) **66** by a MTR-1-P isomerase (encoded in *B. subtilis* by gene *mtnA*). Remarkably, it has been observed that this gene, expressed at a level similar to that of the MTR kinase (*mtnK*), codes for a protein with a sequence as similar to that of the eukaryotic initiation factor eIF2B. Then, MTRu-1-P **66** is further metabolised by a dehydratase (encoded

by gene *mtnW*), an enzyme sharing high similarities to ribulose 1,5-bisphosphate carboxylase/oxygenase (RuBisCO), the most abundant naturally occurring protein.^{4,18,20,21} Further along the pathway, MTR **64** can accumulate and becomes extremely toxic to the cell in the absence of *mtnW*, opening an unexpected target for new antimicrobial drugs.¹⁸

2.1.1.1 5-Deoxy-5-methylthio- α ,D-ribose-1-phosphate isomerases

Abeles and co-workers¹¹ first identified the action of 5-deoxy-5-methylthio- α ,D-ribose-1-phosphate isomerase (MTR-1-P isomerase) in *Klebsiella pneumoniae*, where it was shown that 5-S-methyl-5-thio- α ,D-ribose-1-phosphate (MTR-1-P) **65** undergoes an isomerisation to (3*R*,4*S*)-5-methylthioribulose-1-phosphate (MTRul-1-P) **66** (as illustrated for *B. subtilis* in Scheme 2.1, *vide supra*). A number of MTR-1-P isomerases have since been purified from bacteria²⁰ and yeast²² after gene cloning, and the yeast structure has been solved by X-ray analysis.²²

As previously mentioned, the gene (*mtnA*) of the MTR-1-P isomerase from *Bacillus subtilis* codes for a protein with a sequence annotated as similar to a family of eukaryotic initiation factors, eIF2B.^{4,23} Consequently, the amino acid sequence similarity between the *B. subtilis* MTR-1-P isomerase and related protein sequences, assigned as putative translation initiation factor eIF2B, from *Streptomyces coelicolor*, *Streptomyces avermitilis*, *Klebsiella pneumoniae* and *Saccharomyces cerevisiae* shows a high degree of homology (Figure 2.1, *vide infra*).

CHAPTER 2

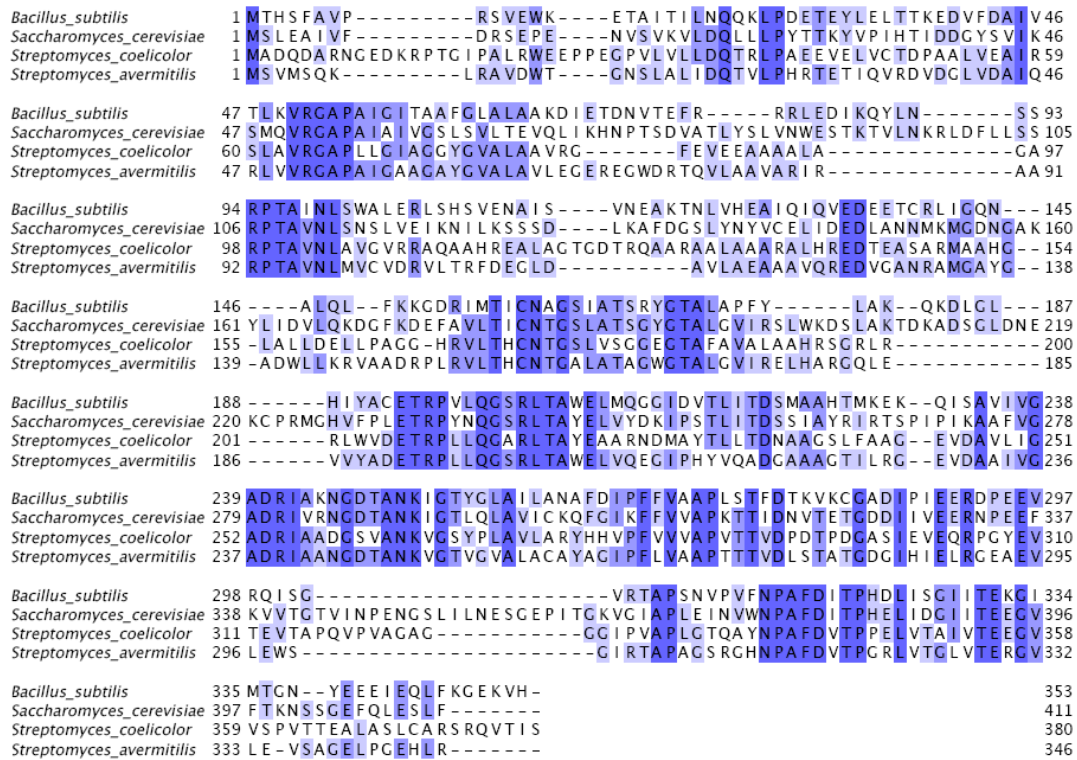


Figure 2.1 MTRP isomerase sequence alignments.

Figure 2.1 illustrates this homology. For example, the *S. coelicolor* eIF2B shows a 32% identity and 52% similarity to the MTR-1-P isomerase from *B. subtilis*. This observation tentatively suggests that these putative translation initiation factors have been misassigned, and they are actually related to MTR-1-P isomerases. Recently, one of these proteins from *S. cerevisiae* (Ypr118w) was crystallised and characterised as a MTR-1-P isomerase.²² It was shown that Ypr118w is required for yeast cells to grow on MTA **63** in the absence of L-methionine **48**, thus confirming the role of Ypr118w in the methionine salvage pathway in *S. cerevisiae*. This yeast isomerase shares 37% sequence identity to that from *B. subtilis* and a 26-28% identity to the eIF2B from *Schizosaccharomyces pombe* and *S. cerevisiae*.²²

2.2 The metabolism of 5'-FDA in *S. cattleya*

Work developed by C. Schaffrath in 2003 (University of St Andrews) focused on the metabolic fate of 5'-FDA **47** in *S. cattleya*.²⁴ It was shown that **47** supports fluorometabolite biosynthesis in *S. cattleya* when incubated in CFEs of the bacterium, generating fluoroacetate **17** and 4-fluorothreonine **39** with other fluorinated intermediates.

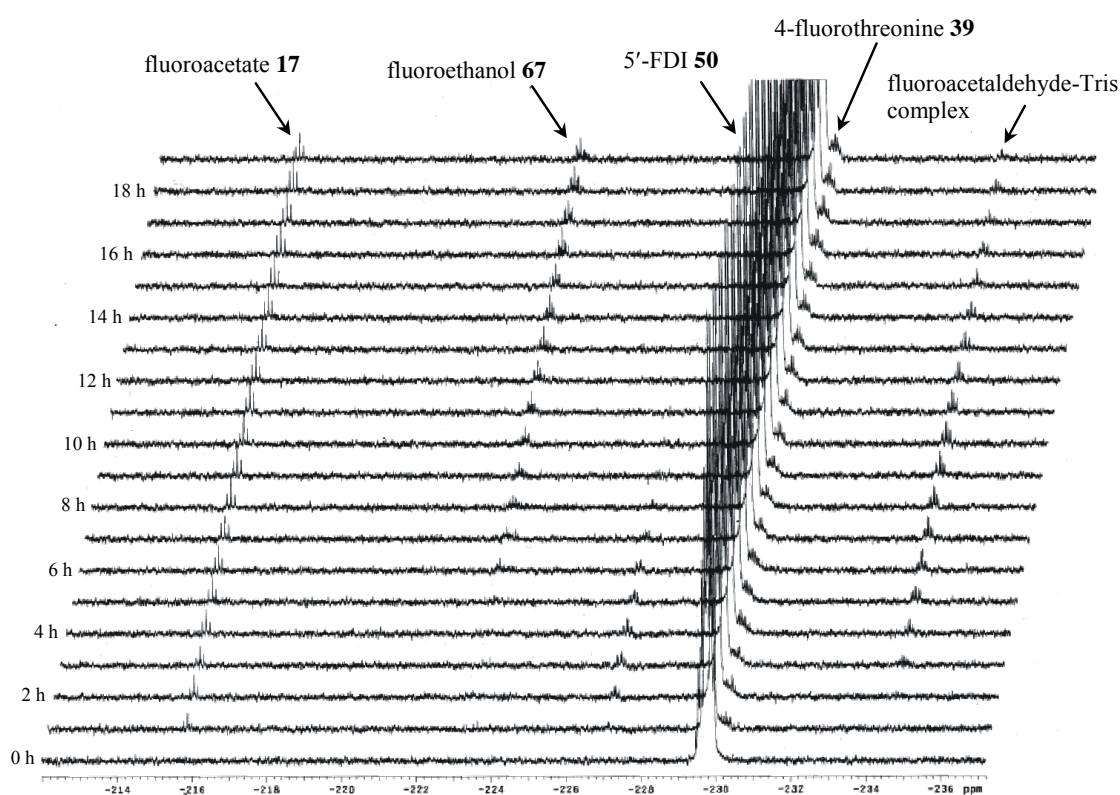
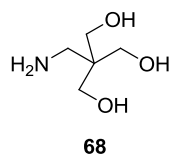
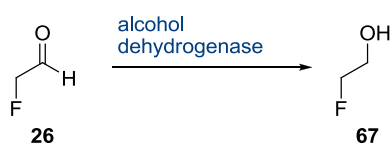


Figure 2.2 $^{19}\text{F}\{^1\text{H}\}$ NMR time course of production of fluorinated intermediates in a CFE of *S. cattleya* when incubated with 5'-FDA **47** (20 mM) at 25 °C for 19 h.

As shown in Figure 2.2 (*vide supra*), the incubation of 5'-FDA **47** in a CFE of *S. cattleya* also led to the formation of a complex between fluoroacetaldehyde **26** and tris(hydroxymethyl)aminoethane **68**, the constituent of Tris buffer.



Surprisingly, fluoroethanol **67** was detected in such incubations, indicating the capacity of the CFE to reduce fluoroacetaldehyde **26** to fluoroethanol **67** (Scheme 2.2)



Scheme 2.2 Biotransformation of fluoroacetaldehyde **26** to fluoroethanol **67** catalysed by an alcohol dehydrogenase in *S. cattleya*.

The fact that 4-fluorothreonine **39** is generated implies that all of the enzymes and co-factors are present in the CFE for its biosynthesis from 5'-FDA **47**. Further work was carried out to investigate the fluorinated intermediates on the biosynthetic pathway to fluoroacetaldehyde **26**. To this end, the biotransformation of 5'-FDA **47** in CFEs of *S. cattleya* was followed in real time by ^{19}F NMR spectroscopy.²⁵ Thus, 5'-FDA **47** (100 μl , 18.6 mM) was incubated in an active CFE (500 μl) at 37 $^{\circ}\text{C}$ and followed by $^{19}\text{F}\{^1\text{H}\}$ NMR hourly. The time course spectra are shown in Figure 2.3 (*vide infra*).

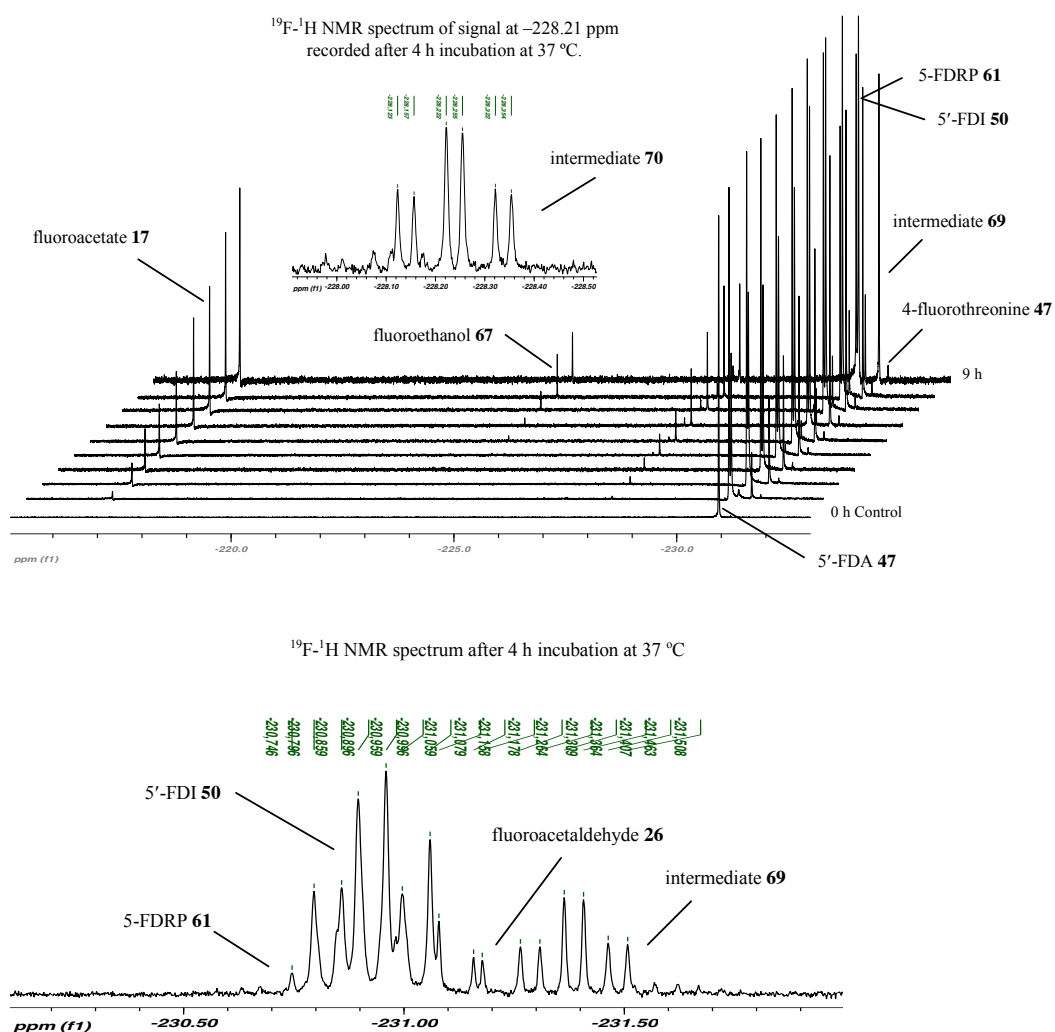


Figure 2.3 $^{19}\text{F}\{^1\text{H}\}$ NMR spectra of 5'-FDA **47** incubation in a CFE of *S. cattleya* at 37°C for 9 h.

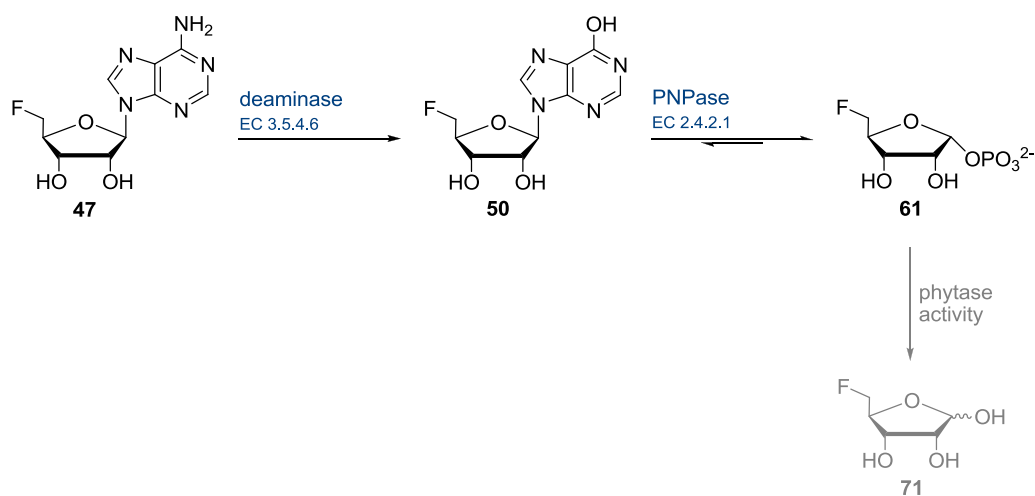
The resultant $^{19}\text{F}\{^1\text{H}\}$ NMR spectra shown in Figure 2.3 clearly indicates a number of fluoro-organic compounds derived from the incubation of 5'-FDA **47**. The time course showed the generation of fluoroacetate **17** and 4-fluorothreonine **39**, consistent with the intermediacy of 5'-FDA **47**. Production of 5-FDRP **61**, the next intermediate after 5'-FDA **47** in the fluorometabolite biosynthetic pathway, was also observed due to the action of a purine-nucleoside phosphorylase (PNPase). The rapid conversion of 5'-FDA **47** to 5'-FDI **50** is apparent by the action of adenosine deaminase present in the CFE. The transformation of

5-FDRP **61** is shown to proceed to compound **69** (−231.34 ppm) which appears after 2 h of incubation and accumulates over time. Production of fluoroacetaldehyde **26** is transient during the time course with later formation of compound **70**. In order to gain an insight into the biosynthesis of the next fluorometabolite in the pathway, the metabolism of 5-FDRP **61** was studied.

2.3 The metabolism of 5-FDRP in *S. cattleya*

2.3.2 Preparation of 5-FDRP **61**

5-Deoxy-5-fluoro- α ,D-ribose-1-phosphate (5-FDRP) **61** was already established as an intermediate on the fluorometabolite pathway.¹ The metabolism of 5-FDRP **61** in a CFE of *S. cattleya* was studied in order to explore the hypothesis that an isomerase enzyme is operating in *S. cattleya*, and to elucidate the remaining fluorinated intermediates on the biosynthetic pathway. With this objective, it was necessary to prepare a sample of **61** for incubation studies with cell free extracts of the bacterium. This was achieved following a chemo-enzymatic approach, as outlined in Scheme 2.3 (*vide infra*).



Scheme 2.3 Chemo-enzymatic preparation of 5-FDRP **61**.

A synthetic sample of 5'-FDA **47** (synthetic procedure described in Chapter 3) was treated with 5'-adenylic acid deaminase (EC 3.5.4.6, from *Aspergillus sp.* Bacterium, Aldrich™) to generate 5'-FDI **50**, the fluorinated unnatural substrate for a purine-nucleoside phosphorylase (supplied by GlaxoSmithKline), as previously described.¹ This PNPase enzyme (EC 2.4.2.1) mediates the reversible phosphorolysis reaction to generate 5-FDRP **61** along with 5-FDR **71**, as a result of a contaminating phytase activity present in the immobilised enzyme preparation. As a consequence, this chemo-enzymatically prepared sample of **61** contains residual 5'-FDI **50** and 5-FDR **71**. However, both **50** and **71** have been studied previously and are not biotransformed to the fluorometabolites in *S. cattleya*. They are recovered intact in CFE incubations of the bacterium.^{1,26}

This chemo-enzymatic preparation of 5-FDRP **61** was used in CFE incubations of the bacterium.

2.3.3 The effect of EDTA on fluorometabolite production

Previous studies showed that the production of FAc **17** was arrested when EDTA was present in CFE incubations. EDTA is a well known chelator of metal ions and it appears to inhibit a zinc-dependent aldolase in the cell-free extract, operating later on in the pathway.²⁵ Accordingly, an experiment was conducted in which an active CFE (500 μ l) was pre-incubated with EDTA (30 mM) at 37 °C for 30 min. After this time, the 5-FDRP **61** preparation, also containing 5'-FDI **50** and 5-FDR **71**, was added to the pre-incubated cell-free extract. The reaction was monitored by ¹⁹F NMR spectroscopy at hourly intervals, and the resultant time course is shown in Figure 2.4 (*vide infra*).

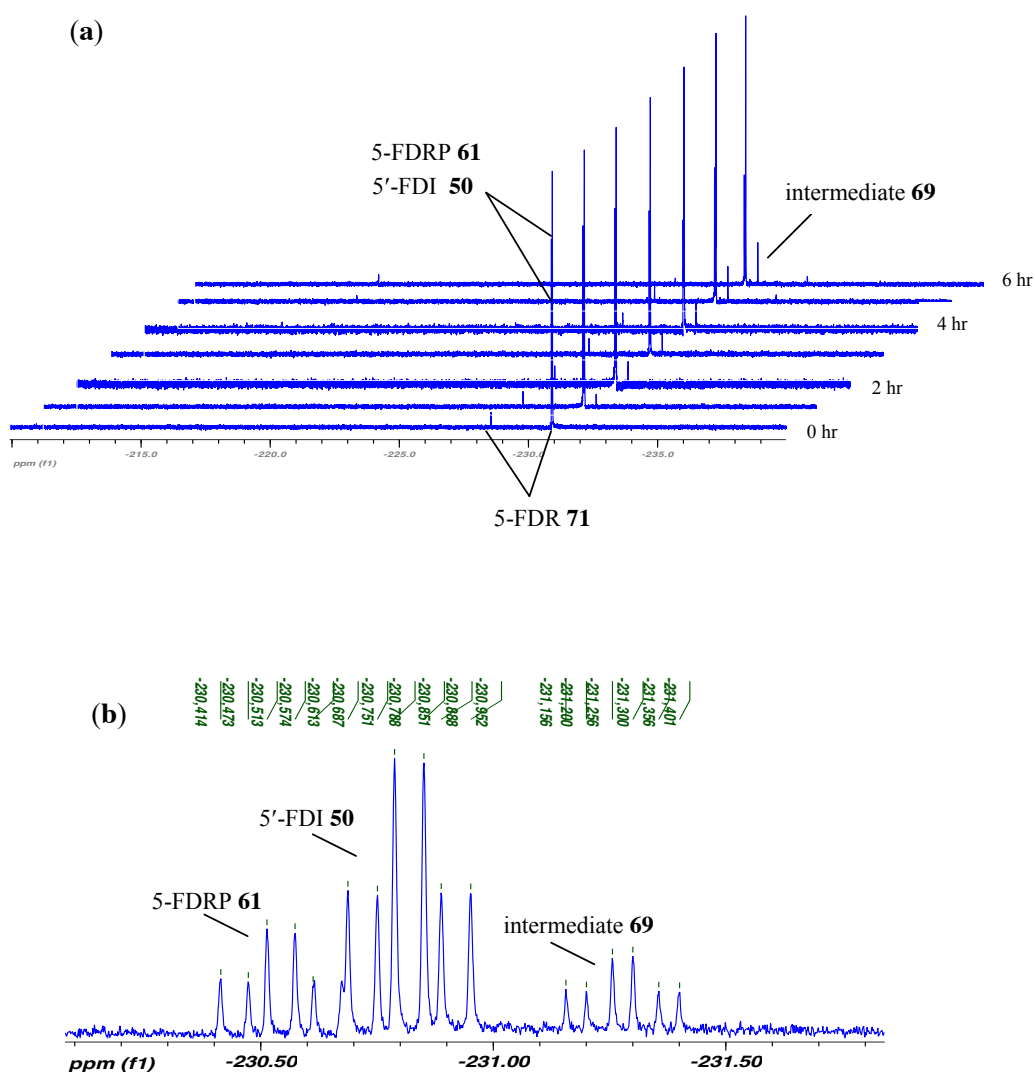


Figure 2.4 (a) $^{19}\text{F}\{^1\text{H}\}$ NMR time course of a CFE of *S. cattleya* incubated with 5-FDRP **61** and EDTA at 37 °C for 6 h. (b) ^{19}F - ^1H NMR spectrum after 6 h, expansion of region -231.10 ppm to -231.80 ppm.

The production of FAc **17** was arrested and this led to the accumulation of a new fluorometabolite clearly evident by ^{19}F NMR (-231.34 ppm, dt, $^2J_{\text{F-H}}$ 47.0 Hz and $^3J_{\text{F-H}}$ 20.9Hz) as shown in Figure 2.4 (*vide supra*), alongside residual 5'-FDI **50** and contaminating 5-FDR **71**.

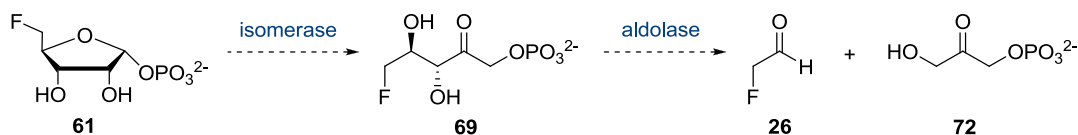
2.3.4 Isomerisation of 5-FDRP to 5-FDRuP

The MTR-1-P isomerase offered a model in metabolism to make the link in the fluorometabolite pathway in *S. cattleya*, where fluorine replaces the methylthio substituent at C-5. An analogous isomerisation on 5-deoxy-5-fluoro- α ,D-ribose-1-phosphate (5-FDRP) **61** would generate 5-deoxy-5-fluoro-D-ribulose-1-phosphate (5-FDRuP) **69**, as outlined in Scheme 2.4 (*vide infra*).



Scheme 2.4 Putative isomerisation of 5-FDRP **61** to 5-FDRuP **69** in *S. cattleya*.

The presence of an isomerase enzyme in *S. cattleya* yielding 5-FDRuP **69** is an attractive hypothesis, as ribulose phosphates are classical products/substrates of DHAP-dependent aldolase enzymes.^{27,28,29} An aldolase could then mediate a reverse aldol reaction to give dihydroxyacetone phosphate (DHAP) **72** and fluoroacetaldehyde **26**, which has been already established as a biosynthetic intermediate.² Such an isomerase to aldolase sequence represents a realistic metabolic pathway that could account for the conversion of 5-FDRP **61** to FAd **26**, as outlined in Scheme 2.5.



Scheme 2.5 Putative enzymes for the conversion of 5-FDRP **61** to FAd **26** in *S. cattleya*.

In order to test this hypothesis, the stepwise metabolism of 5-FDRP **61** in *S. cattleya* was investigated.

2.3.4.1 5-FDRuIP as a biosynthetic intermediate

The product mixture of 5-FDRP **61** (100 μ l) was incubated in a cell-free extract of *S. cattleya* (500 μ l) at 37 °C, and the biosynthetic fate of **61** was followed by ^{19}F NMR spectroscopy at hourly intervals for 6 h. The $^{19}\text{F}\{^1\text{H}\}$ NMR time course of this incubation is shown in Figure 2.5.

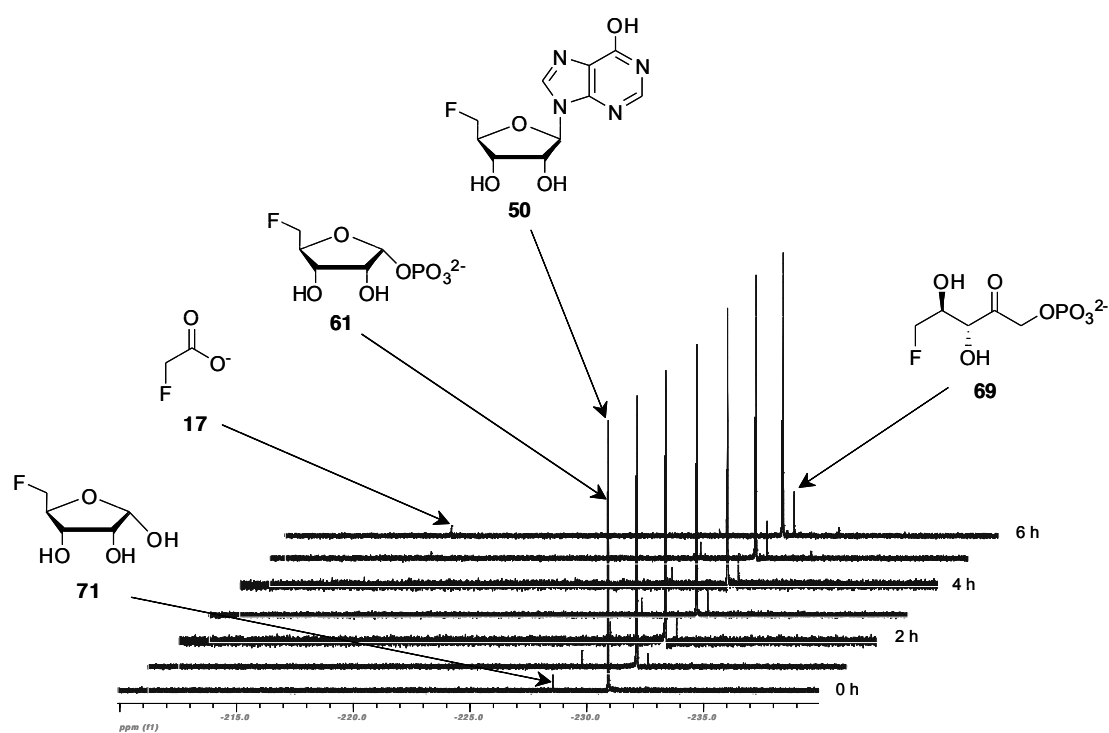


Figure 2.5 $^{19}\text{F}\{^1\text{H}\}$ NMR time course of a CFE of *S. cattleya* incubated with a sample of 5-FDRP **61** at 37 °C for 6 h.

The incubation of **61** showed the accumulation of FAc **17**, consistent with its conversion in the cell free extract. The production of fluoroacetate **17** is consistent with the previously reported ability of 5-FDRP **61** to support fluorometabolite biosynthesis in *S. cattleya*.¹ However, a new signal corresponding to the next formed fluorometabolite was also observed

in this experiment. It was initially attributed to 5-deoxy-5-fluoro-D-ribulose-1-phosphate (5-FDRulP) **69**, the product of a putative isomerase operating in *S. cattleya*.

A product mixture of 5-FDRulP **69** was also analysed by GC-MS after derivatisation with *N*-methyl-*N*-(trimethylsilyl)trifluoroacetamide (MSTFA) following the method described by Hamilton *et al.*³⁰ to generate the persilylated ribulose phosphate derivative. Control experiments with GC-MS (CI -ve ion mode) were carried out on the substrate and the product mixtures as their persilylated derivatives, illustrated in Figure 2.6.

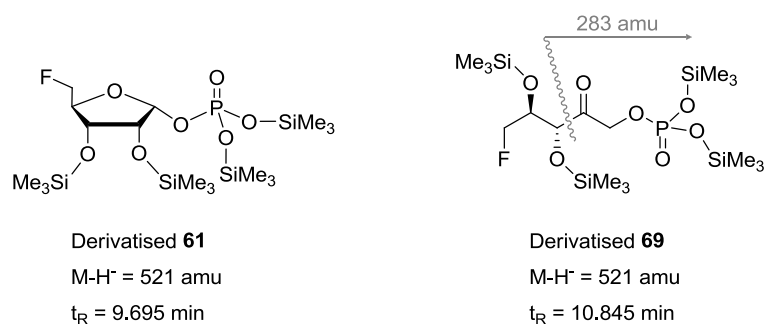


Figure 2.6 Persilylated derivatives of 5-FDRP **61** and 5-FDRulP **69** analysed by GC-MS (CI) after treatment with MSTFA.

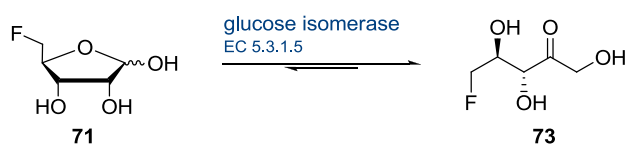
Despite the identical molecular masses for these isomers, the product 5-FDRulP **69** was clearly distinguished from the incubated 5-FDRP **61** by very different retention times. A molecular ion on 521 amu was the predominant ion and the location of the phosphate at the C-1 position was confirmed by the presence of a mass ion at 283 amu.

A. Preparation of 5-FDRul **73**

Immobilised glucose isomerase (EC 5.3.1.5, Sweetzyme T) has been reported to convert (2*R*,3*R*)-configured aldotetrose as well as D-ribofuranoses, modified at C-5, into the

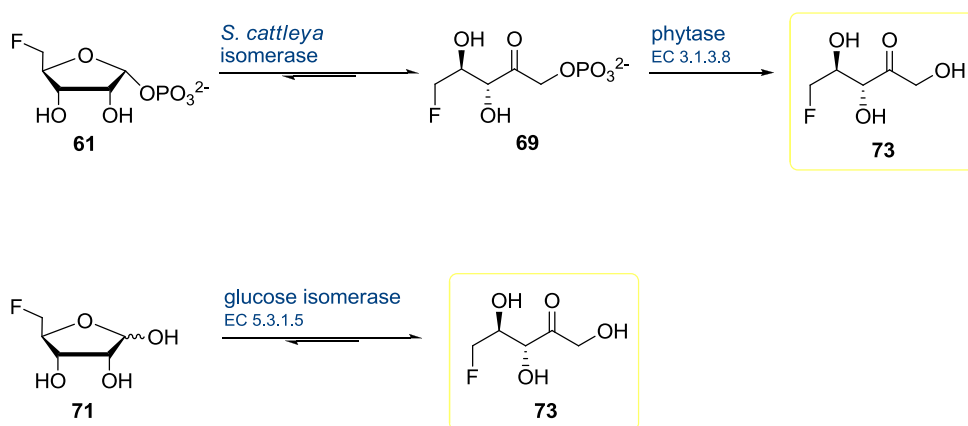
corresponding open-chain 2-ketoses, the latter being the predominant products of the isomerisation reactions.^{31,32}

The product of the isomerisation reaction on 5-FDR **71** is 5-deoxy-5-fluoro-D-ribulose (5-FDRul) **73**, the de-phosphorylated analogue of 5-FDRulP **69**, a postulated biosynthetic intermediate in the fluorometabolite pathway. Scheme 2.6 illustrates this enzyme-catalysed isomerisation reaction.³¹



Scheme 2.6 Chemo-enzymatic synthesis of 5-FDRul **73** with commercial glucose isomerase.

Therefore, to further secure the identity of 5-FDRulP **69**, it was envisaged that the stereochemistry of 5-FDRulP **69** could be established by correlation, by investigating the stereochemistry of 5-FDRul **73**. The strategy is shown in Scheme 2.7.



Scheme 2.7 Strategy to establish the stereochemistry of the intermediate 5-FDRulP **69** in *S. cattleya* by dephosphorylation and cross reference to 5-FDRul **73**.

Accordingly, each of the resulting samples of 5-FDRuIP **69** from the experiment illustrated in Figure 2.5 (*vide supra*), was treated with a commercial phosphatase (EC 3.1.3.8, from *Aspergillus ficuum*, Aldrich™) (100 μ l, 10 mg/ml). This resulted in an immediate change of the ^{19}F NMR chemical shift of the fluorinated metabolite **69** from -231.34 ppm to -231.22 ppm, indicating that a chemical transformation had occurred, consistent with phosphate cleavage. The results are presented in Figure 2.7.

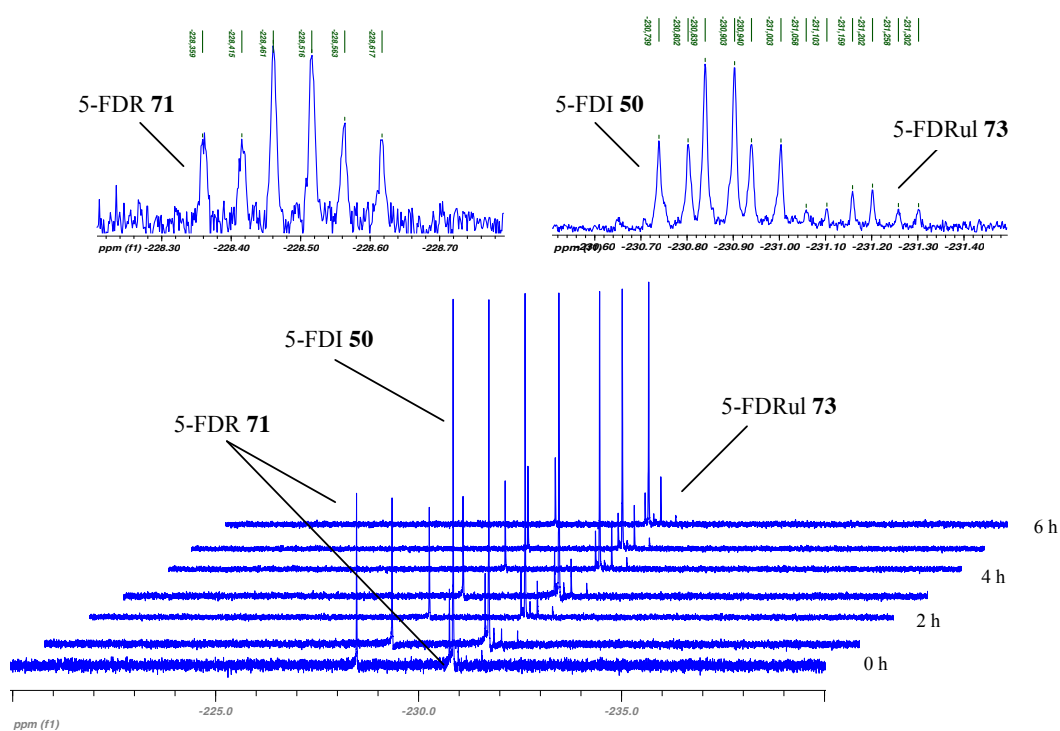


Figure 2.7 $^{19}\text{F}\{^1\text{H}\}$ NMR spectra after addition of a phytase to the samples from time course in Figure 2.5. Insets are ^{19}F NMR expansions of the product peaks without $\{^1\text{H}\}$ decoupling.

CHAPTER 2

This set of experiments supported the conversion of 5-FDRP **61** to 5-FDRulP **69**, and then to the free sugar 5-deoxy-5-fluoro-D-ribulose (5-FDRul) **73** by the action of the added phosphatase.

For further confirmation, a sample of 5-deoxy-5-fluoro-D-ribose (5-FDR) **71** was prepared independently as a reference compound to cross reference the product generated from the sequence of biotransformations described above. Open-chain 2-keto sugars have been synthesised from glucose isomerase catalysed isomerisation of the corresponding D-ribo and D-xylofuranoses as shown in Scheme 2.6 (*vide supra*).^{31,32}

Therefore, a stereochemically pure sample of 5-FDR **71** was prepared by synthesis as described in Chapter 3. Immobilised glucose isomerase (EC 5.3.1.5, Sweetzyme T from *S. murinus*) was used for the production of 5-FDRul **73** from 5-FDR **71**. Accordingly, an aqueous solution of 5-FDR **71** (4.7 mM) was incubated with immobilised glucose isomerase (30 mg) at 37 °C. The reaction was monitored by ¹⁹F NMR spectroscopy and a time course is illustrated in Figure 2.8 (*vide infra*).

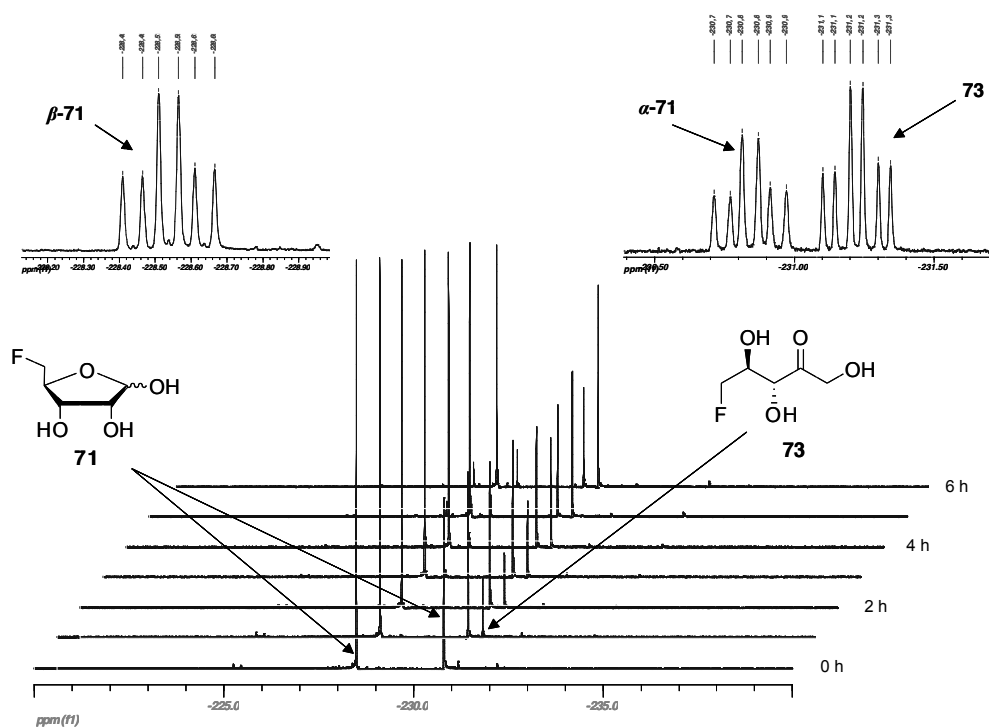


Figure 2.8 $^{19}\text{F}\{^1\text{H}\}$ NMR time course of 5-FDR **71** (4.7 mM) incubated with a commercial immobilised glucose isomerase at 37 °C. Insets are non-decoupled ^{19}F NMR expansions of the product signals. Traces of product 5-FDRul **73** are detected by ^{19}F NMR in the 0 h sample due to the initial running time of the experiment (approx. 30 min.).

The two anomers of the 5-FDR **71** starting material, (β -anomer: -228.53 ppm, dt, $^2J_{\text{F-H}}$ 46.5 Hz and $^3J_{\text{F-H}}$ 26.0 Hz; α -anomer: -230.83 ppm, dt, $^2J_{\text{F-H}}$ 46.5 Hz and $^3J_{\text{F-H}}$ 27.9 Hz) dominated at the outset and over time the 5-FDRul **73** product signal at -231.22 ppm (dt, $^2J_{\text{F-H}}$ 46.9 Hz and $^3J_{\text{F-H}}$ 20.5 Hz) accumulates. Incubation times longer than 6 h did not result in further accumulation of product due to the reversible reaction reaching an equilibrium. Notably the ^{19}F NMR product signal at -231.22 ppm for **73** has an identical chemical shift and coupling pattern to the product observed after incubating 5-FDRP **61** and EDTA with the cell free extract of *S. cattleya*, followed by phosphatase treatment.

Co-addition of the glucose isomerase reaction product to that of the EDTA-cell-free extract/phosphatase reaction gave identical products as judged by ^{19}F NMR as shown in Figure 2.9.

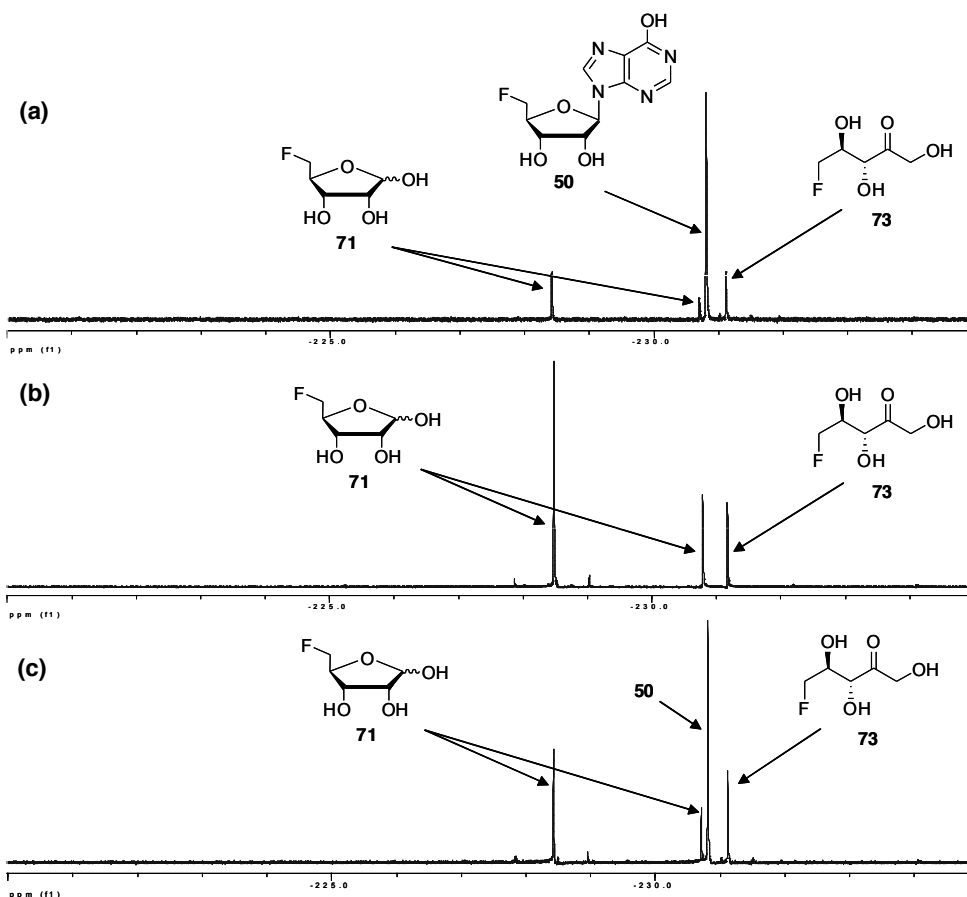
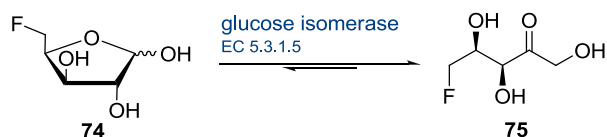


Figure 2.9 $^{19}\text{F}\{^1\text{H}\}$ NMR spectra of : (a) *S. cattleya* cell-free extract incubation of 5-FDRP **61**/5'-FDI **50** and subsequent treatment with phosphatase. (b) 5-FDRul **73** generated by incubation of synthetic 5-FDR **71** with glucose isomerase. (c) Co-addition of these samples indicating that the $^{19}\text{F}\{^1\text{H}\}$ NMR signal for **73** perfectly overlaps.

For comparison, a sample of 5-deoxy-5-fluoro-D-xylose (5-FDX) **74** was also prepared by synthesis (outlined in Chapter 3) in a stereospecific manner. Incubation of this furanose isomer with glucose isomerase would then generate 5-deoxy-5-fluoro-D-xylulose

(5-FDXul) **75**. The strategy for the chemo-enzymatic preparation of the diastereoisomer of **73** is illustrated in Scheme 2.8.



Scheme 2.8 Chemo-enzymatic synthesis of 5-FDXul **75**.

The synthesis of 5-FDX **74** was achieved *via* the synthetic procedure described in Chapter 3. With **74** in hand, a glucose isomerase catalysed isomerisation reaction was carried out by incubating an aqueous solution of 5-FDX **74** (1 ml, 4.7 mM) with glucose isomerase (30 mg) at 37 °C for 3 h. The reaction was monitored by ^{19}F NMR spectroscopy every hour. The resultant ^{19}F NMR time course is illustrated in Figure 2.10 (*vide infra*).

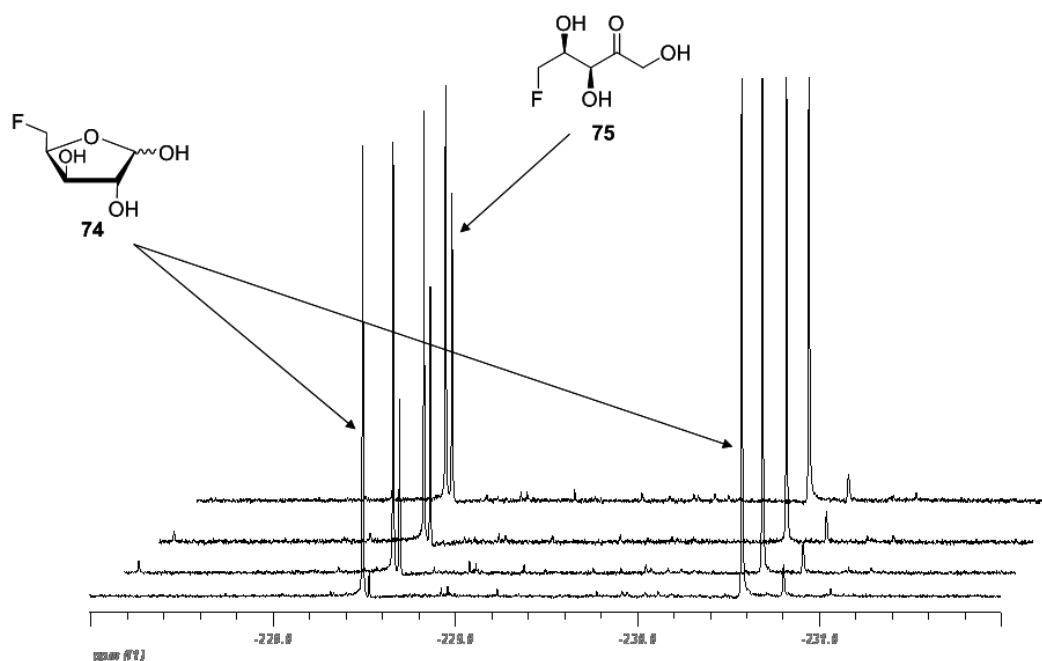


Figure 2.10 ^{19}F $\{^1\text{H}\}$ NMR time course of 5-FDX **74** (4.7 mM) incubated with a commercial immobilised glucose isomerase at 37 °C for 3 h. Traces of product 5-FDXul **75** are detected by ^{19}F NMR in the 0 h sample due to the initial running time of the experiment (approx. 30 min.).

After 1 h of incubation, the ^{19}F NMR spectrum showed the production of **75** with a new fluorine signal at -228.55 ppm (dt, $^2J_{\text{F-H}}$ 46.2 Hz and $^3J_{\text{F-H}}$ 15.3 Hz). The product of this reaction, 5-FDXul **75** does not correlate with the product of the cell-free extract plus phytase treatment. These results confirm that the product of the cell-free extract is indeed diastereoisomer **73**, as expected, and not diastereoisomer **75**.

Taken together, this set of complementary biotransformations secures 5-FDRulP **69** as an intermediate formed immediately after 5-FDRP **61** on the pathway to the secondary fluorometabolites FAc **17** and 4-FT **39** in *S. cattleya*. The reaction involves an isomerisation, which finds precedent in the isomeration of the methylthiosugars in the methionine salvage pathway.

B. The role of 5-FDRul **73**

The capability of 5-FDRul **73**, the dephosphorylated product of 5-FDRulP **69**, to support fluoroacetate **17** and 4-fluorothreonine **39** production was explored. The aforementioned chemo-enzymatic approach was used to prepare a sample of 5-FDRul **73** for incubation studies. Accordingly, 5-deoxy-5-fluoro-D-ribose **71** was prepared by synthesis (as described in Chapter 3) and incubated with the enzyme. This preparation of 5-FDRul **73** also contained 5-FDR **71**, which has already shown to be metabolically inert within *S. cattleya*. Consequently, an active CFE (500 μ l) was incubated with this 5-FDRul **73** preparation (100 μ l) for 16 h at 37 $^{\circ}$ C. The resulting spectra of the biotransformation are shown in Figure 2.11.

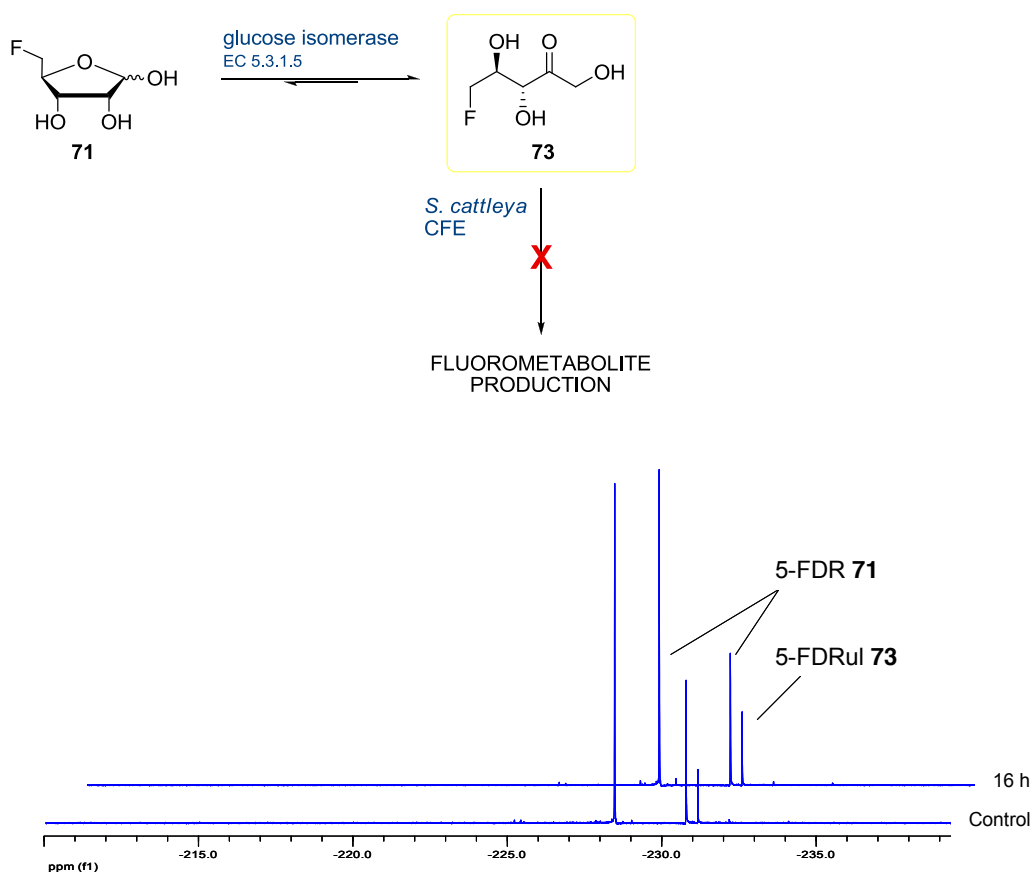


Figure 2.11 ^{19}F $\{^1\text{H}\}$ NMR spectra of 5-FDRul **73** incubated in a CFE of *S. cattleya*.

CHAPTER 2

The ^{19}F $\{^1\text{H}\}$ NMR spectra clearly show that no biotransformation occurred when the product of the glucose isomerase reaction on 5-FDR **71**, 5-FDRul **73**, was incubated in a CFE of *S. cattleya*, indicating that 5-FDRul **73** does not support the biosynthesis of fluoroacetate **17** and 4-fluorothreonine **39**.

2.3.4.2 Purification of the isomerase

A. Assay for isomerase activity

In order to purify the isomerase enzyme from *S. cattleya*, a suitable assay was required. Thus, the conversion of 5-FDRP **61** to 5-FDRulP **69** catalysed by the isomerase was monitored by ^{19}F NMR spectroscopy. The assay is described in detail in Chapter 5, and was used at each purification stage.

B. Step 1: Ammonium sulfate precipitation

In the first stage of the isomerase purification, the crude cell-free extract was subjected to ammonium sulfate precipitation to salt out the desired protein. Accordingly, ammonium sulfate $(\text{NH}_4)_2\text{SO}_4$ was added to an active CFE and the solution was left to stir for 20 min at 4 °C. Protein precipitations were carried out using four $(\text{NH}_4)_2\text{SO}_4$ cuts (0-35%, 35-50%, 50-60%, 60-80%). After this time the precipitated protein was removed by centrifugation (14000 rpm, 20 min) and the supernatant used for the next $(\text{NH}_4)_2\text{SO}_4$ cut. Each of the $(\text{NH}_4)_2\text{SO}_4$ cuts was assayed in the following manner. Partially purified CFE (200 μl) was supplemented with 5-FDRP **61** prepared by the method outlined in Chapter 5 and incubated for 16 h at 37 °C. The resulting samples were then analysed by ^{19}F NMR spectroscopy. The resultant ^{19}F NMR spectra are shown in Figure 2.12 (*vide infra*).

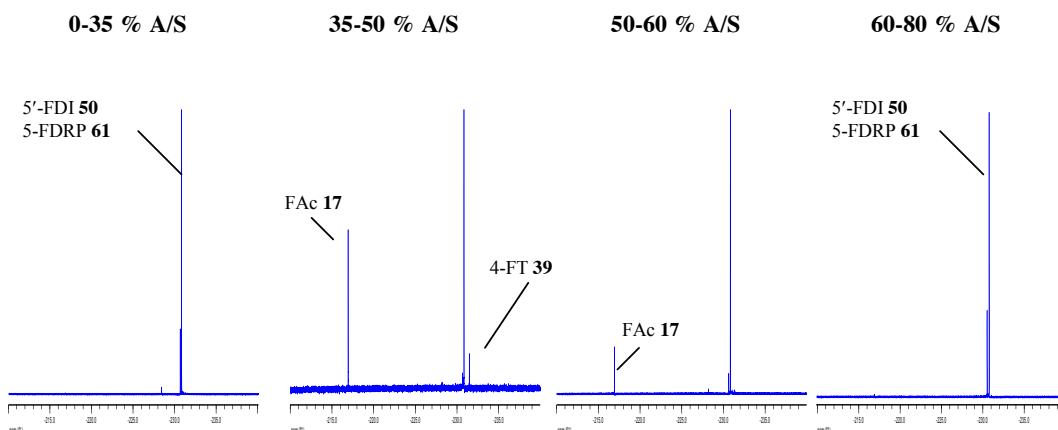


Figure 2.12 ^{19}F $\{^1\text{H}\}$ NMR spectra of ammonium sulfate cuts of the isomerase incubated with 5-FDRP **61**.

Analysis of the ammonium sulfate cuts actually revealed that the 35-60% cut contained all of the biosynthetic enzymes and co-factors required to support fluoroacetate **17** and 4-fluorothreonine **39** biosynthesis. The isomerase activity is found predominantly in the 35-50% cut with a less activity in the 50-60 % cut. No isomerase activity was detected in any of the other fractions, which only showed presence of 5-FDRP **61** and 5'-FDI **50**.

The isomeration of 5-FDRP **61** to 5-FDRuIP **69** could not be detected in real time because assay of the samples involved pre-incubation with EDTA. The 35-50% cut (100 μl) was pre-incubated with EDTA for 25 min at 37 $^{\circ}\text{C}$. After this time, the pre-incubated sample was supplemented with 5-FDRP **61** and incubated for 16 h at 37 $^{\circ}\text{C}$. Analysis by ^{19}F NMR spectroscopy (Figure 2.13) showed that the 35-50% cut was able to support the synthesis of 5-FDRuIP **69**, implying that the addition of a metal ion co-factor is not required for the isomerisation reaction.

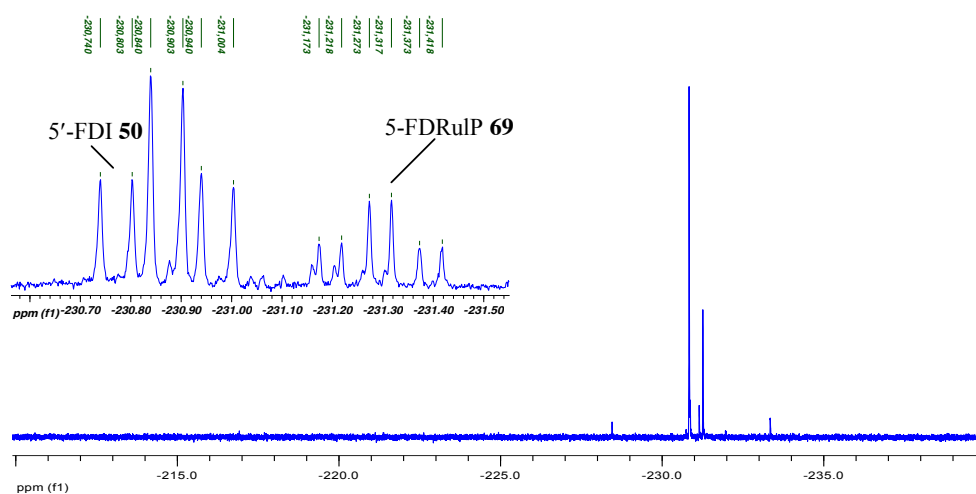


Figure 2.13 ^{19}F $\{^1\text{H}\}$ NMR spectrum of 35-50% $(\text{NH}_4)_2\text{SO}_4$ cut incubated with 5-FDRP **61** and EDTA for 16 h at 37 °C. Inset shows a non-decoupled ^{19}F NMR expansion of the product signals.

The generation of 5'-FDI **50** was confirmed by comparison with a reference sample on admixing.

C. Step 2: Hydrophobic interaction chromatography

A hydrophobic interaction chromatography (HIC) column (Phenyl HP, 40 ml) was equilibrated with phosphate buffer (50 mM, pH 6.8) supplemented with 1 M $(\text{NH}_4)_2\text{SO}_4$. The 35-50% $(\text{NH}_4)_2\text{SO}_4$ precipitate was re-dissolved in equilibration buffer (6 ml, 20 mg / ml). The sample was injected and eluted under a $(\text{NH}_4)_2\text{SO}_4$ gradient following the protocol detailed in Chapter 5. Figure 2.14 shows the resulting protein elution chromatogram (*vide infra*).

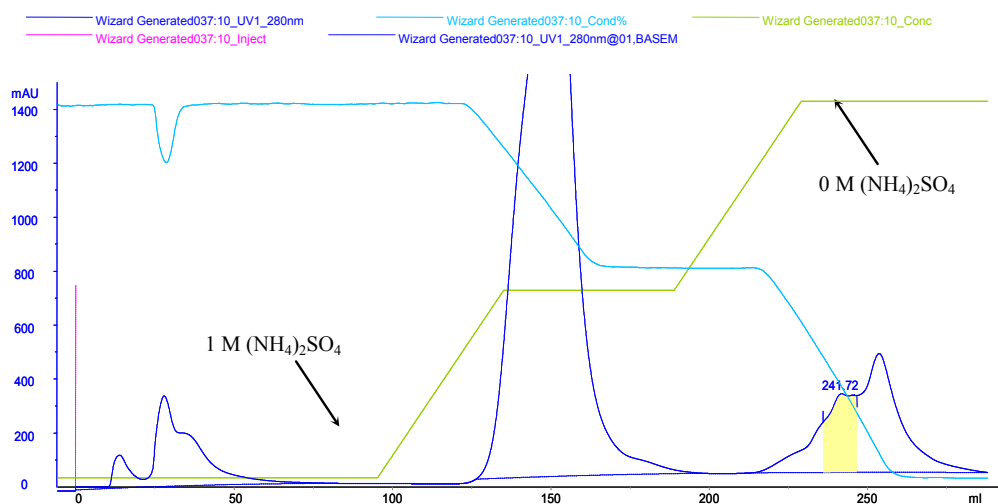


Figure 2.14 Protein elution chromatogram at step 2 of the isomerase purification protocol after ammonium sulfate precipitation and the HIC column.

Each of the protein fractions collected after this second step of purification was assayed for isomerase activity. Thus, a small volume of protein solution (200 μl) was incubated with 5-FDRP **61** at 37 °C for 16 h and then analysed by ^{19}F NMR spectroscopy. It was found that the partially purified isomerase elutes at the end of the gradient (highlighted area). This indicates a strong affinity to the resin. It is clear from the chromatogram that purification by hydrophobic interaction eliminated a substantial amount of undesired protein.

D. Step 3: Size exclusion chromatography

Size exclusion chromatography was the next step chosen for the purification of the isomerase. After the HIC step, there is no ammonium sulfate in the partially purified isomerase, which allows direct injection of this sample onto a size exclusion column. Thus, after concentration of the sample, the partially purified isomerase (2 ml, ~8 mg / ml) was applied to a pre-equilibrated Superdex 200 column. Figure 2.15 shows the resulting protein elution chromatogram.

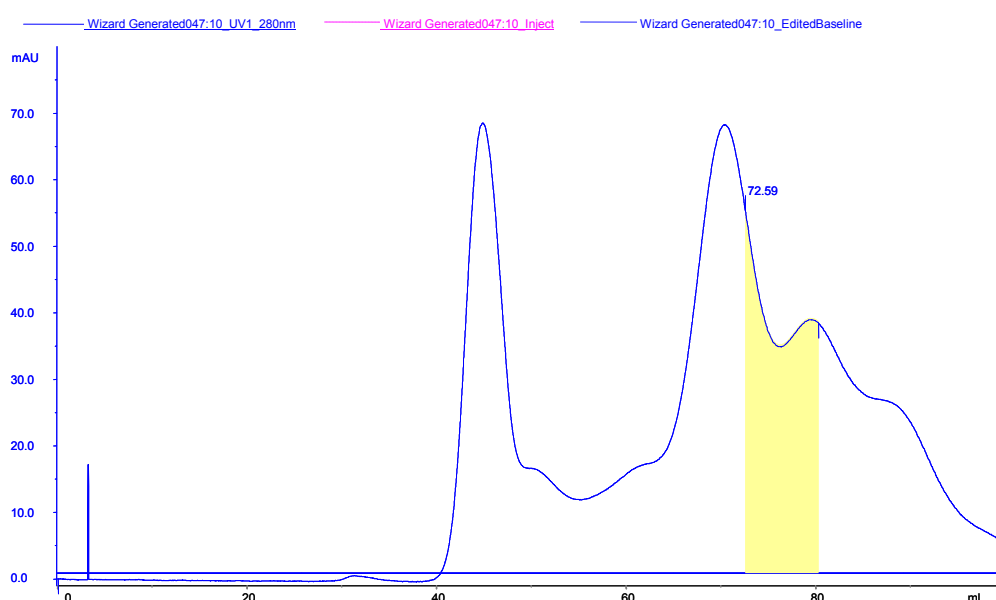


Figure 2.15 Step 3 for the purification of the isomerase enzyme from *S. cattleya*.

As previously carried out, protein fractions were assayed for isomerase activity. The isomerase enzyme was found to be in the 72–80 ml fraction (highlighted area) with a protein concentration of ~ 0.5 mg/ml. Baseline separation was not achieved and therefore a further purification step was clearly required.

E. Step 4: Anion exchange chromatography

Anion exchange chromatography was now explored to purify further the active fractions following the protocol detailed in Chapter 5. The active fractions after step 3 were combined (8 ml) and concentrated (2 ml) by centrifugation. The concentrated protein was then passed through a desalting column (HiTrap™ desalting, 5 ml) and re-concentrated again (~ 2 ml). This sample was loaded onto a strong anion exchange column (Q, 5 ml, Amersham Biosciences) and was pre-equilibrated with Tris buffer (50 mM, pH 7.2). Elution was achieved using a stepwise gradient following the protocol described in Chapter 5. The protein elution profile is shown in Figure 2.16.

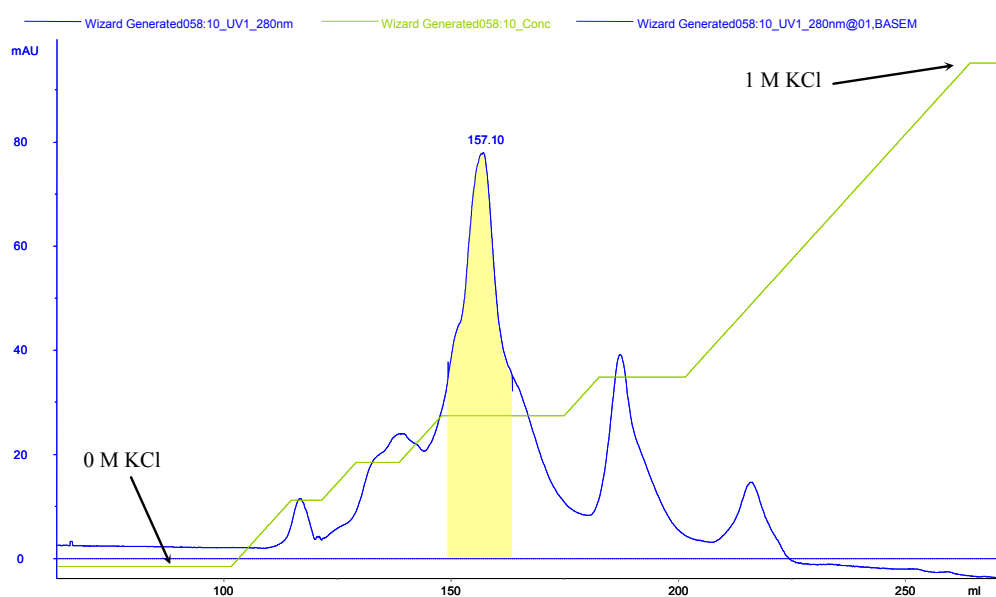


Figure 2.16 Step 4: Protein elution chromatogram obtained by anion exchange using a Q, 5 ml column after injection of sample (2 ml) after size exclusion purification. Active fraction is highlighted in the chromatogram.

Each fraction was assayed for isomerase activity using the assay outlined in Chapter 5. It emerged that the desired activity eluted after 250 mM KCl addition with a total protein

concentration of 1.5 mg / ml. It is clear from the trace in Figure 2.16 that the isomerase enzyme is still not homogenous and further purification is required.

F. Isomerase analysis by SDS-PAGE

Each stage of the isomerase purification was monitored by SDS-PAGE and the resultant gel is shown in Figure 2.17.

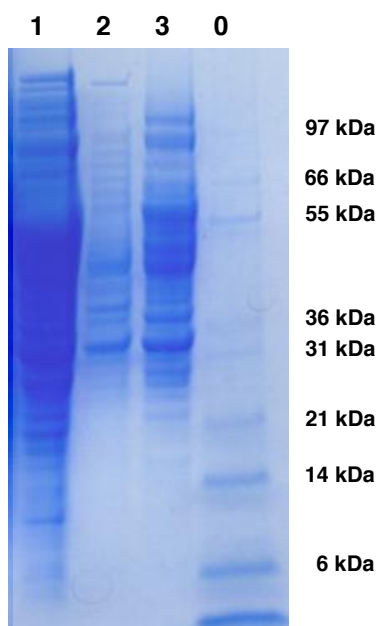


Figure 2.17 SDS-PAGE gel (4-12% acrylamide) showing active protein fractions containing isomerase activity during each purification step. Lanes: 0, molecular markers; 1, hydrophobic interaction chromatography; 2, size exclusion chromatography; 3, anion exchange chromatography.

Finally, the partially purified isomerase was shown to catalyse the biotransformation of 5-FDRP **61** to 5-FDRulP **69**, confirming purification of the isomerase enzyme operating in *S. cattleya*.

2.3.4.3 Identification of the isomerase gene in *S. cattleya*

Contemporaneous work carried out by Dr H. Deng in the research group led to the identification of the analogous isomerase gene in *S. cattleya*.³³ The protein sequences of *S. coelicolor* and *S. avermitilis* genomes highlighted 2 genes SCO3014 (*S. coelicolor*) and SAV6658 (*S. avermitilis*), previously annotated as ‘eukaryotic translation initiation factors 2’ (eIF2B). The amino acid sequences had a 35% amino acid identity to the *B. subtilis* MTRP isomerase and therefore these genes probably code related isomerases. The SCO3014 gene was amplified by PCR from *S. coelicolor* genomic DNA and the protein was over-expressed in *E. coli* for evaluation. After examination of the conserved domains of SCO3014 and SAV6658, DNA primers were designed for PCR amplification using *S. cattleya* genomic DNA as a template. This proved successful. The resulted sequenced open reading frame (ORF), with ~75% identity to the putative isomerase from *S. coelicolor*, was over-expressed in *E. coli*. The purified protein showed a molecular weight of approximately 40 kDa by SDS-PAGE, and the sequence was confirmed by MS-MS analysis. Biotransformation assays of this *S. cattleya* isomerase revealed that this enzyme also catalyses the conversion of 5-FDRP **61** to 5-FDRuIP **69**.³³

Analysis of the sequence similarity between the MTRP isomerase from *Bacillus subtilis*, *Saccharomyces cerevisiae* and *Kebsiella pneumoniae*, and related protein sequences from *Streptomyces avermitilis*, *Streptomyces coelicolor* and *Streptomyces cattleya* are shown in Figure 2.18 (*vide infra*).

CHAPTER 2

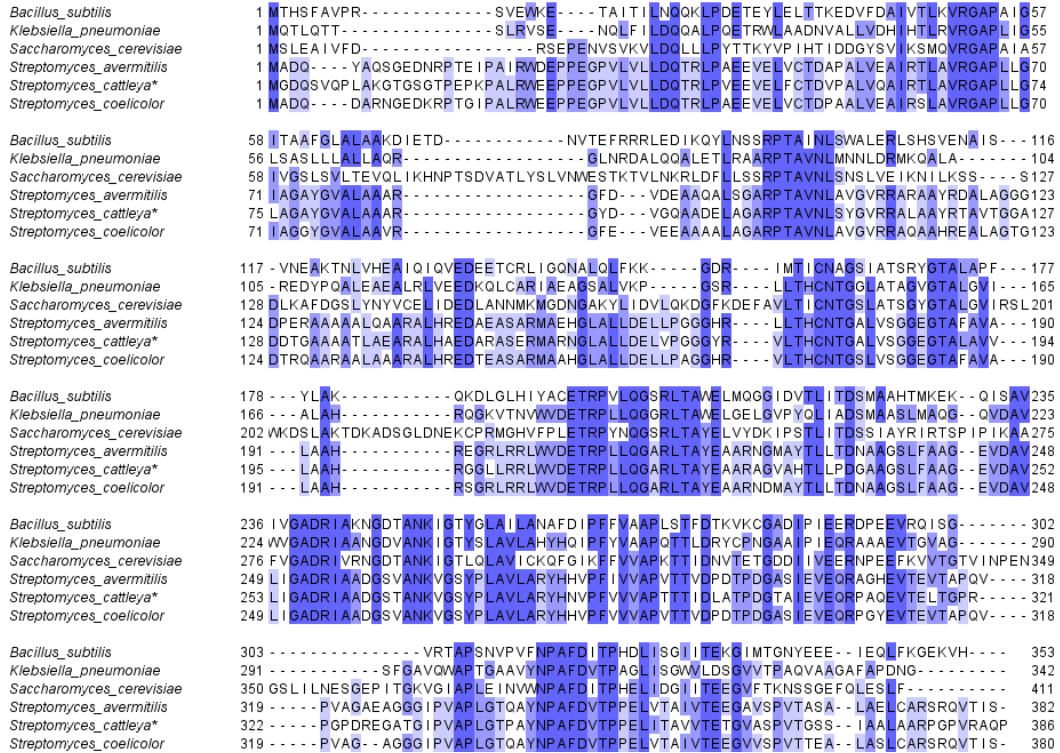
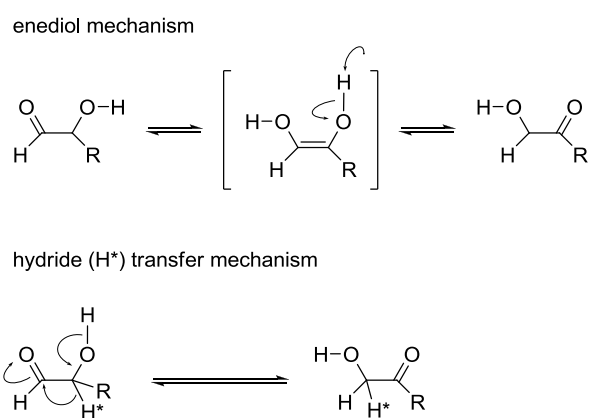


Figure 2.18 MTR-1P isomerase sequence alignments for *B. subtilis*, *K. pneumoniae*, *S. cerevisiae*, *S. avermitilis*, *S. cattleya* and *S. coelicolor*.

There is clearly a high level of conserved residues between the genes from the *Streptomyces* species. This high homology suggests that the gene from *S. cattleya* is likely to have the same function as that of SCO3014 and SAV6658. The fact that the *S. cattleya* enzyme has the ability also to catalyse the isomerisation of 5-FDRP **61** to 5-FDRuP **69** suggests a possible dual function, which is consistent with the observation that no obvious isomerase gene has been found in the gene cluster associated with the fluorinase (*flA*) and PNP (*flB*) genes.^{33,34}

2.3.4.4 Mechanism of the isomerase enzyme

Recently the crystal structure of the 5-methylthioribose-1-phosphate isomerase (EC 5.3.1.23) from *Bacillus subtilis* has been solved in a complex with its product, MTRu-1-P **68**.³⁵ This finding has shed some light on possible mechanisms for the isomerisation reaction. The putative catalytic mechanisms for such an aldose-ketose isomerisation are shown in Scheme 2.9.



Scheme 2.9 Mechanisms for the isomerisation of an aldose to a ketose.

Unlike the substrates of other aldose-ketose isomerases, that normally bear hydroxyl groups on the cyclic C-1, MTR-1-P **67** has a phosphate group on the corresponding C-1 position. The crystal structure of the *B. subtilis* isomerase with MTRu-1-P **68** (Figure 2.19, *vide infra*) shows binding of the phosphate group at the active site, suggesting its requirement and involvement in the catalysis of the isomerisation reaction.

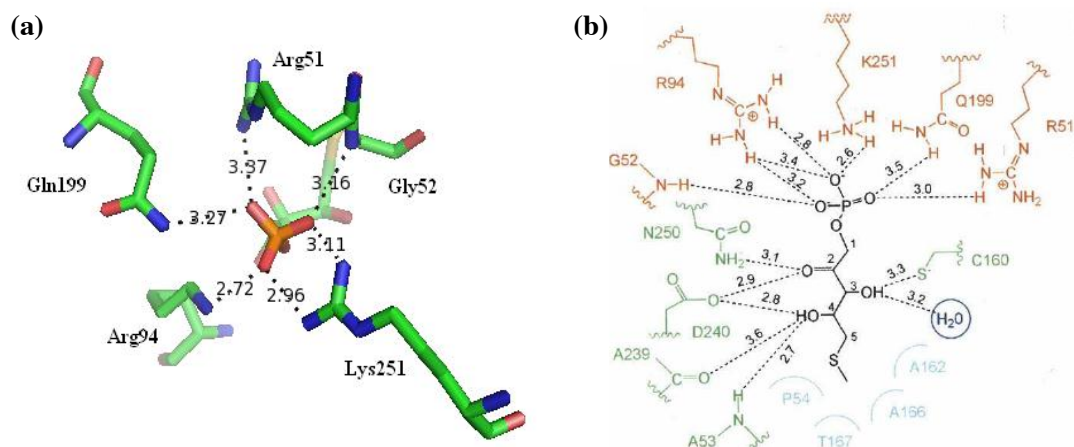
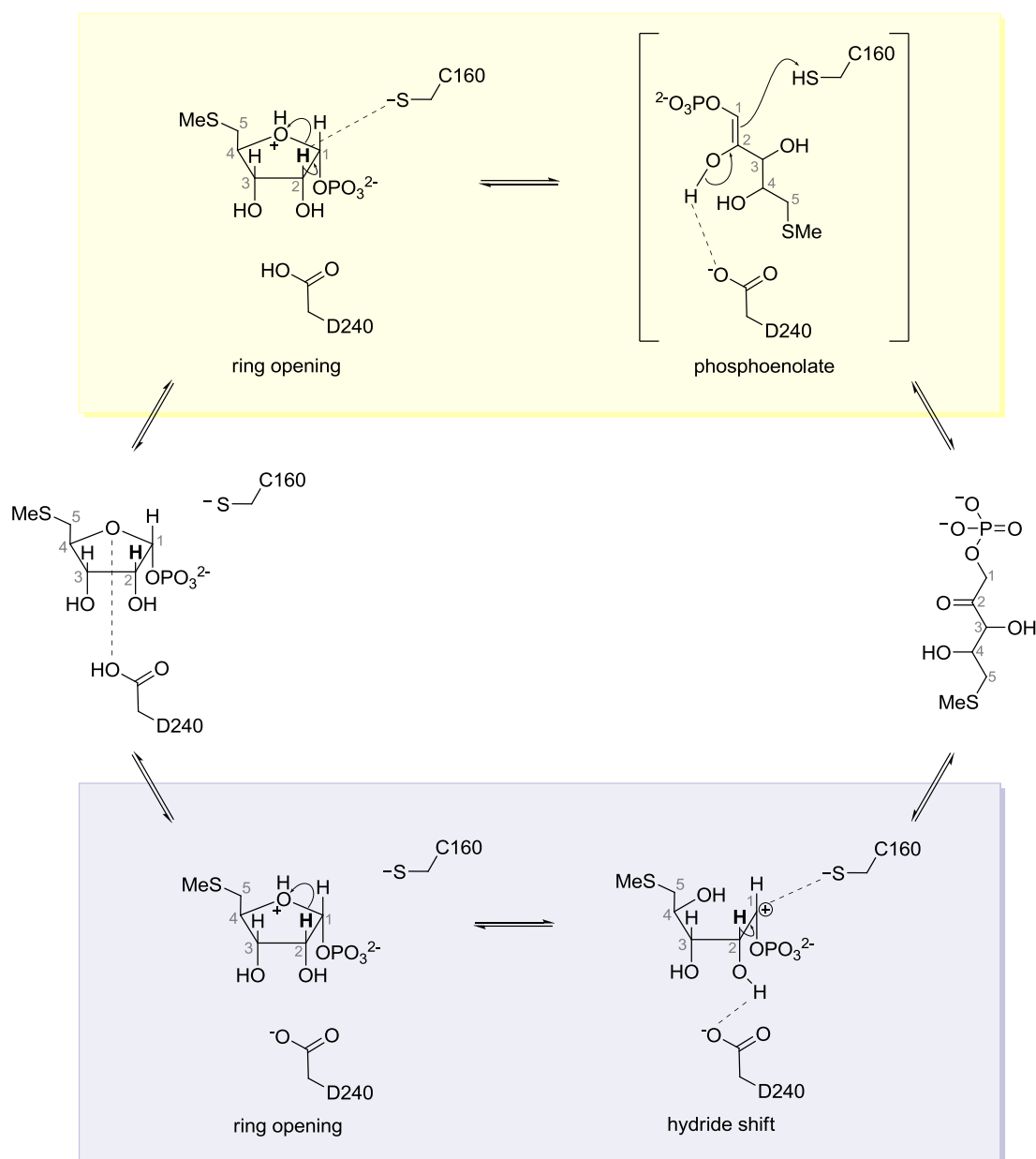


Figure 2.19 Active-site structure of Bs-M1Pi. **(a)** Close-up stereoview of the MTR-1-P isomerase active site in complex with MTRu-1-P **68** showing the interactions with the phosphate group (in orange and red). **(b)** Schematic representation deduced from X-ray crystallography data of hydrogen bonding contacts of MTRu-1-P **68** in the active site structure. Dashed lines: hydrogen bonds with the distance (Å); cyan semicircles: the hydrophobic interactions; the residues involved in the binding of the phosphate group (highlighted in orange) and the backbone oxygens of MTRu-1-P (shown in green).

In *S. cattleya* it has been shown that such a phosphate group is a requirement for the isomerisation of FDRP **61**, since FDR **71** is not further biotransformed and remains metabolically inert in CFEs of the bacterium.¹ Scheme 2.10 illustrates two possible but distinct mechanisms for the isomerisation reaction of MTR-1-P **67** based on crystallographic data.³⁵



Scheme 2.10 Two possible mechanisms. The cis-enediol proton transfer (upper site in yellow box) and 1,2-hydride shift (underside in purple box) reaction of MIPi based on the crystal structure of its product complex. D240 protonates the ring oxygen of MTR-1-P. C1-O bond cleavage could be accompanied by a hydride shift to quench the generating carbocation.

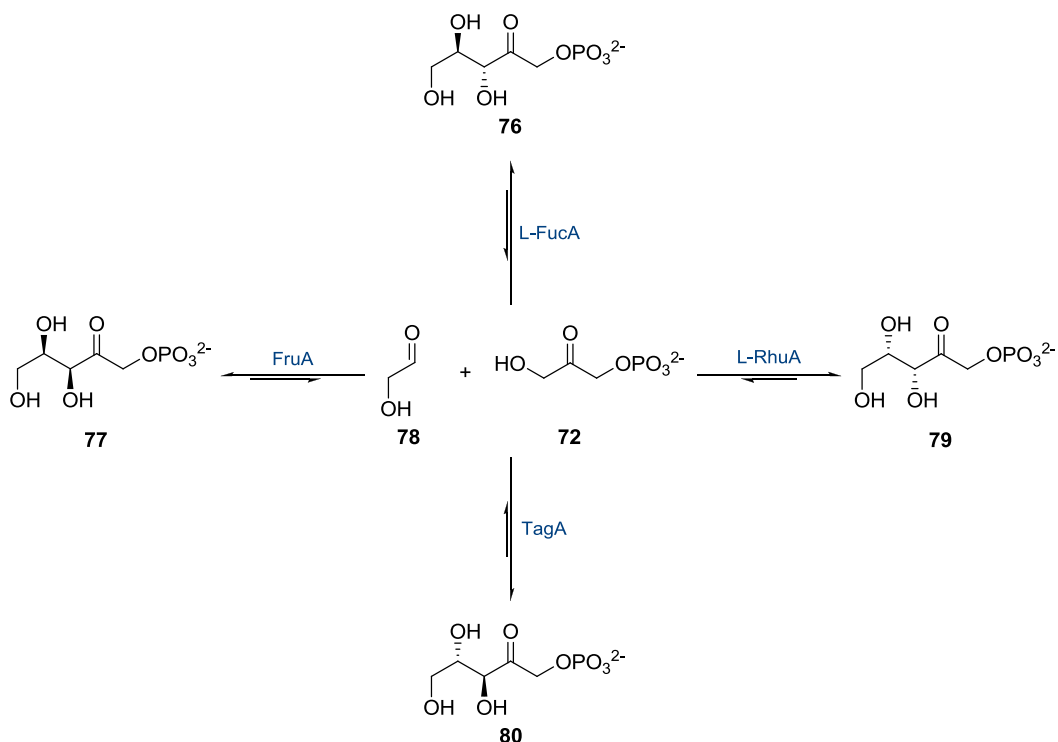
In a similar manner to the mechanism of xylose isomerase^{36,37,38,39} the side chain of Asp240 donates a proton to the ring oxygen to promote the ring-opening step during catalysis (Scheme 2.10, *vide supra*). In addition, previous NMR and mass spectrometry studies of BsM1Pi in D₂O showed some analogy with those of xylose isomerase, which adopts the hydride transfer mechanism.³⁷ However, it remains to be elucidated whether the mechanism of this reaction proceeds *via* a direct hydride transfer or *via* a *cis*-enediol intermediate, since the crystal structure does not discriminate between these mechanisms.³⁵ Currently work is being undertaken within our research group to shed some light on this mechanism.

2.4 The metabolism of 5-FDRuIP in *S. cattleya*

2.4.1 Aldolases in *S. cattleya*

Aldolases (EC 4.1.2.X) are an ubiquitous class of enzymes that catalyse *in vivo* the reversible asymmetric addition of dihydroxyacetone phosphate (DHAP) **72** to D-glyceraldehyde-3-phosphate (G3P) or L-lactaldehyde. These enzymes have attracted particular attention because of their application in organic synthesis (*i.e.*, chiral synthetic processes), since they catalyse the regio- and stereospecific aldol addition of DHAP **72** with a wide range of acceptor aldehydes to generate products with two new stereogenic centres.^{40,41,42}

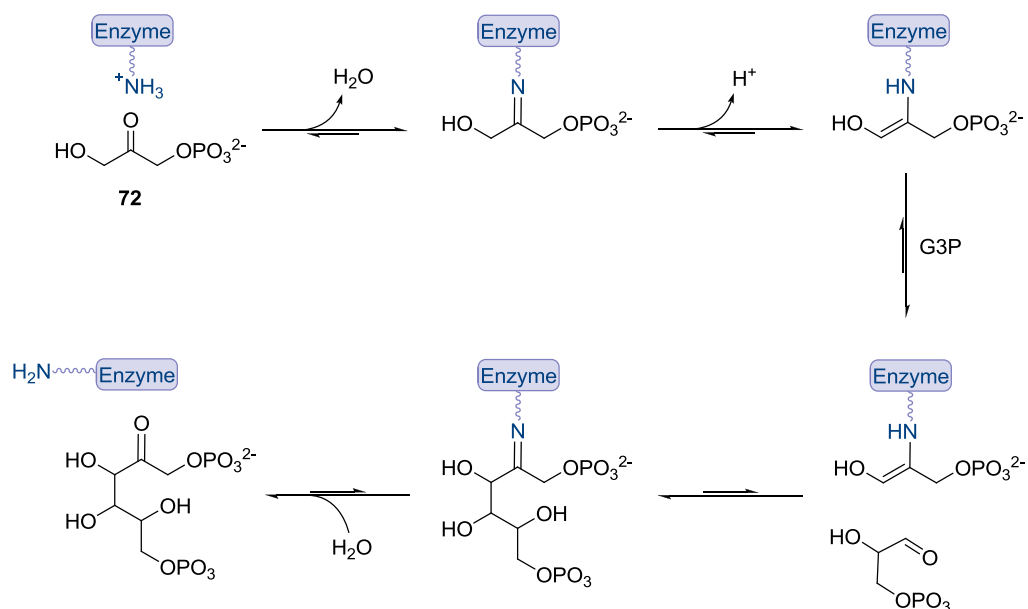
There are four different types of DHAP-dependent aldolase enzymes and each one mediates the formation of a distinct stereoisomer.^{27,28,29} The stereochemistry of the products formed during each enzymatic aldol reaction has been extensively studied, and is shown in Scheme 2.11 (*vide infra*).



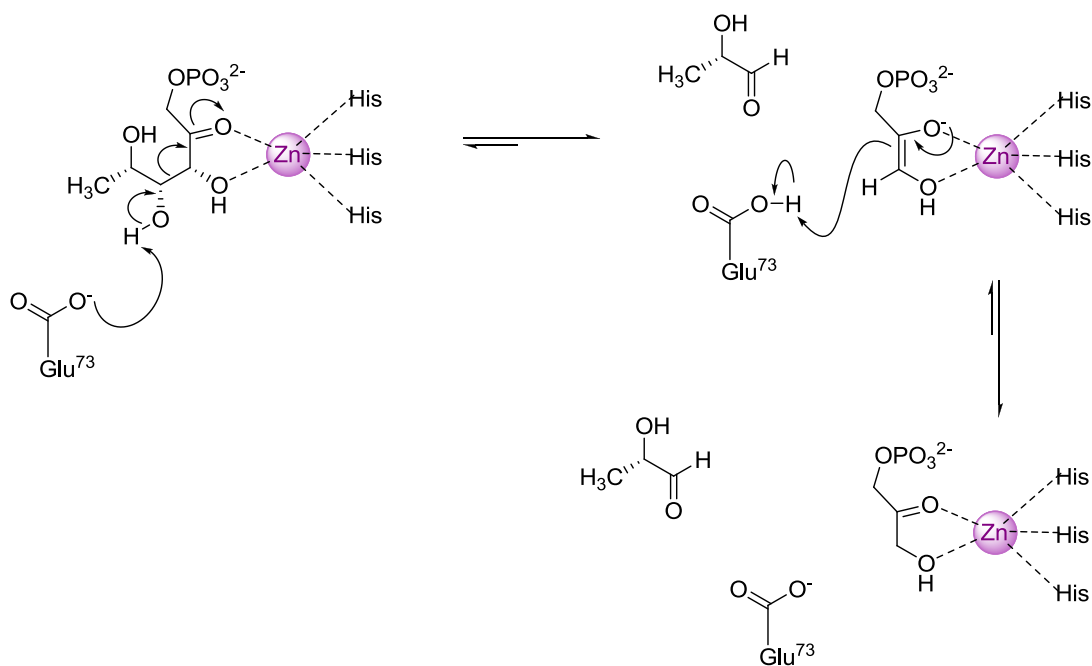
Scheme 2.11 The four DHAP-dependent aldolases: L-fucose-1-phosphate aldolase (L-FucA, EC 4.1.2.17), L-rhamnulose-1-phosphate aldolase (L-RhuA, EC 4.1.2.19), tagatose-1,6-bisphosphate aldolase (TagA, EC 4.1.2.40) and fructose-1,6-bisphosphate aldolase (FruA, EC 4.1.2.13)

Aldolases have been divided into two classes according to their mode of donor activation. These two types of aldolases also vary in structure, since they are phylogenetically distinct.⁴³ Class I aldolases, which are present in all groups of living organisms, from prokaryotes to eukaryotes, achieve stereospecific deprotonation of the substrate by means of covalent linkage to an active site lysine residue (imine/enamine formation).^{44,45} Class II aldolases occur only in prokaryotes and lower eukaryotes such as bacteria, yeast, algae and fungi; and they utilise transition metal ions (usually Zn^{2+}) as essential Lewis acid co-factors to facilitate deprotonation.^{29,46} Type I aldolases are inactivated by treatment with sodium borohydride, while type II aldolases are inactivated by chelating compounds such as EDTA.

Scheme 2.12 illustrates the general mechanism for class I DHAP-dependent aldolases.⁴⁴ The mechanism for catalysis by class II DHAP-dependent aldolases is shown in Scheme 2.13.⁴⁶

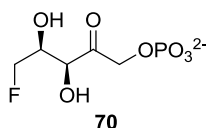


Scheme 2.12 General mechanism for Class I DHAP-dependent aldolase.

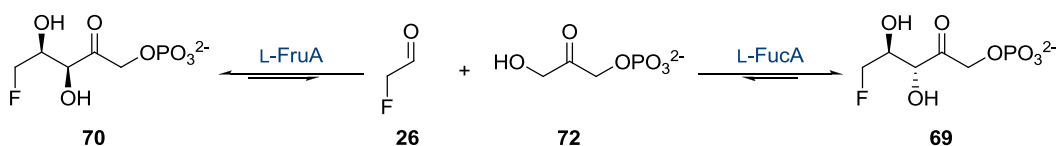


Scheme 2.13 Mechanism of Class II DHAP-dependent aldolase.

Previous work identified two DHAP-dependent aldolases,²⁵ one of which, a class II L-fuculose aldolase (L-FucA), is involved in fluorometabolite biosynthesis in *S. cattleya* and generates fluoroacetaldehyde **26** from 5-deoxy-5-fluoro-D-ribulose-1-phosphate (5-FDRuP) **69**. The other one, a L-fructose 1,6-bisphosphate aldolase (L-FruA) was purified to homogeneity and appears to be responsible for the formation of intermediate **70** (Figure 2.3, *vide supra*). The product of this L-FruA has been tentatively assigned as 5-deoxy-5-fluoro-D-xyulose-1-phosphate (5-FDXuP) **70** after comparison studies with 5-FDXul **75**.



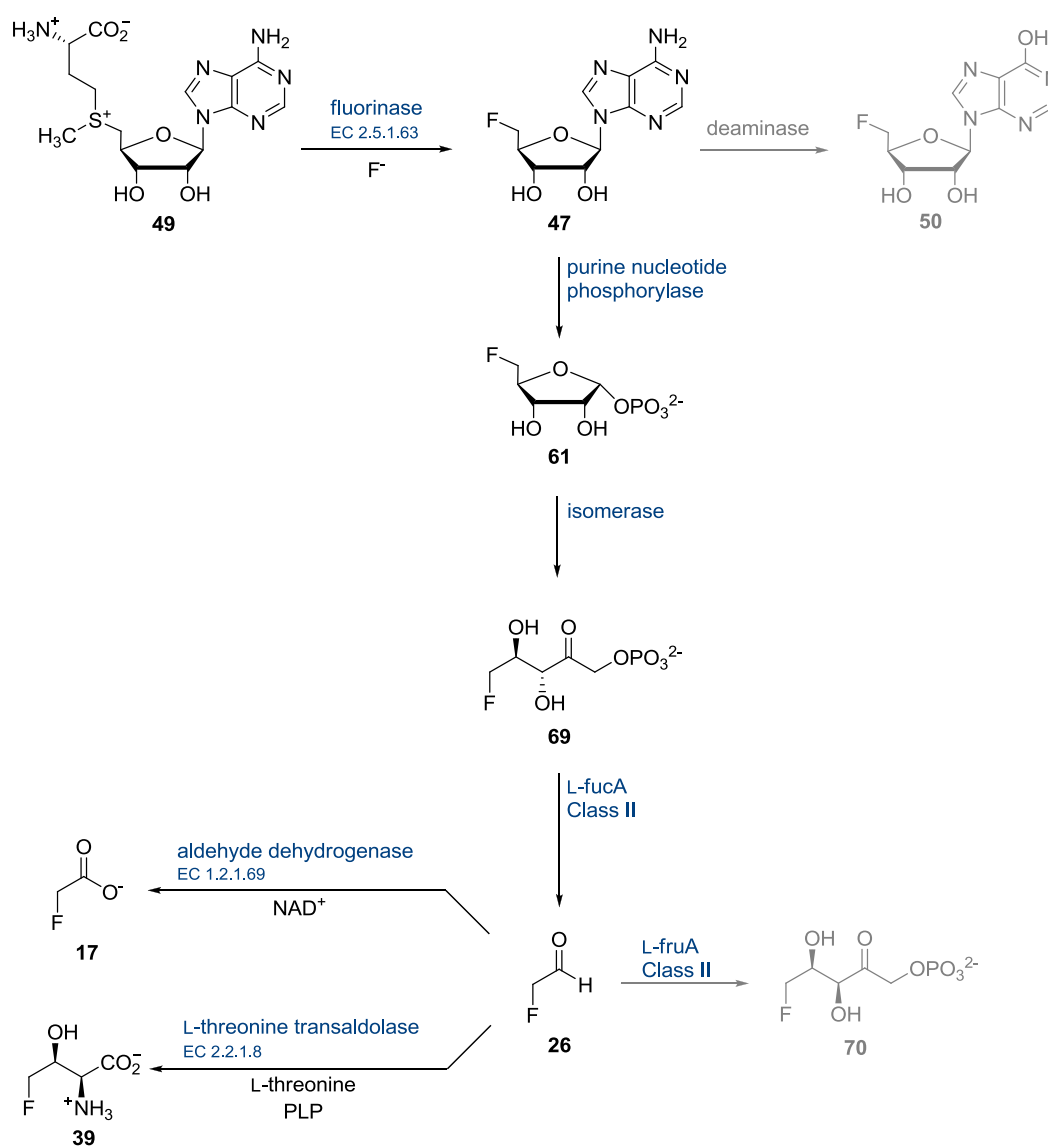
This L-FruA was shown to catalyse an aldol reaction between DHAP **72** and fluoroacetaldehyde **26** to generate 5-FDXuP **70**. This enzyme is also a class II aldolase, requiring a divalent metal ion such as Zn^{2+} , Mg^{2+} , Mn^{2+} , Co^{2+} , Ni^{2+} , Fe^{2+} or Ca^{2+} for catalytic activity. L-FruA was purified to homogeneity and showed homology to a L-FruA from *Streptomyces galbus*.^{25,47} The purified protein showed a molecular weight of approximately 40 kDa by SDS-PAGE, and a native mass of 160 kDa was observed by gel filtration, indicating a tetramer. The amino acid sequence showed similarity to other bacterial L-FruAs.²⁵ Biotransformation assays of this *S. cattleya* aldolase suggested its relationship to primary metabolism and the formation of 5-FDXuP **70** as a shunt product. Scheme 2.14 outlines the formation of **69** and **70** from fluoroacetaldehyde **26** in *S. cattleya*.



Scheme 2.14 The stereochemical relationships of the two aldolases in the *S. cattleya* CFE.

Purification of the L-FucA operating in *S. cattleya* proved to be unsuccessful.²⁵ Recent work by S. Cross focused on the isolation of the gene for L-FucA, putatively involved in fluorometabolite production in *S. cattleya*. Unfortunately, all attempts to isolate such gene from *S. cattleya* genomic DNA were also unsuccessful.³³

The metabolic relationships and enzymes involved in the biosynthesis of fluoroacetate **17** and 4-fluorothreonine **39** in *S. cattleya* are summarised in Scheme 2.15.



Scheme 2.15 Overview of the fluorometabolite biosynthetic pathway in *S. cattleya*.

2.5 Conclusions

(3*R*,4*S*)-5-Deoxy-5-fluoro-D-ribulose-1-phosphate (5-FDRulP) **69** has been identified as the third fluorinated intermediate on the biosynthetic pathway to fluoroacetate **17** and 4-fluorothreonine **39**. 5-FDRulP **69** is generated after formation of 5'-deoxy-5'-fluoroadenosine (5'-FDA) **47** and then phosphorolysis of 5'-FDA **47** to 5-fluoro-5-deoxy- α ,D-ribose-1-phosphate (5-FDRP) **61** occurs by the action of a purine-nucleoside phosphorylase. An isomerase mediates the conversion of 5-FDRP **61** to 5-FDRulP **69**. The identity of the (3*R*,4*S*) diastereoisomer of 5-FDRulP **69** was established by comparative $^{19}\text{F}\{^1\text{H}\}$ NMR studies whereby 5-FDRulP **69** that accumulated in a cell free extract of *S. cattleya*, was treated with a phytase to generate the non-phosphorylated sugar, 5-deoxy-5-fluoro-D-ribulose (5-FDRul) **73**.

This *S. cattleya* product was compared to the product of an *in vitro* biotransformation where separately 5-deoxy-5-fluoro-D-ribose (5-FDR) **71** and 5-deoxy-5-fluoro-D-xylose (5-FDX) **74** were converted to 5-deoxy-5-fluoro-D-ribulose (5-FDRul) **73** and 5-deoxy-5-fluoro-D-xylulose (5-FDXul) **75**, respectively, by the action of a glucose isomerase. It was demonstrated that 5-FDR **71** gave the identical diastereoisomer to that observed from 5-FDRulP **69**.

2.6 References

1. S. L. Cobb, H. Deng, J. T. G. Hamilton, R. P. McGlinchey and D. O'Hagan, *Chem. Commun.*, 2004, 592-593.
2. S. J. Moss, C. D. Murphy, J. T. G. Hamilton, W. C. McRoberts, D. O'Hagan, C. Schaffrath and D. B. Harper, *Chem. Commun.*, 2000, 2281-2282.
3. M. Onega, R. P. McGlinchey, H. Deng, J. T. G. Hamilton and D. O'Hagan, *Bioorg. Chem.*, 2007, **35**, 375-385.
4. A. Sekowska and A. Danchin, *BMC Microbiology*, 2004, **4**, 1-17.
5. H.-S. Choi, J. D. Stoeckler and R. E. Parks Jr., *J. Biol. Chem.*, 1986, **261**, 599-607.
6. M. E. Houston Jr., D. L. Jagt and J. F. Honek, *Bioorg. Med. Chem. Lett.*, 1991, **1**, 623-628.
7. S. A. Christopher, P. Diegelman, C. W. Porter and W. D. Kruger, *Cancer Res.*, 2002, **62**, 6639-6644.
8. M. K. Riscoe, A. J. Ferro and J. H. Fitchen, *Antimicrob. Agents Chemother.*, 1988, **32**, 1904-1906.
9. J. R. Sufirin, S. R. Meshnick, A. J. Spiess, J. Garofalo-Hannan, X.-Q. Pan and C. J. Bacchi, *Antimicrob. Agents Chemother.*, 1995, **39**, 2511-2515.
10. P. C. Trackman and R. H. Abeles, *Biochem. Biophys. Res. Commun.*, 1981, **103**, 1238-1244.
11. E. S. Furfine and R. H. Abeles, *J. Biol. Chem.*, 1988, **263**, 9598-9606.
12. R. W. Myers and R. H. Abeles, *J. Biol. Chem.*, 1990, **265**, 16913-16921.
13. R. W. Myers, J. W. Wray, S. Fish and R. H. Abeles, *J. Biol. Chem.*, 1993, **268**, 24785-24791.
14. J. W. Wray and R. H. Abeles, *J. Biol. Chem.*, 1995, **270**, 3147- 3153.

CHAPTER 2

15. J. Heilbronn, J. Wilson and B. J. Berger, *J. Bacteriol.*, 1999, **181**, 1739-1747.
16. Y. Dai, T. C. Pochapsky and R. H. Abeles, *Biochemistry*, 2001, **40**, 6379-6387.
17. I. Pirkov, J. Norbeck, L. Gustafsson and E. Albers, *FEBS J.*, 2008, **275**, 4111-4120.
18. A. Sekowska and A. Danchin, *BMC Microbiology*, 2002, **2**, 1-14.
19. F. R. Tabita, T. E. Hanson, H. Li, S. Satagopan, J. Singh and S. Chan, *Microbiol. Mol. Biol. Rev.*, 2007, **71**, 576-599.
20. H. Ashida, Y. Saito, C. Kojima, K. Kobayashi, N. Ogasawara and A. Yokota, *Science*, 2003, **302**, 286-290.
21. T. E. Hanson and F. R. Tabita, *Proc. Natl. Acad. Sci. USA*, 2001, **98**, 4397-4402.
22. M. Bumann, S. Djafarzadeh, A. E. Oberholzer, P. Bigler, M. Altmann, H. Trachsel and U. Baumann, *J. Biol. Chem.*, 2004, **279**, 37087-37094.
23. S. R. Kimball, *Int. J. Biochem. Cell Biol.*, 1999, **31**, 25-29.
24. C. Schaffrath, Ph.D. Thesis, *Biosynthesis and Enzymology of Fluorometabolite Production in Streptomyces cattleya*, University of St Andrews, 2002.
25. R. P. McGlinchley, Ph.D. Thesis, *Intermediates and enzymes involved in fluorometabolite biosynthesis in Streptomyces cattleya*, University of St Andrews, 2006.
26. S. L. Cobb, H. Deng, J. T. G. Hamilton, R. P. McGlinchey, D. O'Hagan and C. Schaffrath, *Bioorg. Chem.*, 2005, **33**, 393-401.
27. R. Schoevaart, F. van Rantwijk and R. A. Sheldon, *J. Org. Chem.*, 2000, **65**, 6940-6943.
28. R. Schoevaart, F. van Rantwijk and R. A. Sheldon, *Chem. Commun.*, 1999, 2465-2466.
29. R. Schoevaart, Ph.D. Thesis, *Application of aldolases in organic synthesis*, Technische Universiteit Delft, 2000.

CHAPTER 2

30. J. T. G. Hamilton, C. D. Murphy, M. R. Amin, D. O'Hagan and D. B. Harper, *J. Chem. Soc., Perkin Trans. I*, 1998, 759-767.
31. M. Ebner and A. E. Stütz, *Carbohydr. Res.*, 1998, **305**, 331-336.
32. P. Hadwiger, P. Mayr, B. Nidetzky, A. E. Stütz and A. Tauss, *Tetrahedron Asymm.*, 2000, **11**, 607-620.
33. H. Deng, S. M. Cross, R. P. McGlinchey, J. Hamilton and D. O'Hagan, *Chem. Biol.*, 2008, **15**, 1268-1276.
34. F. Huang, S. F. Haydock, D. Spitteller, T. Mironenko, T.-L. Li, D. O'Hagan, P. F. Leadlay and J. B. Spencer, *Chem. Biol.*, 2006, **13**, 475-484.
35. H. Tamura, Y. Saito, H. Ashida, T. Inoue, Y. Kai, A. Yokota and H. Matsumura, *Protein Sci.*, 2008, **17**, 126-135.
36. G. K. Farber, A. Glasfeld, G. Tiraby, D. Ringe and G. A. Petsko, *Biochemistry*, 1989, **28**, 7289-7297.
37. C. A. Collyer and D. M. Blow, *Proc. Natl. Acad. Sci. USA*, 1990, **87**, 1362-1366.
38. T. D. Fenn, D. Ringe and G. A. Pestko, *Biochemistry*, 2004, **43**, 6464-6474.
39. A. Y. Kovalevsky, A. K. Katz, H. L. Carrell, L. Hanson, M. Mustyakimov, S. Z. Fisher, L. Coates, B. P. Schoenborn, G. J. Bunick, J. P. Glusker and P. Langan, *Biochemistry*, 2008, **47**, 7595-7597.
40. C. Augé and D. H. G. Crout, *Carbohydr. Res.*, 1997, **305**, 307-312.
41. E. J. Toone, E. S. Simon, M. D. Bednarski and G. M. Whitesides, *Tetrahedron*, 1989, **45**, 5365-5422.
42. H. J. M. Gijzen, L. Qiao, W. Fitz and C.-H. Wong, *Chem. Rev.*, 1996, **96**, 443-473.
43. W. J. Rutter, *Fed. Proc.*, 1964, **23**, 1248-1257.
44. C. Y. Lai, N. Nakai and D. Chang, *Science*, 1974, **183**, 1204-1206.
45. A. J. Morris and D. R. Tolan, *Biochemistry*, 1994, **33**, 12291-12297.

CHAPTER 2

46. W.-D. Fessner, A. Schneider, H. Held, G. Sinerius, S. Walter, M. Hixon and J. V. Schloss, *Angew. Chem., Int. Ed.*, 1993, **35**, 2219-2221.
47. U. F. Wehmeier, *FEMS Microbiol. Lett.*, 2001, **197**, 53-58.

CHAPTER 3

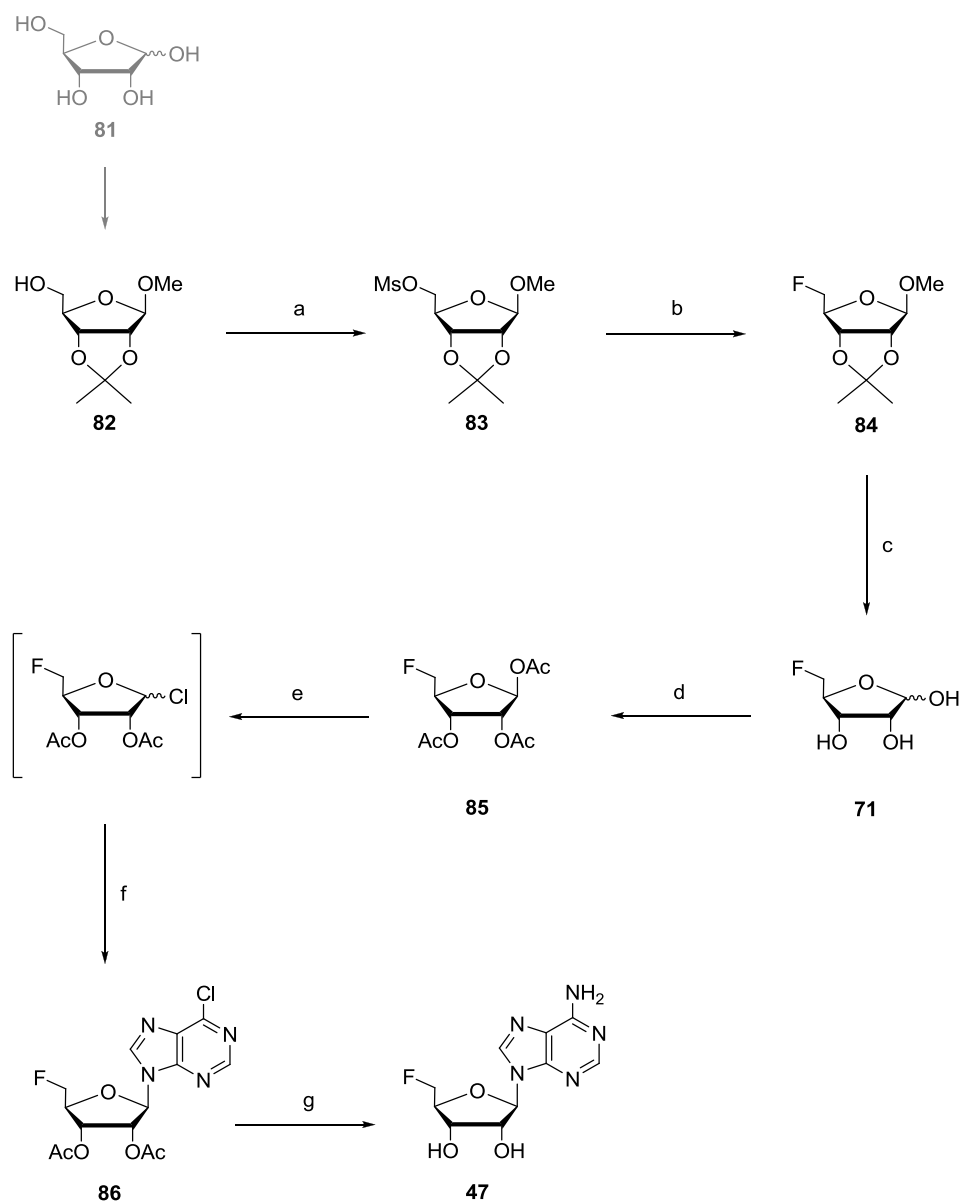
Synthesis of key molecules

Synthesis of key molecules

3.1 Synthesis of 5'-deoxy-5'-fluoroadenosine **47**

As described in Chapter 1, 5'-deoxy-5'-fluoroadenosine (5'-FDA) **47** is the product of the fluorinase in *S. cattleya*. This metabolic intermediate is capable of supporting the biosynthesis of fluoroacetate (FAc) **17** and 4-fluorothreonine (4-FT) **39** when incubated in a cell-free extract. Consequently, 5'-FDA **47** is a key intermediate for detailed studies on the fluorometabolite pathway, and it is continually required in this research project. Therefore, a straightforward synthesis of 5'-FDA **47** was necessary to carry out cell-free extract incubation experiments to support the research programme.

Few examples of the synthesis of mono-fluorinated nucleosides at C-5' are found in the literature. Moreover, there was only one reported synthesis of the target molecule 5'-FDA **47**, at the outset of this work.¹ The synthesis is illustrated in Scheme 3.1 (*vide infra*).



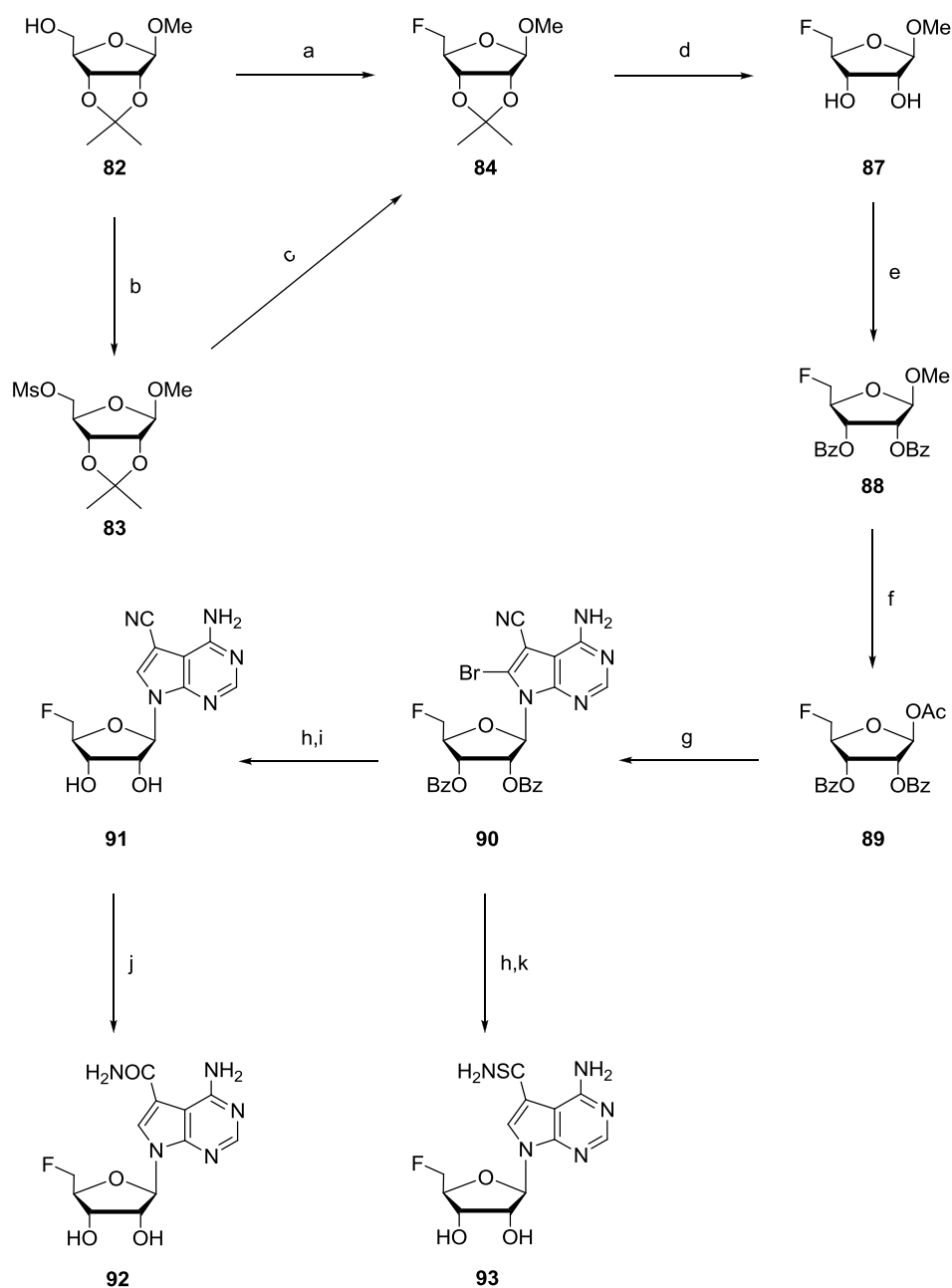
Scheme 3.1 The synthesis of 5'-FDA **47** reported by Kissman and Weiss.¹

Reagents and conditions: (a) Pyridine / MsCl, 3 °C, 71% (b) KF / MeOH, 160 °C, 68% (c) 0.02 N H₂SO₄, 100 °C, 100% (d) Pyridine / acetic anhydride, 21% (e) Acetyl chloride, HCl / ether, 3 °C (f) Chloromercuri-6-chloropurine / xylene, 140 °C, 54% (g) NH₃ / MeOH, 100 °C, 64%.

CHAPTER 3

The overall yield for this synthesis as reported by Kissman and Weiss, was 4% without including the additional step that is required for the preparation of **82**, a starting material prepared from ribose **81**. The fluorinated intermediate **84** is obtained by nucleophilic displacement of a mesylate group using anhydrous KF.¹ Although the yield of the reaction is quite good (68%), the required reaction conditions are fairly harsh (Scheme 3.1, step b).

Other reported 5'-fluorinated nucleosides have been generated as a result of an attempt to synthesise molecules resistant to phosphorylation at C-5'.² Among those are the fluorinated derivatives of toyocamycin **91** and the antibiotics, sangivamycin **92** and thiosangivamycin **93**, shown in Scheme 3.2 (*vide infra*).



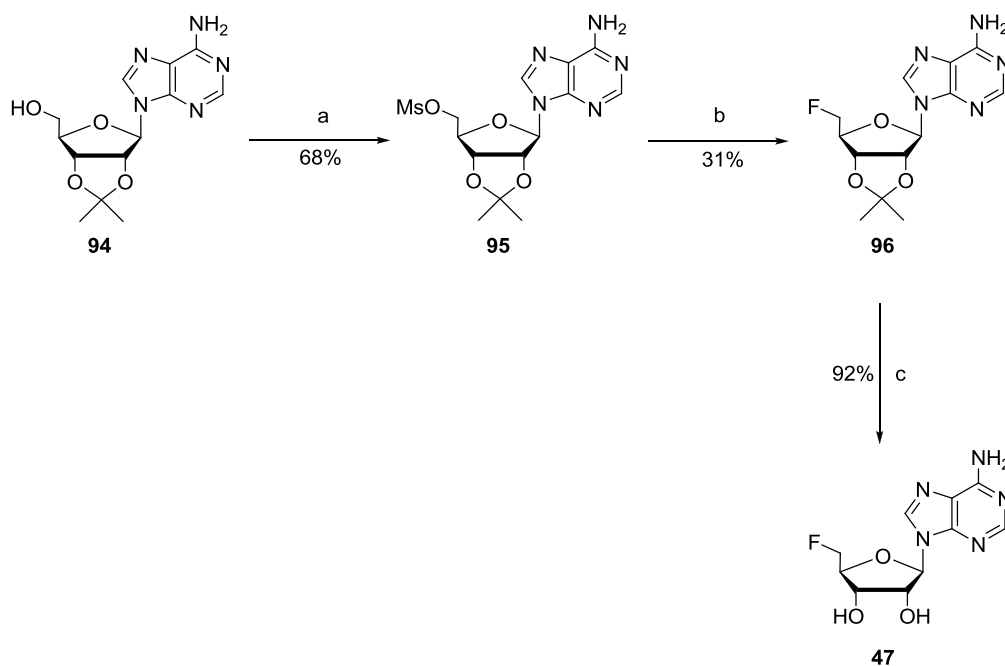
Scheme 3.2 The synthesis of 5'-fluoro-nucleosides **91**, **92** and **93** as reported by Sharma *et al.*² Reagents and conditions: (a) DAST, benzene, 80 °C, 3 h, 35% (b) MsCl, pyridine, 0 °C, 24 h, 78% (c) TBAF, MeCN, reflux, 24 h, 90% (d) Formic acid (60% crude) (e) Pyridine, benzoyl chloride, 0 °C, 95% (f) Acetic acid / acetic anhydride, 78% (g) 4-Amino-6-bromo-5-cyanopyrrolo[2,3-d]pyrimidine / hexamethyldisilazane, TMSTF, 77% (h) Et₃N, Pd charcoal / H₂, 90% (i) NH₃ / MeOH, 91% (j) NH₄OH, H₂O₂, 75% (k) Hydrogen sulfide / pyridine, then NH₃ / MeOH, 27% (over two steps).

The synthesis of **47**, **91**, **92** and **93**, derive from 5'-deoxy-5'-fluoro-2,3-*O*-isopropylidene- β -D-ribofuranoside **83** (Schemes 3.1 and 3.2, *vide supra*).

Sharma *et al.* improved the yield of the fluorination step to **84** to 90% by employing tetrabutylammonium fluoride (TBAF) as the fluorinating reagent (Scheme 3.2, step c). They also showed the practicality of direct fluorination of the C-5' hydroxyl group using DAST as a fluorinating agent (Scheme 3.2, step a). However, the reaction yield is lower than that achieved with TBAF, even when taking the mesylation step into consideration.²

As illustrated in Schemes 3.1 and 3.2, the synthesis of 5'-fluorinated nucleosides involves the incorporation of a fluorine atom into a suitably protected sugar and subsequent coupling to the desired base by a ribosylation reaction.^{3,4} Such a synthetic approach allowed the preparation of 5'-fluoro analogs of several purine and pyrimidine nucleosides.¹ However, the condensation reaction between the 5'-fluorinated protected sugar and the base often presents some disadvantages, such as a low reaction yield, formation of undesired nucleosides and also the use of toxic mercury based reagents.¹

In order to overcome these inconveniences, a new synthetic route to 5'-FDA **47** was developed at St Andrews by S. Cobb.⁵ The route involved a combination of the procedures detailed in Schemes 3.1 and 3.2, and was especially designed to avoid the glycosylation step. Thereby, the synthesis of 5'-FDA **47** was initially carried out following this new procedure. The synthetic sequence is shown in Scheme 3.3.

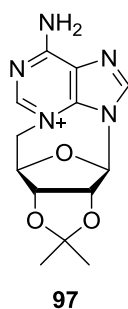


Scheme 3.3 Reagents and conditions: (a) MsCl, pyridine, RT, 4 h (b) TBAF.3H₂O, MeCN, reflux, 17 h (c) 0.02 M H₂SO₄, reflux, 5 h.

The starting material **94** can be easily prepared from adenosine using a standard protection protocol using acetone and 2,3-dimethoxypropane with an acid catalyst.⁶ However, widespread application for the preparation of modified nucleosides has resulted in **94** becoming commercially available. The first step of the synthesis involves the activation of the C-5' hydroxyl group in **94** via a mesylation reaction. Therefore, 2',3'-O-isopropylidene-5'-O-mesyloxyadenosine **95** was prepared according to known procedures.⁷ The mesylation reaction furnished the desired product in good yield (68%), and the analytical and spectroscopic data for the compound were in full agreement with the literature.

Fluorination of **95** used tetrabutylammonium fluoride (TBAF) as the fluorinating reagent. TBAF is available as its trihydrate form (TBAF.3H₂O), and although there are procedures detailed to prepare anhydrous TBAF⁸ there are problems associated with the stability of anhydrous TBAF and there is evidence that its use increases the formation of elimination

products due to the increased basicity of dry fluoride ion and the presence of hydroxide ion.⁹ Therefore, mesylate **95** was subjected to fluoride substitution conditions using 2.5 equivalents of TBAF.3H₂O in refluxing acetonitrile for 16 h. The fluorination, although successful, resulted in a significant decrease of the yield (31%). It is worth noting that the free amine at the C-6 position of the adenine base in **94** did not participate in, or complicate, the reaction and only the 5'-*O*-mesyl compound **95** was isolated. Thus, no formation of unwanted 3',5'-cyclo-nucleoside **97** was observed, a compound previously identified in C-5' activation protocols.⁷

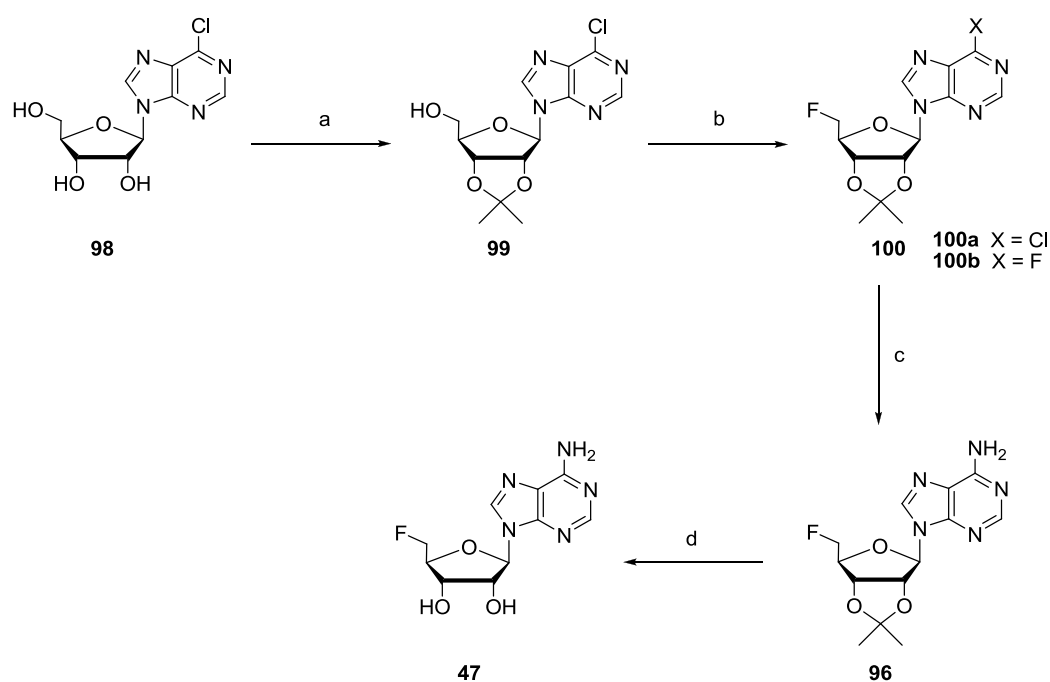


Finally, the 2',3'-isopropylidened-5'-FDA **96** was deprotected under acidic conditions. However, this synthesis resulted in a poor yield of the desired 5'-fluorinated product **47**. The mesylate is generally prepared in good yield (68%), but once subjected to fluoride substitution conditions the yield decreased significantly. Consequently, the recovery of 5'-FDA **47** is poor. While this work was in progress, an improved synthesis of 5'-deoxy-5'-fluoroadenosines was reported in the literature by Ashton and Scammells.¹⁰ So far, the synthesis of 5'-FDA **47** and related compounds involved the conversion of the 5'-OH group to the corresponding sulfonate leaving group, *i.e.*, the tosylate or mesylate. This is then followed by substitution using a suitable fluoride nucleophile under S_N2 conditions. However, such synthetic sequences typically result in poor yields. Different factors contribute to the decreased efficiency of this synthetic method, including the instability of the sulfonated intermediates. The 5'-sulfonates

are regarded as poor precursors for nucleophilic substitution due to a competing intramolecular reaction between N-3 of the adenine ring and C-5' of the ribose moiety to give undesired cyclic nucleosides (*e.g.*, **97**). This process is activated by the lone pair on the *exo*-cyclic N^6 -nitrogen of the adenine ring. Protection of that N^6 -nitrogen would reduce the effect of the lone pair but would also lengthen the synthetic route.^{11,12,13}

Ashton and Scammells envisaged that an electron withdrawing group at N-6 of the adenine ring would negate the formation of any intramolecular cyclised product. Besides, using a 6-chloropurine moiety would also have the advantage of being a good starting point for the preparation of a range of N^6 -substitution adenosine derivatives.¹⁰

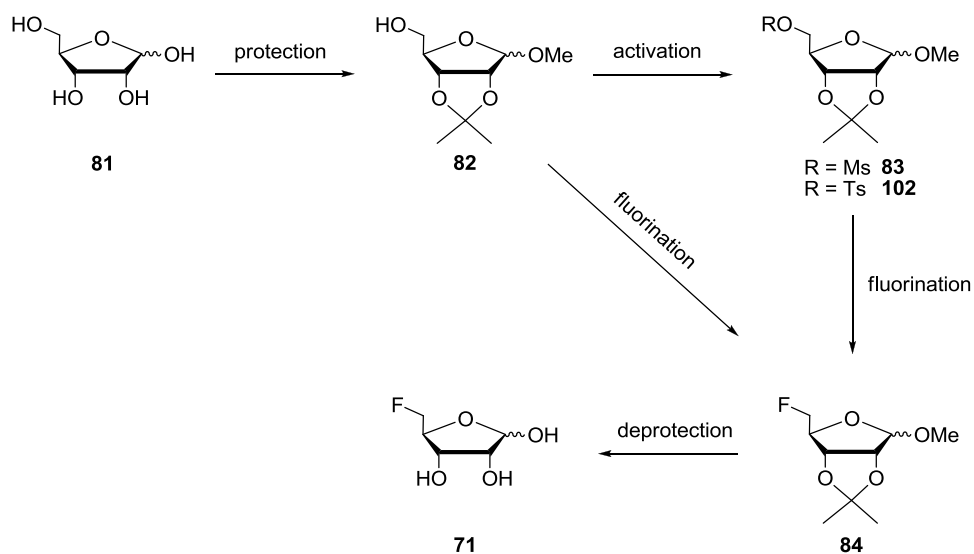
This new synthetic route to 5'-FDA **47** was therefore explored for the first time in the lab following the literature as outlined in Scheme 3.4 (*vide infra*).



Scheme 3.4 Reagents and conditions: (a) Acetone, 2,2-dimethoxypropane, *p*-toluenesulfonic acid monohydrate, RT, 4 h, 73% (b) TsF, TBAF, THF, 66 °C, 22 h, 81% (c) NH₃, *t*-BuOH, sealed tube, 90 °C, 24 h, 92% (d) TFA (90%), RT, 25 min, 85%.

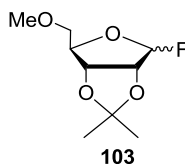
The synthesis starts with 2',3'-isopropylidene-6-chloropurine riboside **99** (Scheme 3.4, *vide supra*), which, although commercially available, is easily prepared from 6-chloropurine riboside **98**.¹⁴ Then, the free 5'-OH is dehydroxyfluorinated by refluxing in THF with tosyl fluoride (TsF) and tetrabutylammonium fluoride (TBAF) following the method previously described by Shimizu.¹⁵ The generation of the tosylate in the presence of excess fluoride was predicted to minimise the formation of any undesired cyclic nucleoside **97**. However, under such conditions, fluorine substitution at the *N*⁶-position of **99** was also observed, giving rise to the resultant aryl fluoride **100b**. Therefore **100a** and **100b** were obtained as a mixture and carried through to the next step. The mixture of **100a** and **100b** was then aminated smoothly by heating in a *t*-BuOH solution saturated with NH_{3(g)}. The desired 2',3'-isopropylidened-5'-deoxy-5'-fluoroadenosine **96** was formed in excellent yield (92%). Deprotection to give **47** was then achieved in good yield using 90% trifluoroacetic acid (TFA).¹⁶

This new synthetic route to 5'-FDA **47** proved very successful in our hands, showing good yields in all of the steps and it has emerged as our route of choice to 5'-FDA **47**.

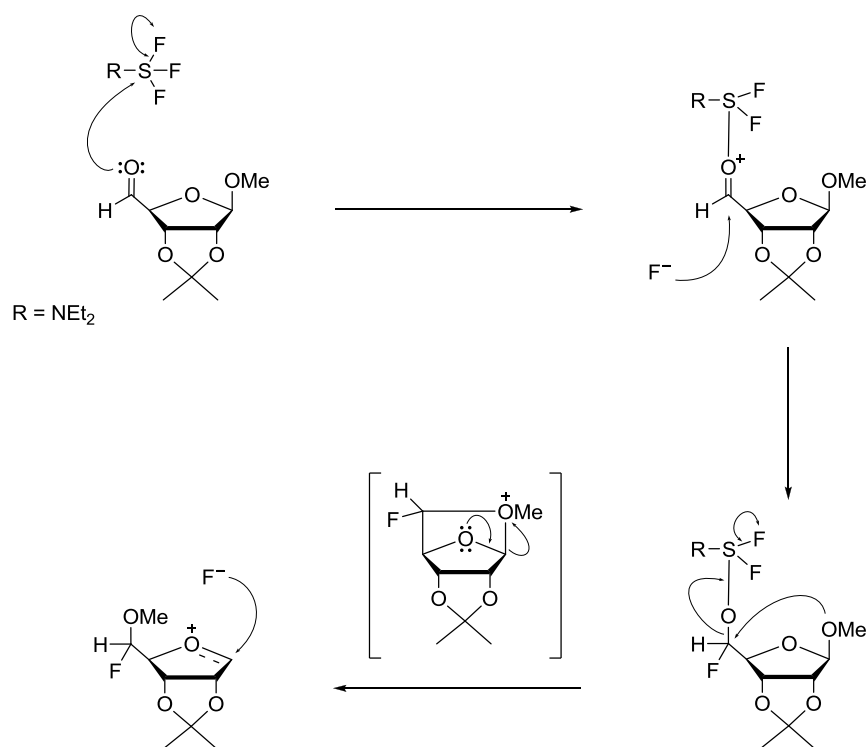


Scheme 3.6 Potential synthetic approaches to 5-FDR **71**.

With D-ribose **81** as starting material, the synthetic route involved formation of the dimethyl acetal and then a selective protection of the 2,3-hydroxyl groups, leaving the 5-OH free, generating methyl-2,3-*O*-isopropylidene- β -D-ribofuranoside **82**.¹⁸ This was easily achieved by using BF_3 in ether as the catalyst and a mixture of 2,2-dimethoxypropane and acetone.¹⁹ With **82** in hand, direct fluorination with DAST was attempted. Despite Sharma *et al.* reporting a 35% yield for this fluorination reaction, it was found that the desired fluorinated ribofuranoside **84** was formed in only very low yield. Instead, the major product of the reaction was found to be 2,3-*O*-isopropylidene-5-*O*-methyl-ribofuranosyl fluoride **103**.



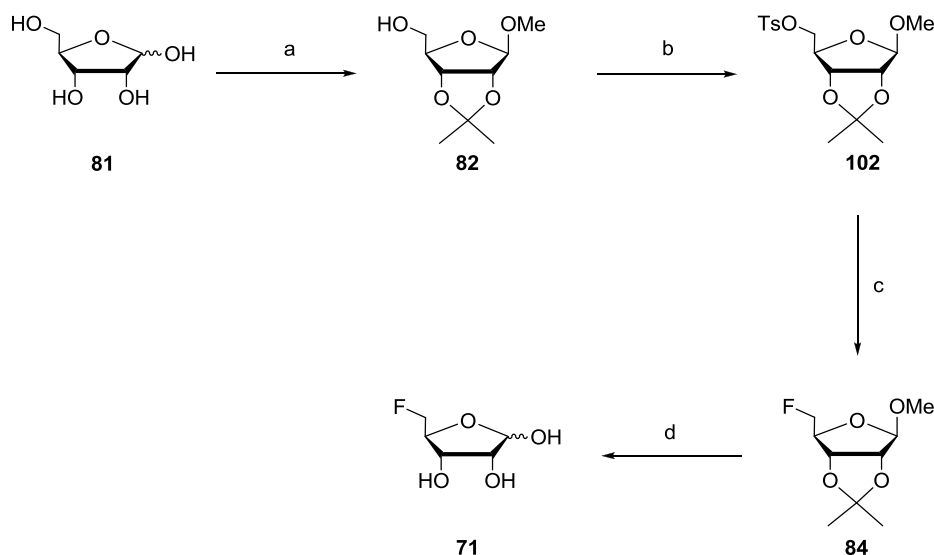
This result is consistent with the findings previously published by Lloyd and co-workers.²⁰ They investigated the migration of the methoxyl group from C-1 to C-5 in different carbohydrates when treated with DAST and they also proposed a mechanism, illustrated below in Scheme 3.7.



Scheme 3.7 Proposed mechanism for the 1,5-migration of the -OCH₃ group in furanosides treated with DAST.²⁰

Despite the existence of these reported synthetic routes, the procedure of choice to produce 5-FDR **71** involved a modification of the first route reported by Kissman (Scheme 3.1), following the sequence protection→activation→fluorination→deprotection. As previously described, fluorination reactions are usually carried out on reactive sulfonates. Thus, it was envisaged that activation of **82** via the formation of a 5-*O*-tosylate **102** could facilitate the subsequent nucleophilic displacement by fluoride using TBAF. Having prepared the

fluorinated protected sugar **83**, removal of the methyl ether and the isopropylidene protecting groups would then furnish 5-FDR **71**. Scheme 3.8 outlines this synthetic route to 5-FDR **71**.



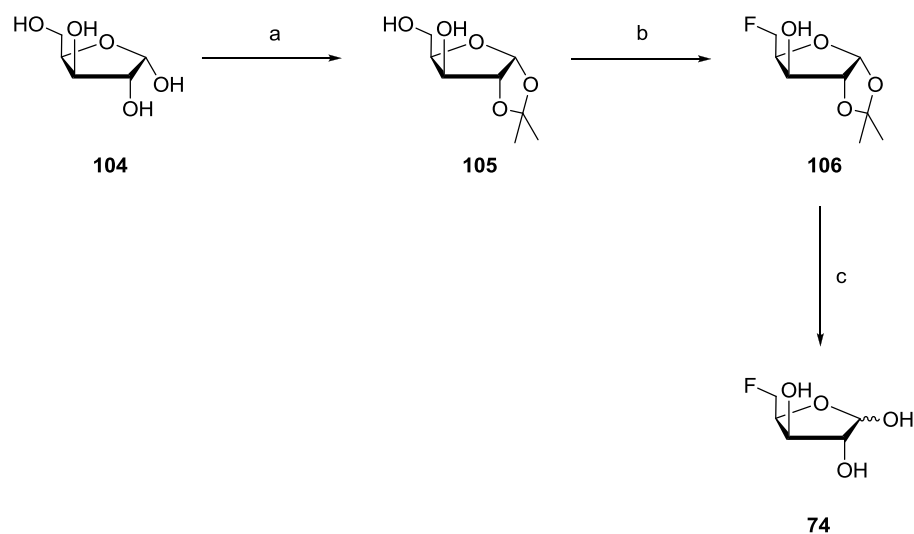
Scheme 3.8 Reagents and conditions: (a) MeOH, acetone, 2,2-dimethoxypropane, $\text{BF}_3 \cdot \text{ether}$, RT, 20 h, 57% (b) TsCl, pyridine, RT, 3 h, 76% (c) TBAF.3H₂O, MeCN, reflux, 22 h, 59% (d) 0.02 M H₂SO₄, reflux, 5 h, 95%.

Accordingly, after generation of methyl-2,3-O-isopropylidene-β-D-ribofuranoside **82**, the 5-hydroxyl group was then activated *via* the corresponding tosylate **102**. It was found that **102** could easily be prepared under standard reaction conditions in very good yield.²¹ Treatment of **102** with TBAF.3H₂O (2.5 molar eq.) in acetonitrile and under reflux, resulted in the formation of the desired product methyl-2,3-O-isopropylidene-5-deoxy-5-fluoro-β-D-ribofuranoside **84** in moderate yield. Analytical and spectroscopic data for **84** were in good agreement with the literature.^{1,2} Removal of the methyl ether and isopropylidene protecting groups of the fluorinated and protected sugar **84** was easily achieved under acidic conditions.¹ As expected, the product was the free fluorinated ribose **71**. Analysis by ¹⁹F NMR

(D₂O, 25 °C) showed an anomeric mixture in 2:1 ratio, in which the major anomer was determined to be the β-anomer, by comparison with the literature.

3.3 Synthesis of 5-deoxy-5-fluoro-D-xylose **74**

The synthesis of 5-deoxy-5-fluoro-D-xylose (5-FDX) **74** has also been reported in the literature. The first route was published by Kent and Young,²² however it is a lengthy and not convenient synthetic method to 5-FDX **74**. Later, another synthetic approach to **74** was reported by Hadwiger and co-workers.^{23,24} This synthetic procedure is outlined in Scheme 3.9.



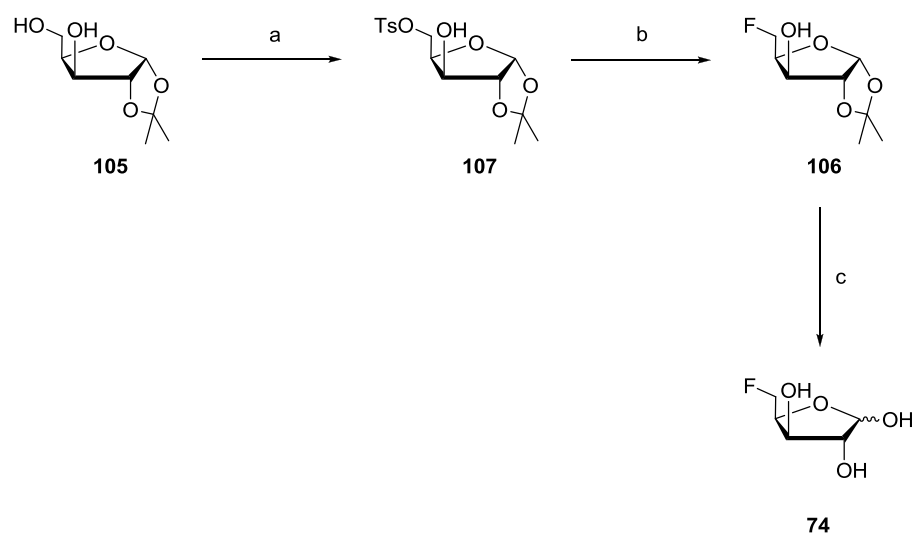
Scheme 3.9 Synthesis of 5-FDX **74** reported by Hadwiger *et al.*^{23,24}

Reagents and conditions: (a) 0.66 M H₂SO₄, acetone, 20 °C, 2.5 h, 80% (b) DAST, CH₂Cl₂, -40 °C, 34% (c) IR 120, H₂O/MeCN, 50 °C, 48%.

The first step of the synthesis involved the selective protection of the hydroxyl groups at C-1 and C-2 of xylose. This can be easily achieved following a standard one-pot procedure.²⁵ However, 1,2-di-*O*-isopropylidene- α -D-xylofuranose **105** is a common intermediate in the

syntheses of different biologically active compounds (*i.e.*, antibiotics, nucleosides, herbicides, anti-HIV agents) and is nowadays commercially available.

With 1,2-di-*O*-isopropylidene- α ,D-xylofuranose **105** in hand, direct fluorination of the free 5-OH was attempted using DAST as the fluorinating reagent, as reported by Hadwiger *et al.* The poor yield of the reaction, together with the formation of by-products rendered it unsuitable. Thus, another synthetic strategy was explored for the preparation of 5-FDX **74**, based on the previous strategy: protection \rightarrow activation \rightarrow fluorination \rightarrow deprotection. Scheme 3.10 illustrates the synthetic route that eventually gave **74**. All of the reactions steps proceeded in moderate to good yields.



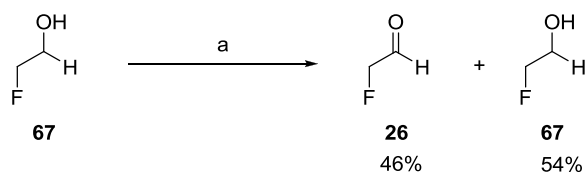
Scheme 3.10 Reagents and conditions: (a) TsCl, pyridine, RT, 3 h, 80% (b) TBAF.3H₂O, MeCN, reflux, 24 h, 57% (c) 0.02 M H₂SO₄, reflux, 4 h, 90%.

Starting with commercially available 1,2-di-*O*-isopropylidene- α ,D-xylofuranose **105**, introduction of the fluorine atom at C-5 was envisaged using a suitably protected 5-sulfonate. Consequently, **107** was prepared by tosylation of **105** with *p*-toluenesulfonyl chloride in the usual manner.²⁶ The reaction gave 1,2-di-*O*-isopropylidene-5-*O*-tosyl- α ,D-xylofuranose **107**

exclusively, with no side-product formation or undesired tosylates. Thereby, tosylate **107** was then subjected to fluoride substitution using TBAF as the fluorine source. The fluorination reaction was found to proceed successfully and in a moderate yield to furnish 5-deoxy-5-fluoro-1,2-di-*O*-isopropylidene- α ,D-xylofuranose **106**. Analytical and spectroscopic data were in good agreement with the literature.^{22,23,24} Finally, fluorinated xylofuranose **106** was hydrolysed under acidic conditions to afford 5-FDX **74**, as a mixture of anomers.

3.4 Synthesis of fluoroacetaldehyde **26**

The synthesis of fluoroacetaldehyde (FAd) **26** was carried out using the previously described procedure as outlined in Scheme 3.11.²⁷ Fluoroethanol **67** is oxidised using pyridinium dichromate (PDC) in dichloromethane (DCM) to generate fluoroacetaldehyde **26** which is collected as its hydrate by distillation directly into water. The oxidation reaction never goes to completion and ¹⁹F NMR analysis of the resultant FAd **26** (−231.0 ppm, dt, ²*J*_{F-H} 46.7 and ³*J*_{F-H} 10.0 Hz) typically shows 54% residual fluoroethanol **67** (−224.5 ppm, tt, ²*J*_{F-H} 47.6 and ³*J*_{F-H} 32.1 Hz). This preparation has been used in cell-free studies by previous co-workers and in this thesis. The contaminating fluoroethanol **67** is metabolically inert and does not generally prove problematic.



Scheme 3.11 Reagents and conditions: (a) PDC, DCM, reflux, 16 h.

3.5 References

1. H. M. Kissman and M. J. Weiss, *J. Am. Chem. Soc.*, 1958, **80**, 5559-5564.
2. M. Sharma, Y. X. Li, M. Ledvina and M. Bobek, *Nucleos. Nucleot.*, 1995, **14**, 1831-1852.
3. *US Pat.*, 5998388, 1999.
4. Sz. Lehel, G. Horváth, I. Boros, P. Mikecz, T. Márián and L. Trón, *J. Radioanal. Nucl. Chem.*, 2000, **245**, 399-401.
5. S. L. Cobb, Ph.D. Thesis, *The origin and metabolism of 5'-FDA in Streptomyces cattleya*, University of St Andrews, 2005.
6. S. B. Ha and V. Nair, *Tetrahedron Lett.*, 1996, **37**, 1567-1570.
7. D. Gani and A. W. Johnson, *J. Chem. Soc., Perkin Trans. I*, 1982, 1197-1204.
8. R. K. Sharma and J. L. Fry, *J. Org. Chem.*, 1983, **48**, 2112-2114.
9. D. P. Cox, J. Terpinski and W. Lawrynowicz, *J. Org. Chem.*, 1984, **49**, 3216-3219.
10. T. D. Ashton and P. J. Scammells, *Bioorg. Med. Chem. Lett.*, 2005, **15**, 3361-3363.
11. V. M. Clark, A. R. Todd and J. Zussman, *J. Chem. Soc.*, 1951, 2952-2958.
12. Sz. Lehel, G. Horváth, I. Boros, T. Márián and L. Trón, *J. Radioanal. Nucl. Chem.*, 2002, **251**, 413-416.
13. V. Bakthavachalam, L.-G. Lin, X. M. Cherian and A. W. Czarnik, *Carbohydr. Res.*, 1987, **170**, 124-135.
14. F. Kappler and A. Hampton, *J. Med. Chem.*, 1990, **33**, 2545-2551.
15. M. Shimizu, Y. Nakahara and H. Yoshioka, *Tetrahedron Lett.*, 1985, **26**, 4207-4210.
16. C. D. Cadicamo, J. Courtieu, H. Deng, A. Meddour and D. O'Hagan, *ChemBioChem*, 2004, **5**, 685-690.
17. M. Ebner and A. E. Stütz, *Carbohydr. Res.*, 1998, **305**, 331-336.

CHAPTER 3

18. A. P. Rauter, F. Ramôa-Ribeiro, A. C. Fernandes and J. A. Figueiredo, *Tetrahedron*, 1995, **51**, 6529-6540.
19. G. Ceulemans, F. Vandenriessche, J. Rozenski and P. Herdewijn, *Nucleos. Nucleot.*, 1995, **14**, 117-127.
20. A. E. Lloyd, P. L. Coe R. T. Walker and O. W. Howarth, *J. Fluorine Chem.*, 1993, **60**, 239-250.
21. F. Sarabia-García and F. J. López-Herrera, *Tetrahedron*, 1996, **52**, 4757-4768.
22. P. W. Kent and R. C. Young, *Tetrahedron*, 1971, **27**, 4057-4064.
23. P. Hadwiger, P. Mayr, A. Tauss, A. E. Stütz and B. Nidetzky, *Bioorg. Med. Chem. Lett.*, 1999, **9**, 1683-1686.
24. P. Hadwiger, P. Mayr, B. Nidetzky, A. E. Stütz and A. Tauss, *Tetrahedron Asymm.* 2000, **11**, 607-620.
25. J. Moravcová, J. Capková and J. Stanek, *Carbohydr. Res.*, 1994, **263**, 61-66.
26. Y. Li and G. Just, *Tetrahedron*, 2001, **57**, 1677-1687.
27. C. Schaffrath, Ph.D. Thesis, *Biosynthesis and Enzymology of Fluorometabolite Production in Streptomyces cattleya*, University of St Andrews, 2002.

C_{HAPTER} 4

**The fluorinase as a tool
for the synthesis of new
fluorine-18 labelled sugars
for positron emission
tomography**

The fluorinase as a tool for the synthesis of new fluorine-18 labelled sugars for positron emission tomography

There is an increasing interest in the preparation of [^{18}F]-labelled radiopharmaceuticals with potential application in positron emission tomography (PET), one of the most common techniques in medical imaging. This requires an efficient route to incorporate fluorine-18 into a drug molecule. However, the incorporation of fluorine-18 into a radiotracer is not always easy to achieve.

A possibility for the synthesis and formation of C- ^{18}F bonds from [^{18}F]fluoride ion became available with the discovery of the fluorinase from *S. cattleya* (EC 2.5.1.63). In this project the enzymatic preparation of [^{18}F]-labelled sugars using the fluorinase, as potential radiotracers for positron emission tomography, has been investigated. In addition, imaging studies with human cancer cell lines and small rodents have been accomplished.

Because of the requirement for fluorine-18 and some human cancer cell lines, this work has been carried out in collaboration, initially with Dr Christophe Plisson at GlaxoSmithKline (PET Laboratory at Mount Vernon Hospital in Northwood, U.K.), and more recently with Dr Lutz Schweiger, Dr Juozas Domarkas and Dr Timothy A. D. Smith at the University of Aberdeen (John Mallard PET Centre in Aberdeen, U.K.).

4.1 Introduction to positron emission tomography

Positron emission tomography (PET) is a high-resolution, sensitive, non-invasive imaging technique in nuclear medicine that permits the assessment and quantification of specific biological and pharmacological processes at the molecular level in humans and animals. This medical imaging method can measure the spatial and temporal concentration of a positron emitting isotope in a volume element of tissue. It was developed in the mid-1970s by Phelps *et al.*,¹ and is the most advanced technology currently available for studying *in vivo* molecular interactions in terms of distribution, pharmacokinetics and pharmacodynamics.^{2,3} Its applications are very varied, and a growing number of diverse physiological parameters in humans and animals (*i.e.*, blood flow, glucose metabolism, receptor properties, enzyme activity and drug distribution and mechanisms) have been investigated using this technique. Although PET has been extensively applied to studies of the brain, heart and tumours, its use goes beyond these systems.^{3,4} Within the last few years, it has been increasingly implemented in clinical diagnosis,⁵ becoming the main technique in the study of the brain^{6,7} heart disease,⁸ and neurological and psychiatric disorders. Diseases such as Alzheimer's disease,⁹ dementia,¹⁰ epilepsy,¹¹ depression,^{12,13} and schizophrenia¹⁴ have all benefitted from PET. In recent years, PET imaging has been applied in drug abuse research, providing information on the mechanisms responsible for substance abuse, addiction, and dependence.^{15,16,17}

However, the outstanding feature of PET is that it allows the visualization of tissue malfunction *in vivo*, thereby representing an important technique for the development of anticancer strategies and for assessing the response to cancer therapy.^{18,19,20,21} In addition to the major role that PET plays in oncology research,^{22,23} it is also used to perform pharmacokinetic studies *in vivo*, providing information on functional activity, biochemical transformations and distribution of organic compounds in the body.²⁴ Such studies may be among the most valuable research applications of PET, and leave open the future possibility

of testing drug effectiveness on humans to obtain data much more quickly than is currently possible.²⁵

PET employs mainly short-lived positron-emitting radiopharmaceuticals. The common positron emitting isotopes (^{18}F , ^{11}C , ^{13}N , ^{15}O) are those of the common elements in organic chemistry (Table 4.1, *vide infra*). The availability of such isotopes offers a wide range of possibilities for the investigation of various biochemical pathways, since they are constituents of the physiological substrates, proteins, and neurochemicals that regulate and sustain biological processes. The use of positron-emitting isotopes of these natural elements allows the preparation of labelled tracer molecules that have chemical and biological behaviour identical to the authentic, unlabelled molecules.³

Table 4.1 Comparative physical properties of radionuclides for PET imaging.^{3,26}

| Nuclide | Half-life | Maximum Energy (MeV) | Decay |
|------------------|-----------|----------------------|-------------------|
| ^{11}C | 20.4 min | 0.96 | β^+ (99%) |
| ^{13}N | 9.96 min | 1.19 | β^+ (99%) |
| ^{15}O | 2.07 min | 1.723 | β^+ (99.9%) |
| ^{18}F | 109.7 min | 0.635 | β^+ (97%) |
| ^{76}Br | 16.1 h | 3.98 | β^+ (57%) |
| ^{124}I | 4.18 days | 2.13 | β^+ (24%) |

The four most widely used positron emitters are carbon-11, nitrogen-13, oxygen-15 and fluorine-18. Three properties of all of these isotopes: the short half-life, the chemistry which is applicable to labelling organic molecules, and the high specific activity, contribute to their implementation to tracer studies in humans. Nevertheless, among those properties is the short

half-life of the positron which dominates the research and application for PET, since isotope production and tracer preparation and analysis must be carried out within a restricted time frame. For this reason, fluorine-18, with the longest half-life and the lowest positron energy (Table 4.1, *vide supra*), is the most suitable positron emitting radionuclide for clinical investigations in PET.^{3,26}

Although there are different methods for its production, fluorine-18 is usually generated in a cyclotron through the proton irradiation of [¹⁸O]-enriched water (*i.e.*, ¹⁸O(p,n)¹⁸F). Several Curies (Ci) may be produced in a single irradiation whereas only 5–15 mCi of radiotracer need to be injected into a human subject for a PET examination. Fluorine-18 is obtained as a solution of [¹⁸F]fluoride ion in the irradiated target water, and the fact that it is obtained as ‘no-carrier added’ increases its specific radioactivity (*i.e.*, the ratio of [¹⁸F]fluoride ion radioactivity to its mass of carrier or total fluoride ion). This enables the administration of radiotracers to human subjects in low mass doses (typically less than 1–10 nmol), with no toxicity or pharmacological effects involved.²⁷

The chemistry of fluorine-18 presents, however, several difficulties. First of all, isotopic labelling is theoretically limited to molecules having an atom of fluorine in their structure. Nevertheless, approximately 30% of molecules of therapeutic interest contain at least one fluorine atom.²⁸ New candidate molecules for ¹⁸F PET studies may be synthesised by substituting one of the atoms of a non-fluorinated molecule by a fluorine atom but, in this case, the biological properties of this new radiotracer have to be assessed independently.

From a chemical point of view, methods for the introduction of a fluorine-18 atom into a chemical structure rely on either electrophilic (*i.e.*, starting from molecular fluorine [¹⁸F]F₂) or nucleophilic (*i.e.*, starting from the fluoride ion [¹⁸F]F⁻) fluorination reactions.^{3,26,27,29}

Many useful positron-emitting radiotracers have been developed and have proven to be attractive candidates for extensive clinical application. The first produced

radiopharmaceutical for PET studies, and the most widely used today, is 2-deoxy-2- ^{18}F fluoro-D-glucose, ^{18}F FDG, [^{18}F]**108**; a fluorinated analog of 2-deoxy-D-glucose (2DG).³⁰ Its major application is as radiotracer of glucose utilisation and metabolism in oncology and neurology.^{31,32} It is also the major PET tracer for examining the effect of a drug on glucose metabolism in tumours,^{33,34} since the ability to sustain high rates of glycolysis is a common feature of rapidly proliferating malignant cells.³⁵ The increased rates of glucose metabolism in cancer cells, compared to healthy cells, is the biochemical principle on which PET is based, making it a molecular imaging technique for the detection and staging of tumours.³⁶ Glucose enters the cell *via* carrier proteins of the GLUT family. It is phosphorylated at O-6 and then undergoes complex metabolism. The modified and radiolabelled glucose analogue, ^{18}F FDG [^{18}F]**108**, is transported into the cell in the same way and is also phosphorylated by hexokinase to ^{18}F FDG-6-P (Figure 4.1, *vide infra*). By contrast to phosphorylated glucose, ^{18}F FDG-6-P undergoes limited metabolism in most tissues and its permeability is quite low. Thus, ^{18}F FDG [^{18}F]**108** is essentially trapped inside the cell, and its accumulation can be measured non-invasively using PET.^{37,38,39}

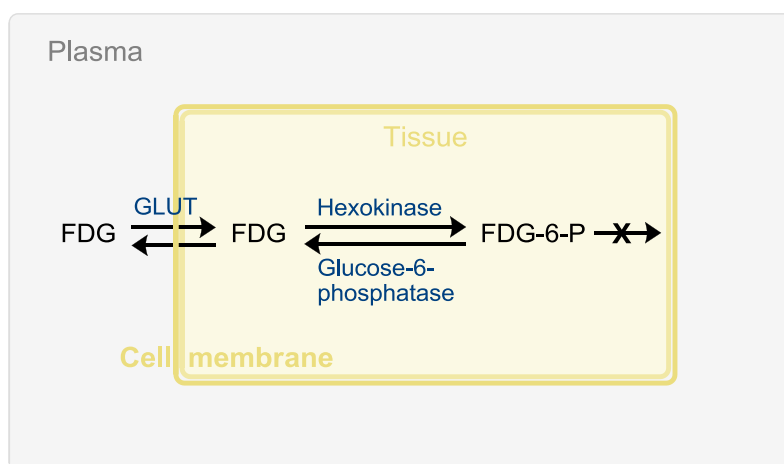
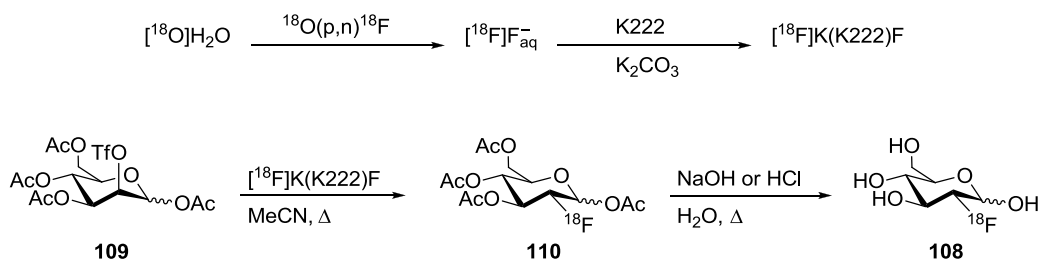


Figure 4.1 Intracellular uptake of ^{18}F FDG [^{18}F]**108** ('metabolic trapping').

CHAPTER 4

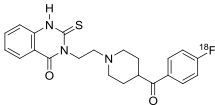
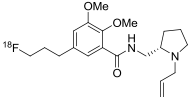
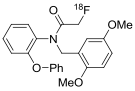
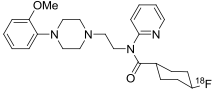
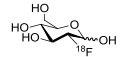
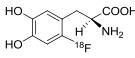
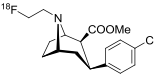
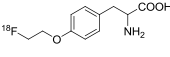
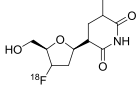
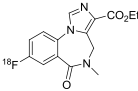
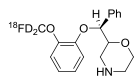
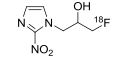
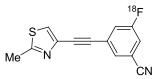
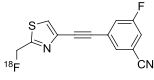
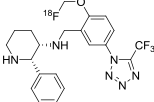
The radiosynthesis of [^{18}F]FDG [^{18}F]**108** is based on the nucleophilic substitution of a modified mannose precursor with [^{18}F]fluoride ion acting as a nucleophile,⁴⁰ as illustrated in Scheme 4.1.



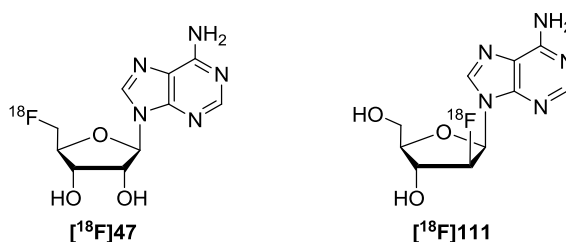
Scheme 4.1 Radiosynthesis of [^{18}F]FDG [^{18}F]**108** (K222: Kryptofix[®] 2.2.2)

The successful use of [^{18}F]FDG [^{18}F]**108** in PET imaging has prompted the design and synthesis of other [^{18}F]-labelled molecules.⁴¹ Some of these fluorinated radiotracers are shown in Table 4.2 (*vide infra*).

Table 4.2 Selected [^{18}F]-labelled PET radiotracers.²⁷

| Radiotracer | Structure | Applications to measurement of: |
|--|---|---|
| [^{18}F]Altanserin |  | Brain 5-HT ₂ receptors |
| [^{18}F]Fallypride |  | Brain D ₂ receptors |
| [^{18}F]FBR |  | Brain "peripheral" benzodiazepine receptors |
| [^{18}F]FCWAY |  | Brain 5-HT _{1A} receptors |
| [^{18}F]FDG |  | Glucose metabolism |
| [^{18}F]FDOPA |  | Brain dopamine metabolism |
| [^{18}F]FECNT |  | Brain dopamine transporters |
| [^{18}F]FET |  | Tumour location |
| [^{18}F]FLT |  | Cellular proliferation |
| [^{18}F]Flumazenil |  | Brain benzodiazepine receptors |
| [^{18}F]FMeNER- <i>d</i> ₂ |  | Noradrenaline transport |
| [^{18}F]FMISO |  | Hypoxia |
| [^{18}F]FMTEB |  | Brain mGluR5 receptors |
| [^{18}F]SP203 |  | Brain mGluR5 receptors |
| [^{18}F]SPA-RQ |  | Brain neurokinin type-1 receptors |

There is an increasing interest in the synthesis of [^{18}F]-labelled sugars and derivatives for clinical investigations.⁴² Among other PET labelled probes which may have potential for the imaging of tumours or receptors in the brain, are the adenosine derivatives.⁴³ The radiolabelled analogue of 9-(2'-deoxy-2'-fluoro- β -D-arabinofuranosyl)adenine, [^{18}F]FAD [^{18}F]111, has shown promise in imaging tumour cell proliferation by PET.⁴⁴



With the stated aim of imaging adenosine receptor systems by the PET technique, the synthesis of 5'-deoxy-5'-[^{18}F]fluoroadenosine, [^{18}F]FDA [^{18}F]47, was attempted for the first time in 2000 by Lehel and co-workers.⁴⁵ However, the introduction of the radioisotope into the molecule proved to be especially difficult, giving extremely low radiochemical yields ($\leq 1\%$). Further unsuccessful efforts to synthesise [^{18}F]FDA [^{18}F]47 led to the conclusion that: "5'-deoxy-5'-[^{18}F]fluoroadenosine cannot be synthesised in preparatively acceptable amounts starting from a precursor of adenosine structure".⁴⁶

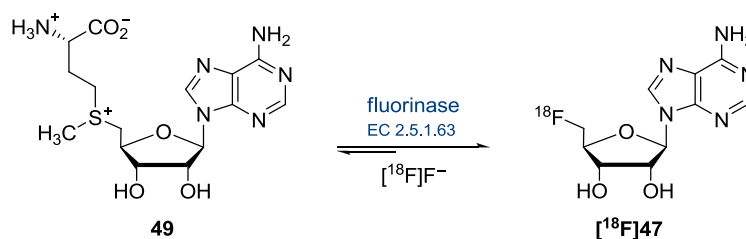
In spite of its sometimes difficult chemistry, fluorine-18 remains the most attractive PET nuclide because of its convenient half-life and low positron energy. The current challenge for [^{18}F]-labelled pharmaceuticals is to develop rapid and clean synthesis methods with straightforward purification protocols for new *in vivo* imaging probes. Enzymatic methods are in principle attractive because of the chemospecificity and low generation of side products. So far there are only a few examples in PET synthesis where enzymes have been used to introduce isotopically labelled atoms, largely because suitable enzymes are not available.^{47,48,49,50}

4.2 Application of the fluorinase enzyme in PET

Studies towards the synthesis of the adenosine derivative 5'-deoxy-5'-[^{18}F]fluoroadenosine, [^{18}F]FDA [^{18}F]**47**, highlighted the difficulty of introducing [^{18}F]fluoride in the 5'-position of the nucleoside; when a series of 5'-halo and 5'-sulfonic acid alkyl and aryl esters failed to produce the expected radiolabelled adenosine derivatives in sufficient yield under the commonly used nucleophilic substitution reaction conditions with [^{18}F]fluoride ion.⁴⁶

With the fluorinase in hand, there was the prospect of the synthesis of [^{18}F]FDA [^{18}F]**47** in one chemical step.

In 2003, the St Andrews lab in collaboration with GlaxoSmithKline reported the first enzymatic radiolabelling method for the production of 5'-deoxy-5'-[^{18}F]fluoroadenosine,⁵¹ [^{18}F]FDA [^{18}F]**47**, by incubating purified wild-type fluorinase from *S. cattleya* with SAM **49** and [^{18}F]F $^-$ (Scheme 4.2).

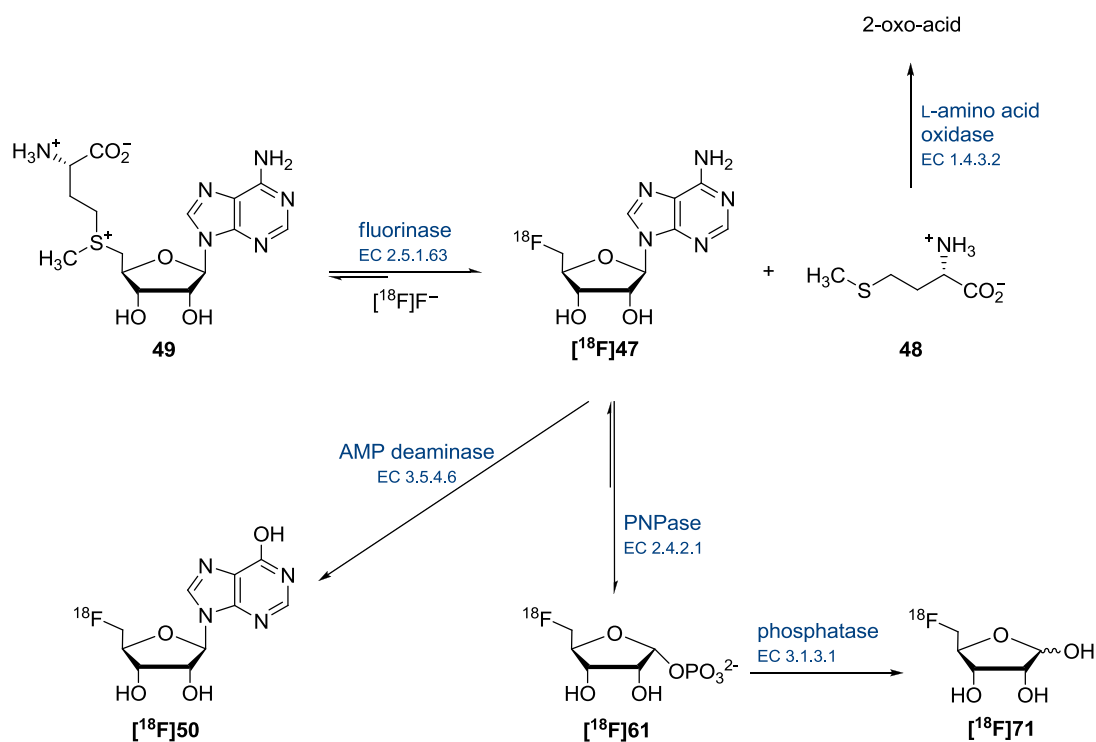


Scheme 4.2 Enzymatic radiolabelling of 5'-deoxy-5'-[^{18}F]fluoroadenosine, [^{18}F]**47**.

In these experiments, the fluorinase enzyme was partially purified by ammonium sulfate precipitation and anion exchange chromatography.⁵² Interestingly, it was shown that the purity of the enzyme had no measurable effect on the radiochemical yield (RCY) of the reaction or the radiochemical purity of [^{18}F]FDA [^{18}F]**47**. Although the radiochemical yield of

the reaction was very low (*ca.* 1%), the successful enzymatic fluorination at the first attempt was significant and provided a foundation for future optimisation.

The subsequent realisation that the fluorination reaction is reversible,⁵³ and that the equilibrium of the reaction must be pulled over towards [¹⁸F]FDA [¹⁸F]47 formation for efficient conversion, led to more satisfactory results. In these latter experiments,⁵⁴ the radiosynthesis of [¹⁸F]47 was improved by using a different coupled enzyme strategy (Scheme 4.3, *vide infra*). This involved over-expressed fluorinase in mg/ml concentrations and the introduction of a second enzyme, an L-amino-acid oxidase (EC 1.4.3.2), which catalyses the oxidation of L-methionine 48 to a 2-oxo-acid, improving the rate of synthesis and the overall conversion to [¹⁸F]FDA [¹⁸F]47 up to 95% under optimum conditions.



Scheme 4.3 Fluorinase coupled reactions for the synthesis of various [¹⁸F]-labelled compounds.

CHAPTER 4

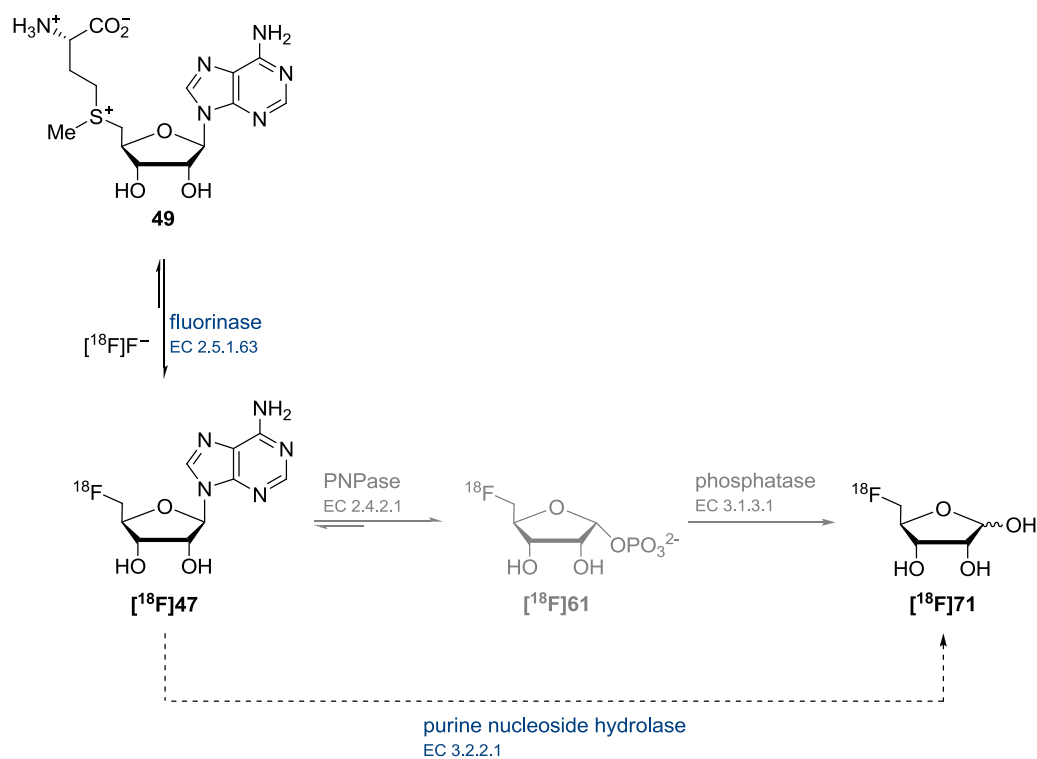
The second approach (*vide supra* Scheme 4.3) involved coupling the fluorinase to an 5'-adenylic acid deaminase (AMP deaminase, EC 3.5.4.6) enzyme to generate [¹⁸F]FDI [¹⁸F]**50** with a RCY of 75% from [¹⁸F]fluoride, achieved over 4 h. Finally, combining the fluorinase reaction with a purine-nucleoside phosphorylase (PNPase, EC 2.4.2.1) and then an alkaline phosphatase (EC 3.1.3.1) resulted in the sequential depurination and phosphate hydrolysis to produce the free ribose sugar [¹⁸F]FDR [¹⁸F]**71** in an overall radiochemical yield of 45% obtained after a 4 h reaction.

These experiments also revealed information about how temperature and fluorinase concentration affect the process. A modest increase in temperature (from 25 °C to 35 °C) had a significant influence on the radiochemical yield, and when increasing the fluorinase concentration (from 8 mg/ml to 24 mg/ml), higher RCY were also obtained and the reaction time could be shortened.

4.2.1 New enzymatic method

for the synthesis of [^{18}F]FDR

The bioconversion of SAM **49** and [^{18}F]fluoride to [^{18}F]FDR [^{18}F]**71** was accomplished in a three enzyme system consisting of the fluorinase (EC 2.5.1.63), an immobilised PNPase (EC 2.4.2.1) and a phosphatase (EC 3.1.3.1). An efficient radiolabelled synthesis of a ribose sugar became a key research objective, given the role that [^{18}F]FDG [^{18}F]**108** has in PET.⁵⁵ Thereby, it was attractive to develop a protocol for the synthesis of [^{18}F]FDR [^{18}F]**71** *via* a shorter route starting from SAM **49**. This envisaged approach for the synthesis of [^{18}F]**71** involved coupling the fluorinase to an enzyme which acts upon [^{18}F]FDA [^{18}F]**47** by direct hydrolysis of the *N*-glycosidic bond, generating [^{18}F]FDR [^{18}F]**71** and adenine **62** in a two step protocol, as illustrated in Scheme 4.4.



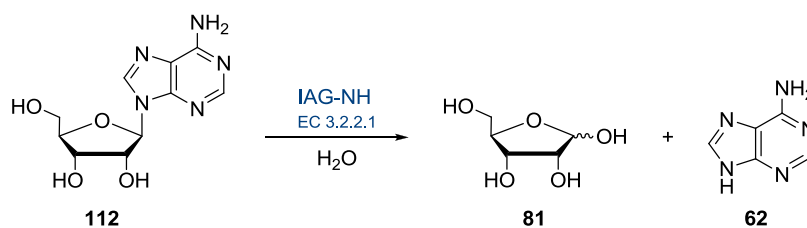
Scheme 4.4 Potential two step route for the synthesis of [^{18}F]FDR [^{18}F]**71** starting from SAM **49**.

Ideally, this new route to [^{18}F]FDR [^{18}F]71 from SAM 49, coupling the fluorinase to a nucleoside hydrolase, could be carried out as a one-pot reaction. With this objective, the best conditions for each enzyme had to be investigated in order to find optimal conditions for a one-pot reaction.

4.2.1.1 Development of the "cold" experiment

A. Nucleoside hydrolases

Nucleoside hydrolases (or nucleoside *N*-ribohydrolases; NHs) are a group of enzymes that catalyse the hydrolysis of the *N*-glycosidic bond (glycosidases, EC 3.2.2.-) between the anomeric carbon atom of ribose and the purine (EC 3.2.2.1) or pyrimidine (EC 3.2.2.8) base of β -ribonucleosides, forming the free nucleic acid base and ribose 81 (Scheme 4.5).⁵⁶



Scheme 4.5 The NH-catalysed hydrolysis of a ribonucleoside exemplified by adenosine *N*-glycosidic bond cleavage.

NHs are widely distributed in nature. These enzymes have been isolated, or the genes of the enzymes have been identified, from a variety of sources, including bacteria,^{57,58,59,60} yeast,⁶¹ protozoa,^{62,63} insects,⁶⁴ mesozoa,⁶⁵ plants.⁶⁶ Although found in most organisms, their physiological role is only well understood in certain parasitic protozoa (*e.g.*, *Trypanosoma*) where they are involved in the purine salvage pathways. Since neither nucleoside hydrolase activity, nor the encoding genes have been found in mammals, they constitute an attractive

target for drug design against a variety of pathogens.^{67,68,69} In addition, nucleoside hydrolases have also been proposed for use as pro-drug activators in chemotherapy.^{70,71}

All characterised nucleoside hydrolases show high specificity for the ribose moiety, but exhibit variability in their preferences for the nature of the nucleoside base. On the basis of the substrate specificity, NHs have been grouped into three subclasses: the inosine-uridine preferring nucleoside hydrolases (IU-NHs),^{72,73} the purine specific inosine-adenosine-guanosine preferring nucleoside hydrolases (IAG-NHs)^{74,75} and the 6-oxo-purine specific inosine-guanosine preferring nucleoside hydrolases (IG-NHs).⁷⁶

The nucleoside hydrolase from *Trypanosoma vivax* (TvNH) has been well characterised kinetically and structurally. This NH catalyses the hydrolysis of the *N*-glycosidic bond of inosine, adenosine and guanosine most efficiently.⁷⁴ The rates for these reactions are very similar, and the k_{cat} values for these substrates are rather low ($\approx 4 \text{ s}^{-1}$ at pH 7.0). The first crystal structure of the *T. vivax* IAG-NH enzyme shows that the enzyme forms hydrogen bonds with all three hydroxyl groups of the ribose moiety. A Ca^{2+} ion is tightly bound at the bottom of the active site (Figure 4.2, *vide infra*).⁷⁴

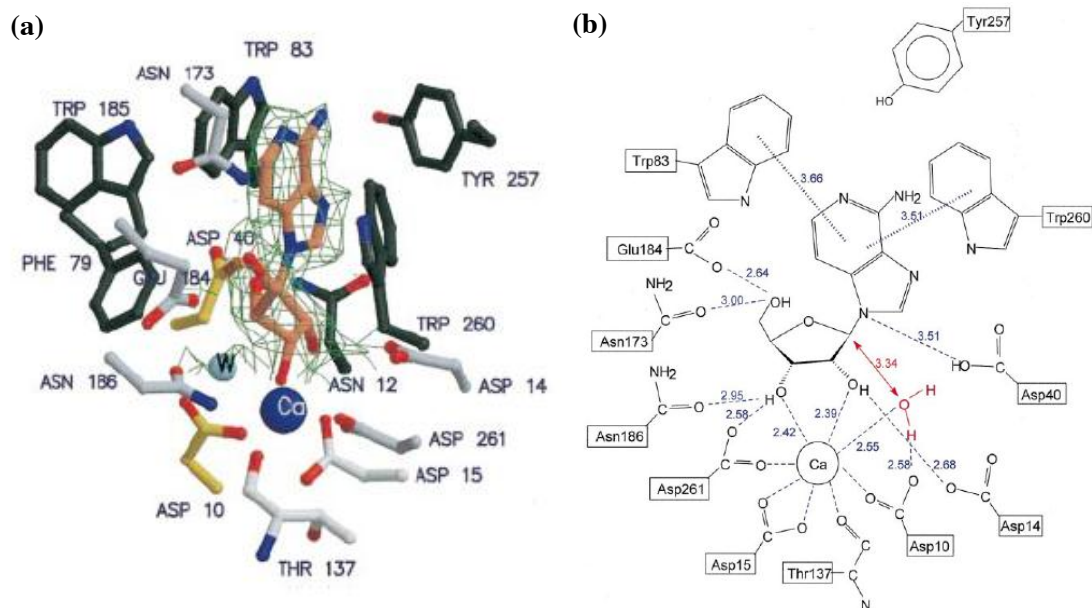


Figure 4.2 (a) Close-up stereoview of the *T. vivax* IAG-NH active site in complex with 3-deaza-adenosine. The calcium ion and the catalytic water molecule are depicted as dark and light blue spheres, respectively. The residues interacting with ribose or the calcium ion are colored light grey. The residues interacting with the 3-deaza-adenine base are colored dark grey. Asp10 (in yellow) is the proposed catalytic base. Asp40 (in yellow) could act as leaving group activator. (b) Schematic representation of interactions in the active site of the *T. vivax* IAG-NH (distances are given in Å).

It was previously shown for the NH from *T. brucei brucei* that interactions with the 5'-OH group mainly contribute to substrate binding, while interactions with the 2'-OH and the 3'-OH groups are important for the stabilisation of the oxocarbenium ion in the transition state.⁷⁵

Studies on substrates or inhibitors of the *T. vivax* NH with the 5'-OH group of the ribose moiety replaced for another atom have not been published so far. This led to a first investigation of 5'-FDA **47** as a potential substrate for TvNH.

CHAPTER 4

Recombinant NH was purified from extracts of *E.coli* strain BL21(DE3)Gold, transformed with the pQE30-IAGNH plasmid (which became available thanks to Dr J. Steyaert, Vrije Universiteit Brussel) according to the procedure outlined in Chapter 5.

A cell-free extract (300 μ l) containing NH activity was incubated with synthetic 5'-FDA **47** (30 μ l, 18.6 mM) in phosphate buffer (400 μ l, 50 mM, 1 mM CaCl₂) at 37 °C for 16 h, and the assay solution was subsequently analysed by ¹⁹F NMR spectroscopy. The presence of 5-FDR **71** (alongside other fluorinated furanoses, due to different activities present in the CFE) confirmed that the *T. vivax* NH catalyses the hydrolysis of the *N*-glycosidic bond of 5'-FDA **47**, producing 5-FDR **71** as shown below in Figure 4.3 (*vide infra*).

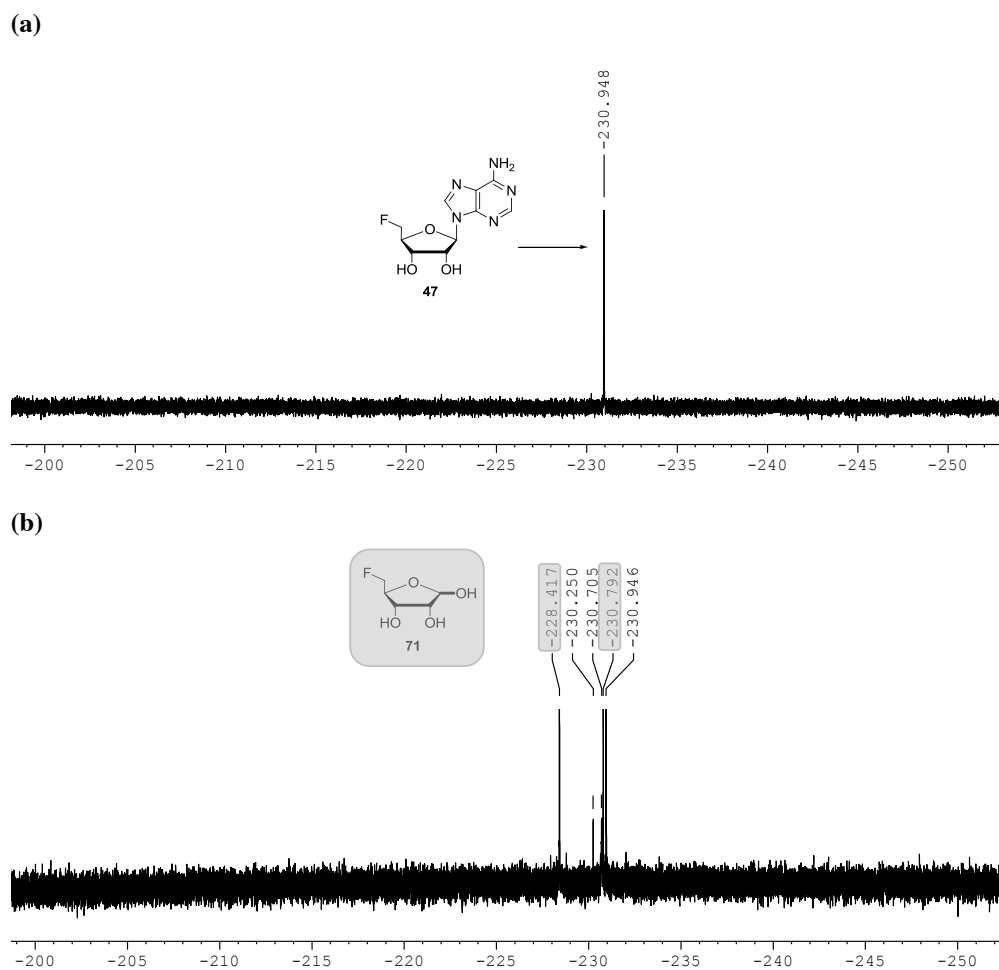
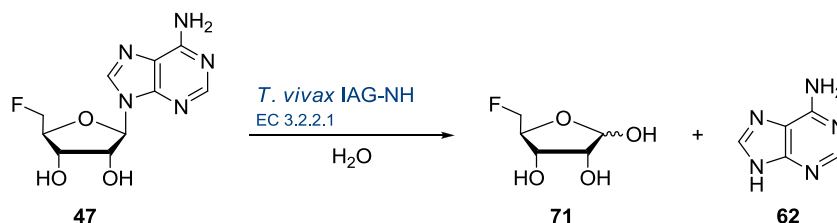


Figure 4.3 $^{19}\text{F}\{^1\text{H}\}$ NMR spectra of: (a) Control sample for the incubation of a CFE of TvNH with synthetic 5'-FDA **47** at time zero. (b) 5-FDR **71** generated after an overnight incubation of a CFE of TvNH with synthetic 5'-FDA **47**.

The initial published studies on TvNH stated that the catalytic power of the enzyme is related to the interactions with the purine base, provided by multiple aromatic stacking interactions with enzyme residues.⁷⁴ It was also found that two functional groups with a pK_a of 5.5 and 8.5 are required to be protonated. Accordingly, Asp10 (Figure 4.2, *vide supra*) acts as the general base in the reaction mechanism, while Asp40 is proposed as a general acid. It was then suggested that the optimum pH of the TvNH is around pH 5.⁷⁴

Experiments on pH profile and temperature were performed in order to investigate the best conditions for the *TvNH* to catalyse the hydrolysis of 5'-FDA **47** (Scheme 4.6).



Scheme 4.6 Hydrolysis of the *N*-glycosidic bond of 5'-FDA **47** catalysed by the *T. vivax* nucleoside hydrolase.

The enzyme was purified from *E. coli* bearing the pQE30-IAGNH plasmid encoding IAG-NH from *T. vivax*. This partially purified IAG-NH was taken directly after nickel column purification and separated into three fractions. Each fraction was dialysed in three different buffers (50 mM MES, pH 5.5; 50 mM PBS, pH 7.0 and 50 mM TRIS, pH 8.5). Experiments were carried out by incubating the *TvNH* (500 μ l, 0.5 mg/ml) with synthetic 5'-FDA **47** (30 μ l, 18.6 mM) in the corresponding buffer (170 μ l) supplemented with $CaCl_2$ (1mM) at 37 °C and 55 °C. The hydrolysis of 5'-FDA **47** was followed by $^{19}F\{^1H\}$ NMR analysis, every two hours. These studies showed a clear influence of the pH on the reaction rate. At pH 5.5 formation of 5-FDR **71** is detected at 0 h time, accumulating due to the running time of the experiment (approximately 30 min), whereas incubation times of 4 h and 2 h respectively, are needed at pH 7.0 and pH 8.5 as shown in Figure 4.4.

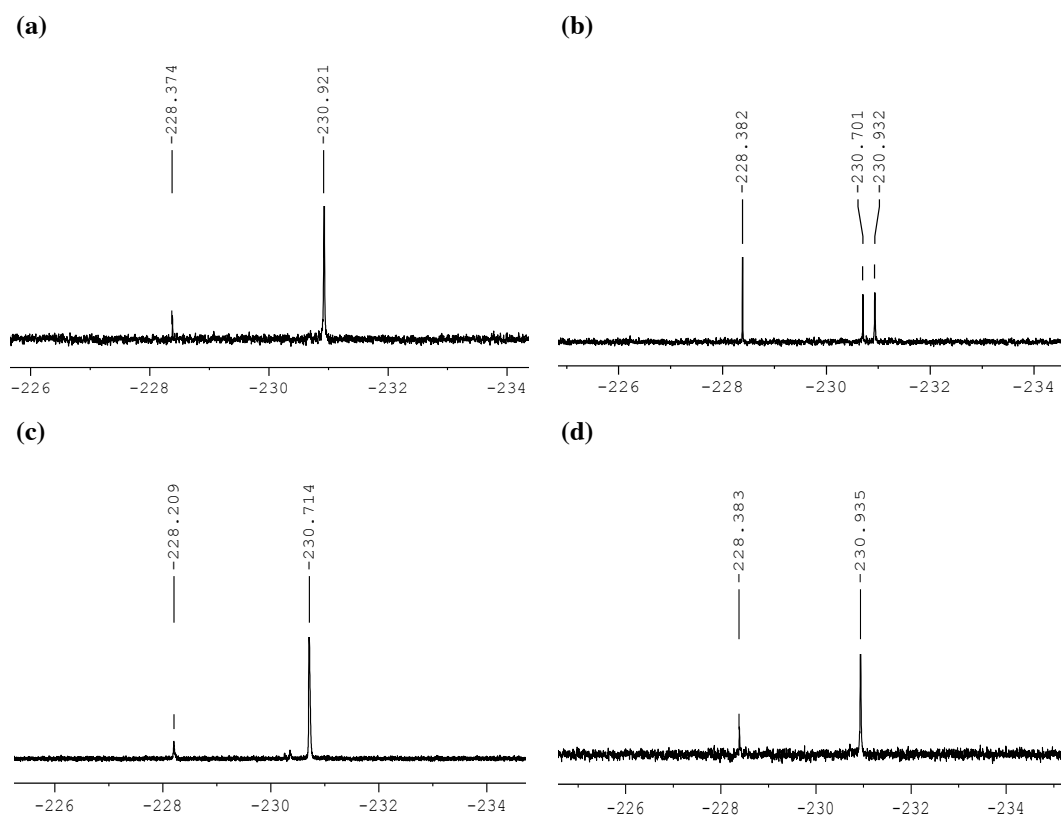


Figure 4.4 $^{19}\text{F}\{^1\text{H}\}$ NMR spectra of partially purified *TvNH* incubated with synthetic 5'-FDA **47** at 37 °C: (a) In 50 mM MES buffer pH 5.5 and time zero (time the spectrum is acquired) (b) In 50 mM MES buffer pH 5.5 after 2 h (c) In 50 mM PBS buffer pH 7.0 after 4 h (d) In TRIS buffer pH 8.5 for 2 h.

The hydrolysis of the *N*-glycosidic bond of 5'-FDA **47** is more rapid when catalysed under acidic conditions by *TvNH*. These results are consistent with the previous report that sets the optimum pH for *T. vivax* NH around pH 5. However, it is important to note that the reduction in activity at pH 7.0 may be attributed to a partial sequestering of the calcium by the phosphate ions in the PBS buffer, rather than just a direct action of pH 7.0.

B. Coupling the fluorinase to a nucleoside hydrolase

The next step in the study involved exploring the fluorinase reaction at pH 5.5 and 37 °C. Previous studies on the fluorinase⁵² have shown that the optimal temperature for the production of 5'-FDA **47** is 55 °C. It is also known from those studies that addition of EDTA (1mM) increases enzyme activity by 25%, suggesting that the fluorinase may be sensitive to trace amounts of metal ions. Nevertheless, there was little known about the optimum pH profile for enzymatic fluorination, and to date all incubations of the fluorinase enzyme had been carried out at neutral or slightly basic pH. A set of experiments was explored by incubating partially purified fluorinase (280 µl, 1.5 mg/ml) with SAM **49** (10 µl, 20 mM), KF (10 µl, 500 mM) and D₂O (100 µl) in the three buffers (170 µl; 50 mM MES, pH 5.5; 50 mM PBS, pH 7.0 and 50 mM TRIS, pH 8.5) at 37 °C. The production of 5'-FDA **47**, was followed by ¹⁹F{¹H} NMR analysis, every two hours. The results of these experiments indicated that the fluorinase is inactive at pH 5.5, and 5'-FDA **47** was observed only at neutral or more basic pH (pH 8.5).

In the light of these results, a two phase experiment was explored. The fluorinase (280 µl, 1.5 mg/ml) was incubated with SAM **49** (10 µl, 20 mM) and KF (10 µl, 500 mM) for a period of 4 h at 37 °C and pH 7.0. After 4 h, production of 5'-FDA **47** was observed by ¹⁹F{¹H} NMR analysis as shown in Figure 4.5a (*vide infra*). This sample was then supplemented with a freshly prepared CFE (400 µl) of TvNH in MES buffer (50 mM, pH 5.5; 1 mM CaCl₂) and incubated for a further 30 min. The sample was analysed by ¹⁹F{¹H} NMR and the spectrum clearly showed two signals at -228.45 ppm and -230.77 ppm corresponding to the β and α anomers of 5-deoxy-5-fluoro-D-ribose, 5-FDR **71**. Thus, the sequential fluorinase and then nucleoside hydrolase reaction was successful in a two-phased one-pot reaction (Figure 4.5b, *vide infra*).

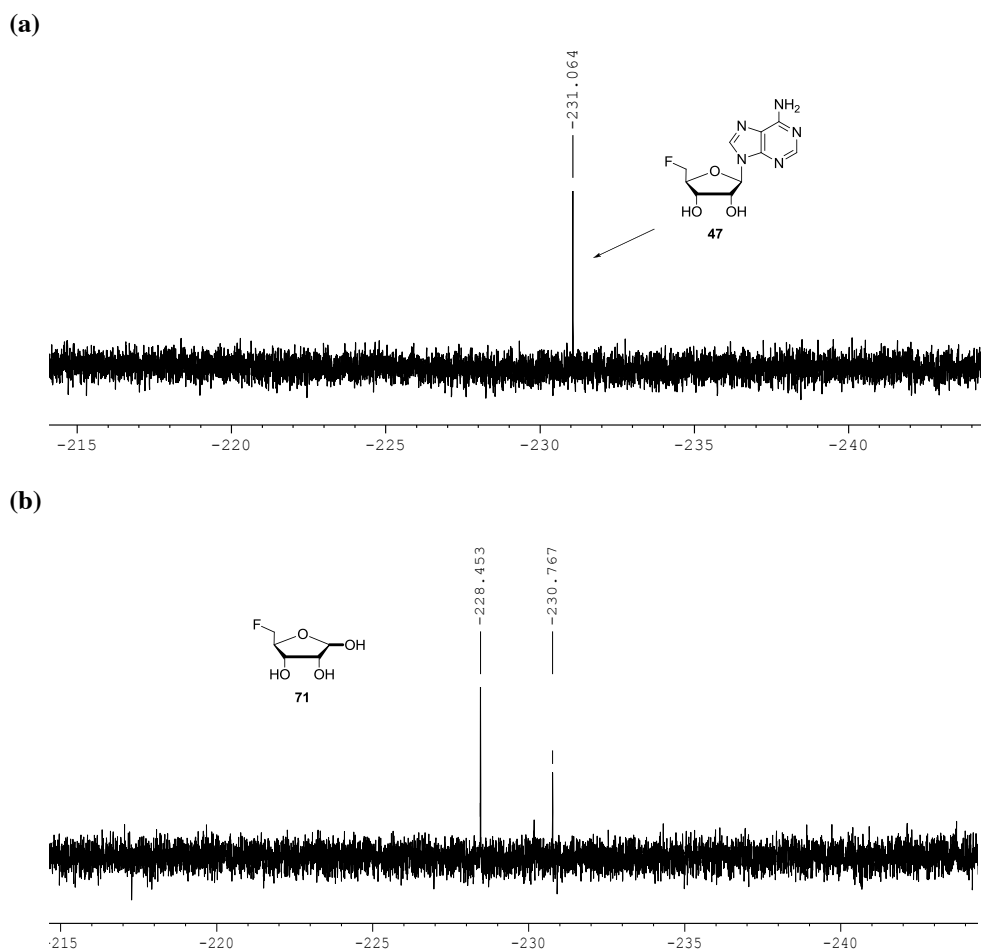
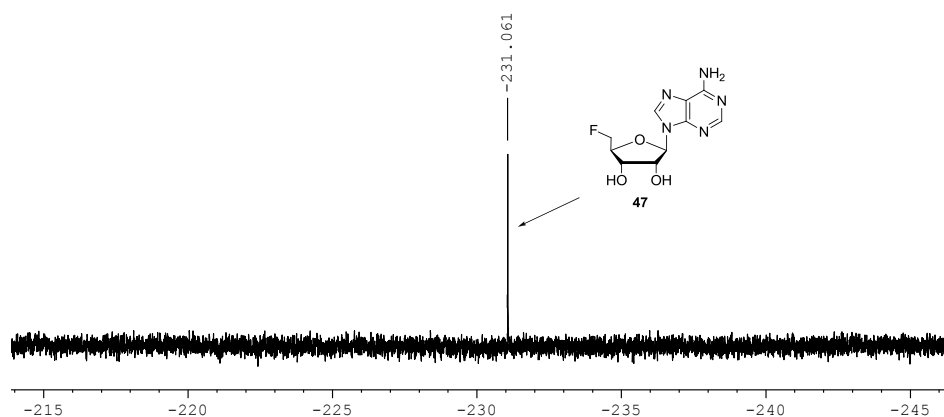


Figure 4.5 $^{19}\text{F}\{^1\text{H}\}$ NMR spectra of: (a) Incubation of the fluorinase with SAM **49** and KF showing production of 5'-FDA **47** at pH 7.0. (b) Addition of *T. vivax* IAG-NH and further incubation of the mixture for 30 min shows 5-FDR **71** formation at pH 5.5.

A similar experiment was then carried out to explore the combination of these two enzymes under more basic conditions. Accordingly, the fluorinase (280 μl , 1.5 mg/ml) was incubated with SAM **49** (10 μl , 20 mM) and KF (10 μl , 500 mM) at pH 7.8 for a period of 3 h at 37 $^{\circ}\text{C}$. $^{19}\text{F}\{^1\text{H}\}$ NMR analysis clearly showed the production of 5'-FDA **47** (Figure 4.6a, *vide infra*). To this sample was added a freshly prepared CFE (400 μl) of the over-expressed *T. vivax* nucleoside hydrolase in phosphate buffer (50 mM, pH 7.8; 1 mM CaCl_2) and the resulting

mixture was then incubated for a further 30 min. After this time, the sample was analysed by $^{19}\text{F}\{^1\text{H}\}$ NMR and the spectrum clearly showed two signals at -228.45 ppm and -230.77 ppm corresponding to the β and α anomers, respectively, of 5-deoxy-5-fluoro-D-ribose, 5-FDR **71**, indicating a successful reaction (Figure 4.6b, *vide infra*).

(a)



(b)

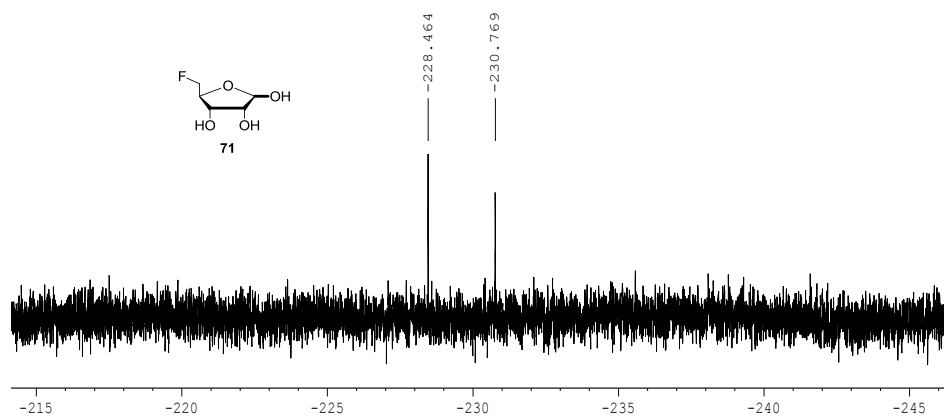


Figure 4.6 $^{19}\text{F}\{^1\text{H}\}$ NMR spectra of: (a) Incubation at 37°C and pH 7.8 of the fluorinase with SAM **49** and KF showing production of 5'-FDA **47** after 3 h. (b) Addition of TvNH and further incubation of the mixture for 30 min at pH 7.8 shows formation of β -FDR **71** and α -FDR **71**.

The next phase in the development of the cold experiment for the enzymatic synthesis of 5-FDR **71** was focused on establishing optimum conditions for coupling both enzymes together in a one-pot reaction. The experiments carried out so far have provided valuable information about the optimum conditions for the fluorinase and for the *T. vivax* nucleoside hydrolase. However, the fluorinase and the *TvNH* show very different preferences in terms of pH and temperature and the presence of metal ions in the reaction mixture. The fluorinase catalyses the fluorination reaction at neutral or basic pH, whereas the *TvNH* proved to be faster under more acidic conditions. The optimal temperature for the fluorinase is 55 °C, whereas *T. vivax* NH shows no catalytic activity at this temperature. Finally, the fluorinase is known to be sensitive to trace amounts of metal ions, increasing its activity up to 25% with EDTA, while the nucleoside hydrolase requires the presence of Ca²⁺ as a co-factor to catalyse the hydrolysis reaction. So the prospects did not look good. A summary of the required conditions for each enzyme for good functioning is represented in Table 4.3.

Table 4.3 Comparative conditions for activity of the enzymes involved in the coupled enzymatic synthesis of 5-FDR **71**.

| | | Fluorinase (EC 2.5.1.63) | <i>TvNH</i> (EC 3.2.2.1) |
|----------------------|-------|------------------------------------|------------------------------------|
| pH | < 7 | ✗ | ✓ |
| | = 7 | ✓ | ✗ |
| | > 7 | ✓ | ✓ |
| T^a | 37 °C | ✓ | ✓ |
| | 55 °C | ✓ | ✗ |
| EDTA | 1 mM | ✓ | ✗ |

A reaction was explored at pH 8.5 and at 37 °C. For that, the fluorinase (280 μ l, 1.5 mg/ml) was incubated with SAM **49** (10 μ l, 20 mM), KF (10 μ l, 500 mM) and a freshly prepared CFE (400 μ l) of the over-expressed *T. vivax* nucleoside hydrolase in phosphate buffer (50 mM, pH 7.8; 1 mM CaCl₂) at 37 °C. After 2 h incubation, the reaction mixture was analysed by ¹⁹F{¹H} NMR. The characteristic ¹⁹F{¹H} NMR signals for the α and β anomers of 5-deoxy-5-fluoro-D-ribose, 5-FDR **71** showed that the product had formed (Figure 4.7a, *vide infra*). One hour later, at a total incubation time of 3 h, the ¹⁹F{¹H} NMR spectrum showed the same two signals for the production of 5-FDR **71**, in a ratio 2:1 β : α (Figure 4.7b, *vide infra*).

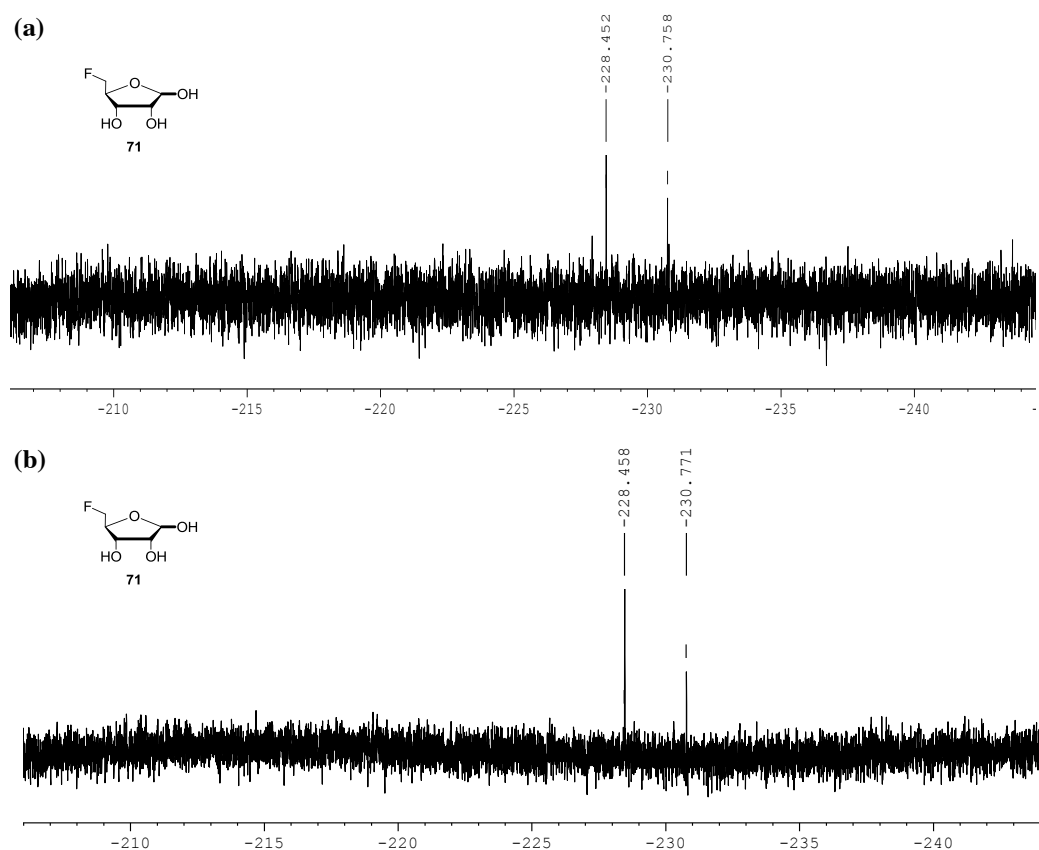
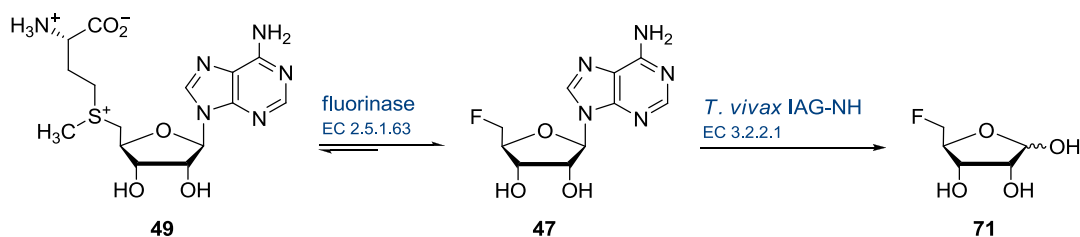


Figure 4.7 ¹⁹F{¹H} NMR spectra following incubation of the fluorinase with SAM **49**, KF and *TvNH* (CFE in PB pH 7.8) at 37 °C showing production of 5-FDR **71** at: (a) 2 h and (b) 3 h.

This experiment confirmed that 5-deoxy-5-fluoro-D-ribose, 5-FDR **71**, can be synthesised from SAM **49** in two steps *via* a fluorinase-NH coupled enzymatic reaction under basic conditions, as shown in Scheme 4.7.



Scheme 4.7 Enzymatic coupled system for the synthesis of 5-FDR **71**.

In order to study the fluorinase-NH coupled reaction in real time, a $^{19}\text{F}\{^1\text{H}\}$ NMR time course experiment was carried out in a NMR tube. Accordingly, a cell free extract containing *T. vivax* IAG-NH (400 μl) in phosphate buffer (50 mM, pH 7.8, 1 mM CaCl_2) was supplemented with fluorinase (280 μl , 1.5 mg/ml), SAM **49** (10 μl , 20 mM), KF (10 μl , 500 mM) and D_2O (100 μl), and incubated at 37 $^\circ\text{C}$. The progress of the reaction was monitored by recording $^{19}\text{F}\{^1\text{H}\}$ NMR (470 MHz) spectra at 30 min intervals over 4 h. Figure 4.8 displays the stacked $^{19}\text{F}\{^1\text{H}\}$ NMR time course spectra resulting from the biotransformation.

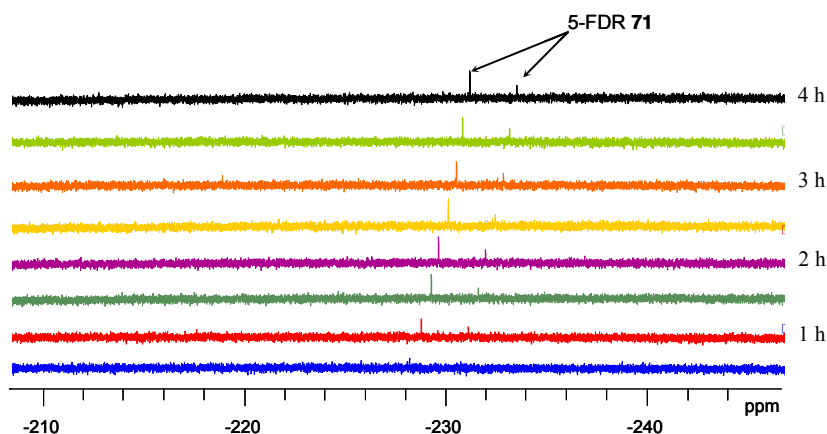


Figure 4.8 $^{19}\text{F}\{^1\text{H}\}$ NMR time course spectra of *TvNH* cell free extract incubated with fluorinase, KF and SAM **49** in phosphate buffer (50 mM, pH 7.8) at 37 °C for 4 h.

The resultant $^{19}\text{F}\{^1\text{H}\}$ NMR data show a product signal at -228.03 ppm corresponding to the β anomer of 5-FDR **71**, appearing just after 30 min of incubation, while the NMR spectrum was being recorded. After 1 h, both anomers of 5-FDR **71** are observed in a 2:1 ratio of β : α and no 5'-FDA **47** is detected. This suggests that the fluorinase is rate limiting and that the *TvNH* hydrolyses the fluorinase-generated 5'-FDA **47** faster than it is being formed.

With this coupled reaction in place, experiments with radiolabelled [^{18}F]fluoride ion were explored.

4.2.1.2 Development of the "hot" experiment

The fluorinase enzyme was over-expressed in *E. coli* and purified following the protocol described in Chapter 5. Initially, an experiment was carried out to explore the production of [^{18}F]FDA [^{18}F]47 in a single step enzyme reaction involving only the fluorinase. The fluorinase enzyme (70 μl , 35.3 mg/ml) was incubated with SAM 49 (30 μl , 20 mM) and aqueous [^{18}F]fluoride (50 μl , solution in [^{18}O]H $_2\text{O}$, 72 MBq) at 37 $^\circ\text{C}$ for 1–5 h. Aliquots were collected at time intervals and analysed by analytical HPLC under the conditions described in Chapter 5. The HPLC system was coupled to a diode array detector followed by a radioactive detector. An aliquot of the reaction mixture was then analysed by radio-HPLC after 3.8 h, showing a radiolabelled compound with a retention time of 5.21 min. The sample was loaded onto a carbohydrate column (Agilent), and formation of [^{18}F]FDA [^{18}F]47 was detected as shown in Figure 4.9 (*vide infra*). A contemporaneous aliquot from the same mixture was analysed by HPLC on a Hypersyl ODS column (Figure 4.10, *vide infra*), confirming production of radiolabelled 5'-FDA [^{18}F]47 after 4 h incubation at 37 $^\circ\text{C}$.

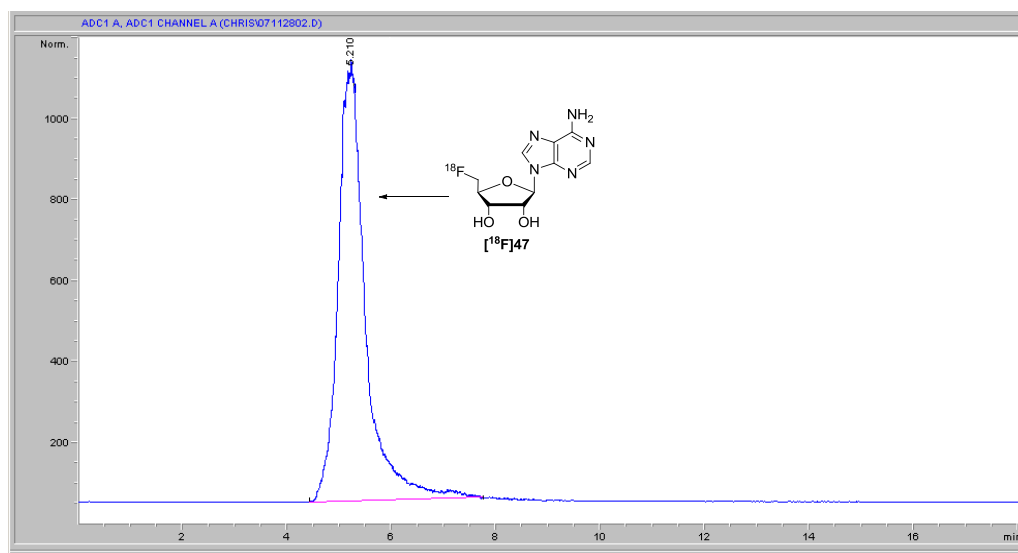


Figure 4.9 HPLC Chromatogram obtained from radioactive detector after injection of a sample collected after 3.8 h of incubation (85:15 ACN/H $_2\text{O}$ as mobile phase).

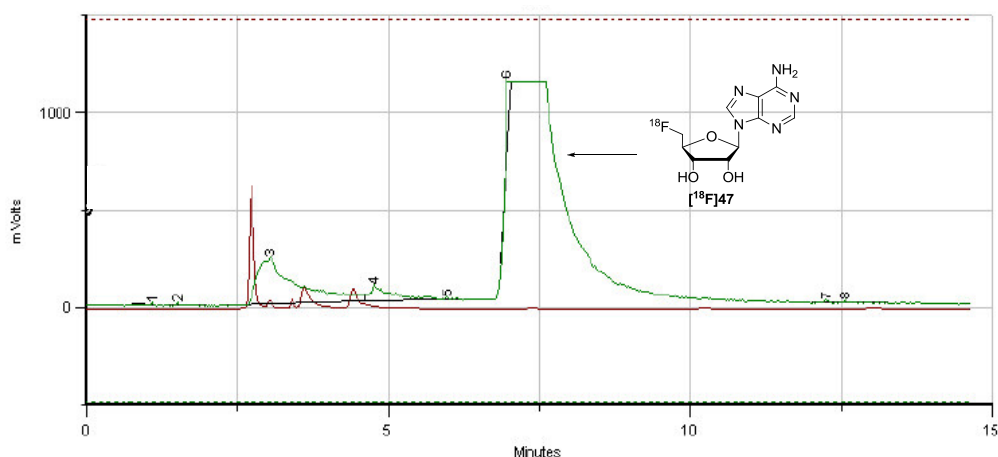


Figure 4.10 HPLC Chromatogram showing both UV (trace in red) and radioactivity (trace in green) detector outputs for the production of [^{18}F]FDA [^{18}F]47 (90:10 $\text{NaH}_2\text{PO}_4/\text{ACN}$ as mobile phase). The first radioactive signal corresponds to unreacted [^{18}F]fluoride.

Production of [^{18}F]FDA [^{18}F]47 was clearly observed after 4 h of incubation and a preparation of purified nucleoside hydrolase in HEPES buffer (100 μL , 16 mg/mL) was added to the remaining fluorinase reaction mixture, as well as a small volume of the buffer (50 μL , 50 mM HEPES, 1 mM CaCl_2) containing the enzyme co-factor (Ca^{2+}) necessary for the hydrolase reaction. Following the addition of *TvNH*, the enzyme cocktail was incubated for a further 45 min at 37 $^\circ\text{C}$, and an aliquot was taken for HPLC analysis. Incubation of the mixture containing [^{18}F]FDA [^{18}F]47 with the *TvNH* enzyme resulted in the formation of a new radiolabelled compound. This was [^{18}F]FDR [^{18}F]71, which had a retention time of 7.2 min as shown by HPLC analysis (Figure 4.11). The ratio between [^{18}F]FDA [^{18}F]47 and [^{18}F]FDR [^{18}F]71 was approximately 9:1, and thus, although successful, the conversion was modest.

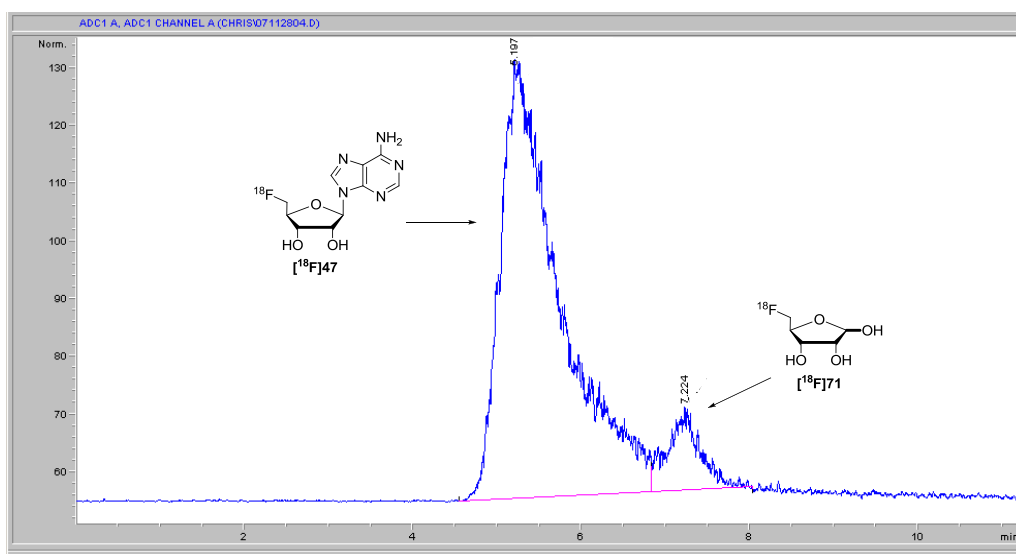


Figure 4.11 HPLC Chromatogram obtained from the radioactivity detector following injection of an aliquot collected after 4.5 h incubation, showing production of $[^{18}\text{F}]\text{FDA}$ $[^{18}\text{F}]\text{47}$ and $[^{18}\text{F}]\text{FDR}$ $[^{18}\text{F}]\text{71}$.

The production of $[^{18}\text{F}]\text{FDR}$ $[^{18}\text{F}]\text{71}$ increased when the reaction mixture was incubated for a further 4 h, as shown by radio-HPLC analysis in Figure 4.12.

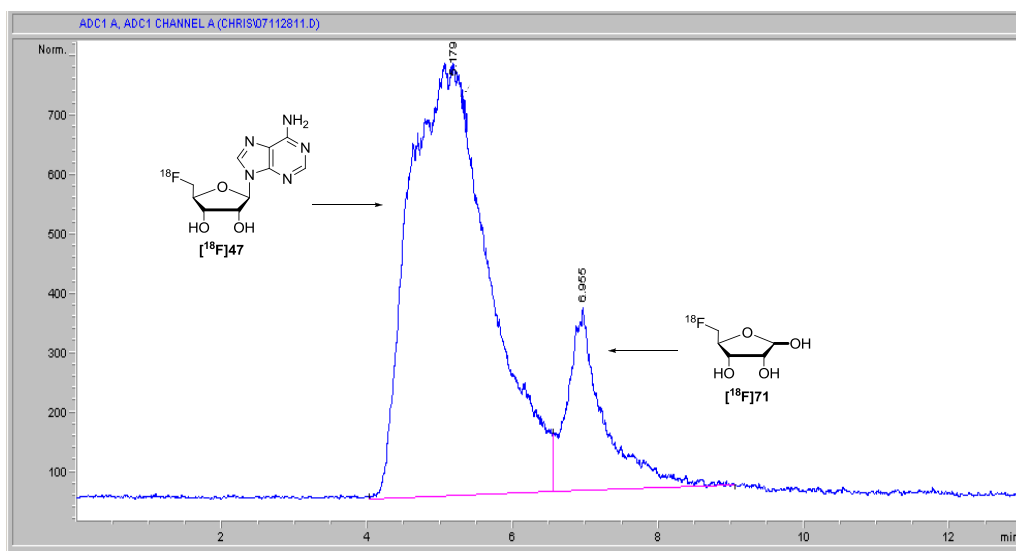


Figure 4.12 HPLC Chromatogram obtained from the radioactivity detector following injection of an aliquot collected after 4.5 h incubation with the fluorinase and additional 4 h incubation with the *TvNH*, showing production of $[^{18}\text{F}]\text{47}$ and $[^{18}\text{F}]\text{71}$.

Another aliquot from the same mixture was also analysed by HPLC on a Hypersyl ODS column (Figure 4.13), confirming production of radiolabelled 5-FDR [^{18}F]71 after 3.5 h of incubation followed *TvNH* addition. The three detected radioactive signals correspond to unreacted [^{18}F]fluoride, [^{18}F]FDR [^{18}F]71 and [^{18}F]FDA [^{18}F]47, as shown in Figure 4.13.

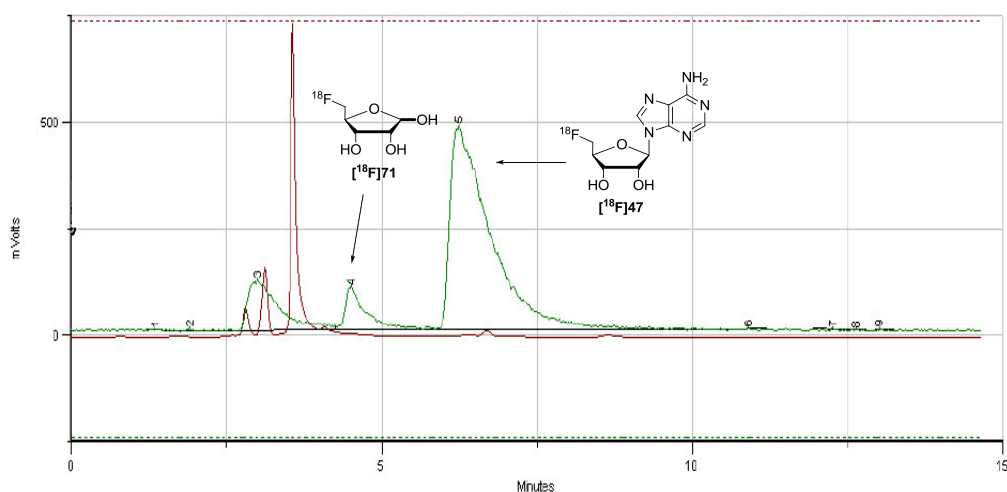


Figure 4.13 HPLC Chromatogram showing both UV (trace in red) and radioactivity (trace in green) detector outputs for the production of [^{18}F]FDA [^{18}F]47 and [^{18}F]FDR [^{18}F]71.

In a second experiment, both enzymes were combined in a one-pot reaction as designed in the cold experiment approach (Section 4.2.1.1, B). The fluorinase enzyme was over-expressed in *E. coli* and purified following the procedure described in Chapter 5. The *TvNH* plasmid was transformed into BL21 or C43(DE3) *E. coli* cells for protein expression and the protein was also purified according to the protocol described in Chapter 5.

A one-pot experiment coupling both enzymes for [^{18}F]FDR [^{18}F]71 production was carried out as follows: the fluorinase enzyme (70 μl , 35.3 mg/ml) was incubated with SAM 49 (30 μl , 20 mM), *TvNH* (100 μl , 12 mg/ml) and aqueous [^{18}F]fluoride (100 μl , solution in [^{18}O]H $_2\text{O}$, 137 MBq) in HEPES buffer (50 μL , 50 mM HEPES pH 8.0, 1 mM CaCl $_2$) at 37 $^\circ\text{C}$. After a 4 h incubation time an aliquot was taken and loaded onto a carbohydrate column (Agilent) for

HPLC analysis. Two radiochemical peaks were evident in this one-pot reaction mixture, one of which is [^{18}F]FDA [^{18}F]**47** and the other [^{18}F]FDR [^{18}F]**71**, with retention times of 5.22 min and 7.20 min, respectively, as shown in Figure 4.14.

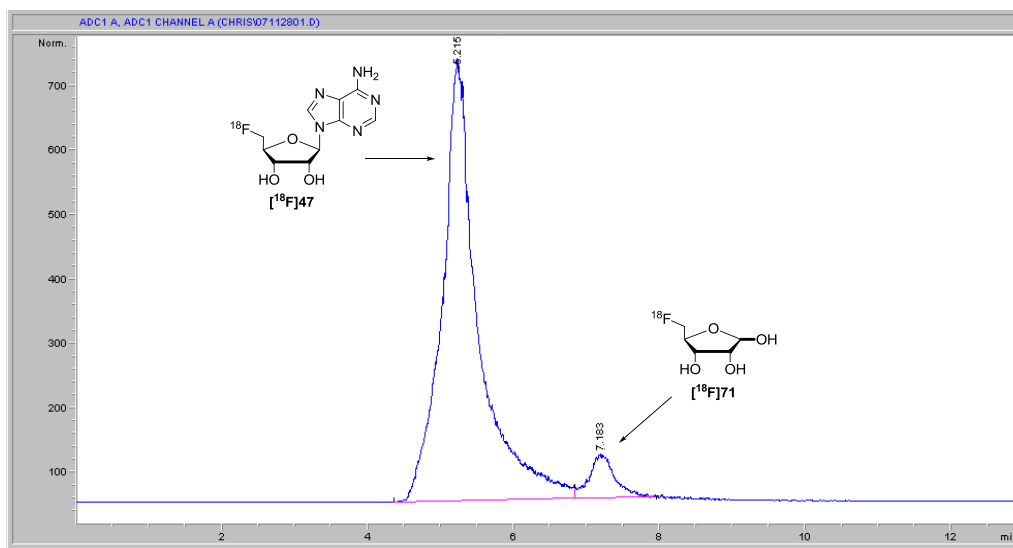


Figure 4.14 HPLC Chromatogram obtained from the radioactivity detector following injection of an aliquot collected from the fluorinase-NH one-pot reaction mixture after 4 h incubation, showing production of [^{18}F]FDA [^{18}F]**47** and [^{18}F]FDR [^{18}F]**71**.

The formation of radiolabelled 5-FDR [^{18}F]**71** after 6 h incubation was also confirmed by HPLC analysis when an aliquot of the enzyme cocktail was loaded on a Hypersyl ODS column using $\text{NaH}_2\text{PO}_4/\text{ACN}$ (90:10) as the mobile phase. These are conditions under which [^{18}F]FDR [^{18}F]**71** elutes before [^{18}F]FDA [^{18}F]**47**, and the unreacted [^{18}F]fluoride and polar products elute first (Figure 4.15).

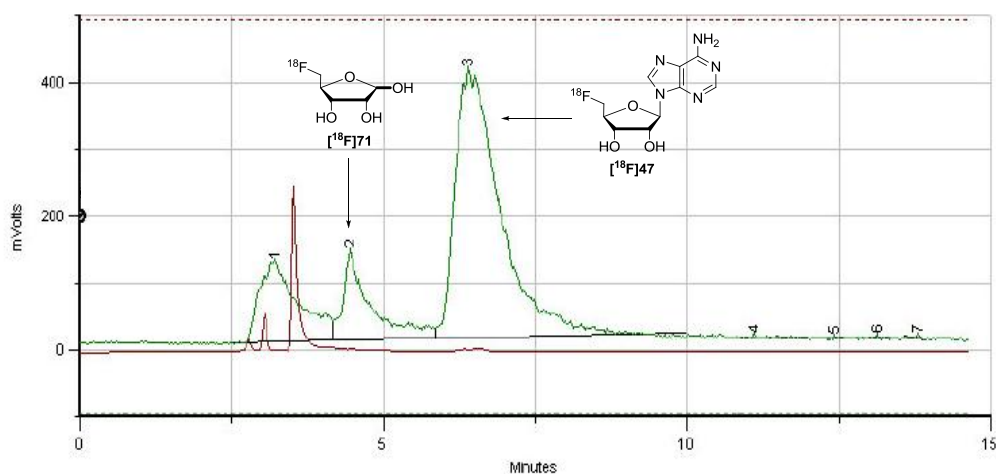


Figure 4.15 HPLC Chromatogram showing both UV (trace in red) and radioactivity (trace in green) detector outputs for the production of [^{18}F]FDA [^{18}F]47 and [^{18}F]FDR [^{18}F]71 after 6 h of combined incubation of fluorinase and TvNH.

Another experiment was carried out coupling the fluorinase and the TvNH, but in this case with a higher concentration of TvNH. Thus, the fluorinase enzyme (70 μL , 35.3 mg/ml) was incubated with SAM 49 (30 μL , 20 mM), TvNH (100 μL , 16 mg/ml) and aqueous [^{18}F]fluoride (100 μL , solution in [^{18}O]H $_2$ O, 136 MBq) in HEPES buffer (50 μL , 50 mM HEPES pH 8.0, 1 mM CaCl $_2$) at 37 $^\circ\text{C}$. After 4.5 h of incubation, analysis by HPLC of the reaction mixture containing the fluorinase and the NH showed an increased conversion to [^{18}F]FDR [^{18}F]71 in the reaction mixture (Figure 4.16, *vide infra*). The formation of radiolabelled 5-FDR [^{18}F]71 related to [^{18}F]FDA [^{18}F]47 is higher than in the previous experiment after a similar incubation time (Figure 4.14, *vide supra*). This is most probably due to the fact that the TvNH enzyme is more concentrated in this latter experiment.

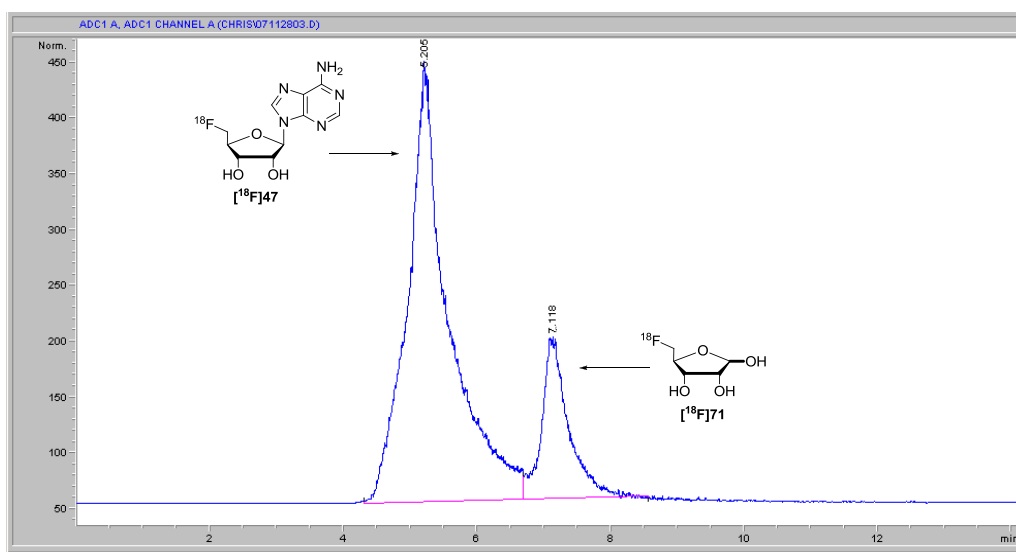


Figure 4.16 HPLC Chromatogram obtained from the radioactivity detector following injection of an aliquot collected from the fluorinase-NH one-pot reaction mixture after 4.5 h incubation, showing production of [18F]FDR [18F]71, which represents approximately 20% of the total radioactivity observed.

Longer incubation times resulted in an increased amount of [18F]FDR [18F]71 formation, as shown by HPLC analysis (Figure 4.17, *vide infra*), reaching an approximately 7:3 [18F]FDA [18F]47 to [18F]FDR [18F]71 ratio after 8.25 hours (Figure 4.18, *vide infra*).

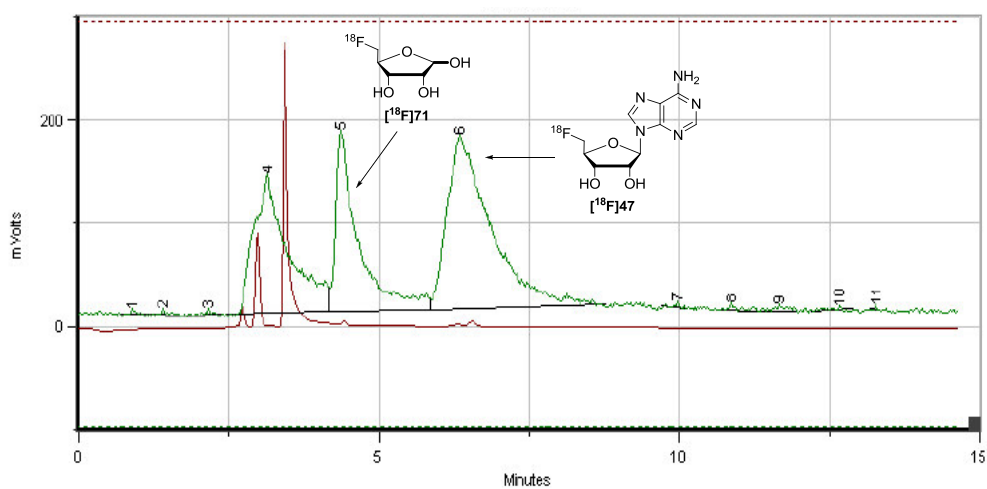


Figure 4.17 HPLC Chromatogram showing both UV (trace in red) and radioactivity (trace in green) detector outputs for the production of [^{18}F]FDA [^{18}F]47 and [^{18}F]FDR [^{18}F]71 after 7 h of combined incubation of fluorinase and *TvNH*. The first radioactive signal corresponds to unreacted [^{18}F]fluoride.

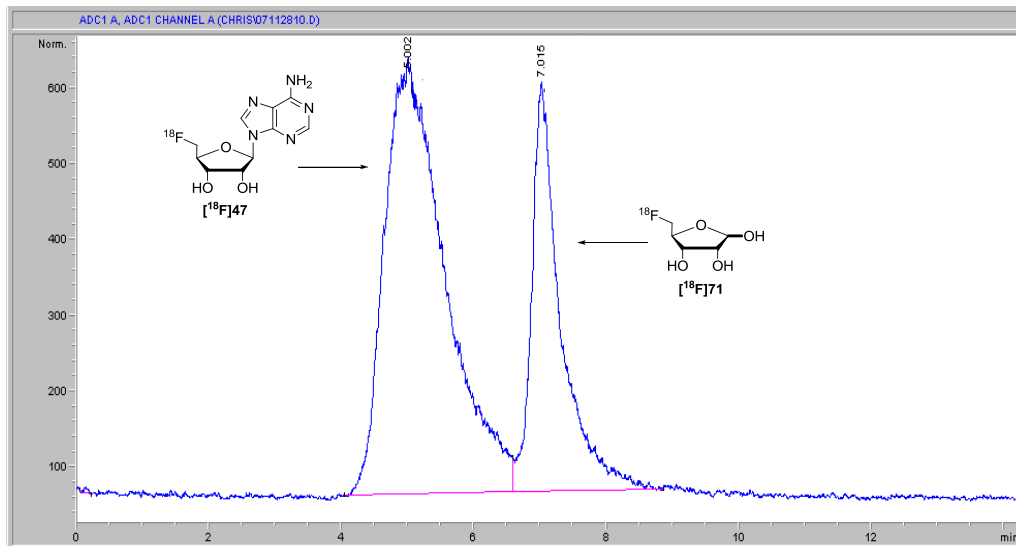
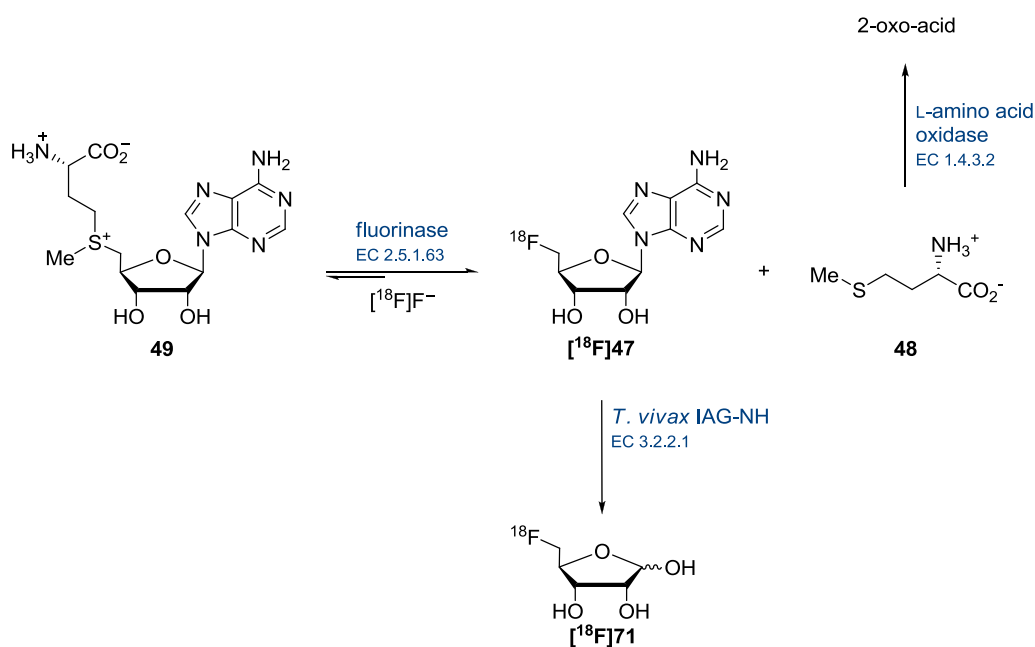


Figure 4.18 HPLC Chromatogram obtained from the radioactivity detector following injection of an aliquot collected from the fluorinase-NH one-pot reaction mixture after 8.25 h of incubation, showing production of [^{18}F]FDR [^{18}F]71, which represents approximately 31% of the total radioactivity observed ([^{18}F]fluoride does not elute from the column under these conditions).

An experiment coupling the fluorinase to a L-amino acid oxidase (EC 1.4.3.2) was also performed, in which a preparation of purified fluorinase (70 μ l, 35.26 mg/ml) was incubated with SAM **49** (30 μ l, 20 mM), L-amino acid oxidase (0.15 units) and aqueous [18 F]fluoride (50 μ l, solution in [18 O]H $_2$ O, 70 MBq) at 37 $^{\circ}$ C for 4 h. The HPLC analysis showed production of [18 F]FDA [18 F]**47** but there was not a real improvement in the synthesis of the radiolabelled nucleoside.

A summary of the reactions explored is illustrated in Scheme 4.8.



Scheme 4.8 Fluorinase coupled enzyme systems for the synthesis of [18 F]FDR [18 F]**71**.

The experiments demonstrate, for the first time, a two-step enzymatic approach to [18 F]FDR [18 F]**71** that can be carried out either in a sequential one-pot reaction or in one-pot reaction system.

4.2.2 Enzymatic synthesis of [^{18}F]FDA

With an improved protocol in hand for the synthesis of [^{18}F]FDA [^{18}F]47 using the fluorinase, it was attractive to generate a sample for investigating its incorporation into cancer cells.

In a typical reaction, the fluorinase enzyme (25 μl , 30 mg/ml) was incubated with SAM 49 (20 μl , 20 mM) and aqueous [^{18}F]fluoride (70 μl , solution in [^{18}O]H $_2\text{O}$, 163 MBq) at 37 $^\circ\text{C}$ for 1 h. After this time, an aliquot was collected and the protein was denatured by heating (95 $^\circ\text{C}$, 1 min) and removed by centrifugation (14,500 rpm, 5 min). The supernatant was then analysed by analytical HPLC under the conditions described in Chapter 5. The HPLC system was coupled to a diode array detector followed by a radioactive detector. The radio-HPLC chromatogram of the reaction mixture showed production of a radiolabelled compound with a retention time of 9 min and 99% conversion. Such product was confirmed to be [^{18}F]FDA [^{18}F]47 when compared with a standard. Figure 4.19 illustrates the HPLC chromatogram obtained.

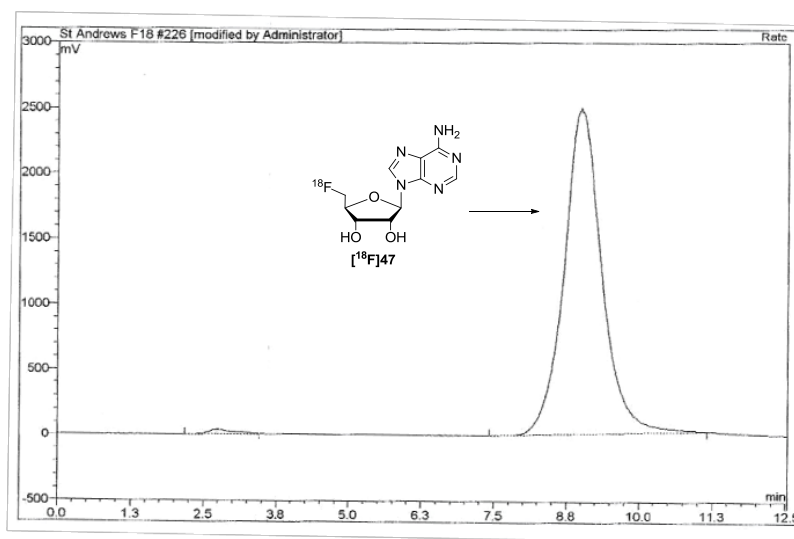


Figure 4.19 Radio-HPLC chromatogram for the production of [^{18}F]47 after a 1 h incubation

Biological studies with [^{18}F]FDA [^{18}F]47 will be discussed in Section 4.3.

4.2.3 Enzymatic synthesis of [^{18}F]FDI

The enzymatic synthesis of [^{18}F]FDI [^{18}F]**50** was achieved by first incubating the fluorinase enzyme (25 μl , 30 mg/ml), SAM **49** (20 μl , 20 mM) and aqueous [^{18}F]fluoride (60 μl , solution in [^{18}O]H $_2\text{O}$, 397 MBq) at 37 $^\circ\text{C}$. After 1 h incubation, an aliquot of the reaction mixture was analysed by HPLC and checked for [^{18}F]FDA [^{18}F]**47** production against a standard following the procedure described in Chapter 5. In most cases almost complete conversion to [^{18}F]FDA [^{18}F]**47** was observed and the fluorinase enzyme in the reaction mixture was denatured by heating (95 $^\circ\text{C}$, 1 min) and removed by centrifugation (14,500 rpm, 5 min). Then 5'-adenylic acid deaminase (3 mg, 0.11 units/mg) was added to the supernatant and incubated for a further 1 h. After this time, an aliquot was collected and the protein was denatured by heating (95 $^\circ\text{C}$, 1 min) and removed by centrifugation (14,500 rpm, 5 min). Radio-HPLC analysis against a standard confirmed the generation of [^{18}F]FDI [^{18}F]**50** with 85% conversion from [^{18}F]fluoride and quantitative conversion from [^{18}F]FDA [^{18}F]**47**, as shown in Figure 4.20.

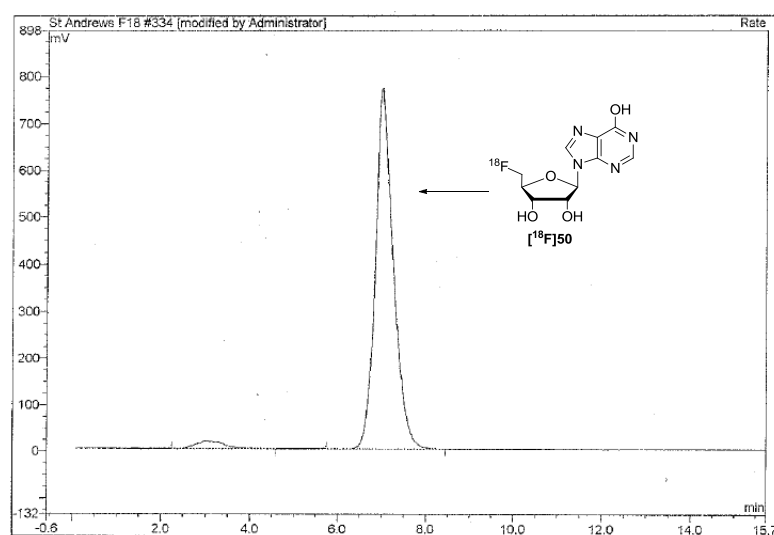


Figure 4.20 Radio-HPLC chromatogram of the enzymatic synthesis of [^{18}F]FDI [^{18}F]**50** after 1 h incubation with fluorinase and then 1 h incubation with deaminase.

4.3 Adenosine analogues as potential radiotracers for investigating adenosine receptors by PET

Adenosine is a natural metabolite, ubiquitous in mammalian cell types. It is related both structurally and metabolically to the bioactive nucleotides adenosine triphosphate (ATP), adenosine diphosphate (ADP), adenosine monophosphate (AMP) and cyclic adenosine monophosphate (cAMP); to the biochemical methylating agent *S*-adenosyl-L-methionine (SAM); and structurally to the co-enzymes NAD, FAD and co-enzyme A; and to RNA. Adenosine, with these related compounds, plays an important role in the regulation of cellular metabolism.⁷⁷ The major pathways responsible for the metabolism (biosynthesis and degradation) and transport of adenosine are shown in Figure 4.21.⁷⁷

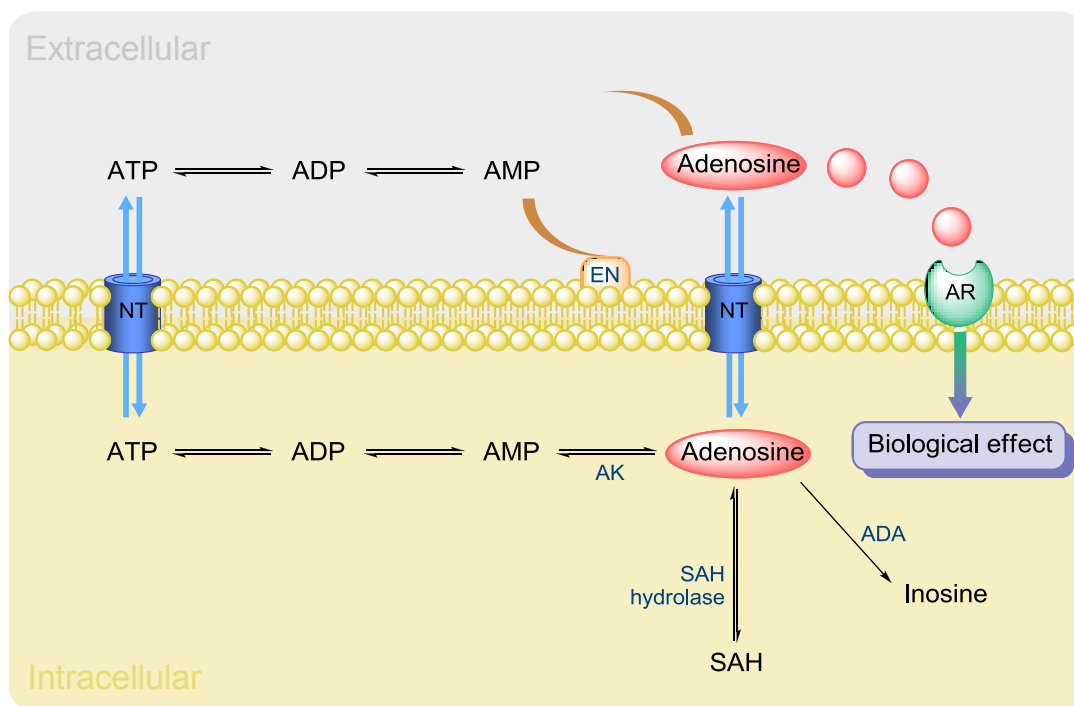


Figure 4.21 Formation, metabolism and uptake of adenosine. EN, ecto-5-nucleotidase; NT, nucleoside transport; AR, adenosine receptor; AK, adenosine kinase; SAH, *S*-adenosylhomocystein; ADA, adenosine deaminase.

The physiological effects of adenosine are mediated by activation of specific cell surface receptors. To date, four adenosine receptors (ARs), namely A₁AR, A_{2B}AR, A_{2A}AR and A₃AR, have been characterised pharmacologically.^{77,78}

Adenosine is reported to be present at high concentrations in solid tumours, with accumulation in the intracellular and extracellular tumour microenvironments. It has also been shown to promote tumour growth and to be involved in the stimulation of angiogenesis and inhibition of inflammatory processes at the site of injury. In addition, a number of observations strongly suggest that adenosine may have a role in cancer. Due to rapid growth, solid tumours routinely experience severe hypoxia and necrosis, which causes adenine nucleotide degradation and adenosine release.⁷⁹ Recent studies have revealed the role that adenosine plays in tumour growth and metastasis.⁸⁰ The activation of the A₃ adenosine receptor (A₃AR) by its natural ligand adenosine, or by synthetic agonists, induces an inhibitory effect on tumour cell growth, attributed to different expression levels of the receptor in tumour and in normal cells.^{81,82} Both the adenosine and the agonists inhibit the growth of various tumour cell types such as melanoma, colon or prostate carcinoma,⁸³ lymphoma,^{84,85} and human breast cancer.⁸⁶ However, the clinical efficacy of anticancer nucleoside drugs is strictly determined by the nucleoside transporters (NTs), which are implicated in the entry of nucleoside drugs into the cells, as all of the nucleoside drugs commonly employed for cancer therapy are hydrophilic molecules and in the absence of transporter-mediated uptake, their access to intracellular targets would be slow.^{87,88,89,90}

Since these transporters are the route of entry for cytotoxic nucleoside analogues used in cancer and viral chemotherapy, imaging adenosine receptors and transporters may be of clinical importance for the investigation of nucleoside metabolism in pathological conditions where adenosine uptake and/or release from certain tissues and organs may be altered (*e.g.*, malignant cell proliferation, cancer, inflammation, hypoxia, asthma).^{91,92} With this objective,

several analogues of adenosine have been synthesised and studied as potential antitumor and antiviral agents.^{93,94,95} In addition, the [¹⁸F]-labelled analogues of adenosine have potential for PET imaging of cell proliferation and/or viral infection.^{96,97}

It has been proposed that 5'-deoxy-5'-[¹⁸F]fluoroadenosine [¹⁸F]**47** and its derivatives could possibly serve as PET isotope-labelled agonist ligands, specific for adenosine receptors, as the modification of the adenine moiety leads to increased selectivity towards receptor subtypes.^{45,46} However, as previously stated, the preparation of 5'-deoxy-5'-[¹⁸F]fluoroadenosine [¹⁸F]**47** by synthetic-chemical procedures proved to be unsatisfactory.^{45,46}

The application of the fluorinase enzyme from *S. cattleya* (EC 2.5.1.63) as a catalyst to incorporate [¹⁸F]fluoride, and the subsequent successful preparation of [¹⁸F]FDA [¹⁸F]**47** permitted further exploration of its role as a potential PET radiotracer.

4.3.1 PET imaging studies *in vitro*

4.3.1.1 5'-Deoxy-5'-[¹⁸F]fluoroadenosine, [¹⁸F]FDA

A. [¹⁸F]FDA uptake in human cancer cells

If FDA **47** is to act as an analogue of adenosine for imaging studies, cell uptake may occur *via* adenosine transporters. In order to investigate this hypothesis, cell uptake studies were carried out with enzymatically prepared [¹⁸F]FDA [¹⁸F]**47**. The incorporation of [¹⁸F]FDA [¹⁸F]**47** in human cancer cells was determined in the absence and presence of high concentration of adenosine (10 mM). Reactions were carried out in triplicate to ensure reproducibility, following the procedure detailed below.

Human breast cancer cells (MDA-MB-453) were seeded in tissue culture flasks (6 x 25 ml flasks) and cultured to 10% confluence level. A sample of [¹⁸F]FDA [¹⁸F]**47** was

collected (0.75 mL, 2 MBq) and an aliquot (100 μ l) was added to (a) Dubbelco's modified Eagle medium (DMEM) culture medium (7.5 ml) and (b) DMEM containing 10 mM adenosine (7.5 ml). A small volume (2 ml) of (a) was added to 3 flasks and of (b) to the other 3 flasks, and the cells were incubated at 37 °C for 30 min. The cells were then washed with phosphate buffered saline (PBS) at 4 °C (5 times) and harvested with trypsin. Uptake of [18 F]FDA [18 F]47 was determined in a cell counter. The cells were then centrifuged and washed once with PBS; the cell pellet was resuspended in aqueous NaOH (100 μ l, 1 M) and left overnight at 37 °C. They were then neutralised with HCl. The protein content was determined using a bicinchoninic acid protein (BCA) assay kit (Sigma-Aldrich™).

The cell count showed that adenosine does not decrease cell viability during the time period of the assay (*i.e.*, the number of cells in flasks with and without adenosine was similar).

However, the addition of adenosine decreased the uptake of [18 F]FDA [18 F]47 into the cells significantly (>99%), as shown in Figure 4.22.

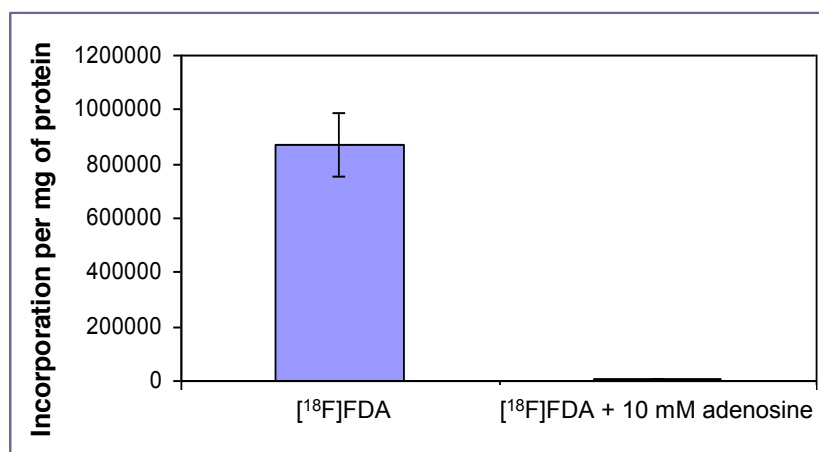


Figure 4.22 [18 F]FDA [18 F]47 uptake by human breast cancer cells (MDA-MB-453) in the absence and presence of a competing concentration of adenosine (10 mM).

These results clearly indicate that [^{18}F]FDA [^{18}F]47 uptake into the cells takes place *via* the adenosine transporters, suggesting that [^{18}F]47 may be useful for imaging adenosine transport/metabolism by positron emission tomography.

B. [^{18}F]FDA transport

In order to investigate whether the cells are also engaged in the reverse process, promoting the release of [^{18}F]FDA [^{18}F]47 out of the cell *via* the adenosine transporters, a cell uptake/efflux experiment was performed.

The same procedure for cell culturing was carried out following the aforementioned protocol. Two set of flasks (6 in total) of human breast cancer cells (MDA-MB-468) were seeded as before. This time, the culture medium was replaced with Dubelcco's modified Eagle medium (DMEM) containing [^{18}F]FDA [^{18}F]47 (2 ml, 1.5 MBq) and the cells were incubated at 37 °C for 30 min. After this time, one set of flasks was used for determining [^{18}F]47 uptake following the procedure described above. The other set had the radioactive medium replaced with new fresh DMEM (2 ml), which was added to each flask. The cells were then incubated at 37 °C for a further 15 min. The residual [^{18}F]FDA [^{18}F]47 and the number of cells and counts per minute (cpm) were determined. The results obtained are illustrated in Figure 4.23 (*vide infra*).

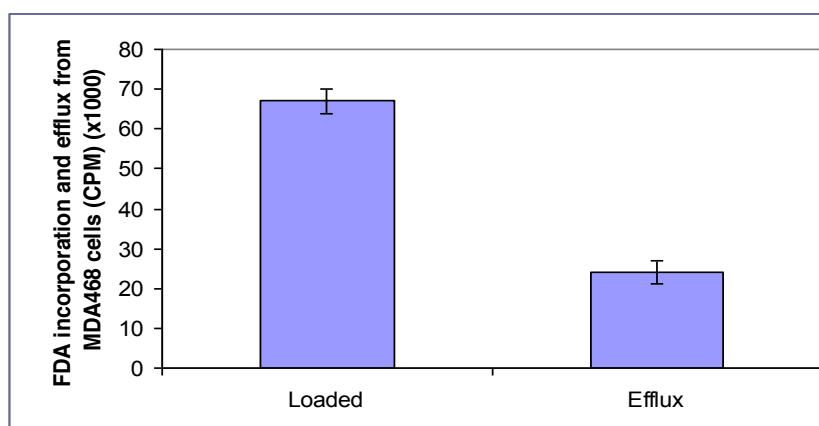


Figure 4.23 [^{18}F]FDA [^{18}F]47 uptake and efflux by human breast cancer cells (MDA-MB-468).

The [^{18}F]FDA [^{18}F]47 uptake and efflux, expressed as counts per minute (cpm) per milligram of protein, shows that not all [^{18}F]FDA [^{18}F]47 that is incorporated remains inside the cell. This indicates the existence of an efflux process. Nevertheless, the results demonstrate that more than 60% of the radiolabelled FDA is retained inside the cell. These findings further support the potential for [^{18}F]FDA [^{18}F]47 as a radiotracer for PET imaging.

4.3.1.2 5'-Deoxy-5'-[^{18}F]fluorinosine, [^{18}F]FDI

A. [^{18}F]FDI uptake in human cancer cells

The incorporation of [^{18}F]FDI [^{18}F]50 in human cancer cells (MDA-MB-468) was determined following the aforementioned protocol for [^{18}F]FDA [^{18}F]47 uptake. Reactions were also carried out in triplicate to ensure reproducibility. Cell culture and counting were performed following the same procedure. In this case, incubation of [^{18}F]FDI [^{18}F]50 in human breast cancer cells (MDA-MB-468) was carried out in the absence and presence of a competing concentration of inosine (20 mM) as encountered *in vivo*. The results obtained after a 10 min incubation are illustrated in Figure 4.24 (*vide infra*).

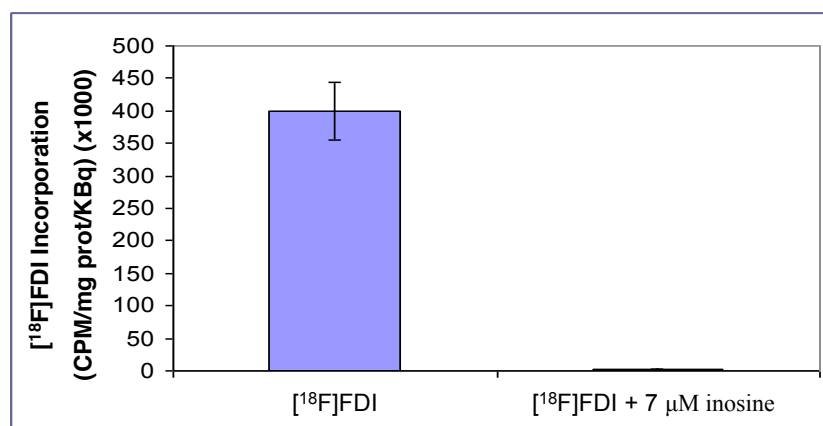


Figure 4. 24 [¹⁸F]FDI **50** uptake by human breast cancer cells (MDA-MB-468) in the absence and presence of inosine.

The results showed that the addition of inosine decreased significantly the uptake of [¹⁸F]FDI [¹⁸F]**50** into the cells.

4.3.2 PET imaging studies *in vivo*: a small animal study with [¹⁸F]FDA

Molecular imaging in small animals has emerged as a powerful technique for investigating disease processes at the molecular and cellular levels.^{98,99} As such, small-animal PET (‘microPET’) has opened the way for imaging tissue biodistribution and metabolism of new markers in nude and genetically-modified rodents.^{100,101,102}

With the purpose of investigating [¹⁸F]FDA [¹⁸F]**47** uptake *in vivo*, an experiment was carried out with a healthy nude rat. After injection (i.v. tail) of a small dose of [¹⁸F]FDA [¹⁸F]**47**, uptake of [¹⁸F]**47** was determined by microPET scanning.

Sagittal and coronal images were acquired after a period of 15 min following intravenous administration of [¹⁸F]FDA [¹⁸F]**47** (1 ml, 18.68 MBq), and are depicted in Figure 4.25 and

Figure 4.26, respectively. A contrast-enhanced microCT scan is shown in both images for anatomic reference.

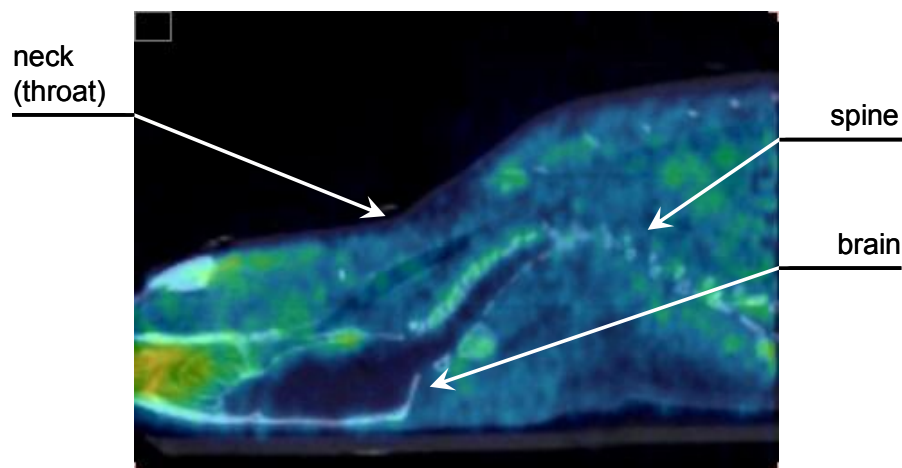


Figure 4.25 Fused CT-PET sagittal view of [^{18}F]FDA [^{18}F]47 uptake in the brain of a male Wistar Han rat following injection of 18.68 Mq, 15 min post-injection. A mixture of ketamine and xylazine was used as an anesthetic agent.

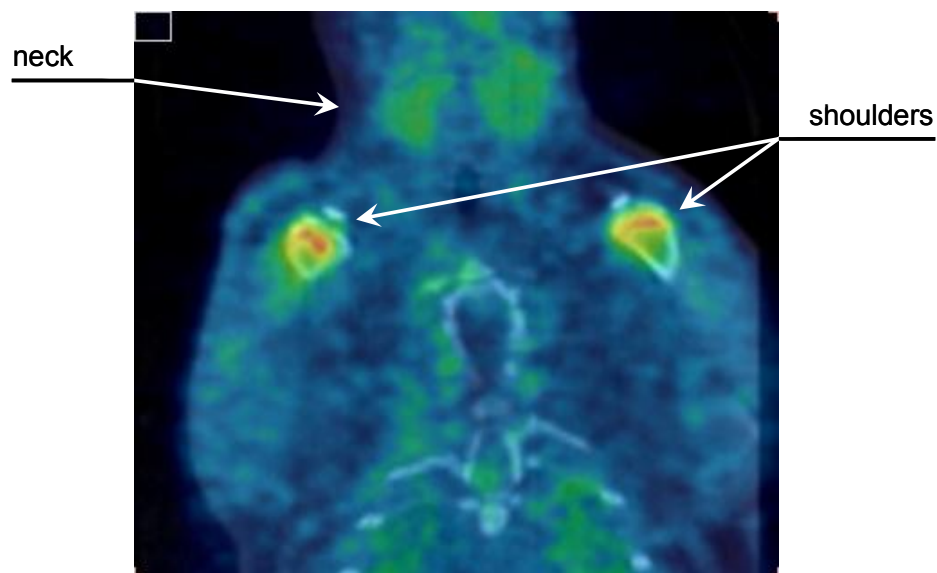


Figure 4.26 Fused CT-PET coronal view through the thorax of a male Wistar Han rat following injection of 18.68 MBq of [^{18}F]FDA [^{18}F]47. Animal was anesthetised with a mixture of ketamine and xylazine.

Uptake of [^{18}F]FDA [^{18}F]47 (Figure 4.25, *vide supra*) is mainly observed in the olfactory bulb. Very low levels of uptake of [^{18}F]FDA [^{18}F]47 are observed in the brain area, with very little definition, indicating virtually no uptake in the brain or spinal cord. This finding suggests that [^{18}F]FDA [^{18}F]47 does not cross the blood brain barrier. However, these are very preliminary results, with not enough information about the pharmacokinetics of [^{18}F]47. Therefore, the possibility that there was insufficient clearance of [^{18}F]FDA [^{18}F]47 from the blood at the time of imaging cannot be discarded.

The experiment demonstrates some accumulation of [^{18}F]FDA [^{18}F]47 in a healthy nude rat with clear concentration in some tissues. [^{18}F]FDA [^{18}F]47 has been generated *via* the fluorinase reaction and in an adequate formulation for a small animal imaging. *In vivo* uptake of [^{18}F]47 has been observed after non-invasive microPET imaging, and happily the animal survived the study.

In order to reduce stress and motion, most small-animal PET scans are carried out with anaesthesia. This may present a problem in PET imaging studies, since the pharmacological action of anaesthetics affect some neuroreceptor systems. However, not only anesthetic agents but also the mode of anesthesia can affect the results of PET studies in small animals. Recently, it has been shown that dietary conditions and temperature during the uptake of the radiotracer influence [^{18}F]FDG [^{18}F]108 biodistribution in mice.^{103,104}

In this context, investigations to gain a deeper knowledge of [^{18}F]FDA [^{18}F]47 biodistribution, and particularly its metabolism, as well as temperature and anesthesia effects, need to be undertaken. Future work will also focus on the exploration of [^{18}F]FDA [^{18}F]47 in tumour and inflammation models.

4.4 Preliminary results of [^{18}F]FDR as a radiotracer of potential diagnostic interest

As aforementioned, nucleoside and sugar tracers have been actively investigated as PET imaging agents for use in tumour detection and/or to monitor response to chemotherapy.^{42,105}

Taking into account the metabolic role of ribose in energy production and recent studies that have reported its benefits in some cardiovascular diseases,^{106,107,108} the development of fluorine-18 labelled ribose, [^{18}F]FDR [^{18}F]71, could offer a new approach to study human energy metabolism and clinical disorders by PET techniques.

To this end, cell uptake studies in human breast cancer cells (MDA-MB-468) were carried out with enzymatically prepared [^{18}F]FDR [^{18}F]71 following the protocol already described for [^{18}F]FDA [^{18}F]47.

The preliminary studies involving incubation of [^{18}F]FDR [^{18}F]71 in breast cancer cells, showed high uptake values when compared to those for [^{18}F]FDG [^{18}F]108 reported for the same cancer cell line, as illustrated in Figure 4.27.

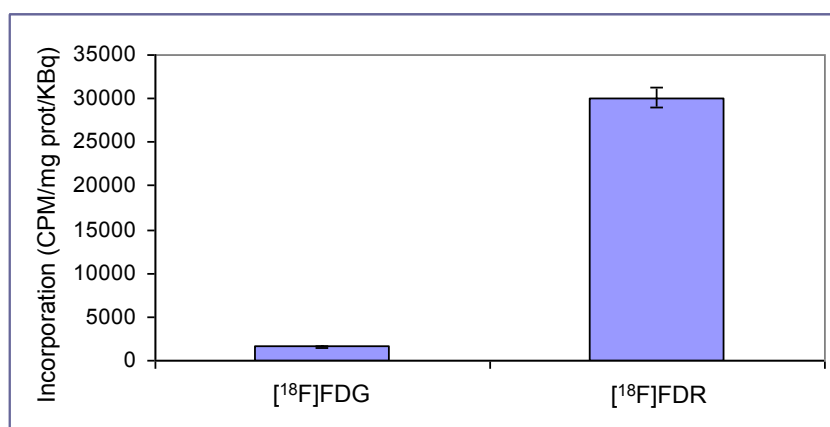


Figure 4.27 Incorporation of [^{18}F]FDG [^{18}F]108 and [^{18}F]FDR [^{18}F]71 in breast cancer cell line MDA-MB-468.

However, the ‘metabolic trapping’ of [^{18}F]FDR [^{18}F]71 needs to be further investigated. Future studies will also focus on the application of [^{18}F]FDR [^{18}F]71 for the evaluation of ribose determination in biological systems.

4.5 Conclusions

The main purpose of this work was to develop a shorter route to [^{18}F]FDR [^{18}F]71 using the fluorinase enzyme as a catalyst for ^{18}F -C bond formation.

A second aim was to develop radiofluorinated FDA [^{18}F]47 and other analogues for non-invasive assessment of adenosine receptors by positron emission tomography (PET).

Human cancer cell lines evaluated *in vitro* showed significant uptake of these radiotracers produced by fluorinase-coupled enzymatic reactions, as summarised in Figure 4.28.

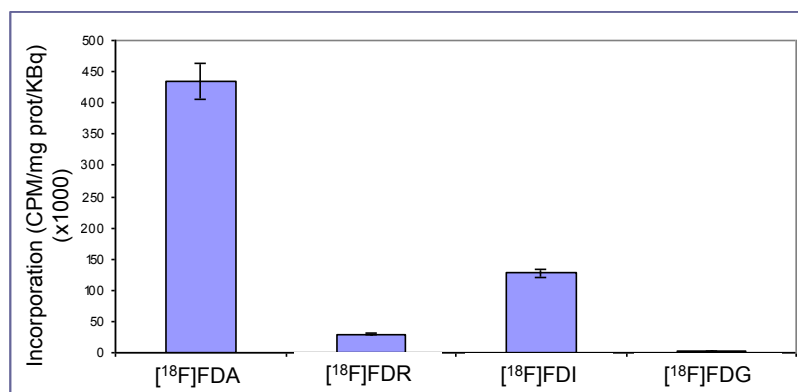


Figure 4.28 Comparative uptake of radiotracers produced by fluorinase reaction with [^{18}F]FDG in human breast cancer cell lines.

These observations stimulated further research on the uptake of [^{18}F]FDA [^{18}F]47, with *in vivo* microPET imaging studies in anaesthetised rat. Nevertheless, further investigations are needed to evaluate the biodistribution and pharmacokinetics of [^{18}F]FDA [^{18}F]47 and these studies should characterise the mode of uptake of these [^{18}F]-labelled sugars and their potential role as radiotracers with clinical use in PET.

4.6 References

1. M. E. Phelps, E. J. Hoffman, N. A. Mullani and M. M. Ter-Pogissian, *J. Nucl. Med.*, 1975, **16**, 210-224.
2. G. Muehllehner and J. S. Karp, *Phy. Med. Biol.*, 2006, **51**, 117-137.
3. F. Dollé, D. Roeda, B. Kuhnast and M.-C. Lasne, *Fluorine-18 Chemistry for Molecular Imaging with Positron Emission Tomography*. In *Fluorine and Health*, Ed. A. Tressaud and G. Haufe, Elsevier, Amsterdam, 2008, pp. 4-65.
4. J. S. Fowler, *The synthesis and Application of F-18 Compounds in Positron Emission Tomography*. In *Organofluorine Compounds in Medicinal Chemistry and Biomedical Applications*, Eds. R. Filler, Y. Kobayashi and L. M. Yagupolskii, Elsevier, Amsterdam, 1993, pp. 309-338.
5. C. Schiepers, *Eur. J. Intern. Med.*, 2004, **15**, 143-146.
6. W. Chen, *J. Nucl. Med.*, 2007, **48**, 1468-1481.
7. D. F. Wong and J. R. Brašić, *Clin. Neurosci. Res.*, 2001, **1**, 35-45.
8. K. Kopka, S. Wagner, M. Schäfers, A. Faust, O. Schober and G. Haufe, *¹⁸F-Labeled PET-Tracers for Cardiological Imaging*. In *Fluorine and Health*, Ed. A. Tressaud and G. Haufe, Elsevier, Amsterdam, 2008, pp. 85-139.
9. K. Någren and J. O. Rinne, *Application of ¹⁸F-PET Imaging for the Study of Alzheimer's Disease*. In *Fluorine and Health*, Ed. A. Tressaud and G. Haufe, Elsevier, Amsterdam, 2008, pp. 67-84.
10. N. L. Foster, J. L. Heidebrink, C. M. Clark, W. J. Jagust, S. E. Arnold, N. R. Barbas, C. S. DeCarli, R. S. Turner, R. A. Koeppe, R. Higdon and S. Minoshima, *Brain*, 2007, **130**, 2616-2635.
11. A. Didelot, P. Ryvlin, A. Lothe, I. Merlet, A. Hammers and F. Mauguière, *Brain*, 2008, **131**, 2751-2764.

CHAPTER 4

12. S. H. Kennedy, K. R. Evans, S. Krüger, H. S. Mayberg, J. H. Meyer, S. McCann, A. I. Arifuzzman, S. Houle and F. J. Vaccarino, *Am. J. Psychiatry*, 2001, **158**, 899-905.
13. M. S. Milak, R. V. Parsey, J. Keilp, M. A. Oquendo, K. M. Malone and J. J. Mann, *Arch. Gen. Psychiatry*, 2005, **62**, 397-408.
14. Y. Okubo, T. Suhara, K. Suzuki, K. Kobayashi, O. Inoue, O. Terasaki, Y. Someya, T. Sassa, Y. Sudo, E. Matsushima, M. Iyo, Y. Tateno and M. Toru, *Nature*, 1997, **385**, 634-636.
15. J. S. Fowler, N. D. Volkow, Y.-S. Ding, J. Logan and G.-J. Wang, in *PET Imaging Studies in Drug Abuse Research*, Brookhaven National Laboratory, New York, 2001.
16. M. R. Gerasimov and S. L. Dewey, *Drug Develop. Res.*, 2003, **59**, 240-248.
17. A. R. Lingford-Hughes, S. J. C. Davies, S. McIver, T. M. Williams, M. R. C. Daglish and D. J. Nutt, *Brit. Med. Bull.*, 2003, **65**, 209-222.
18. L. G. Strauss and P. S. Conti, *J. Nucl. Med.*, 1991, **32**, 623-648.
19. A. A. Neves and K. M. Brindle, *Biochim. Biophys. Acta*, 2006, **1766**, 242-261.
20. J. M. Collins, *Encyclopedia of Cancer*, 2003, **3**, 419-424.
21. W. A. Weber, *J. Nucl. Med.*, 2005, **46**, 983-995.
22. K. Hermann and B. J. Krause, *[¹⁸F]-Labeled PET and PET/CT Compounds in Oncology*. In *Fluorine and Health*, Ed. A. Tressaud and G. Haufe, Elsevier, Amsterdam, 2008, pp. 141-196.
23. C. M. L. West, T. Jones and P. Price, *Nature Rev.*, 2004, **4**, 457-469.
24. N. Gupta, P. M. Price and E. O. Aboagye, *Eur. J. Cancer*, 2002, **38**, 2094-2107.
25. A. D. Gee, *Brit. Med. Bull.*, 2003, **65**, 169-177.

26. M.-C. Lasne, C. Perrio, J. Rouden, L. Barré, D. Roeda, F. Dolle and C. Crouzel, *Chemistry of β^+ -Emitting Compounds Based of Fluorine-18*. In *Topics in Current Chemistry*, Springer-Verlag, Berlin, Heidelberg, 2002, Vol. 2, pp. 201-258.
27. L. Cai, S. Lu and V. W. Pike, *Eur. J. Org. Chem.*, 2008, 2853-2873.
28. C. Isanbor and D. O'Hagan, *J. Fluor. Chem.*, 2006, **127**, 303-319.
29. D. Le Bars, *J. Fluor. Chem.*, 2006, **127**, 1488-1493.
30. T. Ido, W. N. Wan, V. Casella, J. S. Fowler, A. P. Wolf, M. Reivich and D. E. Kuhl, *J. Label. Compd. Radiopharm.*, 1978, **14**, 175-183.
31. M. E. Phelps and J. C. Mazziotta, *Science*, 1985, **228**, 799-809.
32. S. S. Gambhir, J. Czernin, J. Schwimmer, D. H. S. Silverman, R. E. Coleman and M. E. Phelps, *J. Nucl. Med.*, 2001, **42**, 1S-93S.
33. P. Som, H. L. Atkins, D. Bandoypadhyay, J. S. Fowler, R. R. McGregor, K. Matsui, Z. H. Oster, D. F. Sacker, C. Y. Shiue, H. Turner, C.-N. Wan, A. P. Wolf and S. V. Zabinski, *J. Nucl. Med.*, 1980, **21**, 670-675.
34. R. C. Delgado-Bolton, C. Fernández-Pérez, A. González-Maté and J. L. Carreras, *J. Nucl. Med.*, 2003, **44**, 1301-1314.
35. T. A. D. Smith, *Br. J. Biomed. Sci.*, 2000, **57**, 170-178.
36. H. R. Schelbert, C. K. Hoh, H. D. Royal, M. Brown, M. N. Dahlbom, F. Dehdashti and R. L. Wahl, *J. Nucl. Med.*, 1998, **39**, 1302-1305.
37. B. M. Gallagher, J. S. Fowler, N. I. Gutterson, R. R. MacGregor, C.-N. Wan and A. P. Wolf, *J. Nucl. Med.*, 1978, **19**, 1154-1161.
38. K. Wienhard, *Methods*, 2002, **27**, 218-225.
39. M. Mamede, T. Higashi, M. Kitaichi, K. Ishizy, T. Ishimori, Y. Nakamoto, K. Yanagihara, M. Lio, F. Tanaka, H. Wada, T. Manabe and T. Saga, *Neoplasia*, 2005, **7**, 369-379.

40. K. Hamacher, H. H. Coenen and G. Stöcklin, *J. Nucl. Med.*, 1986, **27**, 235-238.
41. L. Varagnolo, M. P. M. Stokkel, U. Mazzi and E. K. J. Pauwels, *Nucl. Med. Biol.*, 2000, **27**, 103-112.
42. B. Beuthien-Baumann, K. Hamacher, F. Oberdorfer and J. Steinbach, *Carbohydr. Res.*, 2000, **327**, 107-118.
43. K. Ishiwata, Y. Kimura, E. F. J. de Vries and P. Elsinga, *Cent. Nerv. Syst. Agents Med. Chem.*, 2007, **7**, 57-77.
44. C.-G. Kim, D. J. Yang, E. E. Kim, A. Cherif, L.-R. Kuang, C. Li, W. Tansey, C. W. Liu, S. C. Li, S. Wallace and D. A. Podoloff, *J. Pharm. Sci.*, 1996, **85**, 339-344.
45. Sz. Lehel, G. Horváth, I. Boros, P. Mikecz, T. Márián and L. Trón, *J. Radioanal. Nucl. Chem.*, 2000, **245**, 399-401.
46. Sz. Lehel, G. Horváth, I. Boros, T. Márián and L. Trón, *J. Radioanal. Nucl. Chem.*, 2002, **251**, 413-416.
47. P. Bjurling, Y. Watanabe, M. Tokushige, T. Oda and B. Långström, *J. Chem. Soc., Perkin Trans. I*, 1989, 1331-1334.
48. P. Bjurling, G. Antoni, Y. Watanabe and B. Långström, *Acta Chem. Scand.*, 1990, **44**, 178-182.
49. E. Lui, R. Chirakal and G. Firnau, *J. Labelled Cpd. Radiopharm.*, 1998, **41**, 503-521.
50. G. Antoni, H. Omura, M. Ikemoto, R. Moulder, Y. Watanabe and B. Långström, *J. Labelled Cpd. Radiopharm.*, 2001, **44**, 287-294.
51. L. Martarello, C. Schaffrath, H. Deng, A. D. Gee, A. Lockhart and D. O'Hagan, *J. Labelled Cpd. Radiopharm.*, 2003, **46**, 1-9.
52. C. Schaffrath, Ph.D. Thesis, *Biosynthesis and Enzymology of Fluorometabolite Production in Streptomyces cattleya*, University of St Andrews, 2002.

53. H. Deng, S. L. Cobb, A. R. McEwan, R. P. McGlinchey, J. H. Naismith, D. O'Hagan, D. A. Robinson and J. B. Spencer, *Angew. Chem., Int. Ed.*, 2006, **45**, 759-762.
54. H. Deng, S. L. Cobb, A. D. Gee, A. Lockhart, L. Martarello, R. P. McGlinchey, D. O'Hagan and M. Onega, *Chem. Commun.*, 2006, 652-654.
55. S. Ben-Haim and P. Ell, *J. Nucl. Med.*, 2009, **50**, 88-99.
56. W. Versées and J. Steyaert, *Curr. Opin. Struc. Biol.*, 2003, **13**, 731-738.
57. C. Petersen and L. B. Møller, *J. Biol. Chem.*, 2001, **276**, 884-894.
58. J. Ogawa, S. Takeda, S.-X. Xie, H. Hatanaka, T. Ashikari, T. Amachi and S. Shimizu, *Appl. Environ. Microbiol.*, 2001, **67**, 1783-1787.
59. L. Liang, X. He, G. Liu and H. Tan, *Microbiology*, 2008, **154**, 1333-1340.
60. M. Porcelli, L. Concilio, I. Peluso, A. Marabotti, A. Facchiano and G. Cacciapuoti, *FEBS J.*, 2008, **275**, 1900-1914.
61. J.-E. Kurtz, F. Exinger, P. Erbs and R. Jund, *Curr. Genet.*, 2002, **41**, 132-141.
62. R. Pellé, V. L. Schramm and D. W. Parkin, *J. Biol. Chem.*, 1998, **273**, 2118-2126.
63. L. Cui, G. R. Rajasekariah and S. K. Martin, *Gene*, 2001, **280**, 153-162.
64. J. M. C. Ribeiro and J. G. Valenzuela, *Insect Biochem. Mol. Biol.*, 2003, **33**, 13-22.
65. W. Versées, E. Van Holsbeke, S. De Vos, K. Decanniere, I. Zegers and J. Steyaert, *Acta Crystallogr. D*, 2003, **59**, 1087-1089.
66. M. Szuwart, E. Starzyńska, M. Pietrowska-Borek and A. Guranowski, *Phytochemistry*, 2006, **67**, 1476-1485.
67. D. M. Santana, G. P. Borja-Cabrera, E. Paraguai de Souza, N. R. Sturm, C. B. Palatnik de Souza and D. A. Campbell, *Mol. Biochem. Parasitol.*, 2002, **120**, 315-319.
68. R. Gamboa-León, E. Paraguai de Souza, G. P. Borja-Cabrera, F. N. Santos, L. M. Myashiro, R. O. Pinheiro, E. Dumonteil and C. B. Palatnik de Souza, *Vaccine*, 2006, **24**, 4863-4873.

69. A. Goeminne, M. Berg, M. McNaughton, G. Bal, G. Surpateanu, P. Van der Veken, S. De Prol, W. Versées, J. Steyaert, A. Haemers and K. Augustyns, *Bioorg. Med. Chem.*, 2008, **16**, 6752-6763.
70. B. Giabbai and M. Degano, *Structure*, 2004, **12**, 739-749.
71. G. Huysmans, A. Ranquin, L. Wyns, J. Steyaert and P. Van Gelder, *J. Controlled Release*, 2005, **102**, 171-179.
72. W. Shi, V. L. Schramm and S. C. Almo, *J. Biol. Chem.*, 1999, **274**, 21114-21120.
73. D. W. Parkin, B. A. Horenstein, D. R. Abdulah, B. Espiñán and V. L. Schramm, *J. Biol. Chem.*, 1991, **266**, 20658-20665.
74. W. Versées, K. Decanniere, R. Pellé, J. Depoorter, E. Brosens, D. W. Parkin and J. Steyaert, *J. Mol. Biol.*, 2001, **307**, 1363-1379.
75. D. W. Parkin, *J. Biol. Chem.*, 1996, **271**, 21713-21719.
76. B. Estupiñán and V. L. Schramm, *J. Biol. Chem.*, 1994, **269**, 23068-23073.
77. S.-A. Poulsen and R. J. Quinn, *Bioorg. Med. Chem.*, 1998, **6**, 619-641.
78. K. A. Jacobson and Z.-G. Gao, *Nat. Rev. Drug Discov.*, 2006, **5**, 247-263.
79. J. Spychala, *Pharmacol. Therapeut.*, 2000, **87**, 161-173.
80. S. Y. Cho, J. Polster, J. M. Engles, J. Hilton, E. H. Abraham and R. L. Wahl, *J. Nucl. Med.*, 2006, **47**, 837-845.
81. P. Fishman, S. Bar-Yehuda, F. Barer, L. Madi, A. S. Multani and S. Pathak, *Exp. Cell Res.*, 2001, **269**, 230-236.
82. L. Madi, A. Ochaion, L. Rath-Wolfson, S. Bar-Yehuda, A. Erlanger, G. Ohana, A. Harish, O. Merimski, F. Barer and P. Fishman, *Clin. Cancer Res.*, 2004, **10**, 4472-4479.
83. J. Blay, T. D. White and D. W. Hoskin, *Cancer Res.*, 1997, **57**, 2602-2605.

CHAPTER 4

84. P. Fishman, S. Bar-Yehuda, G. Ohana, S. Pathak, L. Wasserman, F. Barer and A. S. Multani, *Eur. J. Cancer*, 2000, **36**, 1452-1458.
85. P. Fishman, S. Bar-Yehuda, L. Madi and I. Cohn, *Anti-Cancer Drugs*, 2002, **13**, 437-443.
86. J. Lu, A. Pierron and K. Ravid, *Cancer Res.*, 2003, **63**, 6413-6423.
87. J. A. Thorn and S. M. Jarvis, *Gen. Pharmac.*, 1996, **27**, 613-620.
88. S. A. Baldwin, J. R. Mackey, C. E. Cass and J. D. Young, *Mol. Med. Today*, 1999, **5**, 216-224.
89. M. Pennycooke, N. Chaudary, I. Shuralyova, Y. Zhang and I. R. Coe, *Biochem. Biophys. Res. Commun.*, 2001, **280**, 951-959.
90. V. L. Damaraju, S. Damaraju, J. D. Young, S. A. Baldwin, J. Mackey, M. B. Sawyer and C. E. Cass, *Oncogene*, 2003, **22**, 7524-7536.
91. L. Spicuzza, G. Di Maria and R. Polosa, *Eur. J. Pharmacology*, 2006, **533**, 77-88.
92. R. G. Dip, *Vet. J.*, 2009, **179**, 38-49.
93. W. B. Mathews, Y. Nakamoto, E. H. Abraham, U. Scheffel, J. Hilton, H. T. Ravert, M. Tatsumi, P. A. Rauseo, B. J. Traugher, A. Y. Salikhova, R. F. Dannals and R. L. Wahl, *Mol. Imaging Biol.*, 2005, **7**, 203-208.
94. S. Y. Cho, J. Polster, J. M. Engles, J. Hilton, E. H. Abraham, and R. L. Wahl, *J. Nucl. Med.*, 2006, **74**, 837-845.
95. K.-N. Klotz, N. Falgner, S. Kachler, C. Lambertucci, S. Vittori, R. Volpini and G. Cristalli, *Eur. J. Pharmacol.*, 2007, **556**, 14-18.
96. M. M. Alauddin, J. D. Fissekis and P. S. Conti, *J. Labelled Cpd. Radiopharm.*, 2003, **46**, 805-814.
97. M. M. Alauddin, A. Shahinian, R. Park, M. Tohme, J. D. Fissekis and P. S. Conti, *Nucl. Med. Biol.*, 2007, **34**, 267-272.

CHAPTER 4

98. R. Myers and S. Hume, *Eur. Neuropsychopharmacology*, 2002, **12**, 545-555.
99. D. J. Rowland, J. R. Garbow, R. Laforest and A. Z. Snyder, *Nucl. Med. Biol.*, 2005, **32**, 567-572.
100. B. M. Gallagher, A. Ansari, H. Atkins, V. Casella, D. R. Christman, J. S. Fowler, T. Ido, R. R. MacGregor, P. Som, C. N. Wan, A. P. Wolf, D. E. Kuhl and M. Reivich, *J. Nucl. Med.*, 1977, **18**, 990-996.
101. H. Barthel, M. C. Cleij, D. R. Collingridge, O. C. Hutchinson, S. Osman, Q. He, S. K. Luthra, F. Brady, P. M. Price and E. O. Aboagye, *Cancer Res.*, 2003, **63**, 3791-3798.
102. C. Waldherr, I. K. Mellinghoff, C. Tran, B. S. Halpern, N. Rozengurt, A. Safaei, W. A. Weber, D. Stout, N. Satyamurthy, J. Barrio, M. E. Phelps, D. H. Silverman, C. L. Sawyers and J. Czernin, *J. Nucl. Med.*, 2005, **46**, 114-120.
103. K. H. Lee, B.-H. Ko, J.-Y. Paik, K.-H. Jung, Y. S. Choe, Y. Choi and B.-T. Kim, *J. Nucl. Med.*, 2005, **46**, 1531-1536.
104. B. J. Fueger, J. Czernin, I. Hildebrandt, C. Tan, B. S. Halpern, D. Stout, M. E. Phelps and W. A. Weber, *J. Nucl. Med.*, 2006, **47**, 999-1006.
105. J. Toyohara and Y. Fujibayashi, *Nucl. Med. Biol.*, 2003, **30**, 681-685.
106. H.-G. Zimmer, H. Ibel, U. Suchner and H. Schad, *Science*, 1984, **223**, 712-714.
107. R. Wilson, D. MacCarter and J. St. Cyr, *Heart Drug*, 2003, **3**, 61-62.
108. D. F. Pauly, C. Johnson and J. A. St. Cyr, *Medical Hypotheses*, 2003, **60**, 149-151.

CHAPTER 5

**Chemical and
Biochemical Experimental**

Chemical and biochemical experimental

5.1 Chemical syntheses

5.1.1 General experimental procedures

5.1.1.1 Reagents and solvents

Commercially available reagents and solvents were used when available and purchased from Acros, Aldrich[®], Alfa Aesar[®], Fluka, Lancaster and VWR[®].

All reagents were of synthetic grade and used as supplied, unless otherwise stated. If further purification was required, the procedures detailed by Perrin and Armarego were followed.¹

Diethyl ether (Et₂O) and dry tetrahydrofuran (THF) were dried by refluxing with benzophenone over sodium wire under an atmosphere of nitrogen, and were distilled and collected by syringe as required. Dry methanol (MeOH) and dry dichloromethane (DCM) were dried by refluxing with calcium hydride, they were then distilled and collected by dry syringe as required, or from Pure-Solv[™] Solvent Purification Systems from Innovative Technology, Inc. Dry acetonitrile (MeCN) and dry pyridine were used as supplied by Aldrich[®]. Acetone was used as reagent grade. Light petroleum refers to the fraction boiling between 40–60 °C.

5.1.1.2 Reaction conditions

Air and moisture sensitive reactions were carried out under a positive pressure of nitrogen using oven-dried glassware (140 °C). Room temperature (RT) refers to 20–25 °C. Reaction temperatures of –78 °C to –40 °C were obtained using a bath cooling apparatus LP Technology RP-100-CD. For those at 0 °C, an ice bath was employed. Reactions requiring reflux or heating were carried out using an oil bath equipped with a contact thermometer.

Reaction progress was monitored by thin layer chromatography (TLC).

5.1.1.3 Chromatography

Thin layer chromatography (TLC) was carried out on pre-coated aluminium backed silica gel plates (Machery-Nagel Alugram[®] SIL G, 0.20 mm silica gel) or on pre-coated plastic sheets with silica gel (Machery-Nagel Polygram[®] SIL G/UV₂₅₄, 0.20 mm silica gel). Compounds were visualised using UV light (λ , 254 nm), potassium permanganate, vanillin or a molybdenum based staining agent.

Flash column chromatography was performed using silica gel (Apollo Scientific Ltd, silica gel, 40–63 micron grade). The crude samples were either applied directly to the top of the silica/solvent column or applied as a dry silica gel slurry.

High-performance liquid chromatography (HPLC) analysis was carried out using a Varian series 9012 pump/9050 UV-lamp; analytical HPLC was performed using a Hypersil ODS C-18 column, 5 μ m (250 mm; 4.6 mm ID).

GC-MS analyses were obtained using an Agilent 6890 gas chromatograph equipped with an Agilent 5973N mass-selective detector.

5.1.1.4 Nuclear Magnetic Resonance Spectroscopy (NMR)

Nuclear magnetic resonance (NMR) spectra were recorded on either Bruker Avance 300 (^1H , 300 MHz; ^{13}C , 75 MHz; ^{19}F , 282 MHz), or Bruker Avance 400 (^1H , 400 MHz; ^{13}C , 100 MHz; ^{19}F , 376 MHz), or Bruker Avance 500 (^1H , 500 MHz; ^{19}F , 470 MHz) using GPE Ltd NMR tubes (GPE-S-5-300 NMR tubes). ^{13}C NMR spectra were acquired using the PENDANT sequence.

Chemical shifts for ^1H and ^{13}C NMR spectra were recorded using deuterated solvent as the lock and residual solvent as the internal standard. Where CDCl_3 was employed as the solvent, calibration was carried out on this solvent signal at 7.26 ppm (^1H) and 77.16 (^{13}C).² When D_2O was used, the water signal was designated the internal reference at 4.79 ppm (^1H). ^{19}F NMR spectra were referenced to CFCl_3 as the external standard.

NMR spectra are described in parts per million (ppm) and are reported consecutively as chemical shift (δ_{H} , δ_{C} or δ_{F}), relative integral, multiplicity (s, singlet; d, doublet; dd, doublet of doublets; dt, doublet of triplets; t, triplet; m, multiplet; br.s, broad singlet), coupling constant (J) in Herzt (Hz) and assignment. The abbreviation Ar in the assignment of both ^1H and ^{13}C is used to denote aromatic.

All NMR spectra were recorded at 25 °C, unless otherwise stated and were analysed using Bruker TopSpin (Version 2.0 Bruker BioSpin 2006) software.

5.1.1.5 Mass spectrometry

Low resolution mass spectrometry (MS) were performed using a Micromass LCT (Manchester, UK) mass spectrometer with electrospray ionization (ESI) operating in both positive and negative mode. High resolution mass analysis was carried out by Caroline Horsburgh, spectra were recorded on a Micromass LCT TOF mass spectrometer using ES

ionization in +ve ion mode. Where this method was not adequate CI was employed using a Micromass GCT instrument

5.1.1.6 Melting point analyses

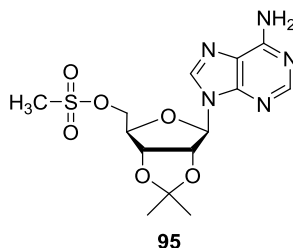
Melting points were obtained using Pyrex[®] capillaries and were measured on a Gallenkamp Griffin MPA350.BM2.5 melting point apparatus.

5.1.1.7 GC-MS

Low resolution GC-MS analysis was carried out using an Agilent 6890 plus gas chromatograph coupled to a 5973N mass selective detector in EI mode, with helium carrier gas. Automatic injections using a 7683 series injector were made into both non-chiral and chiral columns. Separations were achieved with an Agilent HP 19091S-433, 5% phenyl methyl siloxane, 30 m x 250 μ m, film thickness 0.25 μ m, non-chiral column and a β -DEX 120 Superco chiral column. The HP 6890 chemstation software was used for data processing.

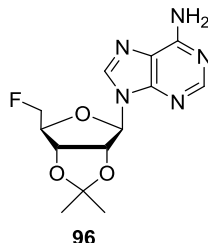
5.1.1.8 LC-MS

Low resolution LC-MS analysis was carried out on a Supelcosil ABZ+PLUS column (3 μ m, 3.3 cm x 4.6 mm ID) eluting with 0.1% HCO₂H and 0.01 M ammonium acetate in water (solvent A), and 95% CH₃CN and 5% water (containing 0.5% HCO₂H) (solvent B). The elution gradient was as follows: 0–0.7 min 0% B, 0.7–4.2 min 0–100% B, 4.2–4.6 min 100% B with a flow rate of 3 cm³ / min. Three modes of detection were used: electrospray in positive mode, electrospray in negative mode which were recorded on a Waters ZQ mass spectrometer and diode array UV detection which was carried out in the range 215–330 nm.

5.1.2 Synthesis of 5'-deoxy-5'-fluoroadenosine **47**5.1.2.1 2',3'-*O*-Isopropylidene-5'-*O*-mesyladenosine **95**³

Methanesulfonyl chloride (2.5 cm³, 31.6 mmol) was added dropwise to a stirred solution of 2',3'-*O*-isopropylidene-adenosine **94** (5 g, 15.8 mmol) in anhydrous pyridine (40 cm³) at 0 °C. The reaction was warmed to RT and stirred for 4 h. Ice-cold water (20 cm³) and 2 M KOH were then added until a neutral pH was reached. The reaction mixture was then concentrated under reduced pressure to give a yellow oil, which was partitioned between chloroform (50 cm³) and water (40 cm³). The organic layer was washed with water (2 x 25 cm³), dried, filtered and concentrated. Purification over silica eluting with CHCl₃:EtOH (10:1) gave **95** (8.27 g, 68%) as an off white powder.

M.p. 225-227 °C (lit.,⁴ 235-236 °C dec.). δ_{H} (300 MHz; CDCl₃): 1.40 (3 H, s, CCH₃), 1.63 (3 H, s, CCH₃), 2.92 (3 H, s, SO₂CH₃), 4.40-4.47 (2 H, m, 2 x H-5'), 4.51-4.56 (1 H, m, H-4'), 5.16 (1 H, dd, *J* 6.3 and 2.9, 3'-H), 5.44 (1 H, dd, *J* 6.3 and 2.0, H-2'), 5.89 (2 H, br s, NH₂), 6.13 (1 H, d, *J* 2.0, H-1'), 7.95 (1 H, s, H-8) and 8.34 (1 H, s, H-2); δ_{C} (75 MHz; CDCl₃): 27.5 (CH₃), 25.7 (CH₃), 21.5 (SO₂-CH₃), 68.8 (CH₂), 81.8 (CH), 84.4 (CH), 85.2 (CH), 91.3 (CH), 115.2 (C), 119.1 (C), 140.5 (C-2), 150.0 (C), 153.2 (C-8) and 155.7 (C).

5.1.2.2 2',3'-*O*-Isopropylidene-5'-deoxy-5'-fluoroadenosine **96**⁴Procedure A⁴

TBAF·3H₂O (9.31 g, 29.5 mmol) in anhydrous MeCN (20 cm³) was added to a solution of 2',3'-*O*-isopropylidene-5'-*O*-mesyl-adenosine **95** (4.54 g, 11.8 mmol) in anhydrous MeCN (80 cm³) at RT and the solution was heated under reflux for 17 h. The reaction was cooled to RT and concentrated under reduced pressure to afford a brown oil, that was partitioned between chloroform (150 cm³) and water (50 cm³). The organic layer was washed with water (2 x 50 cm³), dried, filtered and concentrated. Purification over silica eluting with CHCl₃:EtOH (10:1) furnished **96** (1.12 g, 31%) as an off-white powder. M.p. 156-157 °C (lit.,⁴ 159-160 °C). δ_{H} (300 MHz; CDCl₃): 1.38 (3 H, s, CCH₃), 1.60 (3 H, s, CCH₃), 4.52 (1 H, dm, H-4'), 4.68 (2 H, dm, ²*J*_{H,F} 47.0, 2 x H-5'), 5.10 (1 H, dd, *J* 6.3 and 3.0, H-3'), 5.34 (1 H, dd, *J* 6.3 and 2.2, H-2'), 6.18 (1 H, d, *J* 2.2, H-1'), 6.37 (2 H, brs, NH₂), 7.91 (1 H, s, H-8) and 8.31 (1H, s, H-2); δ_{F} (282 MHz; CDCl₃): -229.29 (dt, ²*J*_{F-H} 46.9 and ³*J*_{F-H} 23.5).

Procedure B⁵

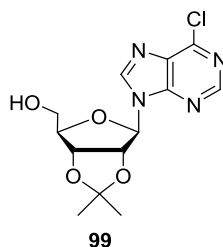
A sealable tube was charged with **100a:100b** (0.188 g, 0.582 mmol) dissolved in *t*-BuOH (6 cm³). A flow of NH_{3(g)} was then bubbled through the solution for 5 min, after which time the tube was sealed and heated at 90 °C for 24 h. The solvent was removed at reduced

CHAPTER 5

pressure, then taken up in CHCl_3 (40 cm^3) and washed using H_2O (30 cm^3) which was extracted further with CHCl_3 (40 cm^3). The combined organic phase was then dried (MgSO_4), filtered and concentrated under reduced pressure to give **96** (0.166 g, 92%) as an off white solid.

Physical and spectroscopic properties were identical to those previously given for **96**.

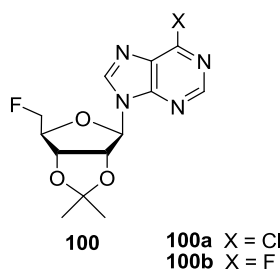
5.1.2.3 Chloro-9-(2',3'-O-isopropylidene- β -D-ribofuranosyl)- purine **99** ⁶



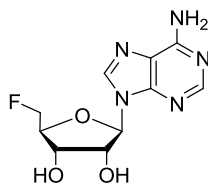
To a stirred suspension of 6-chloro-9- β -D-ribofuranosylpurine **98** (0.5 g, 1.74 mmol) in anhydrous acetone (15 cm³) and 2,2-dimethoxypropane (1.2 cm³, 0.87 mmol) was added *p*-toluenesulfonic acid monohydrate (0.34 g, 1.74 mmol). After 4 h the resulting solution was poured slowly into stirred aqueous 0.5 M NaHCO₃ (30 cm³). The solution was concentrated under reduced pressure and extracted with CHCl₃ (4 x 20 cm³). The combined organic extracts were washed with brine, dried over MgSO₄ and the solvent was evaporated under reduced pressure. The residual off-white solid was crystallised from MeOH to give **99** (0.41 g, 73%) as white crystals; M.p. 158-159 °C (lit.⁶ 159-160). δ_{H} (300 MHz, CDCl₃): 1.39 (3H, s, -CH₃), 1.65 (3H, s, -CH₃), 3.83 (1H, dd, *J* 12.6 and 2.1, H-5'), 3.98 (1H, dd, *J* 12.6 and 1.79, H-5'), 4.55-4.58 (1H, m, H-4'), 5.11 (1H, dd, *J* 6.0 and 1.4, H-3'), 5.20 (1H, dd, *J* 6.0 and 4.6, H-2'), 5.98 (1H, d, *J* 4.6, H-1), 8.25 (1H, s, H-8), 8.77 (1H, s, H-2). *m/z* (ES⁻): 325.04 [M-H] (100%). *m/z* (ES⁺): 348.95 [M+Na]⁺ (100%). HRMS (ES): Found 349.0671. Calcd. for C₁₃H₁₅N₄O₄NaCl, 349.0680.

5.1.2.4 2',3'-*O*-Isopropylidene-5'-deoxy-5'-fluoro-6-chloropurine
riboside **100a**⁵

2',3'-*O*-Isopropylidene-5'-deoxy-5',6-difluoropurine
riboside **100b**⁵



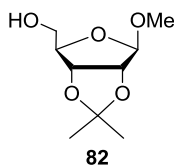
To a stirred solution containing 0.300 g (0.92 mmol) of **99** in dry THF (8.5 cm³) was added TsF (0.320 g, 1.84 mmol; 2 eq) followed by 1 M TBAF in THF (2.8 cm³, 2.8 mmol; 3.0 eq) the resultant solution was heated under reflux. After 22 h the reaction mixture was filtered rinsing with EtOAc. Concentration of this solution under reduced pressure and subsequent purification by column chromatography (hexane:EtOAc, 1:1) gave 0.24 g (0.75 mmol, 81% conversion to primary fluoride) of **100a:100b** as a yellow oil (10:1 mixture). δ_{H} (300 MHz, CDCl₃): 1.35 (3H, s, CH₃), 1.59 (3H, s, CH₃), 4.68-4.44 (3H, m, H-4', 5a'-H, 5b'-H), 5.03 (1H, dd, *J* 6.3 and 2.7, 3'-H), 5.30-5.28 (1H, m, H-2'), 6.26 (1H, d, *J* 2.4, H-1'), 8.24 (s, H-8/2), 8.27 and 8.24 (s, H-8/2, 1:2.2, 1H), 8.71 and 8.60 (s, H-2/8, 1:2.2, 1H). δ_{F} (282 MHz, CDCl₃, H-F decoupled): -230.3.

5.1.2.5 5'-Deoxy-5'-fluoroadenosine **47**⁷**47**Procedure A

2',3'-*O*-Isopropylidene-5'-deoxy-5'-fluoroadenosine **96** (0.075 g, 0.242 mmol) was suspended in 0.02 M sulfuric acid (5 cm³) with stirring. The reaction slurry was then heated (100 °C) and the reaction was monitored by ¹⁹F NMR spectroscopy until such time that no starting material could be detected (5 h). The reaction mixture was cooled and the solvent co-evaporated several times with ethanol to give the title compound as a pale yellow oil which was identified as **47** by HPLC analysis.

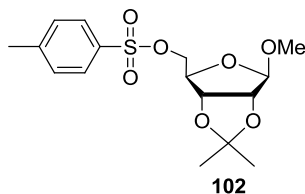
Procedure B⁵

A sample of **100a** and **100b** (0.152 g, 0.491 mmol) was stirred in TFA:H₂O (9:1, 8 cm³) for 25 min at RT, after which time the reaction mixture was cooled and the solvent removed under reduced pressure to afford a pale yellow oil. Recrystallisation in MeOH:Et₂O gave 0.094 g (77%) of **47** as a white solid. M.p. 203-204 °C (lit.,⁷ 204-205 °C); δ_{H} (300 MHz; D₂O): 4.11 (1 H, dm, ³*J*_{H-F} 23.8, H-4'), 4.21-4.30 (1 H, m, H-3'), 4.47-4.63 (1 H, m, H-2'), 4.64 (2 H, dm, ²*J*_{H-F} 47.8, 2 x H-5'), 5.46 (1 H, brs, OH), 5.65 (1 H, brs, OH), 6.01 (1 H, d, *J* 4.8, H-1'), 7.30 (2 H, brs, NH₂), 8.06 (1 H, s, H-8) and 8.15 (1 H, s, H-2); δ_{C} (75 MHz; D₂O): 69.8 (d, ³*J*_{C-F} 6.1, C-3'), 74.3 (C-2'), 81.7 (d, ²*J*_{C-F} 17.8, C-4'), 83.3 (d, ¹*J*_{C-F} 171.8, C-5'), 88.0 (C-1'), 119.4 (C-5), 139.7 (C-8), 149.7 (C), 153.1 (C-2) and 156.4 (C-6); δ_{F} (282 MHz; D₂O): -230.00 (dt, ²*J*_{F-H} 47.4, ³*J*_{F-H} 23.8). *m/z* (ES⁺): 270.04 [M+H]⁺ (100%). HRMS (ES): Found 270.1001. Calcd. for C₁₀H₁₂FN₅O₃, 270.1002.

5.1.3 Synthesis of 5-deoxy-5-fluoro-D-ribose **71**5.1.3.1 Methyl-2,3-*O*-isopropylidene- β -D-ribofuranoside **82**^{8,9}

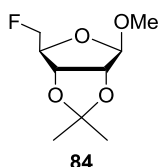
A solution of 2,2-dimethoxypropane (45 cm³) was added to D-(-)-ribose **81** (15.04 g, 100.21 mmol) in a mixture of anhydrous methanol (55 cm³) and anhydrous acetone (70 cm³) at RT with stirring followed by BF₃·Et₂O (3.6 cm³, cat.) and the resulting yellow solution was allowed to stir for 24 h at RT. Sodium bicarbonate was then added until neutral pH was achieved. The reaction mixture was then filtered and concentrated under reduced pressure to afford the crude product as a yellow oil. Vacuum distillation gave the title compound **82** (11.67 g, 57%) as a colourless oil. δ_{H} (300 MHz; CDCl₃): 1.32 (3 H, s, -CH₃), 1.49 (3 H, s, -CH₃), 3.44 (3 H, s, -OCH₃), 3.48 (1 H, brs, -OH), 3.58 (1 H, dd, ²J_{H-H} 12.5 and J 2.6, H-5), 3.66 (1 H, dd, ²J_{H-H} 12.5 and J 3.5, H-5), 4.44 (1 H, t, J 2.7, H-4), 4.59 (1 H, d, J 6.0, H-2), 4.84 (1 H, d, J 6.0, H-3) and 4.98 (1 H, s, H-1); δ_{C} (75 MHz; CDCl₃): 24.7 (CH₃), 26.4 (CH₃), 55.5 (OCH₃), 64.0 (C-5), 81.5 (C-3), 85.8 (C-2), 88.4 (C-4), 110.0 (C-1) and 112.5 (C). *m/z* (GC-MS, EI): 189 (M⁺-CH₃, 52%), 173 (M⁺-OCH₃, 38), 59 (100), 43 (67).

5.1.3.2 Methyl-2,3-*O*-isopropylidene-5-*O*-tosyl- β -D-ribofuranoside **102**¹⁰

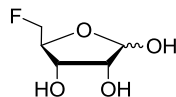


Purified *p*-tosylchloride (6.9 g, 36.2 mmol) was added portion wise to a solution of methyl-2,3-*O*-isopropylidene- β -D-ribofuranoside **82** (5.0 g, 24.5 mmol) in anhydrous pyridine (13 cm³) at 0 °C. After 4 h at RT the reaction was found to be complete by TLC analysis. The reaction mixture was quenched into ice water (25 cm³) and the resulting white precipitate was filtered and washed with ice water (3 x 15 cm³) to remove the excess of pyridine. The white precipitate collected was dissolved in diethyl ether (15 cm³), dried over MgSO₄ and the solvent removed under pressure. Subsequent drying under reduced pressure afforded the tosylate **102** (5.17 g, 76%) as a white solid. M.p. 78-79 °C. (lit.,¹⁰ 78.5-79.5 °C); δ_{H} (300 MHz; CDCl₃) 1.28 (3 H, s, CH₃), 1.45 (3 H, s, CH₃), 2.46 (3 H, s, Ar-CH₃), 3.23 (3 H, s, -OCH₃), 4.01 (2 H, dd, *J* 7.3 and 1.5, H-5), 4.31 (1 H, dt, *J* 7.3 and 0.8, H-4), 4.53 (1 H, d, *J* 6.0, H-2), 4.60 (1 H, dd, *J* 6.0 and 0.8, H-3), 4.93 (1 H, s, H-1), 7.36 (2 H, d, *J* 8.2, Ar-H) and 7.81 (2 H, d, *J* 8.2, Ar-H); δ_{C} (75 MHz; CDCl₃) 22.1 (Ar-CH₃), 25.2 (CH₃), 26.7 (CH₃), 55.4 (OCH₃), 69.6 (CH₂), 81.7 (CH), 83.9 (CH), 85.3 (CH), 109.8 (CH), 113.1 (C), 128.4 (ArC), 130.3 (ArC), 133.1 (C) and 145.5 (C). *m/z* (ES⁺): 380.46 [M+Na]⁺ (100%). HRMS (ES): Found 381.0978. Calcd. for C₁₆H₂₂O₇NaS, 381.0984.

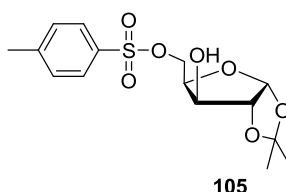
5.1.3.3 Methyl-2,3-*O*-isopropylidene-5-deoxy-5-fluoro- β -D-ribofuranoside **84**⁷



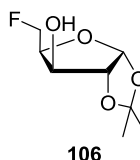
A solution of TBAF.3H₂O (2.2 g, 6.97 mmol) in anhydrous acetonitrile (5.5 cm³) was added to a stirred solution of methyl-2,3-*O*-isopropylidene-5-*O*-tosyl- β -D-ribofuranoside **102** (2.0 g, 5.58 mmol) in anhydrous MeCN (20 cm³) at RT and the reaction was then heated under reflux for 24 h. The reaction mixture was cooled and concentrated under vacuum to give a brown oil. The oil was dissolved in ethyl acetate (15 cm³), washed with water (2 x 15 cm³) and dried over MgSO₄. The solvent was removed under vacuum to give the crude product as a yellow oil which was purified over silica gel eluting with diethyl ether:pet. ether 5:2 to afford **84** (0.86 g, 59%) as a clear oil. δ_{H} (300 MHz; CDCl₃) 1.33 (3 H, s, CH₃), 1.49 (3 H, s, CH₃), 3.33 (3 H, s, OCH₃), 4.28-4.48 (3 H, m, 2 x H-5 and H-4), 4.59 (1 H, dd, *J* 6.0 and 2.4, H-2), 4.69 (1 H, d, *J* 6.0, H-3), 4.99 (1 H, d, *J* 2.4, H-1); δ_{C} (75 MHz CDCl₃); 25.3 (CH₃), 26.8 (CH₃), 55.3 (OCH₃), 81.4 (d, ³*J*_{C-F} 4.2, C-3), 82.2-84.5 (d, ¹*J*_{C-F} 172.5, C-5), 84.7-85.0 (d, ²*J*_{C-F} 22.3, C-4), 85.4 (C-2), 109.6 (C-1), 113.0 (C); δ_{F} (282 MHz, CDCl₃) -225.29 (dt, ²*J*_{F-H} 48.3 and ³*J*_{F-H} 21.4).

5.1.3.4 5-Deoxy-5-fluoro-D-ribose **71** ¹¹**71**

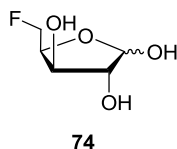
Dilute sulphuric acid (0.02 M, 6 cm³) was added to methyl-2,3-*O*-isopropylidene-5-deoxy-5-fluoro- β -D-ribofuranoside **84** (0.72 g, 3.5 mmol) with stirring. The reaction was then heated under reflux and found to be complete by ¹⁹F NMR spectroscopy within 4 h. Calcium carbonate was added to neutralise the excess of acid and calcium sulfate was removed from the product by centrifugation. The supernatant was filtered through celite and lyophilised to yield 5-deoxy-5-fluoro-D-ribose **71** (0.47 g, 88%) as a pale yellow syrup. The ¹H-NMR (300 MHz, D₂O) spectrum recorded for **71** was too complex to interpret conclusively. δ_C (75 MHz; D₂O): 69.2 (d, ⁴*J*_{C-F} 7.0, α / β , C-3), 69.3 (d, ³*J*_{C-F} 7.2, α / β , C-3), 70.9, 75.4 (α / β , C-2), 80.7 (d, ³*J*_{C-F} 22.5, α / β , C-4), 81.4 (d, ³*J*_{C-F} 17.8, α / β , C-4), 82.5 (d, ¹*J*_{C-F} 168.6, α / β , C-5), 84.8 (d, ¹*J*_{C-F} 168.4, α / β , C-5), 96.8 (α , C-1), 101.4 (β , C-1); δ_F (282 MHz, D₂O): -228.53 (β , dt, and ²*J*_{F-H} 46.5 and ³*J*_{F-H} 26.0), -230.83 (α , dt, ²*J*_{F-H} 46.5 and ³*J*_{F-H} 27.9). *m/z* (GC-MS after derivatisation with MSTFA): 217 (100%), 191 (23), 143 (32), 73 (74).

5.1.4 Synthesis of 5-deoxy-5-fluoro-D-xylose **74**5.1.4.1 1,2-Di-*O*-isopropylidene-5-*O*-tosyl-D-xylofuranose **105** ¹²

Purified *p*-toluenesulfonyl chloride (1.31 g, 6.31 mmol) was added portion wise to a solution of 1,2-di-*O*-isopropylidene-D-xylofuranose **104** (1.20 g, 6.25 mmol) in anhydrous pyridine (15 cm³) at 0 °C and after 4 h at RT the reaction was found to be complete by TLC analysis. The reaction mixture was quenched into ice water (25 cm³) and the resulting white precipitate was filtered and washed with ice water (3 x 15 cm³) to remove the excess of pyridine. The white precipitate collected was dissolved in diethyl ether (15 cm³), dried over MgSO₄ and the solvent removed under reduced pressure. Recrystallisation from THF/Et₂O furnished **105** (1.53 g, 74%) as a white solid; M.p. 85 °C. δ_{H} (300 MHz; CDCl₃): 1.30 (3 H, s, -CH₃), 1.46 (3H, s, CH₃), 2.45 (3 H, s, OCH₃), 3.48 (1 H, s, OH), 4.09-4.18 (1 H, m, H-4), 4.30-4.37 (3 H, m, H-5), 4.51 (1 H, d, *J* 3.6, H-2), 5.88 (1 H, d, *J* 3.6, H-1), 7.36 (2 H, d, *J* 8.2, Ar-H), 7.80 (2 H, d, *J* 8.2, Ar-H). *m/z* (CI⁺): 345.10 [M+H]⁺ (100%). HRMS (CI): Found 345.1011. Calcd. for C₁₅H₂₁O₇S, 345.1008.

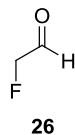
5.1.4.2 1,2-*O*-Isopropylidene-5-deoxy-5-fluoro- α -D-xylofuranose**106**¹³

A solution of TBAF trihydrate (2.2 g, 6.97 mmol) in anhydrous acetonitrile (5 cm³) was added to 1,2-di-*O*-isopropylidene-5-*O*-tosyl-D-xylofuranose **105** (0.98 g, 5.10 mmol) in anhydrous acetonitrile (20 cm³) at 25 °C and the reaction was heated under reflux for 24 h. The reaction mixture was cooled and concentrated under reduced pressure to give an oil. The oil was dissolved in ethyl acetate (15 cm³), washed with water (2 x 15 cm³) and dried over MgSO₄. The solvent was removed under reduced pressure to give the crude product as a yellow oil which was purified over silica gel eluting with diethyl ether:pet. ether 5:2 to afford **106** (0.44 g, 57%) as a white solid. δ_{H} (300 MHz; CDCl₃): 1.33 (3 H, s, CH₃), 1.50 (3H, s, CH₃), 3.48 (1 H, brs, OH), 4.33-4.45 (2 H, dm, H-3 and H-4), 4.53 (1 H, dd, *J* 6.0 and 1.3, H-2), 4.65 (1 H, ddd, *J* 47.1 and 10.2 and 5.1, H-5), 4.81 (1 H, ddd, *J* 47.1 and 10.2 and 5.1, H-5) and 5.98 (1 H, d, *J* 3.7, H-1). δ_{F} (282 MHz, CDCl₃, F-H decoupled): -232.4. *m/z* (CI⁺): 193.09 [M+H]⁺

5.1.4.3 5-Deoxy-5-fluoro-D-xylofuranose **74** ¹³

Dilute sulfuric acid (0.02 M, 6 cm³) was added to 1,2-*O*-isopropylidene-5-deoxy-5-fluoro- α -D-xylofuranose **106** (0.72 g, 3.5 mmol) with stirring at RT. The reaction was heated under reflux and found to be complete by ¹⁹F NMR spectroscopy within 4 h. Calcium carbonate was added to neutralise the excess of acid and the calcium sulfate was removed from the product by centrifugation. The supernatant was filtered through celite and lyophilised to yield 5-deoxy-5-fluoro-D-xylose **74** (0.47 g, 83%) as a pale yellow syrup.

The ¹H-NMR (300 MHz, D₂O) spectrum recorded for **74** was too complex to interpret conclusively. δ_{F} (282 MHz, D₂O): -228.49 (β , dt, and ² $J_{\text{F-H}}$ 47.5 and ³ $J_{\text{F-H}}$ 24.2), -230.60 (α , dt, ² $J_{\text{F-H}}$ 47.5 and ³ $J_{\text{F-H}}$ 24.2).

5.1.5 Fluoroacetaldehyde **26**¹⁴

Fluoroethanol **68** (5 cm³, 85.0 mmol) was added to a suspension of pyridinium dichromate (PDC) (10.0 g, 26.5 mmol) in dichloromethane (60 cm³) and the reaction was heated under reflux for 16 h. The reaction was allowed to cool and the solution distilled into a separating funnel containing water (25 cm³). After mixing, the organic layer was separated and extracted with a further volume of water (15 cm³). The aqueous layers were combined and analysed by ¹⁹F NMR spectroscopy. The sample was shown to approximately 40% fluoroacetaldehyde **26**. δ_{F} (376 MHz, D₂O): -224.44 (60%) (tt, ²J_{F-H} 47.3 and ³J_{F-H} 31.8; fluoroethanol **68**), -231.02 (40%) (dt, ²J_{F-H} 47.3 and ³J_{F-H} 10.3; fluoroacetaldehyde **26**).

5.2 Biochemical protocols

5.2.1 General experimental procedures

5.2.1.1 Reagents and enzymes

Streptomyces cattleya NRRL 8057 was obtained from The Queen's University of Belfast, Microbial Biochemistry Section, Food Science Department, Belfast (originally from United States Department of Agriculture, Agricultural Research Service, Midwest Area Northern Regional Research Laboratories, Peoria, Illinois, USA).

Commercially available reagents and enzymes were used when available and purchased from either Acros, Fermentas, Fluka, Novagen, Promega or Sigma Biochemicals. The details for the enzymes are as follows: immobilised purine nucleoside phosphorylase (PNPase, EC 2.4.2.1, *E. coli*, donated by GlaxoSmithKline), purine nucleoside phosphorylase (PNPase, EC 2.4.2.1, unknown bacterial source, N-8264, 15.5 units/mg), 5'-adenylic acid deaminase (EC 3.5.4.6, from *Aspergillus species*, A 1907, 0.11 units/mg), phytase (EC 3.1.3.8, from *Aspergillus ficuum*, P 9792, 3.5 units/mg), and glucose isomerase (Sweetzyme T, from *Streptomyces murinus*, G-4166, 350 units/mg). The competent cells BL21(DE3), BL21 (DE3) Gold and C43(DE3) were purchased from Invitrogen in 50 µl aliquots.

For [¹⁸F]fluoride production, a CTI RDS-111 cyclotron (CTI/Siemens) and for determination of radioactivity a Capintec well reader (CRC-15R) were used.

5.2.1.2 Cell culture and microbiological work

All microbiological work was carried out under sterile conditions in a Gallenkamp flowhood. All work described involving cells, cell-free extract or protein solutions was performed at 4 °C if not otherwise stated. Glassware, media and consumables were sterilised by

autoclaving. Cell cultures were incubated in a temperature controlled Gallenkamp orbital incubator and resting cells on a temperature controlled Innova 2000 platform shaker. Centrifugation was carried out on a Beckman Avanti instrument at 14,000 rpm, at 20,000 (JA 25.50) or at 9,000 rpm (JLA 9.100). For microcentrifugation (50–1500 μ l), an Eppendorf 5415C centrifuge was used. Sonication was performed with a Sonics & Materials Inc., Vibra Cell apparatus. Lyophilisation was carried out on an FTS, flexi-dry freeze dryer. Protein concentration was determined using a Nanodrop ND1000 spectrophotometer. Samples were concentrated using a SPD1010 Speed Vac system. Ultra-pure water was collected from a USF Elga Maxima water supply system.

5.2.1.3 Nuclear Magnetic Resonance Spectroscopy (NMR)

Nuclear magnetic resonance (NMR) spectra were recorded on either Bruker Avance 400 (^1H , 400 MHz; ^{19}F , 376 MHz), or Bruker Avance 500 (^1H , 500 MHz; ^{19}F , 470 MHz) using GPE Ltd NMR tubes (GPE-S-5-300 NMR tubes). NMR spectra were acquired using D_2O or 10% D_2O in buffer or water.

Chemical shifts for ^1H and ^{19}F NMR spectra were recorded using deuterated solvent as the lock and residual solvent as the internal standard. When D_2O was used, the water signal was designated the internal reference at 4.79 ppm (^1H).² ^{19}F NMR spectra were referenced to CFCl_3 as the external standard.

NMR spectra are described in parts per million (ppm) and are reported consecutively as chemical shift (δ_{H} or δ_{F}), relative integral, multiplicity (s, singlet; d, doublet; dd, doublet of doublets; dt, doublet of triplets), coupling constant (J) in Herzt (Hz) and assignment.

All NMR spectra were recorded at 25 °C, unless otherwise stated and were analysed using Bruker TopSpin (Version 2.0 Bruker BioSpin 2006) software.

5.2.1.4 Gas Chromatography Mass Spectrometry (GC-MS)

GC-MS analysis was performed on a Hewlett Packard 5890 gas chromatograph linked to an HP 5970B mass selective detector controlled by an HP300 series computer. The gas chromatograph was fitted with an autosampler and equipped with an Ultra 1 fused-silica wall-coated open tubular capillary column (12 x 0.2 mm x 0.33 μm) with 5% biphenyl, 95% dimethyl polysiloxane as the bonded phase.

GC-MS Determination of persilylated derivatives

Using the method described by Hamilton *et al.*,¹⁵ lyophilised supernatant (1 ml) of samples was derivatised by the addition of *N*-trimethylsilyl-*N*-methyl trifluoroacetamide (MSTFA) (1 ml) and then heating to 100 °C for 1 h. After cooling to room temperature, the samples were passed through a Pasteur pipette containing a cotton wool plug and analysed by GC-MS under the following conditions. The oven was programmed to start at 100 °C for 1 min and then ramped at 10 °C/min to 300 °C. The injector port temperature was set at 250 °C and the sample (1 μl) injected splitless. The mass spectrometer was operated in the full scan electron impact mode.

5.2.1.5 High Performance Liquid Chromatography (HPLC)

HPLC analyses were carried out on a Varian Prostar HPLC system, consisting of a solvent delivery system (230, Prostar solvent delivery module), a dual wavelength UV-Vis detector (Varian 325, Prostar) and a Prostar 400 autosampler. An analytical Macherey-Nagel C-18 column (Hypersil-ODS, 120-5, 250 x 4.6 mm) was used at a flow rate of 1 ml/min. Sample volumes of 100 μl were used, of which 20 μl was automatically injected. Solvents that were

used were HPLC grade and filtered before use. The mobile phases consisted of 2 solvents; A, 50 mM KH_2PO_4 : acetonitrile (95:5) and solvent B, 50 mM KH_2PO_4 : acetonitrile (80:20). Runs were monitored at 254 nm by gradient elution over 30 min from 0% B to 100% B.

HPLC analysis of radioactive compounds

High performance liquid chromatography (HPLC) was carried out under the conditions described as follows. Aliquots of the reaction mixture were analysed under the conditions stated below at a constant flow rate of 1 ml/min for 15 min.

| Stationary phase | Mobile phase |
|-------------------------------------|---------------------------------------|
| ZORBAX Carbohydrate analysis column | 85:15 MeCN/ H_2O |
| Hypersil ODS | 90:10 NaH_2PO_4 /MeCN |

Analysis of the radiolabelled samples was conducted on a Gynkotek HPLC system composed of a two head gradient pump (P580), a column oven (STHS8S) and a UV detector (UVD340S) coupled in series with a BIOSCAN NaI detector (B-FC-3200), equipped with a Phenomenex Luna C-18 column (250 x 4.5 mm, 5 μm) or a Macherery-Nagel C-18 column (Hypersil-ODS, 120-5, 250 x 4.6 mm).

5.2.1.6 Fast Performance Liquid Chromatography (FPLC)

Protein purification was carried out on an ÄKTA™ HPLC system. Buffers were filtered and kept at 4 °C. Protein elution was monitored at 280 nm collecting samples of 4 ml. Protein purification was carried out on an ÄKTA™ HPLC basic system at room temperature. The following techniques were employed: hydrophobic interaction chromatography (HIC) using

Phenyl Sepharose HP, 40 ml bed volume (Amersham Biosciences); size exclusion chromatography using a HiLoad™ 16/60 Superdex™ 200 gel filtration column (Pharmacia Biotech Inc.) and anion exchange chromatography using a Q, 5 ml bed volume anion exchange column (Amersham Biosciences). Typical flow rates were between 1 ml/min and 2 ml/min.

5.2.1.7 SDS-Polyacrylamide gel electrophoresis (SDS-PAGE)

SDS-PAGE was performed on an Invitrogen XCell *SureLock*™ mini-cell apparatus connected to an Amersham Pharmacia biotech EPS 301 power supply operating at a constant current of 125 mA for 35 min. NuPAGE™ Bis-Tris 10 well gels containing either 10% or 4–12% of acrylamide were used.

A. Sample preparation for SDS-PAGE

Protein samples for SDS-PAGE analysis were prepared as follows. To 20 µl of protein sample was added 5 µl of NuPAGE™ LDS sample buffer, and the protein was denatured at 100 °C for 3 min. A sample (10-20 µl) was then added to the sample wells of the pre-cast NuPAGE™ Bis-Tris gel. Prestained pagemer protein ladder (SM0661, Fermentas) was used as a guide for MW determination.

B. Staining and destaining of SDS gels

The gel was stained by soaking in a solution of Coomassie blue G250 dye for 30–60 min at 4 °C. Destaining was achieved by soaking in distilled water and microwaving for 10 min at full power. The composition of the stain solution is as follows: coomassie blue G250 (2.0g), methanol (400 ml), glacial acetic acid (70 ml) and ultra pure water (530 ml).

5.2.2 Culturing conditions of *S. cattleya*¹⁶

5.2.2.1 Growth and maintenance of *S. cattleya* on agar

Streptomyces cattleya NRRL 8057 was originally supplied by Prof. D. B. Harper at the Queen's University of Belfast, Microbial Biochemistry Section, Food Science Department, Belfast. Cultures were maintained on agar plates containing soybean flour (2% w/v), mannitol (2% w/v), agar (1.5% w/v) and tap water. The plates were incubated at 30 °C for 28 days or until sporulation could be detected. The resultant static cultures were stored at 4 °C.

5.2.2.2 Culture medium and growth conditions of *S. cattleya*

Streptomyces cattleya seed and batch cultures were grown in conical flasks (500 ml) containing chemically defined medium (90 ml). The medium was prepared as follows: sterile ultra-pure water (450 ml) was added to ion solution (150 ml), filtered carbon solution (75 ml), (see Section 5.2.2.3), sterile phosphate buffer (75 ml, 150 mM, pH 7.0) and sterile potassium fluoride (3 ml, 0.5 M). The seed cultures were prepared by transferring spores from a static culture as described above, and added to a conical flask (500 ml) containing chemically defined medium (90 ml). After incubation for 6 days at 28 °C on an orbital shaker (180 rpm), an aliquot (0.3 ml) of spores was used to inoculate the batch cultures. The batch cultures were incubated at 28 °C, on an orbital shaker at 180 rpm for 6–8 days.

5.2.2.3 Media procedure for growing *S. cattleya*

A. Ion solution

The following reagents were added to ultra-pure water (900 ml).

| | |
|--------------------------------------|----------|
| NH ₄ Cl | 6.75 g |
| NaCl | 2.25 g |
| MgSO ₄ .7H ₂ O | 2.25 g |
| CaCO ₃ | 1.13 g |
| FeSO ₄ .7H ₂ O | 0.113 g |
| CoCl ₂ .6H ₂ O | 0.045 g |
| ZnSO ₄ .7H ₂ O | 0.045 g. |

The solution was sterilised by autoclaving prior to use.

B. Carbon source solution

The following reagents were added to ultra-pure water (900 ml).

| | |
|--------------------------------|---|
| glycerol | 45 g |
| monosodium glutamate | 22.5 g |
| <i>myo</i> -inositol | 1.8 g |
| <i>para</i> -aminobenzoic acid | 450 µl of freshly prepared solution 1 mg/ml |

The solution was sterilised by filtration into pre-sterilised Schott bottles.

5.2.3 Preparation of resting cell cultures of *S. cattleya*

After 6 days of growth, *S. cattleya* cells were harvested by centrifugation (9,100 rpm, 25 min) and the resulting pellet was washed three times with phosphate buffer (50 mM, pH 6.8). After the final wash, the bacterial pellet was stored at $-80\text{ }^{\circ}\text{C}$ until required.

5.2.4 Preparation of cell-free extract (CFE) of *S. cattleya*

CFE was prepared by re-suspending frozen cells of *S. cattleya* (0.1–0.4 mg/mL) in an appropriate buffer (50 mM KH_2PO_4 , pH 6.8 or 50 mM Tris-HCl, pH 7.8) and left to stir for 20 min at $4\text{ }^{\circ}\text{C}$. Ultra-sonication (10 x 60 sec, at 60% duty cycle) was used to disrupt the cells and the cell debris was removed by centrifugation (14,000 rpm, 20 min). The resulting clear supernatant was used as a CFE.

5.2.5 Assay to determine biosynthetic activity in a CFE of *S. cattleya*

Assay 1: CFE (500 μl), SAM **49** (50 μl , 20 mM) and KF (10 μl , 0.5 M) was incubated for 16 h at $37\text{ }^{\circ}\text{C}$. The sample was then heated ($100\text{ }^{\circ}\text{C}$, 3 min) and the denatured protein removed by centrifugation (14,000 rpm, 15 min). D_2O (100 μl) was added to the supernatant which was then analysed by ^{19}F NMR spectroscopy. The production of fluoroacetate (FAc) **17** and / or 4-fluorothreonine (4-FT) **39** confirmed that the CFE was active. The presence of **17** or **39** was determined by comparison against reference samples.

Assay 2: CFE (500 μl) and 5'-FDA **47** (100 μl , 18.6 mM) was incubated for 16 h at $37\text{ }^{\circ}\text{C}$. The sample was then heated ($100\text{ }^{\circ}\text{C}$, 3 min) and the denatured protein removed by centrifugation (14,000 rpm, 15 min). D_2O (100 μl) was added to the supernatant which was

then analysed by ^{19}F NMR spectroscopy. The production of FAc **17** and / or 4-FT **39** confirmed that the CFE was active. The presence of FAc **17** or 4-FT **39** was determined by comparison against reference samples.

5.2.6 Protein purification by ammonium sulfate precipitation

A CFE was prepared following the procedure described in Section 5.2.4. According to the volume of the supernatant, ammonium sulfate was slowly added to the desired % saturation level (Table 5.1). After all the ammonium sulfate was dissolved by stirring for 20 min at 4 °C, the precipitated solution was centrifuged (20 min, 14,000 rpm) and the supernatant either discarded or kept for further precipitation. The protein pellet could then be used directly or kept at -80 °C.

Table 5.1 Ammonium sulfate table showing grams of ammonium sulfate added to 100 ml of solution.¹⁷

Final concentration of ammonium sulfate, % saturation at 0°C

| | 20 | 25 | 30 | 35 | 40 | 45 | 50 | 55 | 60 | 65 | 70 | 75 | 80 | 85 | 90 | 95 | 100 |
|------------|---|------|------|------|------|------|------|------|------|------|------|------|------|------|------|------|------|
| | g solid ammonium sulfate to add to 100 ml of solution | | | | | | | | | | | | | | | | |
| 0 | 10.7 | 13.6 | 16.6 | 19.7 | 22.2 | 26.2 | 29.5 | 33.1 | 36.6 | 40.4 | 44.2 | 48.3 | 52.3 | 56.7 | 61.1 | 65.9 | 70.7 |
| 5 | 8.0 | 10.9 | 13.9 | 16.8 | 20.0 | 23.2 | 26.6 | 30.0 | 33.6 | 37.3 | 41.1 | 45.0 | 49.1 | 53.3 | 57.8 | 62.4 | 67.1 |
| 10 | 5.4 | 8.2 | 11.1 | 14.4 | 17.1 | 20.3 | 23.6 | 27.0 | 30.5 | 34.2 | 37.9 | 41.8 | 45.8 | 50.0 | 54.4 | 58.9 | 63.6 |
| 15 | 2.6 | 5.5 | 8.3 | 11.3 | 14.3 | 17.4 | 20.7 | 24.0 | 27.5 | 31.0 | 34.8 | 38.6 | 42.6 | 46.6 | 51.0 | 55.5 | 60.0 |
| 20 | 0 | 2.7 | 5.6 | 8.4 | 11.5 | 14.5 | 17.7 | 21.0 | 24.4 | 28.0 | 31.6 | 35.4 | 39.2 | 43.3 | 47.6 | 51.9 | 56.5 |
| 25 | | 0 | 2.7 | 5.7 | 8.5 | 11.7 | 14.8 | 18.2 | 21.4 | 24.8 | 28.4 | 32.1 | 36.0 | 40.1 | 44.2 | 48.5 | 52.9 |
| 30 | | | 0 | 2.8 | 5.7 | 8.7 | 11.9 | 15.0 | 18.4 | 21.7 | 25.3 | 28.9 | 32.8 | 36.7 | 40.8 | 45.1 | 49.5 |
| 35 | | | | 0 | 2.8 | 5.8 | 8.8 | 12.0 | 15.3 | 18.7 | 22.1 | 25.8 | 29.5 | 33.4 | 37.4 | 41.6 | 45.9 |
| 40 | | | | | 0 | 2.9 | 5.9 | 9.0 | 12.2 | 15.5 | 19.0 | 22.5 | 26.2 | 30.0 | 34.0 | 38.1 | 42.4 |
| 45 | | | | | | 0 | 2.9 | 6.0 | 9.1 | 12.5 | 15.8 | 19.3 | 22.9 | 26.7 | 30.6 | 34.7 | 38.8 |
| 50 | | | | | | | 0 | 3.0 | 6.1 | 9.3 | 12.7 | 16.1 | 19.7 | 23.3 | 27.2 | 31.2 | 35.3 |
| 55 | | | | | | | | 0 | 3 | 6.2 | 9.4 | 12.9 | 16.3 | 20.0 | 23.8 | 27.7 | 31.7 |
| 60 | | | | | | | | | 0 | 3.1 | 6.3 | 9.6 | 13.1 | 16.6 | 20.4 | 24.2 | 28.3 |
| 65 | | | | | | | | | | 0 | 3.1 | 6.4 | 9.8 | 13.4 | 17.0 | 20.8 | 24.7 |
| 70 | | | | | | | | | | | 0 | 3.2 | 6.6 | 10.0 | 13.6 | 17.3 | 21.2 |
| 75 | | | | | | | | | | | | 0 | 3.2 | 6.7 | 10.2 | 13.9 | 17.6 |
| 80 | | | | | | | | | | | | | 0 | 3.3 | 6.8 | 10.4 | 14.1 |
| 85 | | | | | | | | | | | | | | 0 | 3.4 | 6.9 | 10.6 |
| 90 | | | | | | | | | | | | | | | 0 | 3.4 | 7.1 |
| 95 | | | | | | | | | | | | | | | | 0 | 3.5 |
| 100 | | | | | | | | | | | | | | | | | 0 |

5.2.7 Partial purification of an isomerase from *S. cattleya*

S. cattleya CFE (150 ml) was subjected to ammonium sulfate precipitation following the protocol previously detailed. The protein pellet corresponding to the 35-50 % ammonium sulfate cut was dissolved in phosphate buffer (50 mM, pH 6.8) supplemented with 1 M (NH₄)₂SO₄ in a total volume of 6 ml with a protein concentration of ~20 mg / ml. This protein solution was filtered through a 0.45 µm HT Tuffryn® membrane filter. Partially purified fractions (200 µl) were incubated with 5-FDRP **61** (100 µl) for 16 h at 37 °C to assay for isomerase activity. After this time the protein was denatured at 100 °C for 3 min and removed by centrifugation (14,000 rpm / 5 min). The supernatant was retained and assayed

by ^{19}F NMR spectroscopy for isomerase activity. Selected spectroscopic data: δ_{F} (470 MHz, 10% D_2O) 5-FDRulP **69** -231.34 (dt, $^2J_{\text{F-H}}$ 47.0 and $^3J_{\text{F-H}}$ 20.9).

5.2.7.1 Hydrophobic interaction chromatography (HIC)

The dissolved protein pellet (5 ml) was injected onto a 40 ml Phenyl sepharose HP column equilibrated with 2 column volumes of phosphate buffer (50 mM, pH 6.8) containing 1 M $(\text{NH}_4)_2\text{SO}_4$. The column was washed with a further two column volumes and subsequently eluted by applying a step wise gradient at 2 ml/min from 1 M to 0 M $(\text{NH}_4)_2\text{SO}_4$. The protein fractions (12 ml in total, 1.3 mg protein/ml) eluted at the end of the gradient were found to be active when assayed for isomerase activity.

5.2.7.2 Size exclusion chromatography

The eluent (~ 12 ml) from the HIC purification step was concentrated to 2 ml using a 10 kDa Amicon[®] Ultra-15 centrifugal concentrator. The concentrated protein was loaded onto a HiLoad[™] 16/60 Superdex[™] 200 gel filtration column (Pharmacia Biotech Inc.) equilibrated with Tris buffer (50 mM, pH 7.2) supplemented with 0.3 M KCl at a constant flow rate of 1 ml/min. Protein was eluted isocratically over 180 ml. Isomerase activity was found in the protein fractions eluted between 72–80 ml with a protein concentration of 0.5 mg/ml.

5.2.7.3 Ion exchange chromatography (IEC)

The eluent (8 ml) from the size exclusion column was concentrated to 2 ml using a 10 kDa Amicon[®] Ultra-15 centrifugal concentrator. The concentrated protein was then desalted using

a HiTrap™ desalting column (5 ml) to remove KCl. The sample was then re-concentrated to ~2 ml by the same method.

The concentrated protein sample (2 ml) was applied to an anion exchange column (Q, 5 ml sepharose) which was pre-equilibrated with five column volumes of tris buffer (50 mM, pH 7.2). The loaded protein sample was washed with two column volumes and subsequently eluted using a step wise gradient of tris buffer (50 mM, pH 7.2) containing 1 M KCl at a flow rate of 2 ml / min. The peak containing isomerase activity eluted after a gradient of 250 mM KCl with a total protein concentration of 1.5 mg / ml.

5.2.8 Chemo-enzymatic preparation of 5'-FDI **50** ⁴

5'-FDA **47** (100 µl, 18.6 mM) and 5'-adenylic acid deaminase (2 mg) were suspended in phosphate buffer (50 mM, pH 6.8) in a total volume of 1 ml and incubated for 16 h at 37 °C. The sample was then heated (100 °C, 3 min) and the denatured protein removed by centrifugation (14,000 rpm, 15 min). The supernatant was supplemented with D₂O and analysed by ¹⁹F NMR spectroscopy showing 100% conversion to 5'-deoxy-5'-fluorinosine, 5'-FDI **50**. δ_F (470 MHz; D₂O): -231.52 (dt, ²J_{F-H} 47.2 and ³J_{F-H} 29.5); *m/z* (ES⁺): 271.03 [M+H]⁺ (100%).

5.2.9 Chemo-enzymatic preparation of 5-FDRP **61**

5'-Deoxy-5'-fluorinosine, 5'-FDI **50** (5 mg/ml, 1 ml) was incubated with an immobilised PNPase (30 mg) and incubated at 37 °C until the best conversion was observed (approx. 40% conversion to 5-FDRP **61**). The sample was then denatured at 100 °C for 3 min and the precipitated protein removed by centrifugation (14,000 rpm, 15 min). The sample was analysed

by ^{19}F NMR spectroscopy. δ_{F} (470 MHz; D_2O): (5'-FDI **50**, ~60%) -231.52 (dt, $^2J_{\text{F-H}}$ 47.2 and $^3J_{\text{F-H}}$ 29.5) and (5-FDRP **61**, ~40%) -230.75 (dt, $^2J_{\text{F-H}}$ 47.3 and $^3J_{\text{F-H}}$ 28.2).

5.2.10 Chemo-enzymatic preparation of 5-FDRul **73**

Immobilised glucose isomerase (30 mg) was added to an aqueous solution of 5-FDR **71** (1ml, 5 mg/ml KH_2PO_4 buffer, 200 mM, pH 6.8). Samples were incubated at 37 °C for 6 h, following the reaction by ^{19}F NMR spectroscopy every hour. Samples (100 μl) of the reaction mixture were taken every hour and the protein was denatured by heating (100 °C, 3 min) and removed by centrifugation (14,000 rpm, 15 min). The supernatant was then analysed by ^{19}F NMR spectroscopy to reveal the production of 5-FDRul **73**. δ_{F} (470 MHz, D_2O): -231.22 (dt, $^2J_{\text{F-H}}$ 46.9 and $^3J_{\text{F-H}}$ 20.5).

5.2.11 Chemo-enzymatic preparation of 5-FDXul **75**

Immobilised glucose isomerase (30 mg) was added to an aqueous solution of 5-FDX **74** (1ml, 5 mg/ml KH_2PO_4 buffer, 200 mM, pH 6.8). Samples were incubated at 37 °C for 3 h, following the reaction by ^{19}F NMR spectroscopy every hour. Samples (100 μl) of the reaction mixture were taken every hour and the protein was denatured by heating (100 °C, 3 min) and removed by centrifugation (14,000 rpm, 15 min). The supernatant was then analysed by ^{19}F NMR spectroscopy to reveal the production of 5-FDXul **75**. δ_{F} (470 MHz, D_2O): -228.55 (dt, $^2J_{\text{F-H}}$ 46.1 and $^3J_{\text{F-H}}$ 15.4).

5.2.12 Incubations in CFEs of *S. cattleya*

5.2.12.1 Preparation of 5-FDRulP **69**

A stock solution of 5-FDRP **61** was prepared as previously described in Section 5.2.9.

Samples of 5-FDRulP **69** were prepared using the following protocol: *S. cattleya* CFE (400 μ l, 0.1 g cells/ml) was incubated with the 5-FDRP **61** stock solution (100 μ l) and EDTA (30 mM). Samples were incubated at 37 °C for 6 h. The protein was denatured by heating (100 °C, 3 min) and removed by centrifugation (14,000 rpm, 15 min). The supernatant was then analysed by ^{19}F NMR spectroscopy. δ_{F} (470 MHz, D_2O): -231.34 (dt, $^2J_{\text{F-H}}$ 47.0 and $^3J_{\text{F-H}}$ 20.9). m/z (GC-MS, after MSTFA derivatisation): 521 (M $^+$, 100%), 506 (M $^+$ -CH $_3$, 52).

5.2.12.2 Preparation of 5-FDRul **73**

Phytase (100 μ l, 10 mg/ml) was added to a sample of 5-deoxy-5-fluoro-D-ribulose-1-phosphate (5-FDRulP) **69** (500 μ l) prepared using the protocol described above. The sample was incubated at 37 °C for 16 h. The protein was then denatured by heating (100 °C, 3 min) and removed by centrifugation (14,000 rpm, 15 min). The supernatant was then analysed by ^{19}F NMR spectroscopy. Selected spectroscopic data for **73**. δ_{F} (470 MHz, D_2O): -231.22 (dt, $^2J_{\text{F-H}}$ 46.9 and $^3J_{\text{F-H}}$ 20.2).

5.2.12.3 Incubation 5-FDRul **73** in a CFE of *S. cattleya*

A sample of 5-FDRul **73** (100 μ l) containing an excess of 5-FDR **71** was incubated with a CFE (500 μ l) for 16 hrs at 37 °C. After this time the sample was denatured at 100 °C for 3 min and the precipitated protein removed by centrifugation (14,000 rpm, 5 min). The

supernatant was supplemented with D₂O and analysed by ¹⁹F NMR spectroscopy. δ_{F} (470 MHz, 10% D₂O) 5-FDR **71**, -230.83 (α -anomer, dt, ²*J*_{F-H} 46.5 and ³*J*_{F-H} 27.9), -228.53 (β -anomer, dt, ²*J*_{F-H} 46.5 and ³*J*_{F-H} 26.0) and 5-FDRul **73**, -231.22 (dt, ²*J*_{F-H} 46.9 and ³*J*_{F-H} 20.2).

5.2.13 GC-MS Determination of the persilylated derivative of 5-FDRulP **69**

GC-MS analysis of the persilylated 5-deoxy-5-fluoro-D-ribulose-1-phosphate (5-FDRulP) **69** was carried out by Dr J. Hamilton (Queen's University, Belfast). Lyophilised samples of 5-FDRulP **69** were derivatised by the addition of *N*-trimethylsilyl-*N*-methyl trifluoroacetamide (MSTFA) (1 mL) and then heating to 100 °C for 1 h. After cooling to room temperature, the samples were passed through a Pasteur pipette containing a cotton wool plug and analysed by GC-MS under the following conditions. The oven was programmed to start at 100 °C for 1 min and then ramped at 10 °C/min to 300 °C. The injector port temperature was set at 250 °C and the sample (1 μ l) injected splitless. The mass spectrometer was operated in the full scan electron impact mode measuring ion currents between 30 and 550 amu to obtain the mass spectra of fluororibulose phosphate. The molecular weight of 5-FDRulP **69** was confirmed using chemical ionization mass spectrometry with methane as the reagent gas.

5.2.14 Expression of recombinant fIA and purification

E. coli BL21(DE3) transformed with pET28-fIA was grown in Luria Bertrani broth containing 100 µg/ml kanamycin at 37 °C until an absorbance of 0.4–0.6 at 600 nm was reached. Over-expression of fIA was induced by adding isopropylthiogalactoside (IPTG) to 0.2 mM and the incubation was continued at 16 °C overnight. Cells were collected, resuspended in buffer A consisting of 50 mM phosphate buffer (pH 7.8) supplemented with imidazole (10 mM). The cells were lysed by sonication, ten times at 60% duty cycle for 1 min with intervals of cooling for 30 sec depending on the volume. The disrupted cell suspension was centrifuged for 30 min at 10,000 rpm and the clear supernatant was retained. Prior to further purification, this supernatant was first filtered through a 0.45 µm EZEE Syringe filter (Elkay Laboratory Products Ltd.) and then through a 0.22 µm Millex[®]GP Filter Unit (Millipore Corporation). A HisTrap[™] HP column packed with precharged Ni Sepharose[™] High Performance was equilibrated with buffer B. The intracellular fraction was applied to this column and after extensive washing of the column with buffer B, recombinant protein bound on the resin was eluted with buffer C. The fluorinase-containing fractions were pooled together and concentrated using an Amicon[®] Ultra-15 centrifugal filter (Millipore Corporation).

| Buffer A | Buffer B | Buffer C |
|---------------------------|---------------------------|---------------------------|
| 10 mM phosphate pH 7.8 | 10 mM phosphate pH 7.8 | 10 mM phosphate pH 7.8 |
| 10 mM imidazole | 30 mM imidazole | 500 mM imidazole |

The protein was further purified by gel filtration fast protein liquid chromatography (FPLC) on a HiLoad[™] 16/60 Superdex[™] 200 gel filtration column (Pharmacia Biotech Inc.)

equilibrated with 50 mM Tris-HCl buffer (pH 7.8) and eluted at a constant flow rate of 1 ml/min using the same buffer.

The protein was used directly in this buffer or dialysed using dialysis tubing (MW 10 kDa cut off) against 2 l of the required buffer for the corresponding experiment overnight at 4 °C.

For long term storage, the purified recombinant fluorinase was kept at -80 °C.

5.2.14.1 Assay for the over-expressed fIA

A. ¹⁹F NMR assay

The fluorinase enzyme (280 µl, 1.5 mg/ml) was incubated with SAM **49** (10 µl, 20 mM) and KF (10 µl, 500 mM) at 37 °C for 3 h. The sample was heated (100 °C, 3 min) and the denatured protein removed by centrifugation (14,000 rpm, 15 min). D₂O (100 µl) was added to the supernatant which was then analysed by ¹⁹F NMR spectroscopy. A synthetic standard was used to confirm the production of 5'-deoxy-5'-fluoroadenosine, 5'-FDA **47**.

B. HPLC assay

In a total reaction volume of 100 µl, the fluorinase enzyme (80 µl, 1.5 mg/ml) was incubated with SAM **49** (10 µl, 20 mM) and KF (10 µl, 500 mM) at 37 °C for 3 h. The product was heated (100 °C, 3 min) and the denatured protein removed by centrifugation (14,000 rpm, 15 min). HPLC analysis (UV detection) against a synthetic reference compound was used to confirm the production of 5'-FDA **47**.

5.2.15 *T. vivax* IAG-NH over-expression and purification

5.2.15.1 Expression vector

The *T. vivax* IAG-NH recombinant plasmid subcloned into a pQE-30 (Qiagen) expression plasmid vector was supplied by Dr J. Steyaert (Vrije Universiteit Brussel). After its start codon, the pQE-30 expression vector possesses six consecutive histidine codons (coding for a 6 x His-tag). It also encodes a gene for ampicillin resistance and target gene expression is induced by IPTG *via* a T5 promoter.

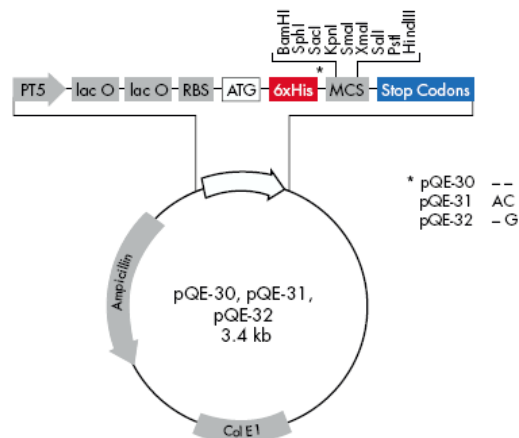


Figure 5.1 pQE-30, pQE-31 and pQE-32 plasmid map (taken from Qiagen, The QIAexpressionist™ 2003) pQE vectors for N-terminal 6xHis tag constructs. PT5: T5 promoter, lac O: lac operator, RBS: ribosome-binding site, ATG: start codon, 6xHis: 6xHis tag sequence, MCS: multiple cloning site with restriction sites indicated, Stop Codons: stop codons in all three reading frames, Col E1: Col E1 origin of replication, Ampicillin: ampicillin resistance gene.

5.2.15.2 Transformation of competent cells with the *iagnh* ORF in pQE-30

Chemically competent *E. coli* cells were purchased from Invitrogen. The competent cells were present in vials containing 50 µl aliquots. To transform these cells, each 50 µl aliquot

was placed on ice and allowed to thaw for 2–5 min, while gently mixing to evenly resuspend the cells. After thawing, addition of 2 μ l of plasmid DNA was added directly to each aliquot, stirring gently and returning the vial on ice for 20 min. Heat shock was performed by heating the vials for 30 seconds in a 42 °C water bath. The vials were then placed on ice for 5 min. LB medium (250 μ l) was added to each vial on ice. The vials were then incubated at 37 °C while shaking at 250 rpm for 1.5 h. An aliquot (100 μ l) of the transformed cells was added onto an agar plate containing the antibiotic ampicillin, and evenly distributed using a plate spreader. The plates were then incubated at 37 °C overnight.

5.2.15.3 Expression of iagNH and purification of IAG-NH

A. Expression trials

Single colonies were picked and grown up in LB (2 ml) containing 2 μ l of ampicillin (100 mg/ml) at 37 °C for ~16 h on an orbital shaker at 250 rpm. After this time, aliquots were used to inoculate fresh growth medium (4 ml) for the over-expression trials. The fresh inoculated LB containing ampicillin was incubated at 37 °C until a $OD_{600} = 0.4$ – 0.6 was reached. Expression was then induced with IPTG. The following variables were altered to optimise expression of soluble IAG-NH.

| <i>E. coli</i> Host strain | Growth Media | IPTG conc. (mM) | Induction T (°C) | Incubation T (°C) |
|-------------------------------|-----------------|--------------------|------------------|-------------------|
| BL21(DE3)Gold | LB | 0.2 | 4 | 16 |
| C43(DE3) | TB | 0.5 | 25 | 25 |
| ----- | ----- | 1 | 42 | ----- |
| ----- | ----- | 2 | ----- | ----- |

CHAPTER 5

For each expression trial, samples (1 ml) were taken at various intervals for analysis. Cells were harvested by centrifugation (14,000 rpm, 5 min) and the resulting pellet was resuspended in phosphate buffer (1 ml, 50 mM, pH 7.0). The cells were then lysed by sonication at 60 cycles for 20 sec. After sonication, the cells were centrifuged (14,000 rpm, 15 min) and the resultant cell pellet and the supernatant were retained as the insoluble and soluble fractions respectively for SDS-PAGE analysis.

B. Large scale expression of IAG-NH

Gene expression was achieved by addition of cell stock (2 μ l) of *E. coli* BL21(DE3)Gold or C43(DE3) cells containing the *iagnh* ORF in pQE-30 in 50% glycerol to LB (20 ml) containing 100 μ g/l ampicillin (20 μ l, 100 mg/ml). The starting cultures were incubated at 37 °C for 16 h. These overnight cultures were used to inoculate 2 l baffled flasks containing LB medium (1 l) and the antibiotic ampicillin (final concentration 100 μ g/l). These were incubated at 37 °C with shaking (180 rpm) until the cells reached an OD₆₀₀ between 0.4 and 0.6. The medium was then cooled to 25 °C and IPTG was added to a final concentration of 0.5 mM to initiate the expression of the recombinant protein. The inoculated flasks were then incubated at 16 °C for 16 h on an orbital shaker (160 rpm). After this time, the cells were harvested by centrifugation (9,000 rpm; 20 min) and the resulting pellet was either stored at -80 °C or used directly for protein purification.

C. Purification of IAG-NH

Cells were resuspended in buffer A consisting of 50 mM phosphate buffer (pH 7.0) supplemented with 1 M NaCl, 1 mM CaCl₂ and protease inhibitor cocktail (1 μ g/ml). The cells were lysed by sonication, ten times at 60% duty cycle for 1 min with intervals of cooling for 30 seconds, depending on the volume. The disrupted cell suspension was centrifuged for 30 min at 10,000 rpm and the clear supernatant was retained as cell-free extract (CFE). Prior

to further purification, this CFE was first filtered through a 0.45 μm EZEE Syringe filter (Elkay Laboratory Products Ltd.) and then through a 0.22 μm Millex[®]GP Filter Unit (Millipore Corporation). A HisTrap[™] HP column packed with precharged Ni Sepharose[™] High Performance was equilibrated with buffer B. The intracellular fraction was applied to this column and after extensive washing of the column with buffer B, the His-tagged nucleoside hydrolase was eluted with buffer C. The nucleoside hydrolase-containing fractions were neutralised with NaOH, combined and concentrated using an Amicon[®] Ultra-15 centrifugal filter (Millipore Corporation).

| Buffer A | Buffer B | Buffer C |
|---------------------------|---------------------------|--------------------------------|
| 50 mM phosphate pH 7.0 | 50 mM phosphate pH 7.0 | 50 mM sodium acetate pH 5.0 |
| 1 M NaCl | 1 M NaCl | 1 M NaCl |
| 1 mM NaCl ₂ | ----- | ----- |

This fraction was then loaded onto a HiLoad[™] 16/60 Superdex[™] 200 gel filtration column (Pharmacia Biotech Inc.) equilibrated with 20 mM Tris-HCl (pH 8.0), 150 mM NaCl and eluted at a constant flow rate of 1 ml/min using the same buffer.

The purified nucleoside hydrolase was then dialysed using dialysis tubing (MW 10 kDa cut off) against 2 l of the required buffer for the experiment overnight at 4 °C. The protein preparation was used directly for the experiments or glycerol was added to a final concentration of 5%, and the protein was snap-frozen in liquid N₂ and stored at -80 °C for later enzymatic assays.

5.2.15.4 Assay for the over-expressed iagNH

A. ^{19}F NMR assay

In a total reaction volume of 700 μl , a preparation of *T. vivax* IAG-NH enzyme (300 μl) was incubated with synthetic 5'-FDA **47** (30 μl , 18.6 mM) in HEPES buffer (370 μl , 50 mM, 1 mM CaCl_2 , pH 8.0) at 37 °C for 2 h. The protein was then denatured by heating (100 °C, 3 min) and removed by centrifugation (14,000 rpm, 15 min). The supernatant was supplemented with D_2O (100 μl) and subsequently analysed by ^{19}F NMR spectroscopy. A synthetic standard was used to confirm the production of 5-deoxy-5-fluoro-D-ribose, 5-FDR **71**.

B. HPLC assay

In a total reaction volume of 100 μl , the *T. vivax* IAG-NH enzyme (30 μl , 1.5 mg/ml) was incubated either with 5'-FDA **47** (30 μl , 18.6 mM) or adenosine **112** (30 μl , 18.6 mM) at 37 °C for 2 h. The product was heated (100 °C, 3 min) and the denatured protein removed by centrifugation (14,000 rpm, 15 min). HPLC analysis (UV detection) against a reference sample of adenine **62** was used to confirm the hydrolysis of 5'-FDA **47** or adenosine **112**.

5.2.16 5'-FDA as a substrate for the *T. vivax* IAG-NH

5.2.16.1 Incubation of 5'-FDA **47** in a CFE of *T. vivax* IAG-NH

A cell-free extract (CFE, 300 μl) containing NH activity was incubated with synthetic 5'-FDA **47** (30 μl , 18.6 mM) in phosphate buffer (400 μl , 50 mM, 1 mM CaCl_2) at 37 °C for 16 h. After this time, the protein was then denatured by heating (100 °C, 3 min) and removed by centrifugation (14,000 rpm, 15 min). The supernatant was supplemented with D_2O (100 μl)

and subsequently analysed by ^{19}F NMR spectroscopy. Selected spectroscopic data for 5-FDR **71**: δ_{F} (470 MHz; 10% D_2O): -228.46 (β , dt, $^2J_{\text{F-H}}$ 46.5, $^3J_{\text{F-H}}$ 26.0), -230.77 (α , dt, $^2J_{\text{F-H}}$ 46.5, $^3J_{\text{F-H}}$ 27.9).

5.2.16.2 pH profile incubations of 5'-FDA **47** with *T. vivax* IAG-NH

Partially purified IAG-NH was taken directly after nickel column purification and divided in three fractions which were dialysed in three different buffers (50 mM MES, pH 5.5; 50 mM PBS, pH 7.0 and 50 mM TRIS, pH 8.5) respectively. Experiments were carried out by incubating the *Tv*NH (500 μl , 0.5 mg/ml) with synthetic 5'-FDA **47** (30 μl , 18.6 mM) in the corresponding buffer (170 μl) supplemented with CaCl_2 (1mM) and D_2O (100 μl) at 37 °C and 55 °C. The hydrolysis of 5'-FDA **47** was followed by recording a $^{19}\text{F}\{^1\text{H}\}$ NMR spectrum every two hours. A synthetic standard was used to confirm the production of 5-deoxy-5-fluoro-D-ribose, 5-FDR **71**.

5.2.17 Enzymatic preparation of 5'-FDA **47**

The fluorinase enzyme (280 μl , 1.5 mg/ml) was incubated with SAM **49** (10 μl , 20 mM) and KF (10 μl , 500 mM) for a period of 4 h at 37 °C. After this time, the sample was heated (100 °C, 3 min) and the denatured protein removed by centrifugation (14,000 rpm, 15 min). The supernatant was supplemented with D_2O (100 μl) and analysed by ^{19}F NMR spectroscopy to reveal the production of 5'-FDA **47**. δ_{F} (470 MHz; 10% D_2O): -231.06 (dt, $^2J_{\text{F-H}}$ 47.6, $^3J_{\text{F-H}}$ 23.8). HPLC analysis (UV detection) against a synthetic reference compound was also used to confirm the production of **47**.

5.2.18 Enzymatic preparation of 5-FDR **71** from SAM **49**

5.2.18.1 Sequential one-pot synthesis

5'-FDA **47** was prepared enzymatically as previously described in Section 5.2.17. This sample containing 5'-FDA **47** was supplemented with a freshly prepared CFE (400 μ l) of *TvNH* in MES buffer (50 mM, pH 5.5; 1 mM CaCl₂) and incubated for further 30 min. The sample was heated (100 °C, 3 min) and the denatured protein removed by centrifugation (14,000 rpm, 15 min). The supernatant was then analysed by ¹⁹F NMR spectroscopy, showing formation of 5-FDR **71**. δ_F (470 MHz; 10% D₂O): β , dt, ²*J*_{F-H} 47.5, ³*J*_{F-H} 24.2), α , dt, ²*J*_{F-H} 47.5, ³*J*_{F-H} 24.2). HPLC analysis (UV detection) against a synthetic reference of adenine **62** was also used to confirm the hydrolysis of 5'-FDA **47**.

5.2.18.2 One-pot synthesis

The fluorinase (280 μ l, 1.5 mg/ml) was incubated with SAM **49** (10 μ l, 20 mM), KF (10 μ l, 500 mM) and a preparation (400 μ l) of the overexpressed *T. vivax* nucleoside hydrolase in phosphate buffer (50 mM, pH 7.8; 1 mM CaCl₂) for a period of 2 h at 37 °C. After this time, the reaction mixture was heated at 100 °C for 3 min and the denatured protein was removed by centrifugation (14,000 rpm, 15 min). The supernatant was supplement with D₂O (100 μ l) and analysed by ¹⁹F NMR spectroscopy. Only production of 5-deoxy-5-fluoro-D-ribose, 5-FDR **71**, was detected. δ_F (470 MHz; 10% D₂O): β , dt, ²*J*_{F-H} 47.5, ³*J*_{F-H} 24.2), α , dt, ²*J*_{F-H} 47.5, ³*J*_{F-H} 24.2). HPLC analysis (UV detection) against a synthetic reference of adenine **62** was also used to confirm the hydrolysis of 5'-FDA **47**.

5.2.18.3 Enzymatic preparation of [^{18}F]FDR [^{18}F]**71** from SAM **49**

A. Sequential one-pot synthesis

The fluorinase enzyme (70 μl , 35.3 mg/ml) was incubated with SAM **49** (30 μl , 20 mM) and aqueous [^{18}F]F $^-$ (50 μl , solution in [^{18}O]H $_2\text{O}$, 72 MBq) at 37 $^\circ\text{C}$ for 4 h. An aliquot of the mixture was analysed by analytical HPLC against a standard 5'-FDA **47**, confirming production of 5'-deoxy-5'-[^{18}F]fluoroadenosine ([^{18}F]FDA) [^{18}F]**47**. A preparation of purified nucleoside hydrolase in HEPES buffer (100 μL , 16 mg/mL; 50 mM, pH 8.0) was added to the remaining fluorinase reaction mixture along with small volume of the buffer (50 μL , 50 mM HEPES, 1 mM CaCl $_2$, pH 8.0) containing the enzyme co-factor necessary for the hydrolase reaction. Following the addition of *T. vivax* IAG-NH, the enzyme cocktail was incubated for a further 45 minutes at 37 $^\circ\text{C}$, and an aliquot was taken for HPLC analysis. Formation of 5-deoxy-5-[^{18}F]fluoro-D-ribose ([^{18}F]FDR) [^{18}F]**71** was observed in a 9:1 ratio of [^{18}F]FDA [^{18}F]**47** to [^{18}F]FDR [^{18}F]**71**.

B. One-pot synthesis

A typical reaction mixture combined the reagents indicated below. Experiments were performed at 37 °C and aliquots of the reaction mixtures analysed by HPLC as previously described.

| | Experiment 1 | Experiment 2 |
|--|----------------------|----------------------|
| Fluorinase (35 mg/ml) | 70 µl | 70 µl |
| SAM (20 mM) | 30 µl | 30 µl |
| <i>T. vivax</i> IAG-NH | 100 µl (16 mg/ml) | 100 µl (35 mg/ml) |
| [¹⁸ F]fluoride in [¹⁸ O]H ₂ O | 100 µl | 100 µl |
| Buffer (50 mM HEPES, 1mM CaCl ₂ , pH 8.0) | 50 µl | 50 µl |

Experiment 1: HPLC analysis confirmed the production of [¹⁸F]FDA [¹⁸F]47 and [¹⁸F]FDR [¹⁸F]71 in a 9:1 ratio (see Chapter 4, Figure 4.14) after 4 h incubation.

Experiment 2: HPLC analysis confirmed the production of [¹⁸F]FDA [¹⁸F]47 and [¹⁸F]FDR [¹⁸F]71 (see Chapter 4, Figure 4.18) after 4.5 h incubation. After 8 h [¹⁸F]FDR [¹⁸F]71 represents 31% of the total radioactivity detected ([¹⁸F]fluoride does not elute from the column under the conditions of the analysis).

5.3 References

1. D. D. Perrin, W. L. F. Armarego and D. R. Perrin, in *Purification of Laboratory Chemicals*, Pergamon Press, Oxford, 4th Ed., 1996.
2. H. E. Gottlieb, V. Kotlyar and A. Nudelman, *J. Org. Chem.*, 1997, **62**, 7512-7515.
3. D. Gani and A. W. Johnson, *J. Chem. Soc., Perkin Trans. I*, 1982, 1197-1204.
4. S. L. Cobb, Ph.D. Thesis, *The origin and metabolism of 5'-FDA in Streptomyces cattleya*, University of St Andrews, 2005.
5. T. D. Ashton and P. J. Scammells, *Bioorg. Med. Chem. Lett.*, 2005, **15**, 3361-3363.
6. F. Kappler and A. Hampton, *J. Med. Chem.*, 1990, **33**, 2545-2551.
7. H. M. Kissman and M. J. Weiss, *J. Am. Chem. Soc.*, 1958, **80**, 5559-5564.
8. A. G. M. Barrett and S. A. Lebold, *J. Org. Chem.*, 1990, **55**, 3853-3857.
9. A. P. Rauter, F. Ramôa-Ribeiro, A. C. Fernandes and J. A. Figueiredo, *Tetrahedron*, 1995, **51**, 6529-6540.
10. F. Sarabia-García and F. J. López-Herrera, *Tetrahedron*, 1996, **52**, 4757-4768.
11. M. Ebner and A. E. Stütz, *Carbohydr. Res.*, 1998, **305**, 331-336.
12. Y. Li and G. Just, *Tetrahedron*, 2001, **57**, 1677-1687.
13. P. Hadwiger, P. Mayr, B. Nidetzky, A. E. Stütz, and A. Tauss, *Tetrahedron Asymm.* 2000, **11**, 607-620.
14. C. Schaffrath, Ph.D. Thesis, *Biosynthesis and Enzymology of Fluorometabolite Production in Streptomyces cattleya*, University of St Andrews, 2002.
15. J. T. G. Hamilton, C. D. Murphy, M. R. Amin, D. O'Hagan and D. Harper, *J. Chem. Soc., Perkin Trans. I*, 1998, 759-767.
16. K. A. Reid, J. T. G. Hamilton, R. D. Bowden, D. O'Hagan, L. Dasaradhi, M. R. Amin and D. B. Harper, *Microbiology*, 1995, **141**, 1385-1393.

CHAPTER 5

17. R. K. Scopes, in *Protein Purification: Principles and Practice*, 3rd Ed., Springer, New York, 1994, p. 346.

Appendix

Appendix

Publications

- **“Fluorinase mediated ^{18}F -C bond formation: a two-step enzymatic route to 5-deoxy-5- ^{18}F fluoro-D-ribose for PET labelling”** Mayca Onega, Juozas Domarkas, Christophe Plisson, Lutz F. Schweiger, Antony D. Gee and David O’Hagan, *in preparation*.
- **“The fluorinase: A tool for the synthesis of fluorine-18 labelled sugars and nucleosides for positron emission tomography”** Mayca Onega, Margit Winkler and David O’Hagan, *Future Medicinal Chemistry*, submitted.
- **“The identification of (3R,4S)-5-fluoro-5-deoxy-D-ribulose-1-phosphate as an intermediate in fluorometabolite biosynthesis in *S. cattleya*”** Mayca Onega, Ryan P. McGlinchey, Hai Deng, John T.G. Hamilton, David O’Hagan, *Bioorg. Chem.* 2007, **35**, 375-385.
- **“Fluorinase mediated C- ^{18}F bond formation, an enzymatic tool for PET labelling”** Hai Deng, Steven L. Cobb, Antony D. Gee, Andrew Lockhart, Laurent Martarello, Ryan P. McGlinchey, David O’Hagan and Mayca Onega, *Chem. Commun.* 2006, 652-654.

Awards

1st Prize for the best poster presentation at the 8th International Symposium on Biocatalysis and Biotransformations (BioTrans 2007), Oviedo (Spain), July 2007: “Fluorometabolite biosynthesis in *Streptomyces cattleya*”.

Conferences and presentations

- 38th RSC Scottish Organic Division Meeting, Aberdeen (UK), Dec 2008.
- 37th RSC Scottish Organic Division Meeting, Glasgow (UK), Dec 2007.
- RSC Bio-Organic Group Meeting: Biosynthesis in Unexpected Places, Fribush (UK), Sep 2007.
- 8th International Symposium on Biocatalysis and Biotransformations (BioTrans 2007), Oviedo (Spain), Jul 2007. Poster presentation (1st Poster prize winner).
- Bio-organic Postgraduate Meeting, Bristol (UK), Jun 2007.
- Organic Chemistry Final Year PhD Symposium, St Andrews, Jun 2007. Oral presentation.
- 36th RSC Scottish Organic Division Meeting, Edinburgh (UK), Dec 2006.
- RSC Chemical Biology: Directing Biosynthesis, Cambridge (UK), Sep 2006. Poster presentation.
- Bio-organic Postgraduate Meeting, Bristol (UK), Jun 2005.
- 35th RSC Scottish Organic Division Meeting, Glasgow (UK), Dec 2005.
- RSC Fluorine Group Meeting, Oxford (UK), Sep 2005. Poster presentation.
- 34th RSC Scottish Organic Division Meeting, St Andrews (UK), Dec 2004.